NOVEL APPLICATIONS OF STEREOTACTIC BODY RADIATION THERAPY (SBRT)

EDITED BY: Debnarayan Dutta, Alexander Muacevic, Rupesh Kotecha and Rakesh Jalali

PUBLISHED IN: Frontiers in Oncology

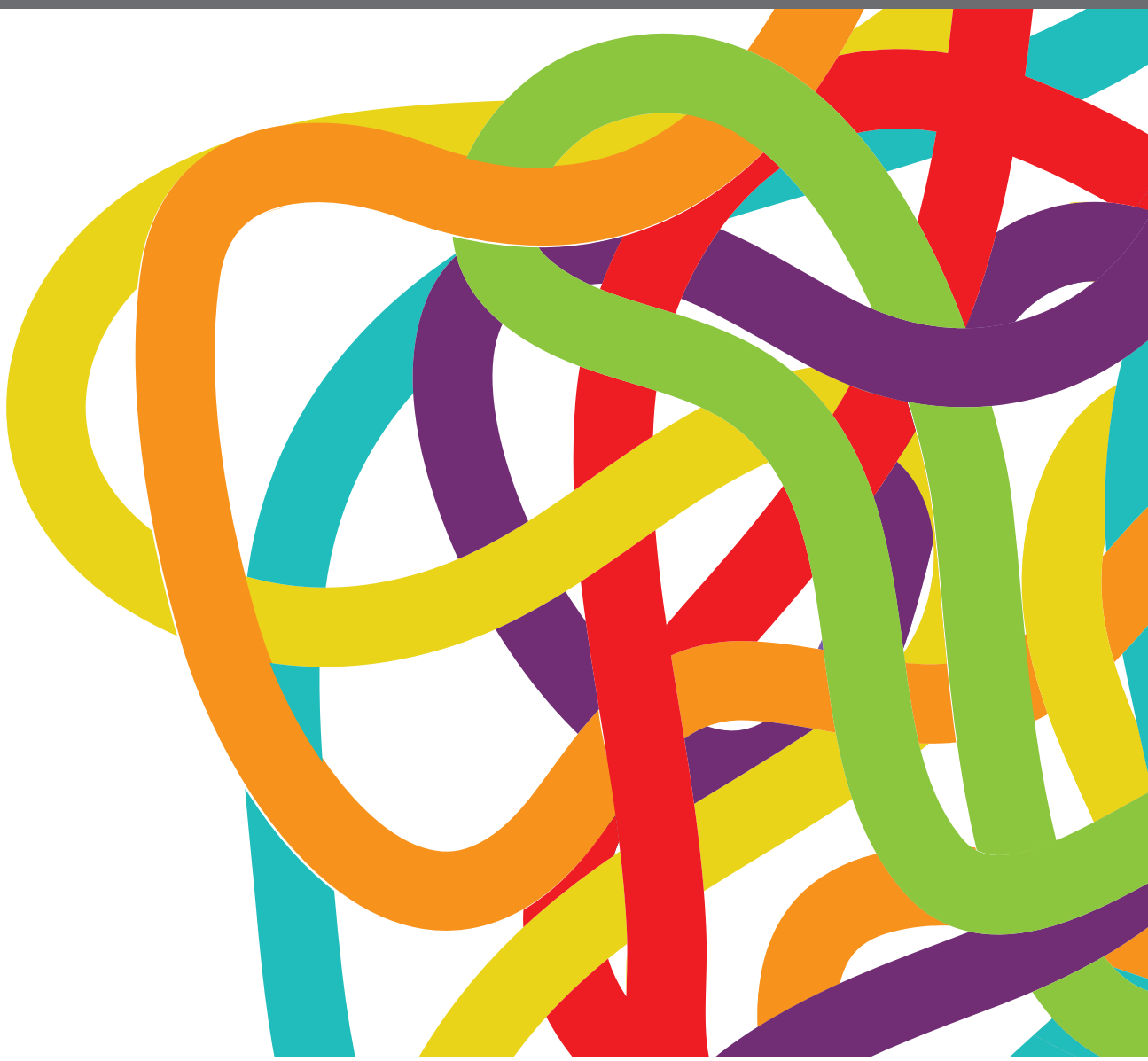

frontiers Research Topics

frontiers

ISSN 1664-8714
ISBN 978-2-88971-518-3
DOI 10.3389/978-2-88971-518-3

About Frontiers

Frontiers is more than just an open-access publisher of scholarly articles: it is a pioneering approach to the world of academia, radically improving the way scholarly research is managed. The grand vision of Frontiers is a world where all people have an equal opportunity to seek, share and generate knowledge. Frontiers provides immediate and permanent online open access to all its publications, but this alone is not enough to realize our grand goals.

Frontiers Journal Series

The Frontiers Journal Series is a multi-tier and interdisciplinary set of open-access, online journals, promising a paradigm shift from the current review, selection and dissemination processes in academic publishing. All Frontiers journals are driven by researchers for researchers; therefore, they constitute a service to the scholarly community. At the same time, the Frontiers Journal Series operates on a revolutionary invention, the tiered publishing system, initially addressing specific communities of scholars, and gradually climbing up to broader public understanding, thus serving the interests of the lay society, too.

Dedication to Quality

Each Frontiers article is a landmark of the highest quality, thanks to genuinely collaborative interactions between authors and review editors, who include some of the world's best academicians. Research must be certified by peers before entering a stream of knowledge that may eventually reach the public - and shape society; therefore, Frontiers only applies the most rigorous and unbiased reviews.
Frontiers revolutionizes research publishing by freely delivering the most outstanding research, evaluated with no bias from both the academic and social point of view. By applying the most advanced information technologies, Frontiers is catapulting scholarly publishing into a new generation.

What are Frontiers Research Topics?

Frontiers Research Topics are very popular trademarks of the Frontiers Journals Series: they are collections of at least ten articles, all centered on a particular subject. With their unique mix of varied contributions from Original Research to Review Articles, Frontiers Research Topics unify the most influential researchers, the latest key findings and historical advances in a hot research area! Find out more on how to host your own Frontiers Research Topic or contribute to one as an author by contacting the Frontiers Editorial Office: frontiersin.org/about/contact

NOVEL APPLICATIONS OF STEREOTACTIC BODY RADIATION THERAPY (SBRT)

Topic Editors:
Debnarayan Dutta, Amrita Institute of Medical Sciences and Research Centre, India
Alexander Muacevic, Ludwig Maximilian University of Munich, Germany
Rupesh Kotecha, Baptist Hospital of Miami, United States
Rakesh Jalali, Apollo Proton Cancer Centre, India

Citation: Dutta, D., Muacevic, A., Kotecha, R., Jalali, R., eds. (2021). Novel Applications of Stereotactic Body Radiation Therapy (SBRT). Lausanne: Frontiers Media SA. doi: 10.3389/978-2-88971-518-3

Table of Contents

frontiers in Oncology

EDITORIAL
published: 03 September 2021
doi: 10.3389/fonc.2021.760078

Editorial: Novel Applications of Stereotactic Body Radiotherapy (SBRT)

Rupesh Kotecha[1,2*], *Debnarayan Dutta*[3], *Rakesh Jalali*[4] *and Alexander Muacevic*[5]

[1] Department of Radiation Oncology, Miami Cancer Institute, Baptist Health South Florida, Miami, FL, United States, [2] Herbert Wertheim College of Medicine, Florida International University, Miami, FL, United States, [3] Amrita Institute of Medical Sciences and Research Centre, Kochi, India, [4] Apollo Proton Cancer Centre, Chennai, India, [5] Ludwig Maximilian University of Munich, Munich, Germany

Keywords: stereotactic body radiotherapy, stereotactic ablative body radiation, oligometastatic, oligoprogressive, hepatocellular carcinoma, arteriovenous malformation

Editorial on the Research Topic

Novel Applications of Stereotactic Body Radiotherapy (SBRT)

The use of stereotactic body radiotherapy (SBRT) or stereotactic ablative radiotherapy (SABR) has undergone a surge in enthusiasm around the world fueled by an improved understanding of the radiobiology of high-fractional dose radiotherapy, technology development and increased availability of high-precision delivery platforms, and the dissemination of published literature through retrospective and prospective studies. Our current knowledge of SBRT/SABR has not only expanded the use of this treatment approach in the historical and classic scenarios of brain and spine SBRT/SABR and lung SBRT/SABR, but also led to new frontiers of clinical applications. In this context, several recent studies were published within a special Research Topic specifically focused on novel and unique applications of SBRT/SABR.

Greve et al. published a large retrospective analysis of patients treated with stereotactic radiosurgery (SRS) for arteriovenous malformations with CT and MRI-based planning approaches and without stereotactically-defined digital subtraction angiography over a 14-year period. In total, this series evaluated the outcomes of 215 patients (53% treated with SRS as a first-line treatment and 55% classified as Spetzler-Martin grade I-III) treated to a median dose of 18 Gy in 1 fraction to a median target volume of 2.4 cm^3. Approximately 47% demonstrated complete obliteration of the arteriovenous malformation, consistent with that observed in other series using different treatment platforms, and supporting the use of this approach.

Although spine SRS/SBRT has been established as an effective treatment in the upfront management of patients with spinal metastasis, Ehret et al. expand the evidence for treatment of recurrent spine metastasis treated with SRS. In their study of 53 patients (initial treatment 36 Gy in 15 fractions treated to a median dose of 18 Gy in 1 fraction), the local control rate was 77% (Ehret et al.). Furthermore expanding indications from metastatic sites to intramedullary lesions, Ehret et al. report on 12 patients with WHO II/III spinal ependymomas treated to a median dose of 15 Gy in 1 fraction with a local control rate of 84%. Together, these series support the role of spine SRS in patients with extramedullary and intramedullary tumors.

Liu et al. reported on patients with hepatocellular carcinoma, and although radiotherapy was not a particular focus of their study, demonstrate potential avenues for evidence development by guiding patient selection for adjuvant treatment. They report on a series of 244 patients with

OPEN ACCESS

Edited and reviewed by:
Timothy James Kinsella, Warren Alpert Medical School of Brown University, United States

***Correspondence:**
Rupesh Kotecha
rupeshk@baptisthealth.net

Specialty section:
This article was submitted to Radiation Oncology, a section of the journal Frontiers in Oncology

Received: *17 August 2021*
Accepted: *20 August 2021*
Published: *03 September 2021*

Citation:
Kotecha R, Dutta D, Jalali R and Muacevic A (2021) Editorial: Novel Applications of Stereotactic Body Radiotherapy (SBRT). Front. Oncol. 11:760078. doi: 10.3389/fonc.2021.760078

hepatocellular carcinoma treated with narrow-margin (<1 cm margin) or wide-margin (≥1 cm margin) resections (Liu et al.). In total, post-operative recurrence was observed in 53% of patients and not only was the risk of recurrence higher in those treated with narrow-margin resections, the pattern of recurrence was also different, with modest rates of marginal recurrence (21 vs. 5%). These recurrence patterns were also hypothesized to affect survival as those patients treated with narrow margins also had reduced overall survival. Interestingly, post-operative SBRT for patients with positive margins yielded no marginal recurrences. In addition, Jiang et al. evaluated the safety and efficacy of transarterial chemoembolization (TACE) and SBRT for Barcelona Clinic Liver Cancer (BCLC) stage B hepatocellular carcinoma. In their series, 57 patients were treated to a dose of 20-50 Gy in 3-5 fractions; at a median follow-up of 42 months, the objective response rate was 86% and the disease control rate was 97%. These results will help inform the clinical practice of SBRT with consideration of post-operative SBRT in patients at high-risk for local recurrence after surgery as well as definitive treatment for those patients too high-risk for invasive interventions.

SBRT for prostate cancer is now endorsed by national and international treatment guidelines and Aghdam et al. describe the demographic characteristics of patients treated with SBRT over a 10-year period. Interestingly, in their analysis of 1,035 patients treated with prostate SBRT, travel distance did not adversely affect use in African Americans, elderly patients, or those from rural locations, supporting the broad adoption and utilization of this treatment approach. Ultimately, the convenience of SBRT over conventionally-fractionated regimens allows for improved patient access to care.

The use of SBRT/SABR for patients with oligometastatic or oligoprogressive disease is an area of intense study and recent reports have supported the cost-effectiveness of this treatment strategy (Mehrens et al.). Even in patients with pancreatic cancer with liver-only oligometastatic disease, SBRT in addition to chemotherapy appears safe and effective (Ji et al.). Yet, treatment of lymph nodes with stereotactic radiotherapy remains an understudied area. Burkon et al. reported on a retrospective analysis of 90 patients treated with SBRT to lymph nodes in the mediastinum, retroperitoneum, or pelvis. The local control rate was modest at 69% at 3 years and the median freedom from widespread dissemination was 14.6 months. Additional studies will evaluate the patterns of failure, optimal dose and fractionation schedule, and patient selection criteria for this treatment approach.

As we look towards the future of SBRT/SABR, the introduction of innovative radiotherapy delivery approaches represents a relatively nascent area of study. Feasibility studies have begun to demonstrate the potential of particle therapy delivery techniques, such as Spot-Scanning Proton Arcs (Liu et al.), and future trials will incorporate these novel technologies with increasing clinical indications.

AUTHOR CONTRIBUTIONS

All authors have reviewed this manuscript. All authors contributed to the article and approved the submitted version.

Conflict of Interest: RK: Honoraria from Accuray Inc., Elekta AB, Viewray Inc., Novocure Inc., Elsevier Inc, Brainlab. Institutional research funding from Medtronic Inc., Blue Earth Diagnostics Ltd., Novocure Inc., GT Medical Technologies, Astrazeneca, Exelixis, Viewray Inc, Brainlab.
RJ: Honoraria from Cipla Limited. AM: Honoraria from Accuray Inc.

The remaining author declares that the research was conducted in the absence of any commercial or financial relationships that could be construed as a potential conflict of interest.

Publisher's Note: All claims expressed in this article are solely those of the authors and do not necessarily represent those of their affiliated organizations, or those of the publisher, the editors and the reviewers. Any product that may be evaluated in this article, or claim that may be made by its manufacturer, is not guaranteed or endorsed by the publisher.

frontiers in Oncology

ORIGINAL RESEARCH
published: 21 January 2021
doi: 10.3389/fonc.2020.610636

Narrow-Margin Hepatectomy Resulted in Higher Recurrence and Lower Overall Survival for R0 Resection Hepatocellular Carcinoma

Lihong Liu[1†], Yongjie Shui[1†], Qianqian Yu[1], Yinglu Guo[1], Lili Zhang[1], Xiaofeng Zhou[1], Risheng Yu[2], Jianying Lou[3], Shumei Wei[4] and Qichun Wei[1*]*

[1] Department of Radiation Oncology, Ministry of Education Key Laboratory of Cancer Prevention and Intervention, the Second Affiliated Hospital, Zhejiang University School of Medicine, Hangzhou, China, [2] Department of Radiology, the Second Affiliated Hospital, Zhejiang University School of Medicine, Hangzhou, China, [3] Department of Hepatobiliary Pancreatic Surgery, the Second Affiliated Hospital, Zhejiang University School of Medicine, Hangzhou, China, [4] Department of Pathology, the Second Affiliated Hospital, Zhejiang University School of Medicine, Hangzhou, China

Purpose: To evaluate the impact of resection margin on recurrence pattern and survival for hepatocellular carcinoma (HCC) with narrow margin resection, with the aim to guide postoperative treatment.

Materials and Methods: Two hundred forty HCC patients after curative hepatectomy between 2014 and 2016 were reviewed retrospectively. The cases were divided into narrow-margin (width of resection margin <1cm, n=106) and wide-margin (width of resection margin ≥1cm, n=134) groups based on the width of resection margin. Recurrence pattern, recurrence-free survival (RFS), and overall survival (OS) were compared between the above two groups. An additional cohort of nine cases with positive margin plus post-operative stereotactic body radiotherapy (SBRT) was also analyzed for the recurrence pattern.

Results: Postoperative recurrence was found in 128 (53.3%) patients. The recurrence rate was significantly higher in narrow-margin group than that in wide-margin group (P=0.001), especially for the pattern of marginal recurrence (20.8 *vs*. 4.5%, P=0.003). The 1-, 2-, 3-year RFS rates for the narrow-margin and wide-margin groups were 55.8, 43.9, 36.9, and 78.7, 67.9, 60.2%, respectively, with significant difference between the two groups (P<0.001). Patients with narrow margin showed a tendency of decreased OS than those with wide margin (P<0.001). As comparison, the nine cases with positive margin treated with postoperative SBRT showed low recurrence rate and no marginal recurrence was found.

Conclusion: Patients with narrow resection margin were associated with higher recurrence rate and worse survival than those with wide resection margin. These patients may benefit from adjuvant local treatment, such as radiotherapy.

Keywords: hepatocellular carcinoma, surgical margin, patterns of recurrence, prognosis, postoperative radiotherapy

OPEN ACCESS

Edited by:
Rupesh Kotecha,
Baptist Hospital of Miami,
United States

Reviewed by:
Michael David Chuong,
Baptist Health South Florida,
United States
Kevin L. Stephans,
Case Western Reserve University,
United States
Adeel Kaiser,
Baptist Hospital of Miami,
United States

***Correspondence:**
Qichun Wei
qichun_wei@zju.edu.cn
Shumei Wei
2307001@zju.edu.cn

[†]These authors have contributed equally to this work

Specialty section:
This article was submitted to Radiation Oncology, a section of the journal Frontiers in Oncology

Received: *26 September 2020*
Accepted: *04 December 2020*
Published: *21 January 2021*

Citation:
Liu L, Shui Y, Yu Q, Guo Y, Zhang L, Zhou X, Yu R, Lou J, Wei S and Wei Q (2021) Narrow-Margin Hepatectomy Resulted in Higher Recurrence and Lower Overall Survival for R0 Resection Hepatocellular Carcinoma. Front. Oncol. 10:610636. doi: 10.3389/fonc.2020.610636

INTRODUCTION

Hepatocellular carcinoma (HCC) is the seventh prevalent malignancy worldwide (1). In China, HCC is the fourth common cancer and the third leading cause of cancer-related mortality (2). Although surgical excision is considered the standard treatment for resectable HCC (3), a high rate of postoperative recurrence was observed after partial hepatectomy, with a marginal recurrence rate up to 30% (4–6). Multiple factors are correlated to high postoperative recurrence, including tumor size, number, microvascular invasion (MVI), tumor capsule invasion, and resection margin status (5, 7–10).

Among these factors, resection margin has been widely evaluated for its effect on the long-term outcomes after resection, however, the conclusion remains controversial. A few studies have shown that an adequate resection margin is indispensable for long-term survival (11–14), but others found that a narrow resection margin does not detract from long-term outcomes (8, 9, 15). It is generally accepted that both surgical curability and postoperative hepatic function preservation are crucial for the successful treatment of patients with HCC. For instance, irregular hepatectomy or meso-hepatectomy were often recommended for centrally located HCCs, especially for those adjacent to the first or second porta hepatis systems (16, 17), but the resection margin is generally less than 1cm in order to meet the criteria both for cure and preservation of the adjacent major vessels simultaneously (18, 19). Therefore, a better understanding of the impact of width of resection margin on recurrence and survival helps to tailor adjuvant therapy against recurrence to improve long-term oncological outcomes.

In this study, based on a retrospectively collected database, we conducted a detailed analysis to reveal the effect of margin width on recurrence pattern and survival outcomes after hepatectomy, in HCC with narrow resection margin. If the rate of marginal recurrence is high, a postoperative local treatment such as radiotherapy might be useful to improve local control.

MATERIALS AND METHODS

Patients

A total of 240 HCC patients in the Second Affiliated Hospital, Zhejiang University School of Medicine (SAHZU) who underwent hepatectomy between April 2014 to December 2016 were enrolled in this study based on the following inclusion criteria: 1) HCC confirmed by postoperative histology. 2) without neoadjuvant treatment before the first hepatectomy. 3) a complete removal of tumor confirmed by postoperative pathology. 4) Child-Pugh class A5, A6, or B7. 5) Eastern Cooperative Oncology Group performance status 0 or 1. 6) with postoperative imaging follow-up of more than 2 months. Those with distant metastasis and second primary tumor were excluded. The clinical information and follow-up data were collected from the electrical records. The tumor differentiation was graded according to the Edmondson and Steiner grading system (20). The MVI status was graded by the guidelines for the pathological diagnosis of primary liver cancer: 2015 update (21). Tumor staging was assessed according to the 8th edition of guidelines of the American Joint Committee on Cancer (AJCC) (22). Tumor capsule invasion were judged by preoperative imaging. Tumor with smooth peripheral rim was defined as presence of capsule, while tumor with irregular or indistinct borders were defined as absence of capsule (23). This study was approved by Institutional Review Board of SAHZU (2020774).

Surgical Procedure

Surgical margin was defined as the shortest distance from the edge of the tumor to the surface of liver transection (24). The cases were divided into narrow-margin (width of resection margin <1cm, n=106) and wide-margin (width of resection margin ≥1cm, n=134) groups. Resection of the liver equal to or larger than two Couinaud's segments was considered major liver resection, and a resection smaller than this was considered minor resection. R0 resection was defined as no cancer cell was found on the surgical margin under microscope. Preoperative and postoperative imaging (contrast-enhanced MRI or CT scans) were used to assess the size and location of tumor, and width of resection margin.

Recurrence

After curative R0 resection, patients were followed up in our hospital every month for 3 times, then every 3 months during the first 2 years and every 6 months during the next 3 years. Biopsy for the recurrent lesion was encouraged. Imaging evidence of tumor recurrence (suspicious new findings and progression of disease documented by serial imaging) was also accepted in patients who did not undergo biopsy. The recurrence pattern and the date of initial disease relapse was recorded when the first suspicious radiologic finding was initially identified. In terms of location of recurrence, two major categories were divided: intrahepatic recurrence and extrahepatic recurrence. Intrahepatic recurrence was subdivided into three patterns: 1) marginal recurrence, 2) intrahepatic single-nodule recurrence, 3) intrahepatic multiple-nodule recurrence. Marginal recurrence was defined as intrahepatic recurrence located less than 1 cm from the resection margin, regardless of any simultaneous recurrence in the distant liver remnant or extrahepatic sites.

Positive Margin Cases with Postoperative Stereotactic Body Radiotherapy

Postoperative radiotherapy such as stereotactic body radiotherapy (SBRT) is not recommended for HCC with wide resection margin and its role in patients with narrow margin resection remains controversial. In our institution, postoperative SBRT is not introduced for HCC with R0 resection, therefore, there are not relevant data to demonstrate the significance of adjuvant SBRT in HCC patients with narrow resection margin.

Abbreviations: CI, confidence interval; GTV, gross target volume; HCC, hepatocellular carcinoma; HR, hazard ratio; IMRT, intensity modulated radiotherapy; ITV, internal target volume; MVI, microvascular invasion; OAR, organs at risk; OS, overall survival; PTV, planning target volume; RFS, recurrence-free survival; RILD, radiation induced liver disease; SBRT, stereotactic body radiotherapy; TACE, transcatheter arterial chemoembolization.

However, for patients with positive margin, adjuvant SBRT was used as an optional treatment for residual lesions following hepatectomy, if the patients possess appropriate performance status (ECOG 0-2) and enough liver function reserve. We compared the difference in recurrence pattern between positive margin HCC who received SBRT and those with R0 resection alone, with the aim to evaluate the role of SBRT in local control.

The tumor bed was marked by surgical clips for patients with positive margin during operation. The gross target volume (GTV) was defined as tumor residual and the tumor bed. The full extent of fluid cavity was not included intentionally. The internal target volume (ITV) was defined as the volumetric sum of GTVs in the multiple phases. The planning target volume (PTV) included ITV with 0.5 cm margin and was adjusted manually to minimize overlapping the gastrointestinal tract when needed. The other radiation treatment details, including dose-volume constrains to organs at risk (OAR), respiratory motion management, image guidance, and evaluation of toxicities after SBRT were referred to our previous article by Shui et al. (25).

Statistical Analysis

The data are presented as the mean ± standard deviation for continuous variables. Comparisons between groups were performed using the chi-square test (or the Fisher's exact test) for nominal variables, and the unpaired t test was used for continuous variables. Overall survival (OS) and recurrence-free survival (RFS) were evaluated by the Kaplan-Meier method and compared by the log-rank test, respectively. OS was calculated from the date of first radical hepatectomy to death for any cause. RFS was measured from the date of first hepatectomy to first recurrence. The Cox regression model was employed in univariate analyses. Surgical resection, tumor number, size, and variables with p value <0.01 in the univariable analyses were retained for the multivariable Cox analysis. All statistical analyses were performed using IBM SPSS Statistics for Windows (Version 23.0; IBM Corp., Armonk, NY) and GraphPad Prism 8.0 software (GraphPad Software Inc., San Diego, CA, USA). P<0.05 was considered statistically significant and indicated by bold values.

RESULTS

Patients Characteristics

The follow-up ended on March 10, 2020. The median follow-up time was 55.2 months [95% confidence interval (CI) 52.2–58.2 months]. Totally 240 patients were included in the final analysis. Of which 106 were divided into the narrow-margin group, and 134 into the wide-margin group based on the width of resection. The patients included 208 (86.7%) male and 32 (13.3%) female cases with an average age of 57.3 (range 22–82) years old at first operation. None of the patients received radiotherapy pre- or post-operatively. A comparison of the baseline demographic and clinicopathological characteristics showed that more patients presented with higher ALT level (P=0.030), larger tumor size (P=0.003), absence of tumor capsule (P=0.027), longer operative time (P<0.001), larger operative blood loss (P=0.019), major liver resection (P<0.001), and more advanced pTNM stage (P=0.008) in the narrow-margin group than that in the wide-margin group (**Table 1**). In this analysis, TACE was administered to 57 patients (57/240, 23.8%), with 29 (29/134, 21.6%) cases from the wide-margin group, the other 28 (28/106, 26.4%) from narrow-margin group. The patient distribution of receiving TACE were largely comparable between the two groups. We further compared the baseline and outcome characteristics of all 240 R0 resection patients with or without postoperative transcatheter arterial chemoembolization (TACE) (**Supplementary Table 1**). The clinicopathological characteristics of patients receiving TACE were comparable to those without receiving TACE.

Patterns of Recurrence

The median time to recurrence is 9.7 months. During the follow-up periods, 128 patients (128/240, 53.3%) had documented tumor recurrence, with 69 patients (69/106, 65.1%) were originally resected with a narrow margin, 59 (59/134, 44.0%) with a wide margin resection (P=0.001). The marginal recurrence rate was 20.8% (22/106) among patients in the narrow-margin group, and the corresponding rate was 4.5% (6/134) in the wide-margin group, with a significant difference between these two groups (P=0.003). The intrahepatic single-nodule recurrence rate was 12.3% (13/106) in the narrow-margin group, and the corresponding rate was 19.4% (26/134) in the wide-margin group, with a significant difference between the two groups (P=0.002). Intrahepatic multiple-nodule recurrences were found in 50 patients. Among them, 34 (34/106, 32.1%) were from the narrow-margin group, and 16 (11.9%) from the wide-margin group, with a significant difference between them (P=0.010). The recurrence patterns were summarized in **Table 2** and **Figure 1**, showing that the incidence of extrahepatic recurrence was low, while marginal recurrence and intrahepatic remnant recurrence were the main recurrence patterns.

Compared with patients with wide margin resection, those with narrow margin resection had a higher rate of recurrence within 12 months after surgery (narrow and wide: 43.4 *vs*. 20.9%, P=0.028). More marginal recurrence occurred in narrow-margin group than wide-margin group at different time points of the first year after surgery (at 3 months: 6.6 *vs*. 0.0%; at 6 months: 10.4 *vs*. 0.7%; at 9 months: 12.3 *vs*. 2.2%; at 12 months: 14.2 *vs*. 2.2%). Similar results were also found for intrahepatic multiple-nodule recurrence (at 3 months: 9.4 *vs*. 3.0%; at 6 months: 18.9 *vs*. 4.5%; at 9 months: 23.6 *vs*. 5.2%; at 12 months: 27.4 *vs*. 6.7%) (**Table 2**).

Recurrence-Free Survival

The 1-, 2-, 3-year RFS rates were 55.8, 43.9, 36.9% in the narrow-margin group and 78.7, 67.9, 60.2% in the wide-margin group, respectively (P<0.001; **Figure 2A**). In the multivariable analysis, narrow margin was significantly associated with worse RFS [wide *vs*. narrow, hazard ratio (HR) =0.608; 95% CI, 0.414–0.893, P=0.011]. Other independent predictors include HBs Ag, tumor capsule, MVI status, and extent of liver resection (**Table 3**). In the subgroup analysis based on MVI status (M0 *vs*. M1 +M2), patients with narrow margin resection correlated with worse RFS, regardless of MVI status (**Figure 3**). Similar results were also found in the subgroup analysis based on tumor size (≤

TABLE 1 | Demographic and clinicopathological characteristics of wide-margin, narrow-margin, and positive-margin plus stereotactic body radiotherapy (SBRT) groups.

Variable	Wide-margin group (n = 134)	Narrow-margin group (n = 106)	*P*-Value (Wide *vs.* narrow)	Positive-margin plus SBRT (n = 9)
Age	87 (64.9%)	61 (57.5%)	0.243	6 (66.7%)
≤60 years old	47 (35.1%)	45 (42.5%)		3 (33.3%)
>60 years old				
Gender	113 (84.3%)	95 (89.6%)	0.231	8 (88.9%)
Male	21 (15.7%)	11 (10.4%)		1 (11.1%)
Female				
HBs Ag	108 (80.6%)	75 (70.8%)	0.075	7 (77.8%)
Positive	26 (19.4%)	31 (29.2%)		2 (22.2%)
Negative				
Cirrhosis	100 (74.6%)	74 (69.8%)	0.407	9 (100.0%)
Yes	34 (25.4%)	32 (30.2%)		0 (0.0%)
No				
Alcohol	75 (56.0%)	57 (53.8%)	0.734	1 (11.1%)
consumption	59 (44.0%)	49 (46.2%)		8 (88.9%)
Yes				
No				
AFP	64 (47.8%)	39 (36.8%)	0.088	5 (55.6%)
≤20 ng/ml	70 (52.2%)	67 (63.2%)		4 (44.4%)
>20 ng/ml				
ALT	94 (70.1%)	60 (56.6%)	**0.030**	6 (66.7%)
≤40 U/L	40 (29.9%)	46 (43.4%)		3 (33.3%)
>40 U/L				
TBIL	87 (64.9%)	72 (67.9%)	0.626	5 (55.6%)
≤17.1umol/L	47 (35.1%)	34 (32.1%)		4 (44.4%)
>17.1umol/L				
ALB	11 (8.2%)	11 (10.4%)	0.563	1 (11.1%)
≤35 g/L	123 (91.8%)	95 (89.6%)		8 (88.9%)
>35 g/L				
PT%			0.189	
<75	9 (6.7%)	6 (5.7%)		1 (11.1%)
75-100	96 (71.6%)	66 (62.3%)		4 (44.4%)
>100	29 (21.6%)	34 (32.1%)		4 (44.4%)
Child-Pugh			0.377	
class	123 (91.8%)	93 (87.7%)		8 (88.9%)
A5	10 (7.5%)	10 (9.4%)		0 (0.0%)
A6	1 (0.7%)	3 (2.8%)		1 (11.1%)
B7				
Tumor size	89 (66.4%)	50 (47.2%)	**0.003**	5 (55.6%)
≤5 cm	45 (33.6%)	56 (52.8%)		4 (44.4%)
>5 cm				
No. of tumor	119 (88.8%)	86 (81.1%)	0.094	8 (88.9%)
Single	15 (11.2%)	20 (18.9%)		1 (11.1%)
Multiple				
Edmondson	104 (77.6%)	78 (73.6%)	0.469	5 (55.6%)
grades	30 (22.4%)	28 (26.4%)		4 (44.4%)
I-II				
III-IV				
Tumor capsule	115 (85.8%)	79 (74.5%)	**0.027**	3 (33.3%)
Present	19 (14.2%)	27 (25.5%)		6 (66.7%)
Absent				
MVI			0.385	
classification				
M0	77 (57.5%)	49 (46.2%)		2 (22.2%)
M1	37 (27.6%)	36 (34.0%)		4 (44.4%)
M2	17 (12.7%)	18 (17.0%)		3 (33.3%)
Unclear	3 (2.2%)	3 (2.8%)		0 (0.0%)
Extent of	88 (65.7%)	47 (44.3%)	**<0.001**	3 (33.3%)
resection	46 (34.3%)	59 (55.7%)		6 (66.7%)
Minor				
Major				
Operative time	172.4 ± 72.0	224.9 ± 99.0	**<0.001**	276.5 ± 83.6
Operative blood loss	276.2 ± 514.7	454.5 ± 608.7	**0.019**	210.0 ± 87.6
pTNM stage	64 (47.8%)	30 (28.3%)	**0.008**	1 (11.1%)
I	52 (38.8%)	48 (45.3%)		7 (77.8%)
II*	3 (2.2%)	7 (6.6%)		0 (0.0%)
III	15 (11.2%)	21 (19.8%)		1 (11.1%)
IVA				
Postoperative	29 (21.6%)	28 (26.4%)	0.446	5 (55.6%)
TACE	105 (78.4%)	78 (73.6%)		4 (44.4%)
Yes				
No				

Values in parentheses are percentages and P<0.05 was indicated by bold values.
HBs Ag, hepatitis B surface antigen; AFP, alpha-fetoprotein; ALT, alanine aminotransferase; TBIL, total bilirubin; ALB, albumin; PT, prothrombin time; MVI, microvascular invasion; pTNM stage, pathologic TNM stage; TACE, transcatheter arterial chemoembolization.
**5 cases that T stage (T1b or T2) was undefined because of unclear MVI status were belonged in category of T2 stage.*

5 cm *vs.* > 5 cm) (**Figure 4**). The 1-, 2-, 3-year RFS rates for patients receiving TACE were 69.7, 51.8, 44.7%, respectively, comparing to 68.9, 59.1, 51.7% accordingly in the no adjuvant TACE group (**Supplementary Figure 1**).

Overall Survival

The 1-, 2-, 3-year OS rates were 83.5, 65.6, 60.6% in the narrow-margin group, and 94.0, 89.5, 84.2% in the wide-margin group, respectively (P<0.001; **Figure 2B**). In the multivariable analysis, narrow margin was significantly associated with worse OS (wide *vs.* narrow, HR=0.518; 95% CI, 0.308–0.871, P=0.013). Other independent predictors include Child-Pugh class, ALT level, tumor capsule, and MVI status (**Table 4**). In the subgroup analysis based on MVI status (M0 *vs.* M1+M2) and tumor size (≤ 5 cm *vs.* > 5 cm), patients with narrow margin resection correlated with worse OS, regardless of MVI status (**Figure 5**) or tumor size (**Figure 6**). The 1-, 2-, 3-year OS rates for patients receiving TACE were 92.9, 89.3, 76.8%, respectively, comparing to 88.4, 75.9, 73.1% accordingly in the no adjuvant TACE group (**Supplementary Figure 1**).

Patterns of Recurrence for Positive Margin Cases With Postoperative Stereotactic Body Radiotherapy

Finally, nine patients who underwent postoperative SBRT after positive margin resection were included in this analysis. The postoperative radiotherapy was given to a total dose of 35Gy/5F to 50Gy/5F (median, 40Gy/5F). The median interval between operation and initiation of postoperative SBRT was 51 days. The incidence and pattern of recurrence have been detailed in **Table 2**.

TABLE 2 | Patterns of recurrence of the wide-margin, narrow-margin, and positive-margin plus stereotactic body radiotherapy (SBRT) groups.

Variable	Wide-margin group (N = 134)	Narrow-margin group (N = 106)	*P*-Value (Wide *vs.* Narrow)	Positive-margin plus SBRT (N = 9)
Total recurrence	59 (44.0%)	69 (65.1%)	**0.001**	2 (22.2%)
Type of recurrence				
Intrahepatic recurrence	54 (40.3%)	67 (63.2%)	0.321	2 (22.2%)
Extrahepatic recurrence	7 (5.2%)	10 (9.4%)	0.662	0 (0.0%)
Sites of intrahepatic recurrence				
Marginal recurrence	6 (4.5%)	22 (20.8%)	**0.003**	0 (0.0%)
Intrahepatic single-nodule	26 (19.4%)	13 (12.3%)	**0.002**	1 (11.1%)
Intrahepatic multiple-nodule	16 (11.9%)	34 (32.1%)*	**0.010**	1 (11.1%)
Unclear	6 (4.5%)	5 (4.7%)	0.556	0 (0.0%)
Time to recurrence				
Total recurrence				
~ 3 months (include 3)	11 (8.2%)	16 (15.1%)	0.530	0 (0.0%)
3~6 months	15 (11.2%)	30 (28.3%)	**0.033**	0 (0.0%)
6~9 months	20 (14.9%)	41 (38.7%)	**0.004**	2 (22.2%)
9~12 months	28 (20.9%)	46 (43.4%)	**0.028**	0 (0.0%)
Marginal recurrence				
~ 3 months (include 3)	7 (6.6%)	0 (0.0%)	**0.022**	0 (0.0%)
3~6 months	11 (10.4%)	1 (0.7%)	0.074	0 (0.0%)
6~9 months	13 (12.3%)	3 (2.2%)	0.164	0 (0.0%)
9~12 months	15 (14.2%)	3 (2.2%)	**0.033**	0 (0.0%)
Intrahepatic multiple-nodule				
~ 3 months (include 3)	10 (9.4%)	4 (3.0%)	0.252	0 (0.0%)
3~6 months	20 (18.9%)	6 (4.5%)	0.088	0 (0.0%)
6~9 months	25 (23.6%)	7 (5.2%)	0.057	1 (11.1%)
9~12 months	29 (27.4%)	9 (6.7%)	**0.010**	1 (11.1%)

**8 of them with concurrent marginal recurrence. P < 0.05 was indicated by bold values.*

Median follow-up period is 15.1 (range 6.8–38.6) months. During the follow-up periods, two patients (2/9, 22.2%) had documented tumor recurrence, with one patient (1/9, 11.1%) developed intrahepatic multiple-nodule recurrence at 7.9 months after surgery, and the other case had intrahepatic single-nodule recurrence far away from the resection margin at 7.5 months post-operation.

Patients with positive margin resection plus SBRT or wide-margin resection showed a significantly lower incidence of total recurrence than that with narrow-margin resection (positive plus SBRT *vs.* wide *vs.* narrow: 22.2 *vs.* 44.0 *vs.* 65.1%). Regarding the pattern of marginal recurrence, a large numerical difference was found among the three groups. Patients with positive margin resection plus SBRT or wide-margin resection experienced a significantly lower rates of marginal recurrence than that with narrow-margin resection (positive plus SBRT *vs.* wide *vs.* narrow: 0.0 *vs.* 4.5 *vs.* 20.8%). With regard to the pattern of intrahepatic multiple-nodule recurrence, patients with positive margin resection plus SBRT or wide-margin resection showed a significantly lower rate of recurrence than that with narrow margin resection (positive plus SBRT *vs.* wide *vs.* narrow: 11.1 *vs.* 11.9 *vs.* 32.1%).

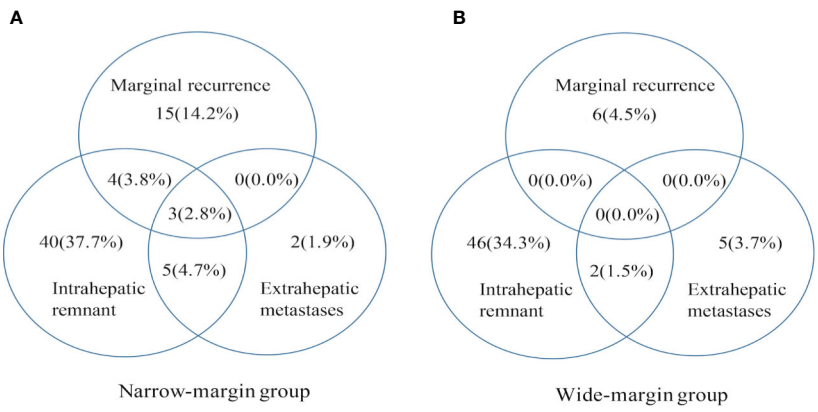

FIGURE 1 | Patterns of initial recurrence for hepatocellular carcinoma (HCC) patients in narrow-margin and wide-margin groups. Patterns of initial recurrence stratified by marginal recurrence, intrahepatic remnant recurrence, and extrahepatic metastases. Values in parentheses are percentages. **(A)** Patterns of initial recurrence in the narrow-margin group. **(B)** Patterns of initial recurrence in the wide-margin group.

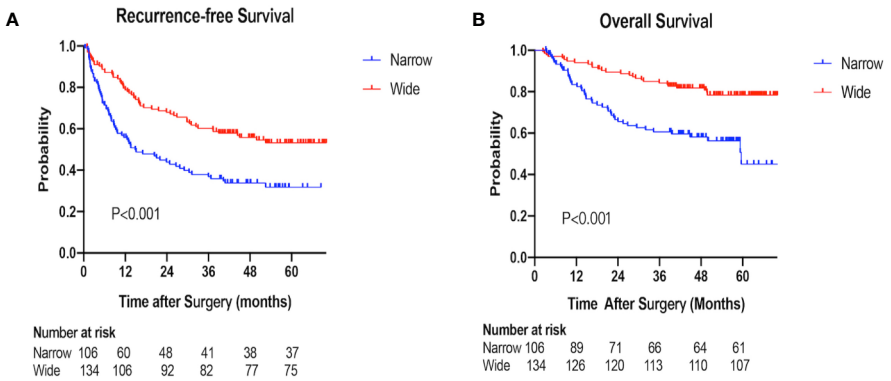

FIGURE 2 | Recurrence-free survival (RFS) and overall survival (OS) of the narrow-margin and wide-margin groups. **(A)** Recurrence-free survival for patients with narrow and wide margin resection. **(B)** Overall survival for patients with narrow and wide margin resection.

TABLE 3 | Prognostic factors of recurrence-free-survival (RFS) for patients with narrow and wide margin resection.

Variable	Univariate analysis		Multivariate analysis	
	HR (95% CI)	*P*-Value	HR (95% CI)	*P*-Value
Surgical margin (narrow/wide)	0.504 (0.356–0.715)	**<0.001**	0.608 (0.414–0.893)	**0.011**
Age (≤60/>60 years old)	0.850 (0.593–1.217)	0.374		
Gender (male/female)	0.724 (0.416–1.261)	0.254		
HBs Ag (negative/positive)	1.917 (1.200–3.062)	**0.006**	2.159 (1.302–3.580)	**0.003**
Cirrhosis (no/yes)	1.070 (0.726–1.579)	0.732		
Alcohol consumption (no/yes)	1.012 (0.714–1.435)	0.946		
AFP (≤20/>20ng/ml)	1.640 (1.144–2.351)	**0.007**	1.413 (0.968–2.063)	0.073
ALT (≤40/>40U/L)	1.904 (1.341–2.702)	**<0.001**	1.422 (0.973–2.076)	0.069
Child-Pugh class		0.166		
A5	Reference			
A6	0.876 (0.444–1.725)	0.701		
A7	2.970 (0.930–9.481)	0.066		
Tumor size (≤5/>5cm)	1.185 (0.835–1.683)	0.341	0.845 (0.570–1.253)	0.402
No. of tumor (single/multiple)	2.330 (1.535–3.536)	**<0.001**	1.281 (0.757–2.167)	0.356
Edmondson grades (I–II/III–IV)	1.287 (0.872–1.900)	0.204		
Tumor capsule (absent/present)	0.394 (0.267–0.581)	**<0.001**	0.447 (0.290–0.691)	**<0.001**
MVI classification		**<0.001**		**0.003**
M0	Reference		Reference	
M1	1.800 (1.214–2.671)	**0.003**	1.138 (0.693–1.868)	0.611
M2	3.364 (2.102–5.381)	**<0.001**	2.394 (1.382–4.147)	**0.002**
Unclear	0.336 (0.047–2.429)	0.280	0.233 (0.031–1.763)	0.158
Extent of liver resection (minor/major)	2.005 (1.415–2.841)	**<0.001**	1.586 (1.070–2.351)	**0.022**
pTNM stage		**<0.001**		0.560
I	Reference		Reference	
II	2.451 (1.611–3.729)	**<0.001**	1.487 (0.862–2.565)	0.154
III	4.978 (2.378–10.420)	**<0.001**	1.475 (0.510–4.264)	0.473
IVA	2.52 3(1.485–4.288)	**0.001**	1.326 (0.691–2.547)	0.396
Postoperative TACE (no/yes)	1.139 (0.769–1.686)	0.517		

Surgical resection, tumor number, tumor size, and variables with p value <0.01 in the univariable Cox analyses were retained for the multivariable Cox analysis. The foreparts of the parentheses were set as the reference groups in the univariable and multivariable Cox analysis.
HBs Ag, hepatitis B surface antigen; AFP, alpha-fetoprotein; ALT, alanine aminotransferase; MVI, microvascular invasion; pTNM stage, pathologic TNM stage; TACE, transcatheter arterial chemoembolization. P < 0.05 was indicated by bold values.

The time interval to recurrence significantly differed among the three groups. Compared with patients with positive margin plus SBRT and with wide margin resection, those with narrow margin resection had a higher rate of recurrence within 12 months after surgery (positive plus SBRT *vs.* wide *vs.* narrow: 22.2 *vs.* 20.9 *vs.* 43.4%).

The toxicity associated with postoperative SBRT is summarized in **Table 5**. Grade 1 myeloid suppression was the most common toxicity encountered during SBRT, followed by grade 1 liver enzyme (44.4%) and bilirubin (33.3%) elevation. One (11.1%) patient combined cirrhosis history experienced

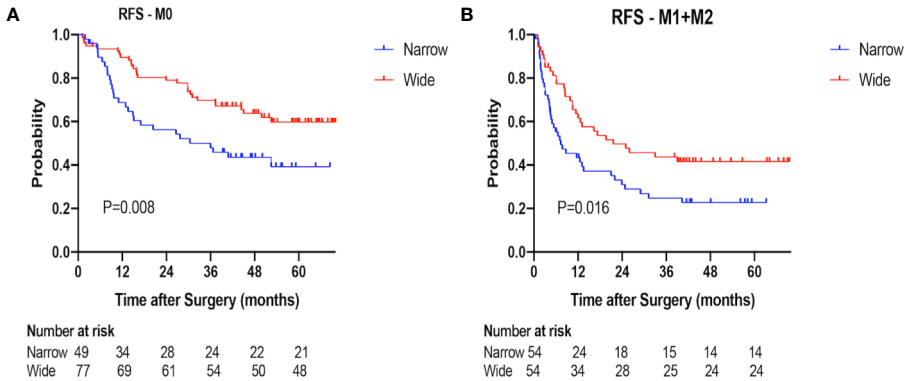

FIGURE 3 | Recurrence-free survival (RFS) of the narrow-margin and wide-margin groups stratified based on microvascular invasion (MVI) status. **(A)** Recurrence-free survival in the subgroup of M0. **(B)** Recurrence-free survival in the subgroup of M1+M2.

grade 2 thrombocytopenia. No grade 3 and 4 toxicities were seen. No radiation induced liver disease was encountered.

DISCUSSION

This study analyzed the association of surgical margin with recurrence pattern. Higher rate of recurrence (especially the pattern of marginal recurrence) and lower overall survival were found in HCC with narrow margin resection compared to that with wide margin resection. The addition of SBRT to patients with positive surgical margin reduced the recurrences, particularly the pattern of marginal recurrence. Our findings implicate the potential feasibility of postoperative SBRT for patients with narrow margin resection.

Narrow margin resection may be the most appropriate procedure for HCC adjacent to major vessels because the premise for survival is the conservation of more normal liver parenchyma (17). Unfortunately, narrow margin resection has been reported to contribute to poor survival outcomes due to the high frequency of recurrence and the clinical significance remains controversial (9, 11, 26–29). Shi et al. investigated the influence of the width of resection margin on postoperative recurrence and found that narrow margin group had significantly higher rate of recurrence than wide margin group (52.4 *vs.* 36.5%, P=0.037), and wide margin resection efficaciously decrease recurrence and improve survival (11). Chau et al. also showed a similar results (narrow and wide: 61.3 *vs.* 36.5%) (29). However, Poon et al. reported that the width of margin did not influence the postoperative recurrence rates (narrow and wide: 64.0 *vs.* 59.4%, P=0.943) (9). It is worth noting that these controversial results might be due to the heterogeneity of tumor characteristics and surgery procedures, such as cirrhosis (Shi's and Poon's: 80.5 *vs.* 46.2%), resection extent ≥3 segments (Shi's and Poon's: 10.1 *vs.* 65.3%), and preoperative transfusion (Shi's and Poon's: 26.6 *vs.* 58.0%). Our results were consistent with the former, showing that HCC patients with narrow margin resection had higher rate of recurrence compared to those with wide margin resection (P=0.001), and multivariable analysis showed that narrow margin was significantly associated with worse RFS and OS, indicating that narrow margin resection alone is insufficient for tumor eradication and adjuvant therapy

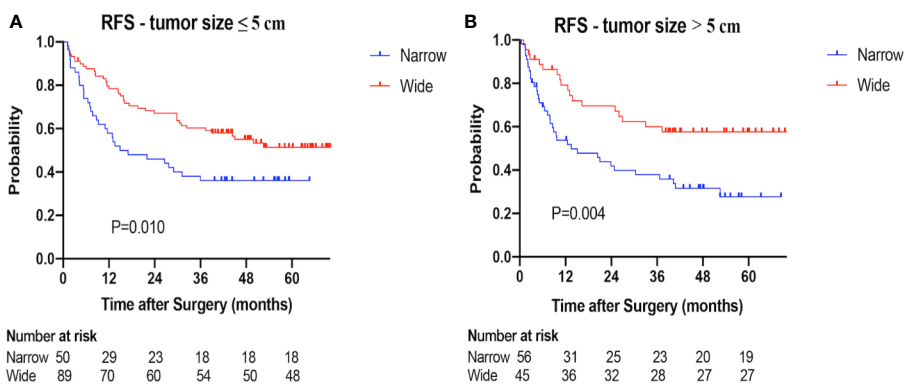

FIGURE 4 | Recurrence-free survival (RFS) of the narrow-margin and wide-margin groups stratified based on tumor size. **(A)** Recurrence-free survival in the subgroup of tumor size ≤ 5 cm. **(B)** Recurrence-free survival in the subgroup of tumor size > 5 cm.

TABLE 4 | Prognostic factors of overall survival (OS) for patients with narrow and wide margin resection.

Variable	Univariate analysis		Multivariate analysis	
	HR (95% CI)	*P*-Value	HR (95% CI)	*P*-Value
Surgical margin (narrow/wide)	0.366 (0.226–0.591)	**<0.001**	0.518 (0.308–0.871)	**0.013**
Age (≤60/>60 years old)	0.960 (0.598–1.542)	0.866		
Gender (male/female)	0.543 (0.235–1.252)	0.152		
HBs Ag (negative/positive)	1.340 (0.747–2.402)	0.326		
Cirrhosis (no/yes)	1.091 (0.646–1.843)	0.744		
Alcohol consumption (no/yes)	0.923 (0.580–1.467)	0.734		
AFP (≤20/>20ng/ml)	2.042 (1.237–3.374)	**0.005**	1.611 (0.949–2.735)	0.077
ALT (≤40/>40U/L)	2.374 (1.494–3.771)	**<0.001**	1.941 (1.190–3.168)	**0.008**
Child-Pugh class		**<0.001**		**0.017**
A5	Reference		Reference	
A6	1.966 (0.975–3.966)	0.059	1.898 (0.882–4.082)	0.101
A7	8.140 (2.911–22.760)	**<0.001**	4.150 (1.355–12.708)	0.013
Tumor size (≤5/>5cm)	1.603 (1.010–2.545)	**0.045**	0.897 (0.531–1.514)	0.683
No. of tumor (single/multiple)	1.985 (1.138–3.462)	**0.016**	0.856 (0.414–1.771)	0.675
Edmondson grades (I–II/III–IV)	1.616 (0.984–2.654)	0.058	1.335 (0.765–2.332)	0.309
Tumor capsule (absent/present)	0.325 (0.201–0.527)	**<0.001**	0.421 (0.244–0.725)	**0.002**
MVI classification		**<0.001**		**<0.001**
M0	Reference		Reference	
M1	2.437 (1.373–4.325)	**0.002**	1.269 (0.633–2.544)	0.501
M2	7.194 (4.003–12.929)	**<0.001**	5.031 (2.510–10.085)	**<0.001**
Unclear	1.048 (0.141–7.784)	0.963	0.988 (0.123–7.929)	0.991
Extent of liver resection (minor/major)	2.440 (1.522–3.912)	**<0.001**	1.437 (0.839–2.462)	0.187
pTNM stage		**<0.001**		0.193
I	Reference		Reference	
II	3.743 (1.955–7.167)	**<0.001**	1.945 (0.874–4.326)	0.103
III	12.758 (5.000–32.555)	**<0.001**	4.547 (1.117–18.499)	**0.034**
IVA	4.454 (2.081–9.529)	**<0.001**	1.785 (0.722–4.416)	0.210
Postoperative TACE (no/yes)	0.921 (0.535–1.588)	0.768		

Surgical resection, tumor number, tumor size, and variables with p value <0.01 in the univariable Cox analyses were retained for the multivariable Cox analysis. The foreparts of the parentheses were set as the reference groups in the univariable and multivariable Cox analysis.

HBs Ag, hepatitis B surface antigen; AFP, alpha-fetoprotein; ALT, alanine aminotransferase; MVI, microvascular invasion; pTNM stage, pathologic TNM stage; TACE, transcatheter arterial chemoembolization. P < 0.05 was indicated by bold values.

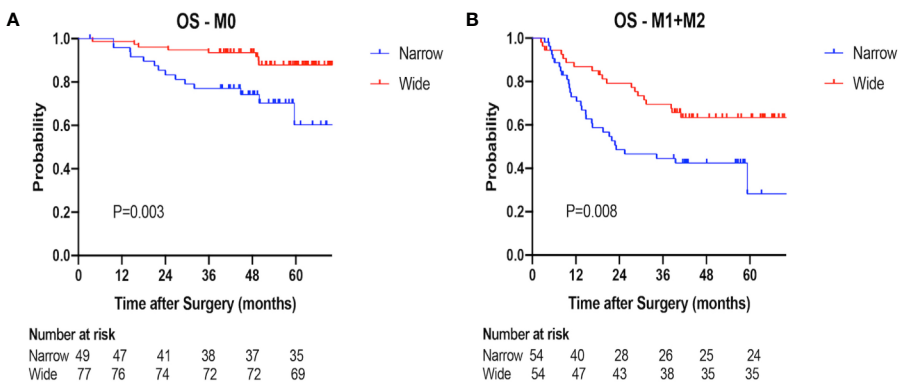

FIGURE 5 | Overall survival (OS) of the narrow-margin and wide-margin groups stratified based on MVI status. **(A)** Overall survival in the subgroup of M0. **(B)** Overall survival in the subgroup of M1+M2.

is imperative to reduce the risk of recurrence. Identifying the failure patterns help to further guide appropriate management of postoperative therapy.

In our study, the intrahepatic recurrence patterns were defined as marginal, intrahepatic single-nodule and multiple-nodule recurrences. We found that patients with narrow margin resection experienced a higher marginal recurrence, as well as intrahepatic multiple nodules recurrence. The findings were consistent with previous reports (11, 29). For example, in the study conducted by Shi et al. all marginal recurrences were observed in narrow margin

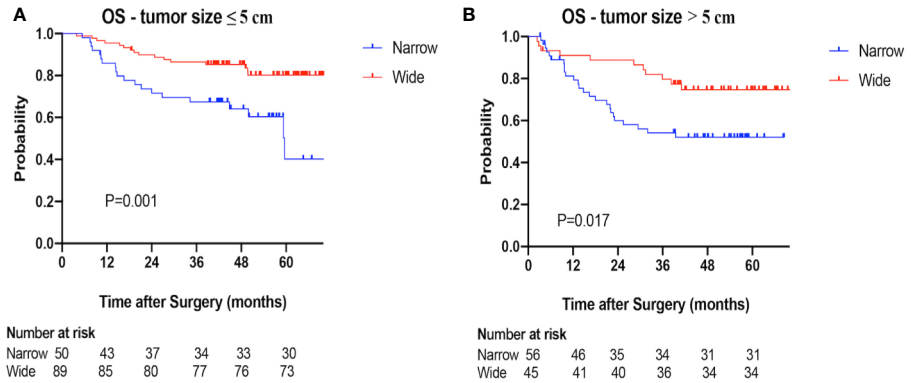

FIGURE 6 | Overall survival (OS) of the narrow-margin and wide-margin groups stratified based on tumor size. **(A)** Overall survival in the subgroup of tumor size ≤ 5cm. **(B)** Overall survival in the subgroup of tumor size >5cm.

TABLE 5 | Toxicity from stereotactic body radiotherapy (SBRT) in patients with positive margin.

Toxicity grade (CTCAE)	0	1	2	3	4
Myeloid suppression					
Leukopenia	4 (44.4%)	5 (55.6%)	0 (0%)	0 (0%)	0 (0%)
Lymphopenia	8 (88.9%)	1 (11.1%)	0 (0%)	0 (0%)	0 ()%)
Thrombocytopenia	7 (77.8%)	1 (11.1%)	1 (11.1%)	0 (0%)	0 (0%)
Constitutional symptoms					
Fatigue	7 (77.8%)	2 (22.2%)	0 (0%)	0 (0%)	0 (0%)
Fever (tympanic)	9 (100.0%)	0 (0%)	0 (0%)	0 (0%)	0 (0%)
Insomnia	9 (100.0%)	0 (0%)	0 (0%)	0 (0%)	0 (0%)
Abdominal pain	9 (100.0%)	0 (0%)	0 (0%)	0 (0%)	0 (0%)
Gastrointestinal					
Anorexia	9 (100.0%)	0 (0%)	0 (0%)	0 (0%)	0 (0%)
Diarrhea	9 (100.0%)	0 (0%)	0 (0%)	0 (0%)	0 (0%)
Constipation	9 (100.0%)	0 (0%)	0 (0%)	0 (0%)	0 (0%)
Nausea	8 (88.9%)	1 (11.1%)	0 (0%)	0 (0%)	0 (0%)
Vomiting	8 (88.9%)	1 (11.1%)	0 (0%)	0 (0%)	0 (0%)
Metabolic/laboratory					
Albumin	9 (100.0%)	0 (0%)	0 (0%)	0 (0%)	0 (0%)
Liver transaminase (ALT or AST)	5 (55.6%)	4 (44.4%)	0 (0%)	0 (0%)	0 (0%)
Bilirubin	6 (66.7%)	3 (33.3%)	0 (0%)	0 (0%)	0 (0%)
Radiation induced liver disease (RILD)	9 (100.0%)	0 (0%)	0 (0%)	0 (0%)	0 (0%)

group and multinodular recurrence was also significantly higher than that in wide margin group (P=0.018) (11). Taken together, postoperative marginal recurrence for patients with narrow margin seems to be common, about 21% of the narrow-margin HCC patients recur within 1cm from the surgical margin in our study, suggesting that adjuvant local therapy might improve the local-regional control.

Higher intrahepatic multiple-nodule recurrences were also seen in patients with narrow margin, and associated with higher marginal recurrence. For multiple-nodule recurrences, it is difficult to identify which lesion occurred first. According to the previous study, micro-metastasis was commonly remnant from resection margin within 1 cm, surgical margin recurrence might occur first, then spread to the whole residual liver *via* portal vein branches (4, 6, 30, 31). Therefore, we cautiously speculate that marginal recurrence may be one of driver factors of intrahepatic multiple recurrence, and multifocal recurrence might be prevented or mitigated if liver marginal recurrence could be well controlled by adjuvant local therapy. However, margin status alone is an insufficient explanation as to why intrahepatic other regions yields recurrence located over 1 cm from the area of resection, inherent imbalance in the tumor characteristics, such as microvascular invasion status, were also related to the recurrence pattern (32).

Our multivariate analysis showed that MVI were negatively related to RFS and OS. Previous studies reached similar conclusion that MVI was closely related to early recurrence and dismal prognosis (27, 30, 33, 34). Additionally, absence of tumor capsule was significantly correlated to poorer long-term outcomes, which was in line with the previous studies (8, 35–38). Therefore, adjuvant therapy may be useful for those with high risk factors.

We also evaluated the influence of postoperative SBRT on the incidence and pattern of recurrence. The rate of marginal and

multiple-nodule recurrences in the group of positive-margin plus SBRT was comparable to that of wide-margin group, and better than that of narrow-margin group, suggesting that the addition of postoperative local radiotherapy could provide an improved local control and mitigate the recurrence risk due to insufficient surgical margin. In spite of the small number of cases, our data does highlight the efficacy of postoperative SBRT in reducing the recurrence risk for patients with positive margin, and presumably a potential effect on narrow margin resection.

Considering the pattern of marginal recurrence itself occurs frequently and it may, subsequently, induce the occurrence of intrahepatic multiple-nodule in patients with narrow margin resection, postoperative local radiotherapy may provide a favorable outcome through its role of local-regional control. To date, with the improvement of radiotherapy techniques, such as intensity modulated radiotherapy (IMRT) and SBRT, a significantly reduced radiation-induced toxicity and increased radiotolerance of normal tissue were obtained (39, 40). A few prospective studies have been carried out to demonstrate the feasibility and advantages of adjuvant radiotherapy (32, 41, 42). For instance, Wang et al. reported that the efficacy of receiving IMRT following narrow margin resection was comparable to that of wide margin hepatectomy and superior to those of narrow margin resection alone, and none of the patients receiving IMRT developed radiation-induced liver disease (42). Yu et al. revealed that patients who underwent three-dimensional conformal radiotherapy following narrow margin resection yielded recurrence-free survival outcomes significantly superior to those of narrow margin resection alone, in patients with HCCs smaller than 5cm (41). Additionally, one clinical trial showed that for HCC patients with MVI, adjuvant three-dimensional conformal or IMRT could result in better survival outcomes than TACE or conservative therapy following narrow margin hepatectomy, considering radiotherapy could eliminate residual micro-metastasis-foci in the remnant liver (32). However, there is a lack of exploration for the efficacy of adjuvant SBRT. SBRT has shown encouraging rates of local control for HCC (43). Compared with standard fractionation radiation, SBRT can achieve more precise delivery of high-dose radiation beams to the lesion, obtaining a much smaller target volume. Meanwhile, it could be finished in a short period which can bring more convenience to patients (25, 40). In our study, the total recurrence rate in the patients with positive-margin plus SBRT (2/9, 22.2%) was satisfied, comparing by patients with negative-margin resection alone (128/240, 53.3%). The marginal recurrence rate with SBRT was relatively lower. Given these compelling results, postoperative radiotherapy may represent an innovative strategy to optimize the amelioration of tumor recurrence. A further large-sample clinical data is warranted to demonstrate the benefits of adjuvant radiotherapy in patients with narrow margin resection, considering the small sample size of above-mentioned studies.

In summary, we found that HCC patients following narrow margin hepatectomy had a higher recurrence rate and poorer prognosis, with 20.8% patients developed marginal recurrence. Postoperative SBRT treatment for patients with positive margin showed low recurrence rate and no marginal recurrence was found. There is a limitation of this study with small patient samples received postoperative SBRT and short patient follow-up. Therefore, high-quality multi-center prospective studies are needed to further confirm the efficacy of adjuvant radiotherapy.

CONCLUSION

Patients with narrow margin were associated with higher recurrence (especially for the pattern of marginal recurrence) and worse survival outcomes than those with wide resection margin. Postoperative local treatment, such as radiotherapy, might bring potential benefit for these patients.

DATA AVAILABILITY STATEMENT

The raw data supporting the conclusions of this article will be made available by the authors, without undue reservation.

ETHICS STATEMENT

The studies involving human participants were reviewed and approved by the Institutional Review Board of Zhejiang University School of Medicine. The patients/participants provided their written informed consent to participate in this study.

AUTHOR CONTRIBUTIONS

LL and YS wrote the article and analyzed the data and statistics. QY and YG analyzed the data and statistics. LZ and XZ reviewed and edited the article. RY and JL were responsible for image evaluation and clinical data analysis. QW and SW designed, revised, and supervised the writing and concept of the article. All authors read and approved the final manuscript. All authors contributed to the article and approved the submitted version.

FUNDING

This work was supported by the National Natural Science Foundation of China (No. 81572952).

SUPPLEMENTARY MATERIAL

The Supplementary Material for this article can be found online at: https://www.frontiersin.org/articles/10.3389/fonc.2020.610636/full#supplementary-material

SUPPLEMENTARY FIGURE 1 | Recurrence-free survival (RFS) and Overall survival (OS) of patients with or without postoperative TACE. **(A)** Recurrence-free survival for patients with TACE and without TACE. **(B)** Overall survival for patients with TACE and without TACE.

REFERENCES

1. Bray F, Ferlay J, Soerjomataram I, Siegel RL, Torre LA, Jemal A. Global cancer statistics 2018: GLOBOCAN estimates of incidence and mortality worldwide for 36 cancers in 185 countries. *CA Cancer J Clin* (2018) 68(6):394–424. doi: 10.3322/caac.21492
2. Chen W, Zheng R, Baade PD, Zhang S, Zeng H, Bray F, et al. Cancer statistics in China, 2015. *CA Cancer J Clin* (2016) 66(2):115–32. doi: 10.3322/caac.21338
3. Hartke J, Johnson M, Ghabril M. The diagnosis and treatment of hepatocellular carcinoma. *Semin Diagn Pathol* (2017) 34(2):153–9. doi: 10.1053/j.semdp.2016.12.011
4. Shindoh J, Hasegawa K, Inoue Y, Ishizawa T, Nagata R, Aoki T, et al. Risk factors of post-operative recurrence and adequate surgical approach to improve long-term outcomes of hepatocellular carcinoma. *HPB (Oxford)* (2013) 15(1):31–9. doi: 10.1111/j.1477-2574.2012.00552.x
5. Tung-Ping Poon R, Fan ST, Wong J. Risk factors, prevention, and management of postoperative recurrence after resection of hepatocellular carcinoma. *Ann Surg* (2000) 232(1):10–24. doi: 10.1097/00000658-200007000-00003
6. Kumar AM, Fredman ET, Coppa C, El-Gazzaz G, Aucejo FN, Abdel-Wahab M. Patterns of cancer recurrence in localized resected hepatocellular carcinoma. *Hepatobiliary Pancreat Dis Int* (2015) 14(3):269–75. doi: 10.1016/S1499-3872(15)60382-4
7. Hasegawa K, et al. Prognostic impact of anatomic resection for hepatocellular carcinoma. *Ann Surg* (2005) 242(2):252–9. doi: 10.1097/01.sla.0000171307.37401.db
8. Lee KT, et al. Is wider surgical margin justified for better clinical outcomes in patients with resectable hepatocellular carcinoma? *J Formos Med Assoc* (2012) 111(3):160–70. doi: 10.1016/j.jfma.2011.02.002
9. Poon RT, et al. Significance of resection margin in hepatectomy for hepatocellular carcinoma: A critical reappraisal. *Ann Surg* (2000) 231(4):544–51. doi: 10.1097/00000658-200004000-00014
10. Predictive factors for long term prognosis after partial hepatectomy for patients with hepatocellular carcinoma in Japan. The Liver Cancer Study Group of Japan. *Cancer* (1994) 74(10):2772–80. doi: 10.1002/1097-0142(19941115)74:10<2772::AID-CNCR2820741006>3.0.CO;2-V
11. Shi M, et al. Partial hepatectomy with wide versus narrow resection margin for solitary hepatocellular carcinoma: a prospective randomized trial. *Ann Surg* (2007) 245(1):36–43. doi: 10.1097/01.sla.0000231758.07868.71
12. Hu W, et al. Relationship of different surgical margins with recurrence-free survival in patients with hepatocellular carcinoma. *Int J Clin Exp Pathol* (2015) 8(3):3404–9.
13. Regimbeau JM, et al. Extent of liver resection influences the outcome in patients with cirrhosis and small hepatocellular carcinoma. *Surgery* (2002) 131(3):311–7. doi: 10.1067/msy.2002.121892
14. Lise M, et al. Prognostic factors affecting long term outcome after liver resection for hepatocellular carcinoma: results in a series of 100 Italian patients. *Cancer* (1998) 82(6):1028–36. doi: 10.1002/(SICI)1097-0142(19980315)82:6<1028::AID-CNCR4>3.0.CO;2-A
15. Nara S, et al. Prognostic impact of marginal resection for patients with solitary hepatocellular carcinoma: evidence from 570 hepatectomies. *Surgery* (2012) 151(4):526–36. doi: 10.1016/j.surg.2011.12.002
16. Stratopoulos C, et al. Central hepatectomy: the golden mean for treating central liver tumors? *Surg Oncol* (2007) 16(2):99–106. doi: 10.1016/j.suronc.2007.05.002
17. Cheng CH, et al. Surgical resection of centrally located large hepatocellular carcinoma. *Chang Gung Med J* (2012) 35(2):178–91. doi: 10.4103/2319-4170.106153
18. Matsui Y, et al. Postoperative outcomes in patients with hepatocellular carcinomas resected with exposure of the tumor surface: clinical role of the no-margin resection. *Arch Surg* (2007) 142(7):596–602; discussion 603. doi: 10.1001/archsurg.142.7.596
19. Miao XY, et al. Null-margin mesohepatectomy for centrally located hepatocellular carcinoma in cirrhotic patients. *Hepatogastroenterology* (2011) 58(106):575–82.
20. Du M, et al. Microvascular invasion (MVI) is a poorer prognostic predictor for small hepatocellular carcinoma. *BMC Cancer* (2014) 14:38. doi: 10.1186/1471-2407-14-38
21. Cong WM, et al. Practice guidelines for the pathological diagnosis of primary liver cancer: 2015 update. *World J Gastroenterol* (2016) 22(42):9279–87. doi: 10.3748/wjg.v22.i42.9279
22. Kamarajah SK, et al. Critical evaluation of the American Joint Commission on Cancer (AJCC) 8th edition staging system for patients with Hepatocellular Carcinoma (HCC): A Surveillance, Epidemiology, End Results (SEER) analysis. *J Surg Oncol* (2018) 117(4):644–50. doi: 10.1002/jso.24908
23. Jeng KS, et al. Is less than 5 mm as the narrowest surgical margin width in central resections of hepatocellular carcinoma justified? *Am J Surg* (2013) 206(1):64–71. doi: 10.1016/j.amjsurg.2012.06.010
24. Lai EC, et al. The pathological basis of resection margin for hepatocellular carcinoma. *World J Surg* (1993) 17(6):786–90; discussion 791. doi: 10.1007/BF01659097
25. Shui Y, et al. Stereotactic body radiotherapy based treatment for hepatocellular carcinoma with extensive portal vein tumor thrombosis. *Radiat Oncol* (2018) 13(1):188. doi: 10.1186/s13014-018-1136-5
26. Shi M, et al. Micrometastases of solitary hepatocellular carcinoma and appropriate resection margin. *World J Surg* (2004) 28(4):376–81. doi: 10.1007/s00268-003-7308-x
27. Hirokawa F, et al. Outcomes and predictors of microvascular invasion of solitary hepatocellular carcinoma. *Hepatol Res* (2014) 44(8):846–53. doi: 10.1111/hepr.12196
28. Nakashima Y, et al. Portal vein invasion and intrahepatic micrometastasis in small hepatocellular carcinoma by gross type. *Hepatol Res* (2003) 26(2):142–7. doi: 10.1016/S1386-6346(03)00007-X
29. Chau GY, et al. Prognostic significance of surgical margin in hepatocellular carcinoma resection: an analysis of 165 Childs' A patients. *J Surg Oncol* (1997) 66(2):122–6. doi: 10.1002/(SICI)1096-9098(199710)66:2<122::AID-JSO9>3.0.CO;2-F
30. Zhou XP, Quan ZW, Cong WM, Yang N, Zhang HB, Zhang SH, et al. Micrometastasis in surrounding liver and the minimal length of resection margin of primary liver cancer. *World J Gastroenterol* (2007) 13(33):4498–503. doi: 10.3748/wjg.v13.i33.4498
31. Fidler IJ. The pathogenesis of cancer metastasis: the 'seed and soil' hypothesis revisited. *Nat Rev Cancer* (2003) 3(6):453–8. doi: 10.1038/nrc1098
32. Wang L, Wang W, Yao X, Rong W, Wu F, Chen B, et al. Postoperative adjuvant radiotherapy is associated with improved survival in hepatocellular carcinoma with microvascular invasion. *Oncotarget* (2017) 8(45):79971–81. doi: 10.18632/oncotarget.20402
33. Sumie S, et al. The significance of classifying microvascular invasion in patients with hepatocellular carcinoma. *Ann Surg Oncol* (2014) 21(3):1002–9. doi: 10.1245/s10434-013-3376-9
34. Roayaie S, et al. A system of classifying microvascular invasion to predict outcome after resection in patients with hepatocellular carcinoma. *Gastroenterology* (2009) 137(3):850–5. doi: 10.1053/j.gastro.2009.06.003
35. Ko S, et al. Significant influence of accompanying chronic hepatitis status on recurrence of hepatocellular carcinoma after hepatectomy. Result of multivariate analysis. *Ann Surg* (1996) 224(5):591–5. doi: 10.1097/00000658-199611000-00001
36. Nagasue N, et al. Incidence and factors associated with intrahepatic recurrence following resection of hepatocellular carcinoma. *Gastroenterology* (1993) 105(2):488–94. doi: 10.1016/0016-5085(93)90724-q
37. Dong S, et al. Effect of surgical margin in R0 hepatectomy on recurrence-free survival of patients with solitary hepatocellular carcinomas without macroscopic vascular invasion. *Medicine (Baltimore)* (2016) 95(44):e5251. doi: 10.1097/MD.0000000000005251
38. Cheng Z, et al. Risk factors and management for early and late intrahepatic recurrence of solitary hepatocellular carcinoma after curative resection. *HPB* (2015) 17(5):422–7. doi: 10.1111/hpb.12367
39. Mornex F, et al. Feasibility and efficacy of high-dose three-dimensional-conformal radiotherapy in cirrhotic patients with small-size hepatocellular carcinoma non-eligible for curative therapies–mature results of the French Phase II RTF-1 trial. *Int J Radiat Oncol Biol Phys* (2006) 66(4):1152–8. doi: 10.1016/j.ijrobp.2006.06.015
40. Baumann BC, et al. Stereotactic Body Radiation Therapy (SBRT) for Hepatocellular Carcinoma: High Rates of Local Control With Low Toxicity. *Am J Clin Oncol* (2018) 41(11):1118–24. doi: 10.1097/COC.0000000000000435

41. Yu W, et al. Adjuvant radiotherapy in centrally located hepatocellular carcinomas after hepatectomy with narrow margin (<1 cm): a prospective randomized study. *J Am Coll Surg* (2014) 218(3):381–92. doi: 10.1016/j.jamcollsurg.2013.11.030
42. Wang WH, et al. Survival benefit with IMRT following narrow-margin hepatectomy in patients with hepatocellular carcinoma close to major vessels. *Liver Int* (2015) 35(12):2603–10. doi: 10.1111/liv.12857
43. Wahl DR, Stenmark MH, Tao Y, Pollom EL, Caoili EM, Lawrence TS, et al. Outcomes After Stereotactic Body Radiotherapy or Radiofrequency Ablation for Hepatocellular Carcinoma. *J Clin Oncol* (2016) 34(5):452–9. doi: 10.1200/JCO.2015.61.4925

Conflict of Interest: The authors declare that the research was conducted in the absence of any commercial or financial relationships that could be construed as a potential conflict of interest.

frontiers in Oncology

ORIGINAL RESEARCH
published: 05 February 2021
doi: 10.3389/fonc.2020.616494

Stereotactic Body Radiotherapy for Lymph Node Oligometastases: Real-World Evidence From 90 Consecutive Patients

Petr Burkon[1,2], Iveta Selingerova[3], Marek Slavik[1,2], Petr Pospisil[1,2], Lukas Bobek[1], Libor Kominek[1], Pavel Osmera[4], Tomas Prochazka[1,2], Miroslav Vrzal[1], Tomas Kazda[1,2,5] and Pavel Slampa[1,2]*

[1] Department of Radiation Oncology, Masaryk Memorial Cancer Institute, Brno, Czechia, [2] Department of Radiation Oncology, Faculty of Medicine, Masaryk University, Brno, Czechia, [3] Research Center for Applied Molecular Oncology (RECAMO), Masaryk Memorial Cancer Institute, Brno, Czechia, [4] Department of Nuclear Medicine and PET Center, Masaryk Memorial Cancer Institute, Brno, Czechia, [5] Central European Institute of Technology, Masaryk University, Brno, Czechia

OPEN ACCESS

Edited by:
Rupesh Kotecha, Baptist Hospital of Miami, United States

Reviewed by:
Aditya Juloori, University of Chicago Medical Center, United States
Michael David Chuong, Baptist Health South Florida, United States

***Correspondence:**
Iveta Selingerova
iveta.selingerova@mou.cz

Specialty section:
This article was submitted to Radiation Oncology, a section of the journal Frontiers in Oncology

Received: *12 October 2020*
Accepted: *24 December 2020*
Published: *05 February 2021*

Citation:
Burkon P, Selingerova I, Slavik M, Pospisil P, Bobek L, Kominek L, Osmera P, Prochazka T, Vrzal M, Kazda T and Slampa P (2021) Stereotactic Body Radiotherapy for Lymph Node Oligometastases: Real-World Evidence From 90 Consecutive Patients. Front. Oncol. 10:616494. doi: 10.3389/fonc.2020.616494

Aims: To evaluate the efficacy and toxicity of extracranial stereotactic body radiotherapy (SBRT) in the treatment of oligometastatic lymph node involvement in the mediastinum, retroperitoneum, or pelvis, in a consecutive group of patients from real clinical practice outside clinical trials.

Methods: A retrospective analysis of 90 patients with a maximum of four oligometastases and various primary tumors (the most common being colorectal cancers). The endpoints were local control of treated metastases (LC), freedom from widespread dissemination (FFWD), progression-free survival (PFS), overall survival (OS), and freedom from systemic treatment (FFST). Acute and delayed toxicities were also evaluated.

Results: The median follow-up after SBRT was 34.9 months. The LC rate at three and five years was 68.4 and 56.3%, respectively. The observed median FFWD was 14.6 months, with a five-year FFWD rate of 33.7%. The median PFS was 9.4 months; the three-year PFS rate was 19.8%. The median FFST was 14.0 months; the five-year FFST rate was 23.5%. The OS rate at three and five years was 61.8 and 39.3%, respectively. Median OS was 53.1 months. The initial dissemination significantly shortened the time to relapse, death, or activation of systemic treatment—LC (HR 4.8, $p < 0.001$), FFWD (HR 2.8, $p = 0.001$), PFS (HR 2.1, $p = 0.011$), FFST (HR 2.4, $p = 0.005$), OS (HR 2.2, $p = 0.034$). Patients classified as having radioresistant tumors noticed significantly higher risk in terms of LC (HR 13.8, $p = 0.010$), FFWD (HR 3.1, $p = 0.006$), PFS (HR 3.5, $p < 0.001$), FFST (HR 3.2, $p = 0.003$). The multivariable analysis detected statistically significantly worse survival outcomes for initially disseminated patients as well as separately in groups divided according to radiosensitivity. No grade III or IV toxicity was reported.

Conclusion: Our study shows that targeted SBRT is a very effective and low toxic treatment for oligometastatic lymph node involvement. It can delay the indication of cytotoxic chemotherapy and thus improve and maintain patient quality of life. The aim of

further studies should focus on identifying patients who benefit most from SBRT, as well as the correct timing and dosage of SBRT in treatment strategy.

Keywords: stereotactic body radiotherapy, lymph node metastases, oligometastases, local therapy, radiotherapy

INTRODUCTION

Oligometastatic disease (OD), commonly defined as the presence of five or fewer metastatic lesions located in a limited number of organs (1), is now diagnosed more often due to the increased availability of positron emission tomography (PET/CT) scanning, which has become an integral part of the follow-up examination schedule. OD is supposedly an intermediate step between localized and disseminated cancer (2, 3). Local therapies such as surgery, radiofrequency ablation (RFA), cryoablation, or targeted radiotherapy have the potential to achieve local control (LC) with minimal toxicity. In many cases, it can be assumed that if the cancer is in the stage where pathogenic changes leading to dissemination have not yet been promoted, the local treatment of such involvement will lead to a long-term asymptomatic period, or even cure (2–5). Moreover, the possibility of delaying the administration of potentially toxic systemic therapy may significantly affect the quality of life of these patients (6).

Stereotactic body radiotherapy (SBRT) is a non-invasive method of treating localized tumor lesions by applying high doses of ionizing radiation in a small number of fractions. This is possible by employing specially equipped linear accelerators, modern immobilization devices, and imaging methods. SBRT is a short-term treatment that is very well tolerated, non-invasive, and does not require hospitalization or any complicated special preparation, all of which is important, especially in palliative treatment. Compared to standard radiotherapy (RT) techniques, SBRT allows for significantly higher doses to be delivered with less damage to surrounding healthy tissues due to its accuracy (7, 8).

Outstanding local control, improved overall survival, and minimal side effects rank SBRT among the standard treatment methods for localized non-small cell lung cancer and oligometastatic involvement of various sites and different primary tumors (9–11). Most evidence of the use of SBRT in the treatment of oligometastases is mainly related to liver and lung metastases with two-year LC of approximately 80%, the 2 to 3-year disease-free survival (DFS) of approximately 20%, and the 2 to 3-year overall survival (OS) of 25–40% (12–14).

Currently, there is limited data on the use of SBRT in the treatment of lymph node metastases. The number of fractions, and the dose per fraction depend on the location, size, and number of affected nodes. The dose is, of course, limited by the sensitivity of the surrounding structures. Because of their localization, the doses administered in stereotactic irradiation of the affected lymph nodes are lower than in the SBRT of lung or liver lesions. In addition, SBRT is often used repeatedly on a patient.

The aim of this retrospective study is to evaluate the efficacy and toxicity of SBRT in the treatment of 90 consecutive patients with oligometastatic involvement of lymph nodes located in the mediastinum, retroperitoneum, or pelvis. The study was approved by Ethical Board of Masaryk Memorial Cancer Institute (MMCI; approval No. 2020/2802/MOU).

PATIENTS AND METHODS

Patients

The patients screened for eligibility were those who indicated for SBRT in the Masaryk Memorial Cancer Institute between 2011 and 2019. Eligibility criteria included an age of ≥ 18 years, a Karnofsky index of ≥70%, and oligometastatic involvement of lymph nodes located in the mediastinum, retroperitoneum, or pelvis described on a diagnostic CT scan. Before initiating radiotherapy planning, the extent of involvement was confirmed in all patients by PET/CT examination. If additional lesions were found, the SBRT indication was re-evaluated and the patient not meeting the criteria of OD was referred to an oncologist to start systemic treatment. Patients who experienced new metastasis during follow-up after their primary SBRT oligometastases were not re-included in this analysis, even if this metastasis was indicated for another SBRT. In these cases, the evaluation of local control after initial SBRT, time to indicate systemic treatment, and overall survival continued.

Oligometastatic Disease Classification and Tumor Grouping

OD was classified according to the patient's history of metastatic disease before diagnosing the treated OD and according to relation to systemic therapy following the system currently presented by the European Society for Radiotherapy and Oncology and the European Organization for Research and Treatment of Cancer (15). The first-time diagnosis of OD is referred to as *de-novo OD*. The term *repeat OD* is used if the patient has a history of oligometastases before the treated OD. Any previous history of polymetastatic disease is referred to as *induced OD*. The development of OD during the systemic treatment-free interval is referred to as *oligorecurrence*. *Oligopersistent* OD is defined as a stable residual disease or partial response occurring during active systemic therapy. The term *oligoprogression* refers to growing or newly developed oligometastases during active systemic therapy. The used system for OD classification is summarized in **Supplementary Table 1**.

Primary tumors were divided into groups considering sensitivity to radiotherapy—*radiosensitive tumors* including breast, head and neck, gynecologic and prostatic (16, 17); *radioresistant tumors* including colorectal, renal, bladder, pancreas, melanoma, sarcoma, and lung tumors (18, 19). In

relation to the primary tumor diagnosis irrespective of future OD status, initial disease staging was considered. Initially localized tumors are referred to as *M0*, and patients with initially disseminated disease as *M1* under TNM classification.

Radiotherapy Technique

A stable, reproducible, and comfortable position of the patient during irradiation was ensured by vacuum-formable mattresses placed freely or in combination with a fixed frame on an linear accelerator couch (20). Until the end of 2015, the combination of vacuum mattresses with the Elekta rigid stereotactic frame (SBF, stereotactic body frame) (21) was used to prevent rotational shifts on the couch. Since January 2016, Frameless fixation of Orfit Industries and CIVCO Medical Solutions has been used in combination with the patient's position correction in six planes using the Varian PerfectPitch 6DoF couch.

Four-dimensional CT (4DCT) and respiratory gating (management of respiratory movements) during each fraction of irradiation using a linear accelerator with integrated imaging systems and a patient's respiratory control system were used during treatment planning and subsequent irradiation (22). Gross Tumor Volume (GTV) was defined in 2–3 mm planning CT scans as a lesion visible on CT or CT/MR or CT/PET fusion in all scan sets. This individual GTV from different breath phases was subsequently fused to create an ITV (Internal Target Volume) that included all of the breathing positions. In the case of significant breathing movements, the deep inspiration breath hold technique (DIBH) (23) was used. In this case, the GTV was drawn only at this stage (breath hold). To create the Planning Target Volume (PTV), the GTV was expanded by 3 to 5 mm in all directions (3 mm margin for very well localizable lesions, or when the movements of the tumor were minimal). The prescribed dose was subsequently optimized for this PTV (24).

The risk-adaptive concept was used to prescribe and calculate the radiotherapy dose, where the dose per fraction and the total dose are adjusted to the dose–volume histogram (DVH) of the risk structures (OAR) around the target PTV volume (25, 26). Because of the very close spatial proximity of radiosensitive gastrointestinal structures and spatial instability during repeated fractions (especially in the case of the small intestine), the dose 35 Gy in five fractions was most frequently prescribed, and the median biological equivalent dose (BED_{10Gy}) was 60 Gy (in the range of 48–112 Gy).

Dose calculation was carried out with the Eclipse planning system (Varian Medical Systems, Palo Alto, USA) with the Analytical Anisotropic Algorithm (AAA), enabling heterogeneity correction. Adequate coverage of the target volume was achieved when 98–100% of PTV was covered with 95–100% of the prescribed dose. The best possible treatment plan was also identified by evaluation of the gradient of the radiation dose to the surrounding tissue. This is assessed by 1) the ratio of the isodose volume for which the dose is prescribed to the volume of PTV, 2) the ratio of the volume of 50% isodose to the volume of PTV, and 3) the maximum dose at 2 cm from PTV in all directions. The prescribed dose was applied using the Varian Clinac iX and Varian TrueBeam STX ver. 2.5 linear accelerators equipped with Volumetric Modulated Arc Therapy (VMAT) technology (27) and flattening filter free (FFF) beams, *i.e.*, radiation beams without homogenizing filters. Patient pre-treatment correction was performed online on-board using cone-beam computed tomography (CBCT), which is an integral part of these linear accelerators (28). To ensure patient safety, each RT plan was dosimetrically verified by gamma analysis as part of the standard RT quality assurance process. A typical treatment plan is shown in **Figure 1** and dose constraints are listed in **Supplementary Table 2**.

Follow-Up, Toxicity, and Effectivity

Patient follow-up during and after SBRT was based on established standards of care in our institution. Follow-up consists of imaging, clinical examination, blood tests, and supplementary examinations according to the irradiated site. The effectiveness of SBRT treatment was monitored in all patients using PET/CT to ensure an accurate comparison with baseline data. If the PET/CT findings were repeatedly negative, more economical contrast computed tomography for the next examination was allowed. The follow-up schedule is as follows: in the first two years after 3–4 months, in the next three years every six months, and then once a year.

Progressive disease was defined according to EORTC-RECIST criteria (30, 31) as a new lesion in the irradiated area or as an increase of ≥20% from the baseline with significant avidity in PET examination compared to threshold activity in the liver. Unclear findings led to the indication of early PET/CT control, biopsy, or surgery. Both acute and late post-radiation changes were evaluated according to the National Cancer Institute's Common Toxicity Criteria for Adverse Events scale (CTCAE). Acute toxicity occurs during treatment or within the following 90 days. Toxicity evaluation was based on clinical examination and laboratory or imaging data.

Statistical Analysis and Endpoint Definition

Time-to-event endpoints were outcomes in terms of local control of treated metastases (LC), freedom from widespread dissemination (FFWD), progression-free survival (PFS), overall survival (OS), and freedom from systemic treatment (FFST). All cited events were observed from the date of SBRT termination. LC was determined as the time to progression or recurrence within the PTV. FFWD was defined as the time to distant progression, not amenable to resection or locally ablative therapy. PFS was determined as the time to progression (including local, regional, or distant progression) or death from any cause. OS was defined as the time to death from any cause. FFST was considered as the time to activation of systemic therapy. Patients without the observed event were censored at the date of the last appropriate visit.

Patient and treatment characteristics were described using standard summary statistics, *i.e.*, median and interquartile range (IQR) for continuous variables and frequencies and proportions for categorical variables. SBRT characteristics in patient groups were compared using Fisher's exact test, the chi-squared test, or the Mann–Whitney test, as appropriate. Survival probabilities were calculated using the Kaplan–Meier method. Survival curves

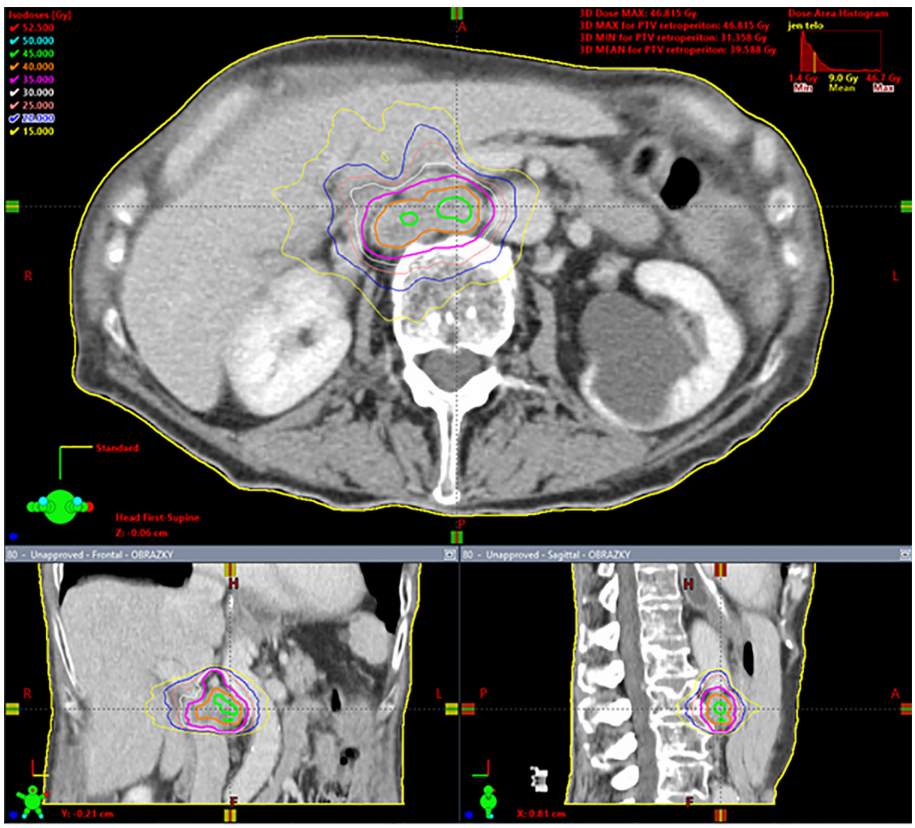

FIGURE 1 | Spinocellular carcinoma of the esophagus in a 63 year-old woman, solitary metastasis in the retroperitoneal lymph node, 35 Gy in five fractions, dose prescription at 80% isodose, PTV = 29.6 cm3, Dmin = 31.4 Gy, Dnear min = 35 Gy, Dmean in PTV = 39.6 Gy, Dnear max = 45.5 Gy, Dmax = 46.8 Gy. Gy, Gray; PTV, planning target volume; Dmin, minimum dose in the PTV; Dnear min, near-minimum dose in the PTV; Dmean in PTV, mean dose in PTV; Dnear max, near-maximum dose in the PTV; Dmax, maximum dose inthe PTV. Dnear min and Dnear max according to ICRU report 83 (29).

were compared using the log-rank or Gehan–Wilcoxon test, as appropriate. The Cox proportional hazard model was used to calculate hazard ratios. The proportional hazard assumption was verified based on scaled Schoenfeld residuals. Multivariable analysis was performed using backward stepwise selection based on the Akaike information criterion. All statistical analyses were performed employing R version 4.0.2 (32), and a significance level of 0.05.

RESULTS

Baseline Characteristics

The basic patient and tumor characteristics are summarized in the left part of **Table 1**. A total of 90 patients were analyzed. Men and women were evenly represented, and the median age at diagnosis was 66 years (range 25–80 years). All patients indicated for SBRT were in good general condition, with a Karnofsky index of at least 70%. The most common primary tumors were colorectal cancers (37 patients, 41%). The initial dissemination of the primary tumor was in 19 (21%) patients. Within 12 months of their primary tumor, another 26 (29%) patients developed metastases. In half of the cohort, the first metastases occurred after 12 months.

The description characteristics of OD currently intended for SBRT are listed in the right column of **Table 1**. Metastatic lymph nodes were most frequently located in the retroperitoneum (40 patients, 44%) and mediastinum (33 patients, 37%). In the majority of cases, one metastatic node was irradiated (60 patients, 67%). Patients with two lesions (21 patients, 23%), three lesions (seven patients, 8%), and four lesions (four patients, 2%) made up the remaining cases.

In 32 (36%) patients, the treated oligometastases were the first sign of dissemination (*de-novo* OD). The other 58 (64%) patients had been successfully treated in the past for metastatic disease and were currently indicated for SBRT for new oligodissemination. Half of these patients had a history of oligodissemination (repeat OD), and the other half had former multiple metastases (induced OD). Most patients (66 patients, 73%) were not under active systemic therapy at OD diagnosis. The median time without systemic treatment was eight months (range 1–96 months). The other patients had ongoing systemic therapy with a median duration of 12 months (range 4–80 months) at the time of OD diagnosis. No patient in our cohort was treated with concurrent

TABLE 1 | Patients' clinicopathological characteristics (left) and characteristics of oligometastatic disease intended for SBRT (right).

Clinicopathological characteristics of patients (N = 90)		Characteristics of oligometastatic disease intended for SBRT (N = 90)	
Gender		**Locality of lesions**	
Female	45 (50%)	Mediastinum	33 (37%)
Male	45 (50%)	Pelvis	17 (19%)
Age (years)		Retroperitoneum	40 (44%)
Median (IQR)	66 (55-71)	**Number of lesions**	
Range	25-80	1	60 (67%)
Karnofsky index		2	21 (23%)
70	3 (3%)	3	7 (8%)
80	20 (22%)	4	2 (2%)
90	51 (57%)	**History of dissemination**	
100	16 (18%)	De-novo	32 (36%)
Primary tumor		Repeat	29 (32%)
Colorectal	37 (41%)	Induced	29 (32%)
Gynecologic/Prostatic	6/3 (10%)	**Relation of OD to systemic therapy**	
Renal/Bladder/Pancreas	9/4/1 (16%)	Oligorecurrence	66 (73%)
Breast	9 (10%)	Oligopersistence	7 (8%)
Lung	10 (11%)	Oligoprogression	17 (19%)
Melanoma/Sarcoma	5/3 (9%)	**Months from last therapy (oligorecurrence)**	
Head and neck	3 (3%)	median (IQR)	8 (4–22)
Primary histologic type		range	1–96
Adenocarcinoma	46 (52%)	**Months of ongoing systemic therapy (oligopersistence and oligoprogression)**	
GIST	9 (10%)	median (IQR)	12 (8–23)
IDC	9 (10%)	range	4–80
SCC	9 (10%)		
Other	16 (18%)		
NS	1		
Initial disease staging			
M0 (initially localized)	71 (79%)		
M1 (initially disseminated)	19 (21%)		
Timing of initial dissemination			
At time of primary tumor	19 (21%)		
Within 12 months of primary tumor	26 (29%)		
More than 12 months after primary tumor	45 (50%)		

SBRT, stereotactic body radiation therapy; N, number; IQR, interquartile range; GIST, gastrointestinal stromal tumor; IDC, invasive ductal carcinoma; SCC, spinocellular carcinoma; NS, non-specified; OD, oligodissemination.

chemotherapy; targeted therapy was also always discontinued at least one week before and one week after SBRT.

The parameters of SBRT treatment and lesion size are given in **Table 2**. The median GTV size was 10.6 cm^3 (range 0.4–110.2 cm^3). The tumor lesion size corresponded to the size of PTV (median 27.4 cm^3; range 3.3–218.4 cm^3). Patients were most often irradiated in five fractions; the dose was selected according to dose–volume histograms (DVHs) of risk organs surrounding the target PTV volume. More than one-third of the patients were irradiated utilizing schedule 35 Gy in five fractions (35 patients; 39%). A further 29 (32%) patients were irradiated with 30 Gy in five fractions and 11 (12%) patients with 40 Gy in five fractions. The median biological dose equivalent (at $\alpha/\beta = 10$) was 60 Gy (range 48–112 Gy). Only 19 (21%) patients were indicated for systemic treatment immediately after SBRT. According to ICRU recommendations (33), the minimum and maximum doses in 2 and 98% of GTV and PTV volumes were also evaluated.

Treatment-Related Toxicity

No grade III or IV toxicity was observed. The most common side effect was mild grade I fatigue, often associated with the need to travel for therapy. Other acute adverse events grade I to II occurred in five patients (6%)—nausea and lumbar pain (SBRT of retroperitoneum), difficulty swallowing, anorexia, and increased mucous production (SBRT of mediastinum) and proctitis (SBRT of the pelvis, pararectally located tumors). Late side effects were observed in only two patients. One patient developed a post-radiation cough associated with post-SBRT infiltrate in the left pulmonary hilus. In the second patient who underwent the SBRT of two nodes in the mediastinum, a traumatic vertebral fracture occurred in the previously irradiated terrain.

Treatment Outcomes (Time to Event Data)

The median follow-up after SBRT was 34.9 months (95% CI 32.6–43.0). At the time of analysis in August 2020, 58 patients (64%) were still living, and 28 (31%) patients had died from a cancer-related cause. A total of 34 (38%) patients were free of disease and were free of chemotherapy or biological treatment (four patients medicate with hormonal pills). Local recurrence at the irradiation site occurred in 19 (21%) cases, 16 of them with another distant dissemination. These patients were referred for systemic treatment or symptomatic therapy if their general condition worsened. Any progression types (local, regional, or distant) were observed in 66 patients (73%).

Median LC was not reached. The probability of absence of local progression at three and five years was 68.4% and 56.3%,

TABLE 2 | SBRT characteristics.

(N = 90)			
GTV (cm^3)		**BED_{10} (Gy)**	
median (IQR)	10.6 (5.2–18.5)	median (IQR)	60 (48–60)
range	0.4-110.2	range	48–112
PTV (cm^3)		**Fractionation**	
median (IQR)	27.4 (14.9–45.2)	3 × 15Gy	1 (1%)
range	3.3-218.4	3 × 9Gy	1 (1%)
Dmin (Gy)		5 × 6.5Gy	5 (6%)
median (IQR)	33.5 (29.6–36.9)	5 × 6Gy	29 (32%)
range	23.9-51.9	5 × 7.5Gy	3 (3%)
<30	29 (32%)	5 × 7Gy	35 (39%)
30–37	38 (42%)	5 × 8Gy	11 (12%)
≥37	23 (26%)	5 × 9Gy	4 (4%)
Dmax (Gy)		8 × 5Gy	1 (1%)
median (IQR)	36.1 (31.2–41.6)	**Chemo after SBRT**	19 (21%)
range	30.3-58.6	**Acute side effects**	5 (6%)
<37	54 (60%)	**Late side effects**	2 (2%)
≥37	36 (40%)		

SBRT, stereotactic body radiation therapy; GTV, gross tumor volume; IQR, interquartile range; PTV, planning target volume; Dmin, minimum dose; Dmax, maximum dose; BED, biological equivalent dose; Gy, Gray.

respectively (**Figure 2A**). One-third of patients treated with SBRT for OD of lymph nodes did not develop distant relapse that was not amenable to resection or local ablation therapy (*via* SBRT, radiofrequency ablation, or embolization) within five years. The observed median FFWD was 14.6 months (**Figure 2B**).

The median PFS was 9.4 months. Approximately one-fifth of patients (19.8%) were progression-free within three years from SBRT (**Figure 2C**). The necessity of systemic therapy has a significant effect on patient quality of life. In our cohort of patients, the median time to activate systemic therapy was 14.0 months, with a five-year FFST rate of 23.5% (**Figure 2D**). The overall survival rate at three and five years was 61.8 and 39.3%, respectively (**Figure 2E**). Median OS was 53.1 months. During follow-up, 32 (35.6%) patients died, four of whom died without direct relation to cancer.

Patient demographic characteristics, such as age and gender, did not significantly influence survival outcomes except OS. Men had a higher risk of death (HR 2.5, p = 0.012), apparently concerning the unequal distribution of primary tumors. The nature of the primary tumor, together with the initial occurrence of metastases concurrently with the primary tumor, had a major impact on patient prognosis. Tumor aggressiveness expressed by the time to initial dissemination was a negative prognostic factor. The initial dissemination statistically significantly shortened the time to relapse, death, or activation of systemic treatment—LC (HR 4.8, p < 0.001), FFWD (HR 2.8, p = 0.001), PFS (HR 2.1, p = 0.011), FFST (HR 2.4, p = 0.005), OS (HR 2.2, p = 0.034). These results point to higher aggressiveness of the initially disseminated tumors requiring higher radiation doses combined with the maximum possible systemic treatment. Besides, patients classified as having radioresistant tumors had significantly higher risk in terms of LC (HR 13.8, p = 0.010), FFWD (HR 3.1, p = 0.006), PFS (HR 3.5, p < 0.001), FFST (HR 3.2, p = 0.003). Moreover, multivariable analysis detected significantly worse survival outcomes for initially disseminated patients as well as separately in groups according to radiosensitivity (**Figure 3**).

The patients under systemic therapy at the diagnosis of oligometastatic disease intended for SBRT had longer time to local progression (HR 3.8, p = 0.056, **Figure 4A**). The patient's disease history before a diagnosis of OD intended for SBRT has a crucial role in decision making concerning oncological treatment. We analyzed survival outcomes depending on the patients' previous diagnoses of metastatic disease. Patients with a history of polymetastatic or oligometastatic disease had a higher risk of distant dissemination than patients with *de-novo* OD—FFWD

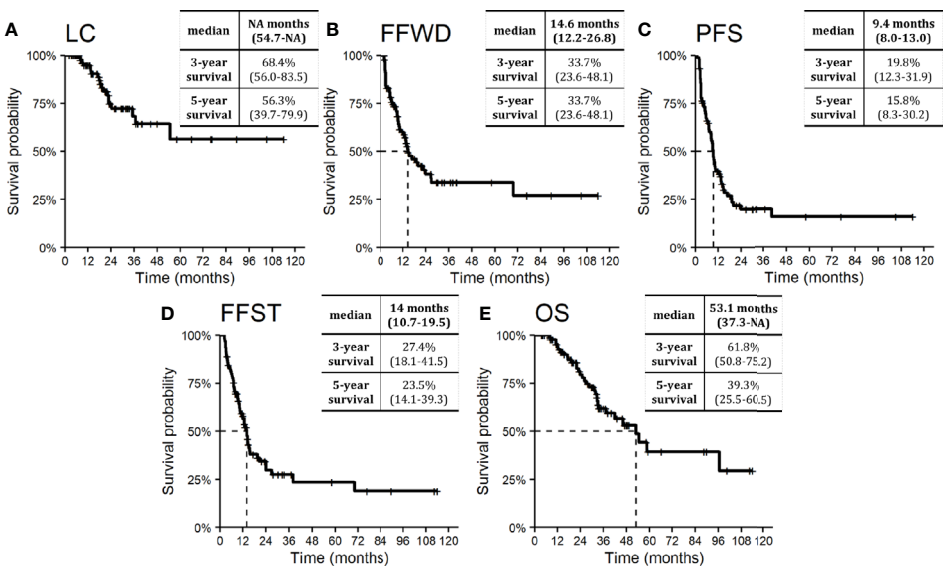

FIGURE 2 | Kaplan–Meier curves for **(A)** local control, **(B)** freedom from widespread dissemination, **(C)** progression-free survival, **(D)** freedom from systematic treatment, and **(E)** overall survival. Dashed lines represent medians. Nested tables include selected characteristics with 95% confidence intervals. NA, Not available.

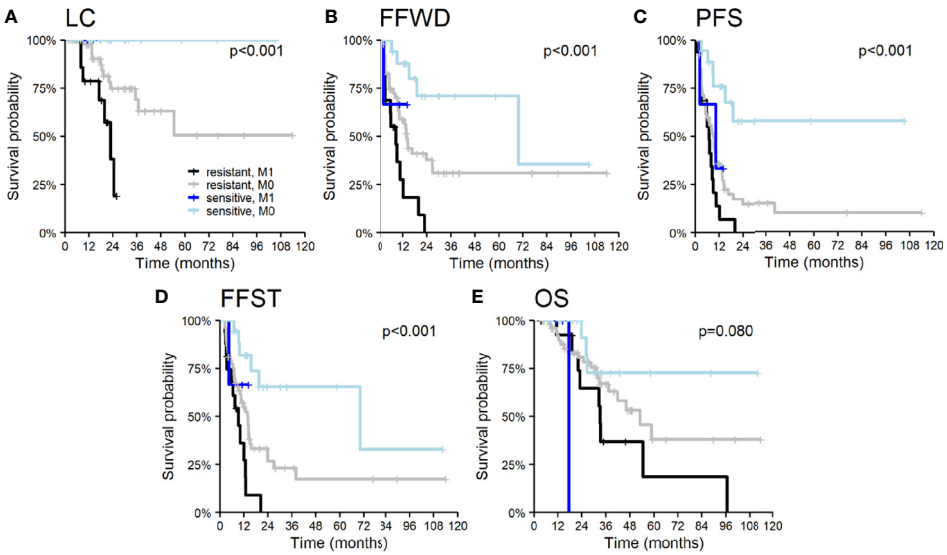

FIGURE 3 | Kaplan–Meier curves according to radiosensitivity of primary tumor and timing of initial dissemination for **(A)** local control, **(B)** freedom from widespread dissemination, **(C)** progression-free survival, **(D)** freedom from systematic treatment, and **(E)** overall survival. The p-values given correspond to the appropriate overall test for the multivariable model.

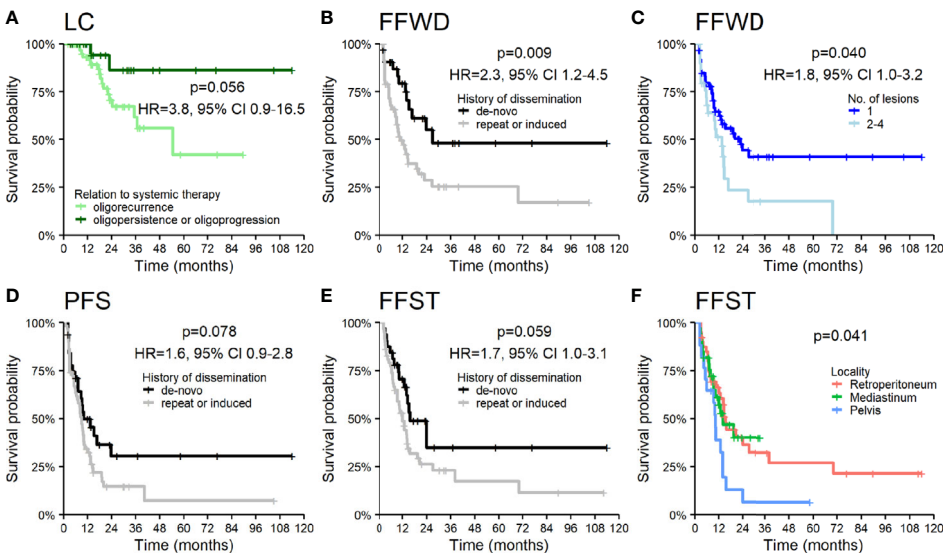

FIGURE 4 | Kaplan–Meier curves for **(A)** local control according to the relation of OD to systemic therapy, **(B)** freedom from widespread dissemination, **(D)** progression-free survival, **(E)** freedom from systematic treatment according to the history of dissemination, **(C)** freedom from widespread dissemination according to the number of lesions, and **(F)** freedom from systematic treatment according to the locality of lesions. Panels include corresponding hazard ratios **(**HR) with 95% confidence intervals (CIs).

(HR 2.3, p = 0.009, **Figure 4B**). The difference in PFS (HR 1.6, p = 0.078) and FFST (HR 1.7, p = 0.059) did not reach statistical significance (**Figures 4D, E**). Neither LC (p = 0.490) nor OS (p = 0.260) was affected by the patient's disease history.

The higher number of treated lesions (two to four lesions) increased the risk of distant dissemination not amenable to resection or locally ablative therapy—FFWD (HR 1.8, p = 0.040, **Figure 4C**). The metastases localized in the pelvic area caused a more frequent disease progression, which was related to an earlier indication for systemic therapy (p = 0.041, **Figure 4F**).

SBRT is a local treatment method for cancer diseases. Thus, the essential treatment parameter is the applied dose (Dmin, Dmax, and BED) and its distribution over time (fractionation). Dose and fractionation are primarily related to the location and

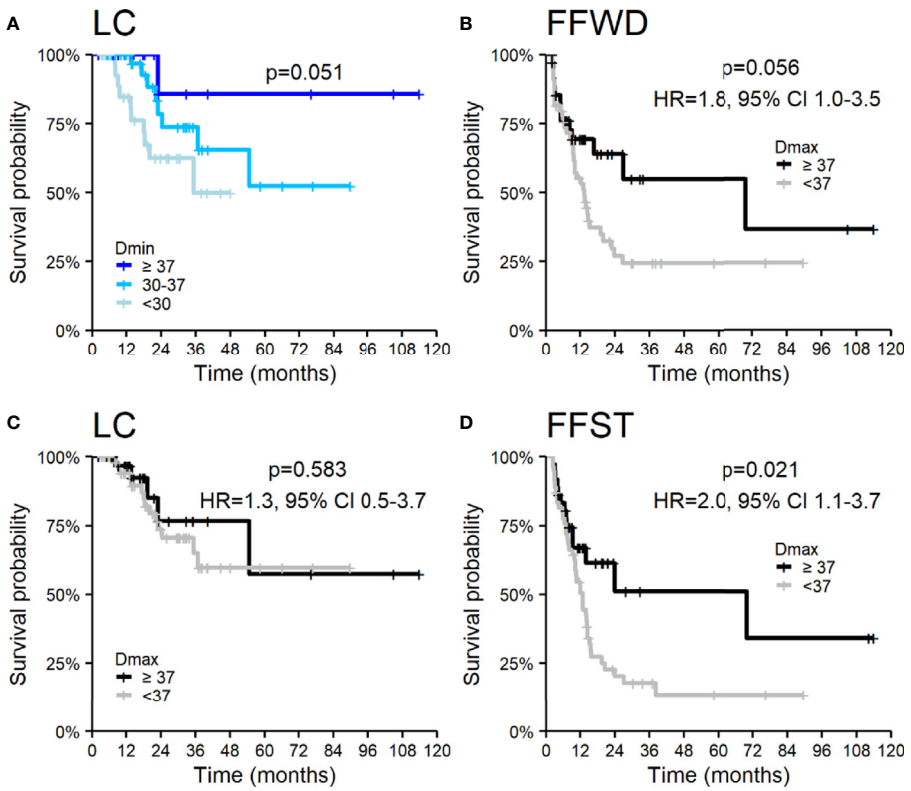

FIGURE 5 | Kaplan–Meier curves according to applied dose expressed by **(A)** Dmin for local control and Dmax **(B–D)** for **(B)** freedom from widespread dissemination, **(C)** local control, and **(D)** freedom from systematic treatment. Panels include corresponding hazard ratios (HR) with 95% confidence intervals (CIs).

dimension of lesions. We observed an association of LC with the minimal applied dose on the borderline of significance but not with maximal applied dose. On the contrary, maximal applied dose affected any distant metastases' appearance and the associated time to activate systemic treatment. The results of the applied dose in relation to survival outcomes are summarized in **Figure 5**, where we categorized Dmin and Dmax into groups using empirically chosen cut-off values. The univariable analysis did not show an association of other SBRT characteristics with the observed survival endpoints.

The complex multivariable analyses with backward elimination (**Table 3**) identified the significance of primary

TABLE 3 | Multivariable analyses for time-to-event endpoints.

	LC p-value HR (95% CI)	FFWD p-value HR (95% CI)	PFS p-value HR (95% CI)	FFST p-value HR (95% CI)
Primary tumor type	p = 0.011	p = 0.006	p = 0.001	p = 0.003
Radioresistant vs radiosensitive	11.2 (1.5,1423)	3.5 (1.4,8.5)	3.4 (1.6,7.1)	3.4 (1.5,7.7)
Timing of initial dissemination	p = 0.007	p = 0.003	p = 0.030	p = 0.007
Initial vs. later	4.1 (1.5,10.8)	2.8 (1.4,5.5)	1.9 (1.1,3.3)	2.5 (1.3,4.7)
Relation to systemic therapy	p = 0.061			
Oligorecurrence vs. Oligoprogression + Oligopersistence	3.1 (1.0,15.3)			
Locality of lesions		p = 0.042		p = 0.036
Mediastinum vs. retroperitoneum		2.7 (1.3,5.8)		1.6 (0.8,3.2)
Pelvis vs. retroperitoneum		1.5 (0.7,3.1)		2.4 (1.2,4.6)
Number of lesions		p = 0.011		p = 0.054
2–4 vs. 1		2.2 (1.2,3.9)		1.7 (1.0,3.1)
Dmax		p = 0.074		
<37 vs. ≥37		1.9 (0.9,4.1)		

LC, local control; FFWD, freedom from widespread dissemination; PFS, progression-free survival; FFST, freedom from systemic treatment; HR, hazard ratio; CI, confidence interval; OD, oligodissemination.

tumor aggressiveness for all treatment endpoints (**Figure 3**), in addition, for LC in combination with relation OD to systemic therapy, and for FFWD and FFST in combination with the lesion locality and number of lesions and (only for FFWD) with Dmax.

DISCUSSION

Oligometastatic involvement of the lymph nodes after treatment of the primary tumor appears in 15–20% of cases and depends on its location and histology (34, 35). Several studies have shown improved patient survival after complete resection of retroperitoneal, intraabdominal, and paraaortic lymphatic relapses (36). However, surgical resection of such involvement is technically challenging, and R0 resection is difficult to achieve (37). Any previous treatment also increases the risk of surgical complications. Such patients are often indicated for systemic treatment—chemotherapy, targeted therapy, or its combination. SBRT, with its potentially ablative doses of radiation, offers an effective alternative to surgery (4). In the present study, local control at 1, 2, 3, 4 and 5 years is approximately 95, 75, 68, 64, and 56%, respectively. Over the same period, PFS is 41, 23, 23, 19, and 19%, and OS is 94, 79, 62, 53, and 39%, respectively.

In Jereczek-Fossa et al. (38), 69 patients underwent the SBRT for oligometastases in lymph nodes (38). The authors report one-year local control of 81.6% and three-year local control of 64.3%. Median PFS was 8.27 months, and three-year PFS was 11.7%. The median OS was 35.4 months. Yeung et al. (39) included 18 patients and reported a one-year local control of 94%, but a two-year local control was only 47%. They also reported a one-year PFS of 39%, a two-year PFS of 17%, a one-year OS of 89%, and a two-year OS of 74%. Despite the high doses (median BED_{10} = 59.5 Gy), the worse local control result could be explained by a high proportion of gastrointestinal tract tumors, especially colorectal cancers, which are considered less sensitive to radiotherapy (37). Loi et al. (40) retrospectively evaluated 87 patients. Their four-year local control and overall survival were high, 79 and 43%, respectively. Franzese et al. (41) recently reported a group of 278 patients with a median follow-up of 15.1 months LC at 1 and 2 years 87.2 and 76.8%, respectively. Better LC was associated with prostate primary tumor, a small tumor volume, oligorecurrence, and BED_{10} ≥75 Gy. One-year OS was 88.4%, and a two-year OS was 73.9%. This study is the most extensive, which includes lymph node oligometastases treated with SBRT. Selected recent SBRT studies evaluating the treatment of lymph node oligometastases are summarized in **Table 4** (6, 38–45).

The local control achieved in our patients is comparable or better to previously published studies. Yeung et al. reported a lower 3-year LC (47%), explained by a higher number of colorectal cancers and application of SBRT alone, without concurrent systemic treatment (39). The same procedure was used in Jereczek-Fossa et al. with similar results (42). In our study, LC was very good (95 and 68% at 1 and 3 years, respectively) despite the high number of colorectal cancers (41%) and irradiation without concomitant systemic treatment. Besides, in our cohort, the minimum dose in target volume (represented by Dmin in GTV) influences local control. The lower Dmin is always related to the undertreatment of part of the target volume, which is in close proximity to an organ at risk (*e.g.*, duodenum). In our study, LC was worse for patients with Dmin <30 Gy. These observations indicated that the volume of lymph node oligometastases irradiated by a lower dose than 30 Gy in five fractions should be as minimal as reasonably

TABLE 4 | Selected recent SBRT studies evaluating the treatment of lymph node oligometastases.

Author, year	No. ofpatients	Primary tumor	Dose	BED_{10}	Local control	Overall survival	Toxicity
Franzese, 2020 (41)	278	various	24–54 Gy/ 3–8 fr.	78.8 Gy (37.5–105.6)	87.2% (1 year) 76.8% (2 years)	88.4% (1 year) 73.9% (2 years)	1× gr. 3
Loi, 2018 (40)	91	various	40–48 Gy/ 5–6 fr.	86 Gy (83–113)	79% (4 years)	43% (4 years)	1× acute gr. 3 no late gr. 3
Yeung, 2017 (39)	18	GIT	31–60 Gy/ 4–10 fr.	59.5 Gy (54.8–105)	47% (2 years)	74% (2 years)	no gr. 3 or 4
Jereczek–Fossa, 2017 (42)	94	prostate	median 24 Gy/3 fr.	43 Gy	84% (2 years)	–	no gr. 3 or 4
Wang, 2016 (43)	22	various	median 39 Gy/5 fr.	70 Gy	91% (1 a 3years)	79% (1 year) 43% (3 years)	–
Ost, 2016 (44)	72	prostate			94% (3 a 5 years)	–	no gr. 3 or 4
Jereczek–Fossa, 2014 (38)	69	various	median 24 Gy/3 fr.	43 Gy	64% (3 years)	50% (3 years)	3× acute gr. 3 1× late gr. 4
Bignardi, 2011 (7)	19	various	24–36 Gy/ 1–5 fr.		78% (2 years)	93% (2 years)	no acute gr. 3 1× late gr. 3
Choi, 2009 (45)	30	cervix, corpus	33–45 Gy/ 3 fr.		67% (4 years)	50% (4 years)	6× acute gr. 3 1× late gr. 3

No., number; Gy, Gray; fr., fraction; gr., grade; GIT, gastrointestinal.

achievable. Nevertheless, the forced undertreatment in the target volume parts near some radiosensitive structure is sometimes inevitable.

Many published studies have also shown better efficacy of ablative doses of radiation (where the biological equivalent of the applied dose exceeds BED_{10} ≥100 Gy) compared to lower doses (46). However, without the most advanced technology, as is MRI guidance, the doses applied to the involved lymph nodes are usually lower. For this reason, the most frequently prescribed fractionation in our population was 35 Gy in five fractions, and the median biological equivalent of BED_{10} was 60 Gy (range 48–112 Gy), corresponding to the gradual development of the learning curve. With appropriate tools and technology, an ablative dose can be given to nodal targets. For example, publications show the feasibility of safely dose-escalating targets such as lymph nodes using MRI guidance (47–49). Even without MRI guidance, Franzese et al. (41) report a higher BED_{10} (median 78.75 Gy). Nevertheless, LC in years 1 and 2 was comparable to our results. A longer follow-up is needed to compare these results further.

In contrast to very good LC, one and three-year PFS was relatively low (41 and 23%), confirming the generally local therapeutic potential of radiotherapy. These values also correspond to the published data; Yeung et al. reported 17% PFS at two years and Jereczek-Fossa 12% PFS at three years. Most of our patients only progressed outside the irradiated area. Whether local progression occurred at the irradiation site, it was almost always associated with multiple dissemination outside the irradiated volume. Reported PFS estimation open discussion about the administration of systemic treatment immediately after solitary lymphatic metastasis is found, or discussion about avoiding indication to SBRT in these cases at all. Conversely, it should be considered that almost a fifth of the patients had been free of signs of disease for five years after the minimal-toxic SBRT and without the need for any other cancer treatment. This number also corresponds to published data after SBRT oligometastasis in the other sites (liver, lung, *etc.*) (7, 50). Approximately 20–25% of oligometastatic patients are free of disease signs for a long period after local treatment, and there is no need to include systemic therapy.

An important observation was the significant difference in all survival parameters in relation to the initial staging of the disease. Specifically, statistically significant differences were found between the group of patients with initially disseminated primary tumor and the group with metastases onset after the completion of primary treatment. Survival differences were observed from both the general disease control point of view (PFS, $p = 0.011$; FFWD, $p = 0.001$; OS, $p = 0.034$; FFST, $p = 0.005$), and in local control parameters (LC, $p < 0.001$). No difference in the volume of PTV as well as in the prescribed dose (Dmin, Dmax, BED) was observed between these two groups. These results indicate higher aggressivity of initially disseminated cancer where it is needed maximum possible systemic treatment and a higher radiotherapy dose. Considering that availability of state-of-the-art RT facility equipped by technology for SBRT (or even more advanced technology employing MR guided systems) is still limited, there are specialized centers which provide service to a large region. Especially for extramural patients referred from distant workplaces, it is important to obtain all clinical data about the patient's disease course irrespective of the possible limited availability of referring medical oncologists.

Future biomarker studies could also identify a subset of patients who have responded to this treatment over an extended period and can benefit from maximum local therapeutical access. These patients could be distinguished from those who would be overtreated by SBRT or even in which the administration of radiotherapy would mean an unnecessary delay in the required chemotherapy (51).

In total, 15 (16.7%) patients of our group progressed beyond the irradiated volume after SBRT again with only oligometastases, which could be re-indicated for local therapy (SBRT, RFA, *etc.*). This allowed further delay of cytotoxic chemotherapy or another type of systemic treatment. Our analysis also assessed the time to multiple progression, which no longer allows the use of local treatment methods (FFWD) and the time to indicate systemic treatment (FFST). Postponing chemotherapy and its side effects thereby improve patients' quality of life.

Regional relapses or distant oligometastases during follow-up after SBRT should not be a reason to contraindicate other local treatment methods; on the contrary, local treatment methods should be indicated wherever possible to postpone systemic treatment initiation further. In accordance with the fact that all these patients are treated *de facto* with palliative intent, an attempt is made to indicate systemic therapy as late as possible; unless, of course, there is no other clear evidence for immediate administration of chemotherapy or another type of systemic treatment. Further studies will also be required to suggest the optimal timing of SBRT in the treatment of these patients.

The overall survival of patients in our study (unselected cohort treated outside of clinical trials, *i.e.*, real-world evidence) did not differ from the published data. Despite further dissemination, the overall survival rate of these patients was high. Such evidence can help raise the level of evidence of SBRT and its use in routine clinical practice.

The toxicity in our cohort was minimal, with very good local control. SBRT is generally a short, well-tolerated treatment (mostly outpatient) requiring no special training or significant reduction in patients' quality of life.

We are aware of some limits of our study; first of all, it is necessary to point out the retrospective character of the monitoring, a limited number of patients, and for this reason, it is currently impossible to statistically evaluate efficacy based on tumor type or histology. Also, dose heterogeneity does not allow an optimal treatment strategy to be identified, especially in patients with tumors at higher risk of local failure or early distant spread. The overall survival assessment is biased, of course, on the heterogeneity of further treatment after SBRT. Nevertheless, for practitioners, the OS indicator is an important

descriptive characteristic for their indication of this sophisticated radiotherapy method (48).

CONCLUSION

Our study has shown that targeted stereotactic radiotherapy, SBRT, is a minimally toxic and very effective local treatment for oligometastatic lymph node involvement. It can delay the use of cytotoxic chemotherapy with minimal patient effort and improve patient quality of life. Less than one-fifth of patients treated in this way survive without signs of disease for an extended period. Identifying patients who benefit most from SBRT in the treatment strategy, as well as its timing and the prescribed dose, should be the subject of further studies.

DATA AVAILABILITY STATEMENT

The raw data supporting the conclusions of this article will be made available by the authors, without undue reservation.

ETHICS STATEMENT

The studies involving human participants were reviewed and approved by the Ethical Committee, Masaryk Memorial Cancer Institute. The patients/participants provided their written informed consent to participate in this study.

AUTHOR CONTRIBUTIONS

PB, TK, MS, PO, and PS conceptualized the study. IS, PB, TK, PP, PO, TP, and MV conducted the data curation. PB, IS, TK, TP, and MV performed the formal analysis. PB, TK, and PS acquired the funding. PB, TK, MS, PP, PO, LB, and LK conducted the investigation. IS, TK, PB, and PP developed the methodology. TK and PB were in charge of the project administration. PS supervised the study. IS, TK, PB, and PP validated the study. PB, IS, TK, and MS wrote the original draft. PB, TK, and IS wrote, reviewed, and edited the manuscript. All authors contributed to the article and approved the submitted version.

FUNDING

This work was supported by grants from the Ministry of Health of the Czech Republic AZV 19-00354 and by the Ministry of Health of the Czech Republic—Conceptual development of a research organization (MMCI 00209805).

SUPPLEMENTARY MATERIAL

The Supplementary Material for this article can be found online at: https://www.frontiersin.org/articles/10.3389/fonc.2020.616494/full#supplementary-material

REFERENCES

1. Lievens Y, Guckenberger M, Gomez D, Hoyer M, Iyengar P, Kindts I, et al. Defining oligometastatic disease from a radiation oncology perspective: An ESTRO-ASTRO consensus document. *Radiother Oncol* (2020) 148:157–66. doi: 10.1016/j.radonc.2020.04.003
2. Hellman S, Weichselbaum RR. Oligometastases. *J Clin Oncol* (1995) 13:8–10. doi: 10.1200/JCO.1995.13.1.8
3. Weichselbaum RR, Hellman S. Oligometastases revisited. *Nat Rev Clin Oncol* (2011) 8:378–82. doi: 10.1038/nrclinonc.2011.44
4. Palma DA, Olson R, Harrow S, Gaede S, Louie AV, Haasbeek C, et al. Stereotactic Ablative Radiotherapy for the Comprehensive Treatment of Oligometastatic Cancers: Long-Term Results of the SABR-COMET Phase II Randomized Trial. *J Clin Oncol* (2020) 38:2830–8. doi: 10.1200/JCO.20.00818
5. Niibe Y, Hayakawa K. Oligometastases and Oligo-recurrence: The New Era of Cancer Therapy. *Jpn J Clin Oncol* (2010) 40:107–11. doi: 10.1093/jjco/hyp167
6. Bignardi M, Navarria P, Mancosu P, Cozzi L, Fogliata A, Tozzi A, et al. Clinical Outcome of Hypofractionated Stereotactic Radiotherapy for Abdominal Lymph Node Metastases. *Int J Radiat Oncol* (2011) 81:831–8. doi: 10.1016/j.ijrobp.2010.05.032
7. Burkoň P, Slávik M, Kazda T, Pospíšil P, Procházka T, Vrzal M, et al. Stereotactic Body Radiotherapy – Current Indications. *Klin Onkol* (2019) 32:10–24. doi: 10.14735/amko201910
8. Chang JS, Sethi RA, Barani IJ. Extracranial Oligometastases. In *Handbook of Evidence-Based Stereotactic Radiosurgery and Stereotactic Body Radiotherapy*. Cham: Springer International Publishing (2016). pp. 203–20. doi: 10.1007/978-3-319-21897-7_12
9. Ettinger DS, Aisner DL, Wood DE, Akerley W, Bauman J, Chang JY, et al. NCCN Guidelines Insights: Non–Small Cell Lung Cancer, Version 5.2018. *J Natl Compr Cancer Netw* (2018) 16:807–21. doi: 10.6004/jnccn.2018.0062
10. Postmus PE, Kerr KM, Oudkerk M, Senan S, Waller DA, Vansteenkiste J, et al. Early and locally advanced non-small-cell lung cancer (NSCLC): ESMO Clinical Practice Guidelines for diagnosis, treatment and follow-up. *Ann Oncol* (2017) 28:iv1–iv21. doi: 10.1093/annonc/mdx222
11. Videtic GMM, Donington J, Giuliani M, Heinzerling J, Karas TZ, Kelsey CR, et al. Stereotactic body radiation therapy for early-stage non-small cell lung cancer: Executive Summary of an ASTRO Evidence-Based Guideline. *Pract Radiat Oncol* (2017) 7:295–301. doi: 10.1016/j.prro.2017.04.014
12. Tree AC, Khoo VS, Eeles RA, Ahmed M, Dearnaley DP, Hawkins MA, et al. Stereotactic body radiotherapy for oligometastases. *Lancet Oncol* (2013) 14:e28–37. doi: 10.1016/S1470-2045(12)70510-7
13. Corbin KS, Hellman S, Weichselbaum RR. Extracranial Oligometastases: A Subset of Metastases Curable With Stereotactic Radiotherapy. *J Clin Oncol* (2013) 31:1384–90. doi: 10.1200/JCO.2012.45.9651
14. Palma DA, Olson RA, Harrow S, Gaede S, Louie AV, Haasbeek C, et al. Stereotactic Ablative Radiation Therapy for the Comprehensive Treatment of Oligometastatic Tumors (SABR-COMET): Results of a Randomized Trial. *Int J Radiat Oncol* (2018) 102:S3–4. doi: 10.1016/j.ijrobp.2018.06.105
15. Guckenberger M, Lievens Y, Bouma AB, Collette L, Dekker A, DeSouza NM, et al. Characterisation and classification of oligometastatic disease: a European Society for Radiotherapy and Oncology and European Organisation for Research and Treatment of Cancer consensus recommendation. *Lancet Oncol* (2020) 21:e18–28. doi: 10.1016/S1470-2045(19)30718-1
16. Laufer I, Rubin DG, Lis E, Cox BW, Stubblefield MD, Yamada Y, et al. The NOMS Framework: Approach to the Treatment of Spinal Metastatic Tumors. *Oncologist* (2013) 18:744–51. doi: 10.1634/theoncologist.2012-0293
17. Spratt DE, Beeler WH, de Moraes FY, Rhines LD, Gemmete JJ, Chaudhary N, et al. An integrated multidisciplinary algorithm for the management of spinal

metastases: an International Spine Oncology Consortium report. *Lancet Oncol* (2017) 18:e720–30. doi: 10.1016/S1470-2045(17)30612-5
18. McPherson CM, Suki D, Feiz-Erfan I, Mahajan A, Chang E, Sawaya R, et al. Adjuvant whole-brain radiation therapy after surgical resection of single brain metastases. *Neuro Oncol* (2010) 12:711–9. doi: 10.1093/neuonc/noq005
19. Paterson R. Classification of Tumours in Relation to Radiosensitivity. *Br J Radiol* (1933) 6:218–33. doi: 10.1259/0007-1285-6-64-218
20. Burkon P, Slampa P, Kazda T, Slavik M, Prochazka T, Vrzal M. Stereotactic body radiation therapy for colorectal cancer liver metastases; early results. *Klin Onkol* (2012) 25(Suppl 2):2S93–7. doi: 10.14735/amko20122S93
21. Nagata Y, Takayama K, Matsuo Y, Norihisa Y, Mizowaki T, Sakamoto T, et al. Clinical outcomes of a phase I/II study of 48 Gy of stereotactic body radiotherapy in 4 fractions for primary lung cancer using a stereotactic body frame. *Int J Radiat Oncol* (2005) 63:1427–31. doi: 10.1016/j.ijrobp.2005.05.034
22. Heinzerling JH, Anderson JF, Papiez L, Boike T, Chien S, Zhang G, et al. Four-Dimensional Computed Tomography Scan Analysis of Tumor and Organ Motion at Varying Levels of Abdominal Compression During Stereotactic Treatment of Lung and Liver. *Int J Radiat Oncol* (2008) 70:1571–8. doi: 10.1016/j.ijrobp.2007.12.023
23. Josipovic M, Persson GF, Bangsgaard JP, Specht L, Aznar MC. Deep inspiration breath-hold radiotherapy for lung cancer: impact on image quality and registration uncertainty in cone beam CT image guidance. *Br J Radiol* (2016) 89(1068):20160544. doi: 10.1259/bjr.20160544
24. Nagata Y, Wulf J, Lax I, Timmerman R, Zimmermann F, Stojkovski I, et al. Stereotactic Radiotherapy of Primary Lung Cancer and Other Targets: Results of Consultant Meeting of the International Atomic Energy Agency. *Int J Radiat Oncol* (2011) 79:660–9. doi: 10.1016/j.ijrobp.2010.10.004
25. Lagerwaard FJ, Haasbeek CJA, Smit EF, Slotman BJ, Senan S. Outcomes of Risk-Adapted Fractionated Stereotactic Radiotherapy for Stage I Non–Small-Cell Lung Cancer. *Int J Radiat Oncol* (2008) 70:685–92. doi: 10.1016/j.ijrobp.2007.10.053
26. Benedict SH, Yenice KM, Followill D, Galvin JM, Hinson W, Kavanagh B, et al. Stereotactic body radiation therapy: The report of AAPM Task Group 101. *Med Phys* (2010) 37:4078–101. doi: 10.1118/1.3438081
27. Ong CL, Verbakel WFAR, Cuijpers JP, Slotman BJ, Lagerwaard FJ, Senan S. Stereotactic radiotherapy for peripheral lung tumors: A comparison of volumetric modulated arc therapy with 3 other delivery techniques. *Radiother Oncol* (2010) 97:437–42. doi: 10.1016/j.radonc.2010.09.027
28. Purdie TG, Bissonnette J-P, Franks K, Bezjak A, Payne D, Sie F, et al. Cone-Beam Computed Tomography for Online Image Guidance of Lung Stereotactic Radiotherapy: Localization, Verification, and Intrafraction Tumor Position. *Int J Radiat Oncol* (2007) 68:243–52. doi: 10.1016/j.ijrobp.2006.12.022
29. Grégoire V, Mackie TR. State of the art on dose prescription, reporting and recording in Intensity-Modulated Radiation Therapy (ICRU report No. 83). *Cancer/Radiothérapie* (2011) 15:555–9. doi: 10.1016/j.canrad.2011.04.003
30. Eisenhauer EA, Therasse P, Bogaerts J, Schwartz LH, Sargent D, Ford R, et al. New response evaluation criteria in solid tumours: Revised RECIST guideline (version 1.1). *Eur J Cancer* (2009) 45:228–47. doi: 10.1016/j.ejca.2008.10.026
31. van Persijn van Meerten EL, Gelderblom H, Bloem JL. RECIST revised: implications for the radiologist. A review article on the modified RECIST guideline. *Eur Radiol* (2010) 20:1456–67. doi: 10.1007/s00330-009-1685-y
32. R Core Team. R: A language and environment for statistical computing. Vienna, Austria: R Foundation for Statistical Computing (2020). Available at: https://www.R-project.org/.
33. Seuntjens J, Lartigau E, Cora S. ICRU Report 91. Prescribing, recording, and reporting of stereotactic treatments with small photon beams. *J ICRU* (2014) 14:1–160. doi: 10.1093/jicru/ndx009
34. van Gestel YRBM, de Hingh IHJT, van Herk-Sukel MPP, van Erning FN, Beerepoot LV, Wijsman JH, et al. Patterns of metachronous metastases after curative treatment of colorectal cancer. *Cancer Epidemiol* (2014) 38:448–54. doi: 10.1016/j.canep.2014.04.004
35. Todo Y, Kato H, Minobe S, Okamoto K, Suzuki Y, Sudo S, et al. Initial failure site according to primary treatment with or without para-aortic lymphadenectomy in endometrial cancer. *Gynecol Oncol* (2011) 121:314–8. doi: 10.1016/j.ygyno.2011.01.019
36. Shibata D, Paty PB, Guillem JG, Wong DW, Cohen AM. Surgical Management of Isolated Retroperitoneal Recurrences of Colorectal Carcinoma. *Dis Colon Rectum* (2002) 45:795–801. doi: 10.1007/s10350-004-6300-3
37. Jereczek-Fossa BA, Ronchi S, Orecchia R. Is Stereotactic Body Radiotherapy (SBRT) in lymph node oligometastatic patients feasible and effective? *Rep Pract Oncol Radiother* (2015) 20:472–83. doi: 10.1016/j.rpor.2014.10.004
38. Jereczek-Fossa BA, Piperno G, Ronchi S, Catalano G, Fodor C, Cambria R, et al. Linac-based Stereotactic Body Radiotherapy for Oligometastatic Patients With Single Abdominal Lymph Node Recurrent Cancer. *Am J Clin Oncol* (2014) 37:227–33. doi: 10.1097/COC.0b013e3182610878
39. Yeung R, Hamm J, Liu M, Schellenberg D. Institutional analysis of stereotactic body radiotherapy (SBRT) for oligometastatic lymph node metastases. *Radiat Oncol* (2017) 12:105. doi: 10.1186/s13014-017-0820-1
40. Loi M, Frelinghuysen M, Klass ND, Oomen-De Hoop E, Granton PV, Aerts J, et al. Locoregional control and survival after lymph node SBRT in oligometastatic disease. *Clin Exp Metastasis* (2018) 35:625–33. doi: 10.1007/s10585-018-9922-x
41. Franzese C, Badalamenti M, Comito T, Franceschini D, Clerici E, Navarria P, et al. Assessing the role of Stereotactic Body Radiation Therapy in a large cohort of patients with lymph node oligometastases: Does it affect systemic treatment's intensification? *Radiother Oncol* (2020) 150:184–90. doi: 10.1016/j.radonc.2020.06.029
42. Jereczek-Fossa BA, Fanetti G, Fodor C, Ciardo D, Santoro L, Francia CM, et al. Salvage Stereotactic Body Radiotherapy for Isolated Lymph Node Recurrent Prostate Cancer: Single Institution Series of 94 Consecutive Patients and 124 Lymph Nodes. *Clin Genitourin Cancer* (2017) 15:e623–32. doi: 10.1016/j.clgc.2017.01.004
43. Wang Z, Wang J, Zhuang H, Wang P, Yuan Z. Stereotactic body radiation therapy induces fast tumor control and symptom relief in patients with iliac lymph node metastasis. *Sci Rep* (2016) 6:37987. doi: 10.1038/srep37987
44. Ost P, Jereczek-Fossa BA, Van As N, Zilli T, Tree A, Henderson D, et al. Pattern of Progression after Stereotactic Body Radiotherapy for Oligometastatic Prostate Cancer Nodal Recurrences. *Clin Oncol* (2016) 28:e115–20. doi: 10.1016/j.clon.2016.04.040
45. Choi CW, Cho CK, Yoo SY, Kim MS, Yang KM, Yoo HJ, et al. Image-Guided Stereotactic Body Radiation Therapy in Patients With Isolated Para-Aortic Lymph Node Metastases From Uterine Cervical and Corpus Cancer. *Int J Radiat Oncol* (2009) 74:147–53. doi: 10.1016/j.ijrobp.2008.07.020
46. Onishi H, Shirato H, Nagata Y, Hiraoka M, Fujino M, Gomi K, et al. Stereotactic Body Radiotherapy (SBRT) for Operable Stage I Non–Small-Cell Lung Cancer: Can SBRT Be Comparable to Surgery? *Int J Radiat Oncol* (2011) 81:1352–8. doi: 10.1016/j.ijrobp.2009.07.1751
47. Winkel D, Bol GH, Werensteijn-Honingh AM, Intven MPW, Eppinga WSC, Hes J, et al. Target coverage and dose criteria based evaluation of the first clinical 1.5T MR-linac SBRT treatments of lymph node oligometastases compared with conventional CBCT-linac treatment. *Radiother Oncol* (2020) 146:118–25. doi: 10.1016/j.radonc.2020.02.011
48. Winkel D, Bol GH, Werensteijn-Honingh AM, Kiekebosch IH, van Asselen B, Intven MPW, et al. Evaluation of plan adaptation strategies for stereotactic radiotherapy of lymph node oligometastases using online magnetic resonance image guidance. *Phys Imaging Radiat Oncol* (2019) 9:58–64. doi: 10.1016/j.phro.2019.02.003
49. Werensteijn-Honingh AM, Kroon PS, Winkel D, Aalbers EM, van Asselen B, Bol GH, et al. Feasibility of stereotactic radiotherapy using a 1.5 T MR-linac: Multi-fraction treatment of pelvic lymph node oligometastases. *Radiother Oncol* (2019) 134:50–4. doi: 10.1016/j.radonc.2019.01.024
50. Burkon P, Kazda T, Pospisil P, Slavik M, Kominek L, Selingerova I, et al. Ablative dose stereotactic body radiation therapy for oligometastatic disease: A prospective single institution study. *Neoplasma* (2019) 66(2):315–25. doi: 10.4149/neo_2018_180731N558
51. Matsushita H, Jingu K, Umezawa R, Yamamoto T, Ishikawa Y, Takahashi N, et al. Stereotactic Radiotherapy for Oligometastases in Lymph Nodes—A Review. *Technol Cancer Res Treat* (2018) 17:153303381880359. doi: 10.1177/1533033818803597. 153303381880359.

Conflict of Interest: The authors declare that the research was conducted in the absence of any commercial or financial relationships that could be construed as a potential conflict of interest.

frontiers in Oncology

ORIGINAL RESEARCH
published: 25 February 2021
doi: 10.3389/fonc.2020.616286

Ten-Year Single Institutional Analysis of Geographic and Demographic Characteristics of Patients Treated With Stereotactic Body Radiation Therapy for Localized Prostate Cancer

*Nima Aghdam[1], Michael Carrasquilla[2], Edina Wang[2], Abigail N. Pepin[2,3], Malika Danner[2], Marilyn Ayoob[2], Thomas Yung[2], Brian T. Collins[2], Deepak Kumar[4], Simeng Suy[2], Sean P. Collins[2] and Jonathan W. Lischalk[5]**

[1] Department of Radiation Medicine, Beth Israel Deaconess Medical Center, Boston, MA, United States, [2] Department of Radiation Medicine, MedStar Georgetown University Hospital, Washington, DC, United States, [3] George Washington University School of Medicine, Washington, DC, United States, [4] The Julius L. Chambers Biomedical Biotechnology Research Institute, North Carolina Central University, Durham, NC, United States, [5] Perlmutter Cancer Center, Langone Medical Center, New York University, New York, NY, United States

OPEN ACCESS

Edited by:
Alexander Muacevic,
Ludwig Maximilian University of Munich, Germany

Reviewed by:
Andrew Wenhua Ju,
The Brody School of Medicine at East Carolina University, United States
Jonathan Haas,
New York University, United States

***Correspondence:**
Jonathan W. Lischalk
Jonathan.Lischalk@nyulangone.org

Specialty section:
This article was submitted to Radiation Oncology, a section of the journal Frontiers in Oncology

Received: 11 October 2020
Accepted: 23 December 2020
Published: 25 February 2021

Citation:
Aghdam N, Carrasquilla M, Wang E, Pepin AN, Danner M, Ayoob M, Yung T, Collins BT, Kumar D, Suy S, Collins SP and Lischalk JW (2021) Ten-Year Single Institutional Analysis of Geographic and Demographic Characteristics of Patients Treated With Stereotactic Body Radiation Therapy for Localized Prostate Cancer. Front. Oncol. 10:616286. doi: 10.3389/fonc.2020.616286

Objectives: Stereotactic Body Radiation Therapy (SBRT) offers definitive treatment for localized prostate cancer with comparable efficacy and toxicity to conventionally fractionated radiotherapy. Decreasing the number of treatment visits from over 40 to five may ease treatment burden and increase accessibility for logistically challenged patients. Travel distance is one factor that affects a patient's access to treatment and is often related to geographic location and socioeconomic status. In this study, we review the demographic and geographic factors of patients treated with SBRT for prostate cancer for a single institution with over a decade of experience.

Methods: Patient zip codes from one thousand and thirty-five patients were derived from a large, prospectively maintained quality of life database for patients treated for prostate cancer with SBRT from 2008 to 2017. The geospatial distance between the centroid of each zip code to our institution was calculated using the R package Geosphere. Characteristics for seven hundred and twenty-one patients were evaluated at the time of analysis including: race, age, and insurance status. To assess the geographic reach of our institution, we evaluated the demographic features of each zip code using US Census data. Statistical comparisons for these features and their relation to distance traveled for treatment was performed using the Mann-Whitney U test. Finally, an unsupervised learning algorithm was performed to identify distinct clusters of patients with respect to median income, racial makeup, educational level, and rural residency.

Results: Patients traveled from 246 distinct zip codes at a median distance of 11.35 miles. Forty percent of patients were African American, 6.9% resided in a rural region, and

22% were over the age of 75. Using K-means cluster analysis, four distinct patient zip-code groups were identified based on the aforementioned demographic features: Suburban/high-income (45%), Urban (30%), Suburban/low-income (17%), and Rural (8%). For each of the clusters, the average travel distance for SBRT was significantly different at 11.17, 9.26, 11.75, and 40.2 miles, respectively (p-value: <0.001).

Conclusions: Distinct demographic features are related to travel distance for prostate SBRT. In our large cohort, travel distance did not prevent uptake of prostate SBRT in African American, elderly or rural patient populations. Prostate SBRT offers a diverse population modern treatment for their localized prostate cancer and particularly for those who live significant distances from a treatment center.

Keywords: racial, disparities (health), machine learning, treatment burden, travel distance, prostate cancer, SBRT (stereotactic body radiation therapy)

INTRODUCTION

Adoption of a new technology in cancer treatment is contingent upon efficacy, safety, and accessibility. The field of radiation oncology has historically been dominated by the concept of fractionation to optimize the therapeutic ratio. However, with the evolution of advanced imaging, precision radiotherapy delivery, and exquisite image guidance, our ability to reliably and precisely treat even moving targets has allowed for an unprecedented movement towards hypofractionation. While the oncologic efficacy and side effect profile of ultra-hypofractionated radiotherapy (UHF-RT) has been found to be comparable to other modes of radiation for localized prostate cancer, UHF- RT is currently offered to a minority of patients (1–3). Ultra-hypofractionated radiotherapy can be delivered in a five-fraction regimen, which has the potential to reduce treatment burden and cost, as well as improve accessibility to patients who may be burdened by fractionated radiation treatments delivered over nine weeks (4–6).

Health services utilization is partially determined by geographical disparity (7–9). Patients who live in areas with scarce healthcare options face greater barriers to accessing appropriate services and are required to travel long distances for cancer treatment (10). Specifically, patients from rural communities have diminished access to newer and novel treatments and practice changing clinical trials (11). Several studies have documented improved cancer outcomes for patients treated at centers with more specialized care (12–14). In general, travel distance to a major cancer center has been noted to contribute to slower adoption of new cancer treatment and poorer outcomes (12, 15). A recent study examining the National Cancer Database for prostate cancer revealed that travel distance may be a contributor to racial disparity for African Americans, Hispanics and other nonwhite races in the adoption of SBRT for treatment of localized prostate cancer (16). While the efficacy of SBRT continues to be evaluated in prospective clinical trials, the inequitable access to SBRT may prove detrimental. Given that nine weeks of daily conventionally fractionated radiation therapy may lead to greater financial toxicity for communities with lower income and decreased access due to geographic disparity, a hypofractionated regimen offers an excellent treatment option to patients with limited access without overwhelming logistical challenges.

To this end, we sought to review a decade of experience at a comprehensive cancer center which was an early adopter of SBRT for localized prostate cancer. Using a large institutional database, we analyzed the geographic and demographic features of our patient population, the utilization of prostate SBRT defined by geodemographic clusters based on zip code, and associated census data points using a machine learning algorithm.

METHODS

From January of 2008 to December of 2017, 1,035 patients with localized prostate cancer were treated at Medstar Georgetown University Hospital with five fraction SBRT or an SBRT boost and supplemental pelvic IMRT. Given that a portion of patients traveled long distances across the United States a threshold for outliers was developed using the Tukey method (**Figure 1**). Subsequently, full records for 923 patients with localized prostate cancer at Georgetown University Hospital were analyzed. Of these, 725 patients were treated with SBRT monotherapy and 198 with an SBRT boost in addition to conventionally fractionated pelvic radiotherapy. Treatment methods have been described elsewhere (17) but briefly; one week after placement of 4 to 6 gold fiducial markers in the prostate, patients underwent a CT simulation of the pelvis. The bladder, prostatic urethra, membranous urethra and rectum were contoured by a single treating radiation oncologist (SPC). Inverse planning was generated with a prescription dose of 35 to 37.25 Gy in five fractions using 6-MV photons calculated on MultiPlan software (Accuray Inc., Sunnyvale, USA). Patients who received supplemental IMRT were treated with robotic SBRT (19.5 Gy in three fractions to the prostate) followed by fiducial-guided IMRT. Patients were initiated on IMRT treatment the week following SBRT. Daily doses of 1.8 Gy were delivered 5 days a week to a total dose of 45–50.4 Gy in 25–28

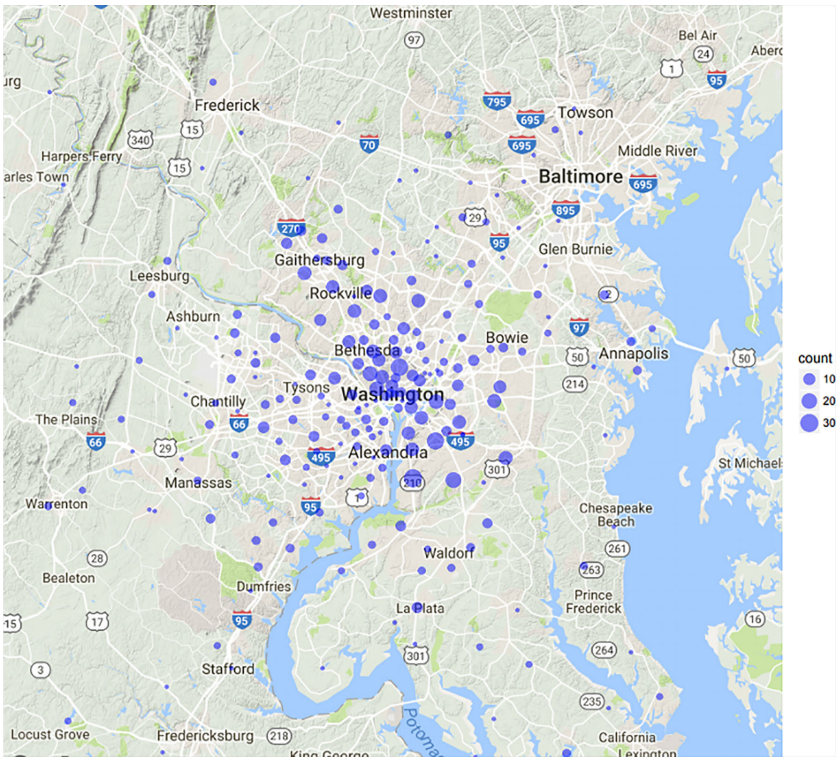

FIGURE 1 | Map patient zip codes.

fractions. Dose volume histograms were constructed to meet clinically established dose objectives and constraints for OARs. Treatment was delivered using the CyberKnife robotic radiosurgical system (Accuray Inc., Sunnyvale, CA, USA). Fiducial tracking using continuous orthogonal x-rays was employed to account for intrafractional target motion.

The patient characteristics were derived from a prospectively maintained quality of life IRB (IRB#: 2009-510) approved institutional trial. Patient zip codes were extracted from the hospital billing database and the US Census database was accessed and linked with patient zip codes. The zip code data points included: median income, proportion of African American and rural residents, education level and proportion of un-insured patients. The geospatial distance between the centroid of each zip code to our cancer center was calculated using the R package Geosphere (CRAN, Vienna, Austria). These distances did not necessarily represent driving distance but rather as the crow flies. Statistical comparisons for these features and their relation to distance traveled for treatment was performed using the Mann-Whitney U test. After standardizing data, an unsupervised learning algorithm called K means clustering using SPSS version 23 (IBM Corp., Armonk, NY) was performed to identify distinct clusters of patients with respect to median income, racial makeup, educational level and rural residency (18). Distance traveled from each cluster was reported in miles. Differences in demographics for each zip code were interrogated to identify the chief discriminant of clusters. Google maps data was used to generate images and zoom levels meant to capture the Maryland and Virginia area from which our cohort lives.

RESULTS

In our cohort, the median age was 69 (range 48–92). Self-reported race was 46% Caucasian, 48% African American, and 6% Other. The majority of patients presented with intermediate risk prostate cancer (55%) per D'Amico criteria, followed by high risk (25%) and low risk (20%) disease. Mean and median travel distance to Georgetown University Hospital was 16.8 and 11.4 miles (0.44–222.2). Additional patient characteristics are presented in **Table 1**.

Mean Travel distance for African American patients was 12.5 miles, which was significantly lower than Caucasian patients, 20.6 miles (p-value<0.001). Travel distance for patients older than 75 was 15.6 miles and not significantly different compared to patients younger than 65 which was 17.8 miles (p-value=0.19) (**Figures 2A, B**). Travel distance for patients with high risk disease was 13.9 miles, significantly lower than those with intermediate and low risk disease at 17.9 miles (p-value=0.014). Patients treated with supplemental IMRT traveled a shorter distance of 13.7 miles compared to monotherapy patients at 17.7 miles (p-value=0.017).

Within a 222 mile radius of the hospital 246 distinct zip codes were identified. The median income of identified zip codes was $107,170 ($34,739–226,386). The median percentage of African

TABLE 1 | Selected patient characteristics.

Median Age (range)	Number (%)
69 (48-92)	
Race	
White	**423** (46%)
Black	**442** (48%)
Other	**58** (6%)
Risk group (D'Amico)	
Low	**185** (11%)
Intermediate	**511** (63%)
High	**228** (26%)
Treatment Modality	
SBRT monotherapy	**725** (79%)
SBRT boost	**198** (21%)
Travel Distance (miles)	
11.8 (0.44-222.2)	
Total Patients: 923	

Bold is number of patients.

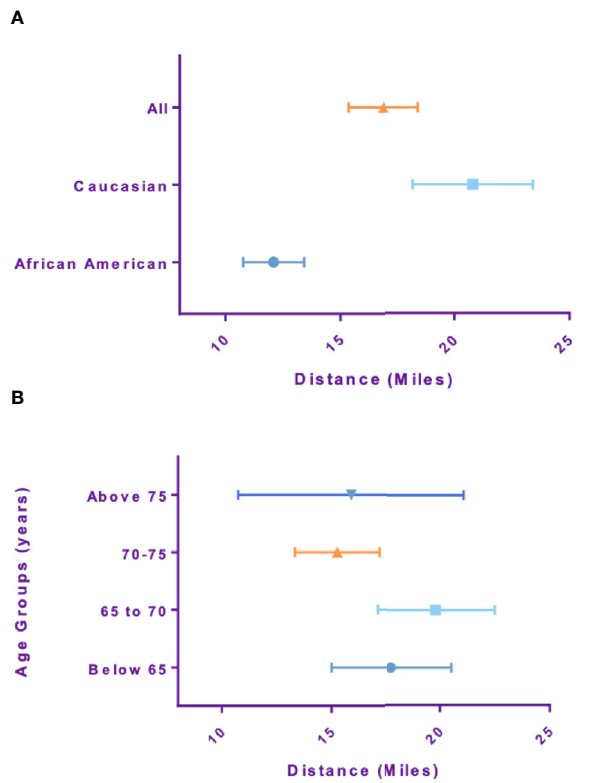

FIGURE 2 | Travel distance stratified by **(A)** race and **(B)** Age.

American residents in the zip codes analyzed was 21.39% (0%–100%). Approximately 6.9% of zip codes analyzed were considered rural based on rural residency (**Table 2**). Using an unsupervised K-means clustering algorithm which included the above characteristics as well as percentage uninsured and percentage high school graduates within each zip code, four distinct clusters with similar demographic features were identified (**Figure 3**). The clusters were characterized based on rural residency, African American population, and income, and

TABLE 2 | Selected patient demographics.

Demographic Feature Median (Range)	
Income (USD)	
	107,170 (34,739-226,386)
% African American Residents	
	21.39% (0%-100%)
% Rural Residents	
	6.9% (0%-100%)
% Un-Insured residents	
	6.5% (0-30.8%)

are referred to as: Urban, Suburban/high income, Suburban/low income and Rural clusters. Mean travel distance for the urban cluster was 9.26 miles, compared to 11.17 miles for Suburban/high income, 11.75 miles for Suburban/low income and 40.2 miles for the rural cluster. For each of the clusters, the average travel distance for SBRT was significantly different (p-value: <0.001). Incomes differed significantly between clusters with the urban clusters having the lowest income with a median income of $63,000 per household and the suburban/high income cluster having highest median income at $125,000 dollars per household. Racial make-up of each cluster differed significantly, with the urban cluster having an 82% African American population compared to suburban/high income at 9% (**Figure 4**).

DISCUSSION

SBRT for localized prostate cancer is increasingly offered as a treatment option that may reduce treatment related burden compared to conventionally fractioned EBRT. This treatment regimen has the potential advantage of being more accessible to patients than conventionally fractionated EBRT. We reviewed the demographic and geographic factors of patients treated with SBRT for localized prostate cancer at a single institution with over a decade of prostate SBRT experience. To our knowledge, this is the first study that examines patient utilization of prostate SBRT based on sociodemographic clusters derived from a machine learning algorithm. In this study, patient age, zip code, and race as well as US census data tied to patient zip codes were entered into an unsupervised K-means clustering algorithm to categorize geographical and demographical clusters.

Studies in the past have demonstrated travel distance as one of the factors that affects a patient's access to treatment and is often a consequence of other sociodemographic factors (15, 16). Mahal et al. identified distinct demographic features that correlate with travel distance specifically for prostate SBRT such as race, income and rural residency (16). In this study, travel distance was found to be a function of race, income and rural residency, consistent with findings from Mahal and colleagues (16). In our study, Caucasian patients traveled significantly further for their treatment than African American patients. However, it is noteworthy that the racial make-up of our study population for the most part, mirrored that of the general population of the community surrounding our institution, the District of Columbia (43% AA

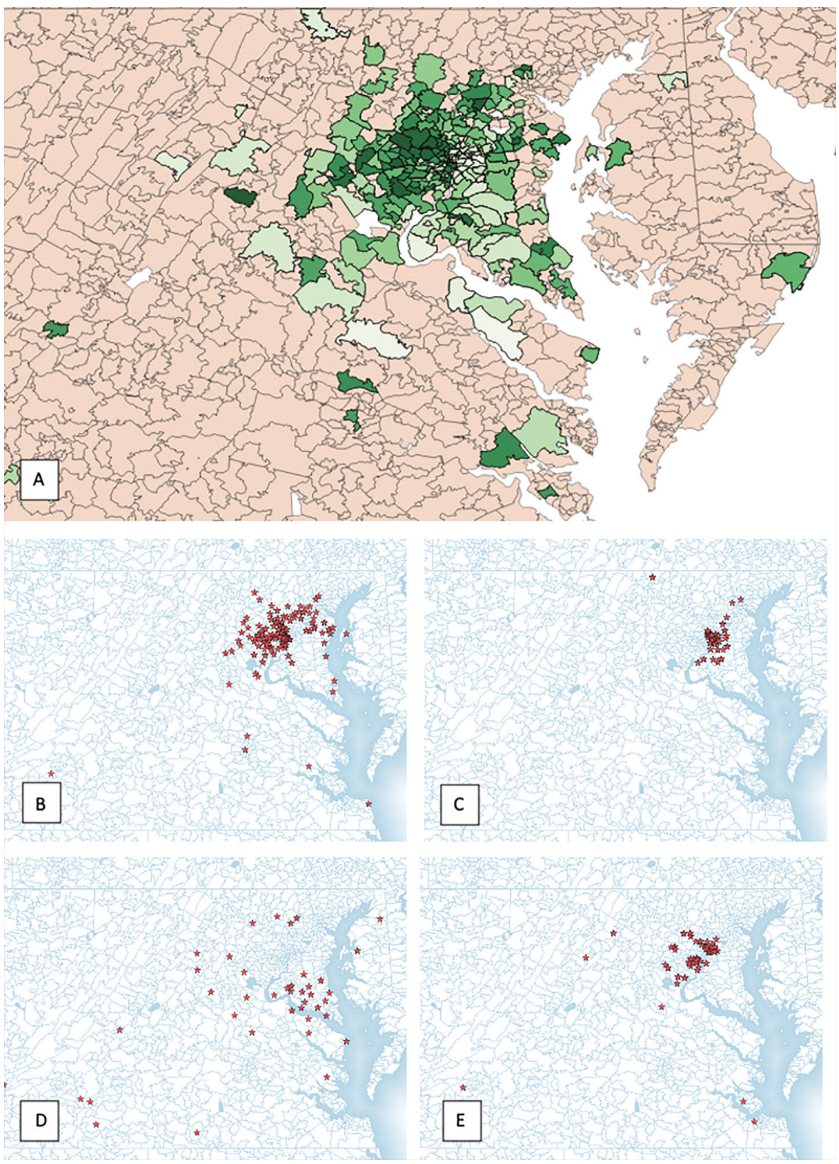

FIGURE 3 | **(A)** All patient zip codes mapped, **(B)** urban cluster, **(C)** suburban/high income cluster, **(D)** suburban/low income cluster and **(E)** rural cluster.

vs 46% AA, 53% Caucasian vs 46% Caucasian, respectively) (19). These findings imply that travel distance may be an incomplete proxy for access to care. Further, we found that our patients came from a relatively balanced mix of socio-demographic backgrounds with the majority coming from Urban, Suburban/low income and Rural clusters but not Suburban/high income. This finding is interesting as the clusters had significantly different median travel distances. Importantly, despite an almost 4-fold greater travel distance compared to their Urban and Suburban counterparts (40.2 vs 10.72 miles), patients from the rural cohort were able to access this treatment regimen. We suspect that this greater geographic accessibility is due to the reduced number of treatment sessions associated with SBRT as compared to conventionally fractionated EBRT. Interestingly, we found that the distance traveled for patients receiving SBRT boost and supplemental IMRT was significantly shorter than patients who were treated with SBRT alone. This is likely a result of the significantly higher number of treatments needed for the SBRT/IMRT combination, resulting in a greater treatment burden and lower geographic accessibility.

Travel distance stratified by risk group demonstrates a significantly lower distance traveled for individuals with high risk disease than with intermediate or low risk groups. Despite this, there was no significant difference in travel distance for individuals requiring a boost. This is likely because boost protocols include high risk and intermediate risk patients.

In prior studies, patients who are African American, under the age of 65, those with low income and/or with a low education

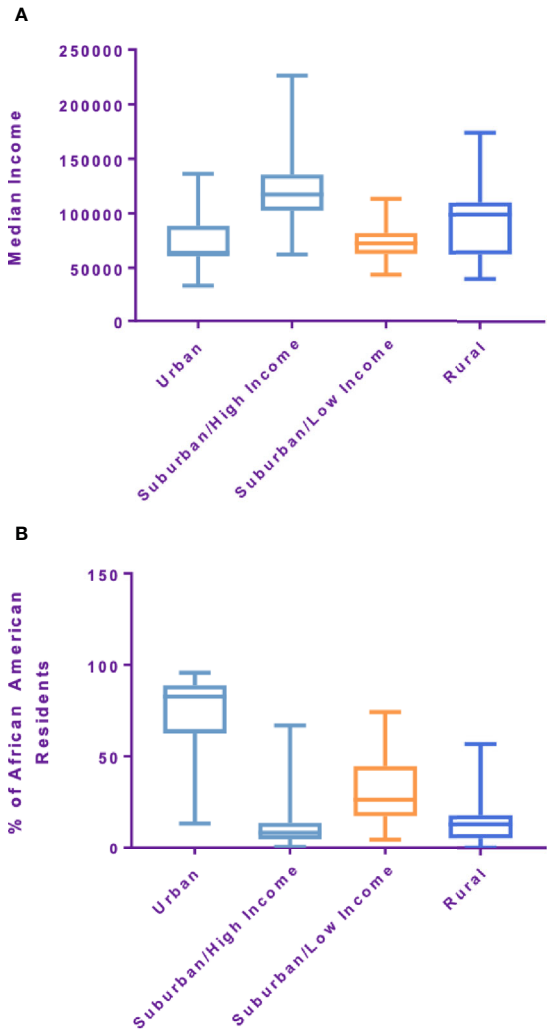

FIGURE 4 | **(A)** median income by cluster and **(B)** racial makeup by cluster.

level were identified as more likely to experience reduced access to cancer treatment (20, 21). In this study, we found significant utilization of prostate SBRT from African American, elderly, low income and rural communities. This suggests that utilization of SBRT for prostate cancer may improve access to patient populations that have historically faced a disproportionate barrier in treatment of their cancer. Decreasing the number of treatments to five may ease treatment burden and increase accessibility for logistically challenged and socioeconomically disenfranchised patients. Furthermore, SBRT may be an option for some patients to reduce financial toxicity related to their cancer care while achieving excellent disease specific outcomes (1).

Potential limitations of our study include the use of indirect patient characteristics based on US Census data, the exclusion of patients who traveled very long distances to receive treatment, the possibility of inaccuracies in the US Census data used and changes in the demographics of patients who utilized SBRT over the study period. Future directions include using artificial intelligence derived clusters to study disease specific end-points, patient reported outcomes and possibly to identify disparities that were missed when only considering single variables.

CONCLUSION

In this study, we examined distinct demographic features and their relationship with travel distance for prostate SBRT. Notably, travel distance did not prevent the uptake of this new technology for our African American, elderly or rural patients. Hence, prostate SBRT is a modern treatment modality that a diverse population can access, particularly for those who live significant distances from a treatment center. This is likely secondary to shortened treatment time offered by this technology compared to conventionally fractionated radiotherapy.

DATA AVAILABILITY STATEMENT

The raw data supporting the conclusions of this article will be made available by the authors, without undue reservation.

ETHICS STATEMENT

The studies involving human participants were reviewed and approved by Georgetown University Hospital IRB#: 2009-510. The patients/participants provided their written informed consent to participate in this study.

AUTHOR CONTRIBUTIONS

NA is lead author who participated in manuscript drafting, table/figure creation, and manuscript revision. MC, EW, and AP aided in table/figure creation and manuscript drafting and revisions. MA, TY, and MD assisted in data collection, organization, and manuscript revisions. SS, SC, DK, BC, and JL are senior authors who aided in drafting the manuscript and manuscript revision. JL is the corresponding author who initially developed the concept, drafted, and revised the manuscript. All authors contributed to the article and approved the submitted version.

FUNDING

This work was supported by NIH Grant P30CA051008 and grant R01MD012767 from the National Institute on Minority Health and Health Disparities (NIMHD), NIH to DK and SC.

REFERENCES

1. Kishan AU, Dang A, Katz AJ, Mantz CA, Collins SP, Aghdam N, et al. Long-term Outcomes of Stereotactic Body Radiotherapy for Low-Risk and Intermediate-Risk Prostate Cancer. *JAMA Netw Open* (2019) 2(2):e188006. doi: 10.1001/jamanetworkopen.2018.8006
2. Widmark A, et al. Ultra-hypofractionated versus conventionally fractionated radiotherapy for prostate cancer: 5-year outcomes of the HYPO-RT-PC randomised, non-inferiority, phase 3 trial. *Lancet* (2019) 394:385–95. doi: 10.1016/S0140-6736(19)31131-6
3. Jacobs BL, et al. The early adoption of intensity-modulated radiotherapy and stereotactic body radiation treatment among older Medicare beneficiaries with prostate cancer. *Cancer* (2017) 123:2945–54. doi: 10.1002/cncr.30574
4. Hodges JC, et al. Cost-effectiveness analysis of stereotactic body radiation therapy versus intensity-modulated radiation therapy: an emerging initial radiation treatment option for organ-confined prostate cancer. *J Oncol Pract* (2012) 8:e31s–7s. doi: 10.1200/JOP.2012.000548
5. Amin N, Sher D, Konski A. Systematic Review of Cost Effectiveness of Radiation Therapy for Prostate Cancer from 2203-2013. *Appl Health Econom Health Policy* (2003) 12:391–408. doi: 10.1007/s40258-014-0106-9
6. Guy G, Ekwueme D, Yabroff KR, Dowling E, Li C, Rodriguez J. Economic Burden on Cancer Survivorship Among Adults in the United States. *J Clin Oncol* (2013) 31:3749–57. doi: 10.1200/JCO.2013.49.1241
7. Ambroggi M, Biasini C, Giovane CD, Fornari F, Cavanna L. Distance as a Barrier to Cancer Diagnosis and Treatment: Review of the Literature. *Oncol* (2015) 20:1378–85. doi: 10.1634/theoncologist.2015-0110
8. Puts MTE, Tu HA, Tourangeau D, Howell D, Fitch M, Springall E, et al. Factors influencing adherence to cancer treatment in older adults with cancer: a systematic review. *Ann Oncol* (2014) 25:564–77. doi: 10.1093/annonc/mdt433
9. Athas WF, Adams-Cameron M, Hunt WC, Amir-Fazli A, Key CR. Travel Distance to Radiation Therapy and Receipt of Radiotherapy Following Breast-Conserving Surgery. *JNCI J Natl Cancer Inst* (2000) 92:269–71. doi: 10.1093/jnci/92.3.269
10. Syed ST, Gerber BS, Sharp LK. Traveling Towards Disease: Transportation Barriers to Health Care Access. *J Community Health* (2013) 38:976–93. doi: 10.1007/s10900-013-9681-1
11. Unger JM, Gralow JR, Albain KS, Ramsey SD, Hershman DL. Patient Income Level and Cancer Clinical Trial Participation: A Prospective Survey Study. *JAMA Oncol* (2016) 2:137–9. doi: 10.1001/jamaoncol.2015.3924
12. Wolfson J, Sun CL, Wyatt L, Hurria A, Bhatia S. Impact of Care at a Comprehensive Cancer Centers on Outcome - Results from a Population-based Study. *Cancer* (2015) 121:3885–93. doi: 10.1002/cncr.29576
13. Paulson EC, Mitra N, Sonnad S, Armstrong K, Kelz RR, Mahmoud NN. National Cancer Institute designation predicts improved outcomes in colorectal cancer surgery. *Ann Surg* (2008) 248:675–86. doi: 10.1097/SLA.0b013e318187a757
14. Onega T, Duell E, Shi X, Demidenko E, Gottlieb D, Goodman D. Influence of NCI Cancer Center Attendance on Mortality in Lung, Breast, Colorectal, and Prostate Cancer Patients. *Med Care Res Rev* (2009) 66:542–60. doi: 10.1177/1077558709335536
15. Meden T, St. John-Larkin C, Hermes D, Sommerschield S. Relationship Between Travel Distance and Utilization of Breast Cancer Treatment in Rural Northern Michigan. *JAMA* (2002) 287:111–1. doi: 10.1001/jama.287.1.111-JMS0102-5-1
16. Mahal BA, Chen YW, Sethi RV, Padilla OA, Yang D, Chavez J, et al. Travel distance and stereotactic body radiotherapy for localized prostate cancer. *Cancer* (2018) 124:1141–9. doi: 10.1002/cncr.31190
17. Kataria S, Koneru H, Guleria S, Danner M, Ayoob M, Yung T, et al. Prostate-Specific Antigen 5 Years following Stereotactic Body Radiation Therapy for Low- and Intermediate-Risk Prostate Cancer: An Ablative Procedure? *Front Oncol* (2017) 7:157–7. doi: 10.3389/fonc.2017.00157
18. Engl E, Smittenaar P, Sgaier S. Identifying population segments for effective design and targeting using unsupervised machine learning: an end-to-end guide. Gates Open Research. (2019). doi: 10.12688/gatesopenres.13029.1
19. U.S. Census Bureau. *QuickFacts: District of Columbia*. (2018). Available at: https://www.census.gov/quickfacts/DC.
20. Pietro GD, Chornokur G, Kumar NB, Davis C, Park JY. Racial Differences in the Diagnosis and Treatment of Prostate Cancer. *Int Neurourol J* (2016) 20:S112–9. doi: 10.5213/inj.1632722.361
21. Bernard DSM, Farr SL, Fang Z. National estimates of out-of-pocket health care expenditure burdens among nonelderly adults with cancer: 2001 to 2008. *J Clin Oncol Off J Am Soc Clin Oncol* (2011) 29:2821–6. doi: 10.1200/JCO.2010.33.0522

Conflict of Interest: SC, BC, and JL serve as clinical consultants to Accuray Inc.

The remaining authors declare that the research was conducted in the absence of any commercial or financial relationships that could be construed as a potential conflict of interest.

frontiers in Oncology

ORIGINAL RESEARCH
published: 09 March 2021
doi: 10.3389/fonc.2020.608750

Magnetic Resonance Imaging-Based Robotic Radiosurgery of Arteriovenous Malformations

Tobias Greve[1], Felix Ehret[2†], Theresa Hofmann[2], Jun Thorsteinsdottir[1], Franziska Dorn[3], Viktor Švigelj[4], Anita Resman-Gašperšič[4], Joerg-Christian Tonn[1], Christian Schichor[1] and Alexander Muacevic[2]*

[1] Department of Neurosurgery, University Hospital, LMU Munich, Munich, Germany, [2] European Cyberknife Center Munich-Grosshadern, Munich, Germany, [3] Institute of Neuroradiology, University Hospital, LMU Munich, Munich, Germany, [4] Division of Neurology, University Medical Center Ljubljana, Ljubljana, Slovenia

OPEN ACCESS

Edited by:
Yidong Yang, University of Science and Technology of China, China

Reviewed by:
Chunhao Wang, Duke University Medical Center, United States
John E. Mignano, Tufts University School of Medicine, United States

***Correspondence:**
Tobias Greve
tobias.greve@med.uni-muenchen.de

†ORCID:
Felix Ehret
orcid.org/0000-0001-6177-1755

Specialty section:
This article was submitted to Radiation Oncology, a section of the journal Frontiers in Oncology

Received: *21 September 2020*
Accepted: *21 December 2020*
Published: *09 March 2021*

Citation:
Greve T, Ehret F, Hofmann T, Thorsteinsdottir J, Dorn F, Švigelj V, Resman-Gašperšič A, Tonn J-C, Schichor C and Muacevic A (2021) Magnetic Resonance Imaging-Based Robotic Radiosurgery of Arteriovenous Malformations. Front. Oncol. 10:608750. doi: 10.3389/fonc.2020.608750

Objective: CyberKnife offers CT- and MRI-based treatment planning without the need for stereotactically acquired DSA. The literature on CyberKnife treatment of cerebral AVMs is sparse. Here, a large series focusing on cerebral AVMs treated by the frameless CyberKnife stereotactic radiosurgery (SRS) system was analyzed.

Methods: In this retrospective study, patients with cerebral AVMs treated by CyberKnife SRS between 2005 and 2019 were included. Planning was MRI- and CT-based. Conventional DSA was not coregistered to the MRI and CT scans used for treatment planning and was only used as an adjunct. Obliteration dynamics and clinical outcome were analyzed.

Results: 215 patients were included. 53.0% received SRS as first treatment; the rest underwent previous surgery, embolization, SRS, or a combination. Most AVMs were classified as Spetzler-Martin grade I to III (54.9%). Hemorrhage before treatment occurred in 46.0%. Patients suffered from headache (28.8%), and seizures (14.0%) in the majority of cases. The median SRS dose was 18 Gy and the median target volume was 2.4 cm^3. New neurological deficits occurred in 5.1% after SRS, with all but one patient recovering. The yearly post-SRS hemorrhage incidence was 1.3%. In 152 patients who were followed-up for at least three years, 47.4% showed complete AVM obliteration within this period. Cox regression analysis revealed Spetzler-Martin grade ($P = 0.006$) to be the only independent predictor of complete obliteration.

Conclusions: Although data on radiotherapy of AVMs is available, this is one of the largest series, focusing exclusively on CyberKnife treatment. Safety and efficacy compared favorably to frame-based systems. Non-invasive treatment planning, with a frameless SRS robotic system might provide higher patient comfort, a less invasive treatment option, and lower radiation exposure.

Keywords: CyberKnife, radiosurgery, stereotactic, arteriovenous malformation, Gammaknife surgery

INTRODUCTION

Cerebral arteriovenous malformations (AVMs) consist of a complex tangle of abnormal blood vessels - the nidus, which does not clearly correspond to an artery or vein and lacks a physiological capillary bed. With an annual detection rate of one per 100,000, AVMs are a rare but significant vascular pathology (1). If ruptured, AVMs can cause substantial morbidity and mortality. Current treatment protocols are based on a detailed assessment of the risk of spontaneous bleeding during the natural course of the disease versus the risk of invasive AVM treatments (2).

Stereotactic radiosurgery (SRS), alone or in combination with embolization, is an important treatment option for intracranial AVMs, especially if the lesion is not eligible for surgery or embolization or if only partial occlusion can be achieved after embolization (3). In general, a high prescription dose between 15 and 25 Gy is required to obliterate AVMs by SRS. However, a prolonged median time to complete obliteration of around three years is described in the literature and is a known limitation of radiosurgery (4–6). Determinants of obliteration latency have been investigated in the past for various SRS systems such as Gamma Knife (7) and LINAC systems (8) but studies focusing on CyberKnife treatment of AVMs is sparse.

The comprehensive diagnostic work-up of AVMs is based on magnetic resonance imaging (MRI) for topography and digital subtraction angiography (DSA) for flow dynamics. Additionally, a planning CT angiography is necessary for image coregistration in all above-mentioned SRS systems. The Gamma Knife system is frame-based (9) and LINAC SRS systems are usually (but not exclusively) frame-based as well (10), meaning that a stereotactic frame has to be mounted to the patient before they receive the planning CT which is later referenced to the MRI. If the practitioner needs an exact overlay of the DSA with the MRI and CT images for nidus definition, the DSA has to be acquired with a stereotactic frame as well (11, 12). The acquisition of a stereotactic DSA is a time-consuming procedure compared to conventional DSA because the frame has to be mounted using local anesthesia and many patients even require general anesthesia throughout the whole acquisition process. DSA with external localizers or fiducials was shown to be feasible but is not yet established in clinical routine (13–15).

In contrast to frame-based systems, the CyberKnife system (Accuray, Inc., Sunnyvale, CA) relies on real-time image correction during the procedure without the necessity of a stereotactic frame (16). Therefore, computerized treatment planning is solely based on CT and MRI data. DSA is usually used solely as adjunct information without exact image-overlay.

Indeed, MR angiography (MRA) was shown to provide the possibility of non-invasive AVM examination without the need for an additional invasive DSA (17–23). The integration of high-resolution MRI scans into the treatment planning process of the CyberKnife and their use in subsequent follow-up studies have been proven feasible (24).

The objective of this study was to analyze the efficacy and safety of CyberKnife SRS treatment of intracranial AVMs in a large cohort of patients. Planning was based on coregistered MRI and CT images only, using a conventional non-coregistered DSA solely as an adjunct.

METHODS

Study Design

In this retrospective, single-center, non-randomized study patient characteristics, pre-treatment status, radiation parameters, and outcome were collected in our database. Between 2005 and 2019, 270 patients received CyberKnife SRS for cerebral AVMs and were screened for eligibility for this study. Patients were excluded if they were below the age of 18 (n = 18), were treated for spinal AVM (n = 9), or if the follow-up period was less than 5 months (n = 23). Five additional patients were excluded due to a combination of those criteria. Accordingly, 215 patients were included in this retrospective analysis (**Figure 1**). Subgroup analysis was performed in patients meeting the inclusion criteria of the ARUBA study ("A Randomized Trial of Unruptured Brain AVMs"): unruptured AVMs, Spetzler-Martin grade < V, no previous treatment and good Karnofsky performance status ≥ 80% before treatment (25). Obliteration rates were evaluated in patients with at least three years of follow-up.

Written consent to use the collected data for this retrospective analysis was obtained from every patient before treatment. All procedures were in accordance with institutional guidelines. This study was approved by the institutional review board (accession number 20-250KB).

Study Parameters

Basic demographics and AVM specifications were extracted from our database. Pre-treatment work-up consisted of a DSA (**Figures 2A, B**), a CT angiography (with contrast injection) as well as a dedicated MRI study with 1 mm slice thickness (**Figures 2C, D**). The pre-treatment non-stereotactic (acquired without stereotactic frame) DSA solely served as adjunct information and was not coregistered with treatment planning CT and MRI studies. AVMs were classified using the Spetzler-Martin grading system (26), with a score of VI being attributed to inoperable lesions. Furthermore, the radiosurgery-based AVM score was calculated (27). It is a score on a continuous scale which includes AVM volume, patient age and deep localization and was previously shown to predict outcome after radiosurgery (28, 29).

CyberKnife Treatment

The CyberKnife robotic SRS system consists of a 6-MV compact linear accelerator mounted on a computer-controlled, 6-axis robotic manipulator (16). Integral to the system are orthogonally positioned x-ray cameras for image acquisition during treatment. These images are processed automatically to identify specific cranial bone structures. The information is then referenced to the CT angiography study to determine the exact position of the SRS target in real-time and to compensate for changes in patient position during treatment. The treatment

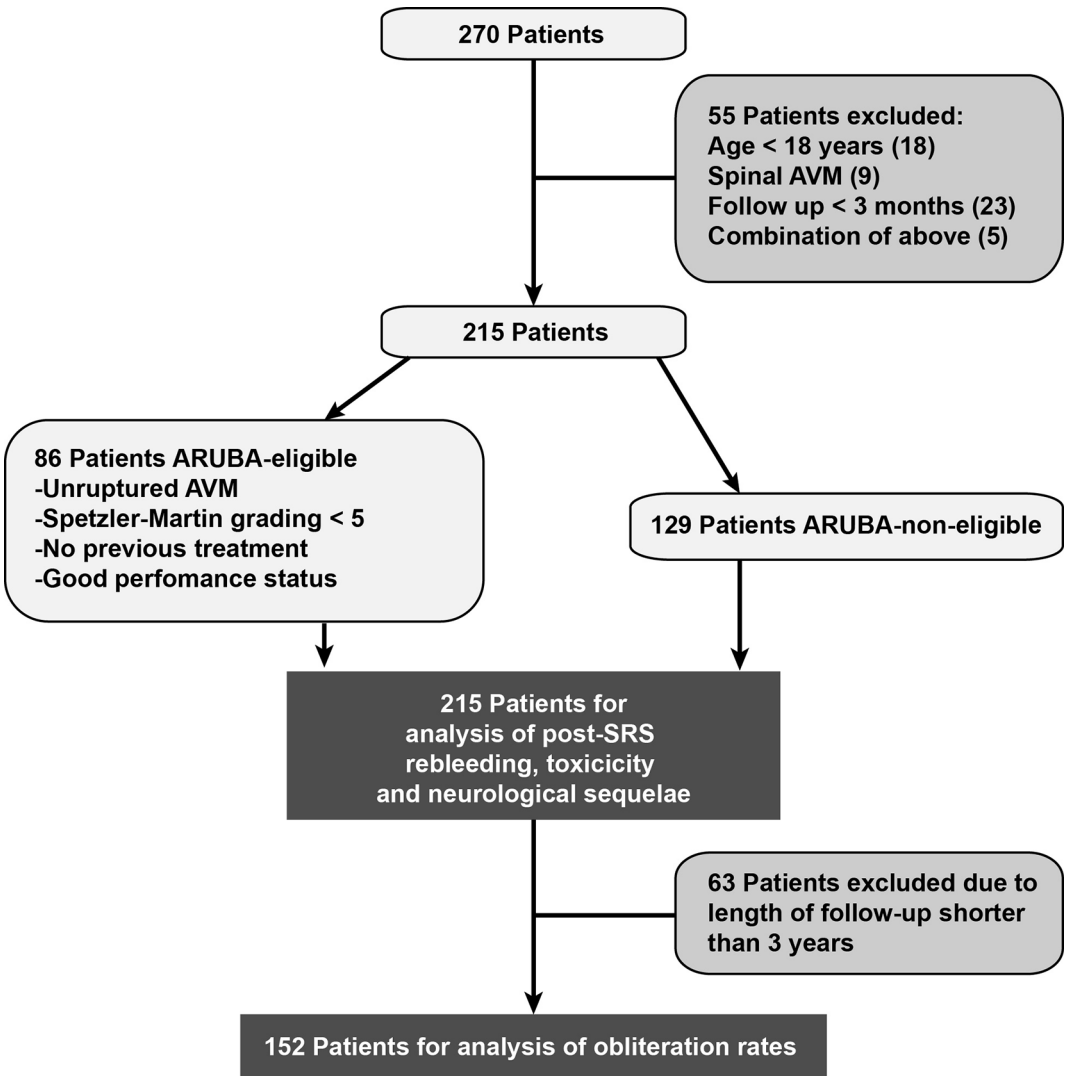

FIGURE 1 | Patient inclusion scheme.

principle of the CyberKnife represents a noncoplanar, nonisocentric dose delivery. The precision of the CyberKnife technology was shown to be comparable to published frame-based SRS systems (30). Dose determination and target volume planning was achieved with various versions of the MultiPlan and Precision planning softwares (Accuray Inc., Sunnyvale, CA, USA) analogously to previous publications (24) (**Figure 3**).

For each patient, a 1 mm isotropic T1 post-gadolinium and a 1 mm isotropic T2 MRI sequence were coregistered with the CT images to verify correct AVM topography during dose planning. Although primary DSA imaging was taken into account during target delineation, it was not coregistered with the other imaging modalities. Volume-staged CyberKnife SRS (subdivision of the target volume with sequential CyberKnife SRS sessions separated by intervals of days to weeks) was not performed. In patients with multiple target volumes, the absolute target volume and dose were used for further analysis.

Definition of Obliteration and Follow-Up

After SRS, patients were followed up clinically and by MRI scans at 6-month intervals. The standard MRI protocol included 1 mm isotropic T1 post-gadolinium and 1 mm isotropic T2 morphological sequences and a 3D TOF MRA. Volumetric characterization of the nidus was performed with various versions of the MultiPlan and Precision planning software (Accuray Inc., Sunnyvale, CA, USA).

In line with existing literature (31), partial obliteration in MRI was defined as a reduction of the original AVM nidus volume of 50-95%. Complete obliteration was defined as > 95% reduction of the original AVM nidus volume combined with absence of early contrast filling of a draining vein in time-resolved MRA (**Figures 2F, G**).

If the MRI scan indicated complete obliteration, the patient was recommended to obtain a DSA to verify complete AVM obliteration. If the MRI did not indicate a complete obliteration, a DSA was recommended after three years at the latest. Although DSA was recommended to all patients, only some of the patients

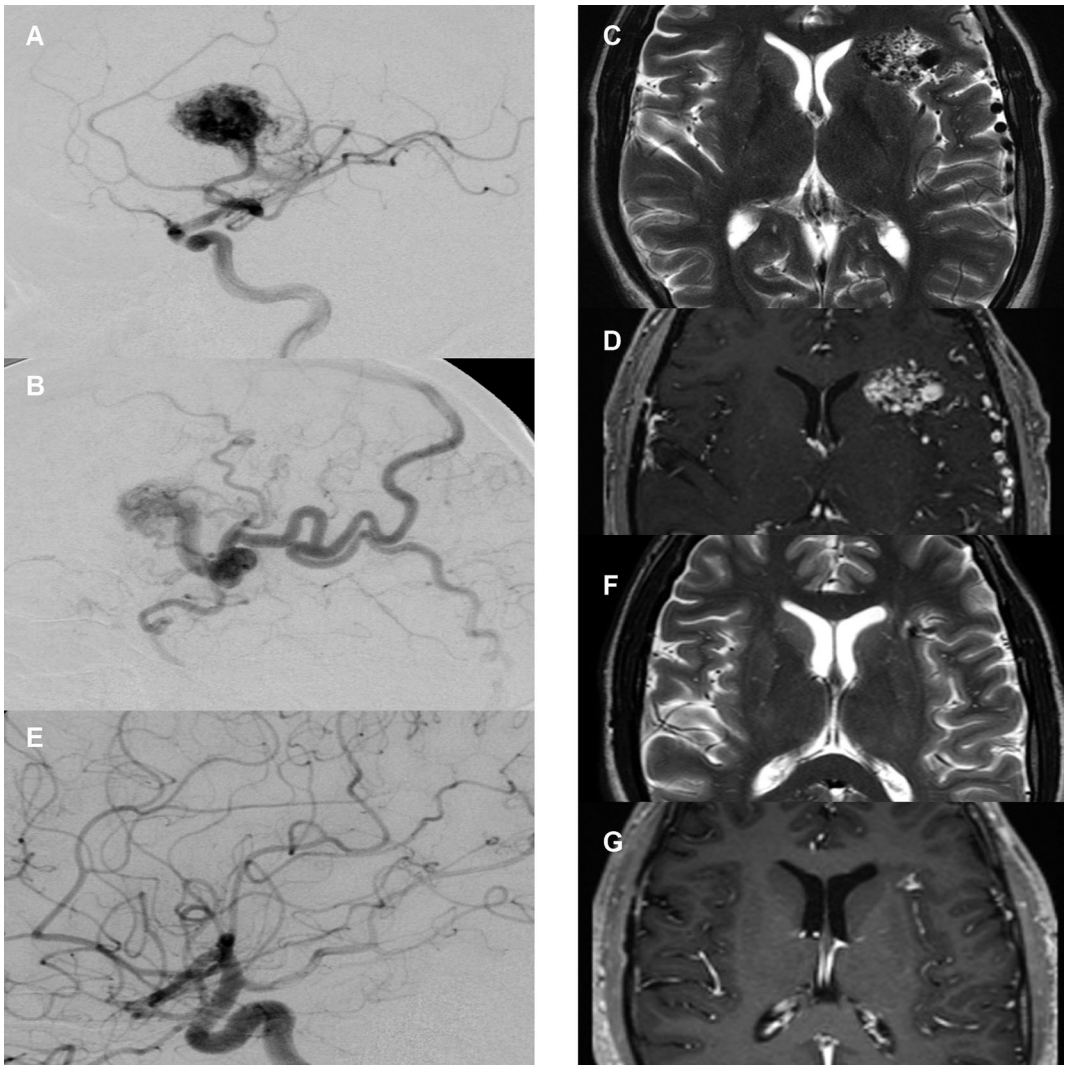

FIGURE 2 | Case illustration. **(A)** Pre-treatment digital subtraction angiography (DSA), lateral view, arterial phase. Depiction of right frontal arteriovenous malformation (AVM) supplied by the medial cerebral artery with large nidus. **(B)** Pre-treatment DSA, lateral view, early venous phase. Depiction of diluted cortical veins. **(C)** Pre-treatment T2-sequence magnetic resonance imaging (MRI) with depiction of AVM nidus and diluted veins. **(D)** Pre-treatment T1-MR-angiography of the same area. **(E)** 2-year post-treatment follow-up DSA, arterial phase with no residual nidus or early venous drainage. **(F)** 2-year post-treatment follow-up T2-sequence MRI with depiction of a small residual lesion without T2-hyperintense radiation induced changes. **(G)** 2-year post-treatment follow-up T1-MR-angiography with depiction of small residual contrast enhancement.

had this test performed. However, both patients with and without follow up DSA were included in the analysis.

In DSA follow-up imaging, partial obliteration was defined as disappearance of the AVM nidus with persistence of an early filling draining vein, indicating that residual shunting is still present. Complete obliteration was defined as disappearance of the AVM nidus without any early filling draining vein (**Figure 2E**).

Statistics

An univariate analysis was performed for factors favoring AVM obliteration within three years. For this purpose, continuous variables were tested for normal distribution using the Shapiro-Wilk test, with only age being found to be normally distributed. Consequently, the descriptive statistics in the tables are listed as median and interquartile range (IQR). IQR measures statistical dispersion in non-normally distributed data, equal to the difference between 75th and 25th percentiles, or between upper and lower quartiles. The t-test was used to compare age and the Mann-Whitney U-test to test all other continuous variables between patients with and without complete obliteration within 36 months. The distribution of ordinal and nominal scaled variables between patients with and without complete obliteration within three years was analyzed using the exact Fisher test and the Chi-square test. The cumulative probability of partial and complete obliteration was evaluated using Kaplan-

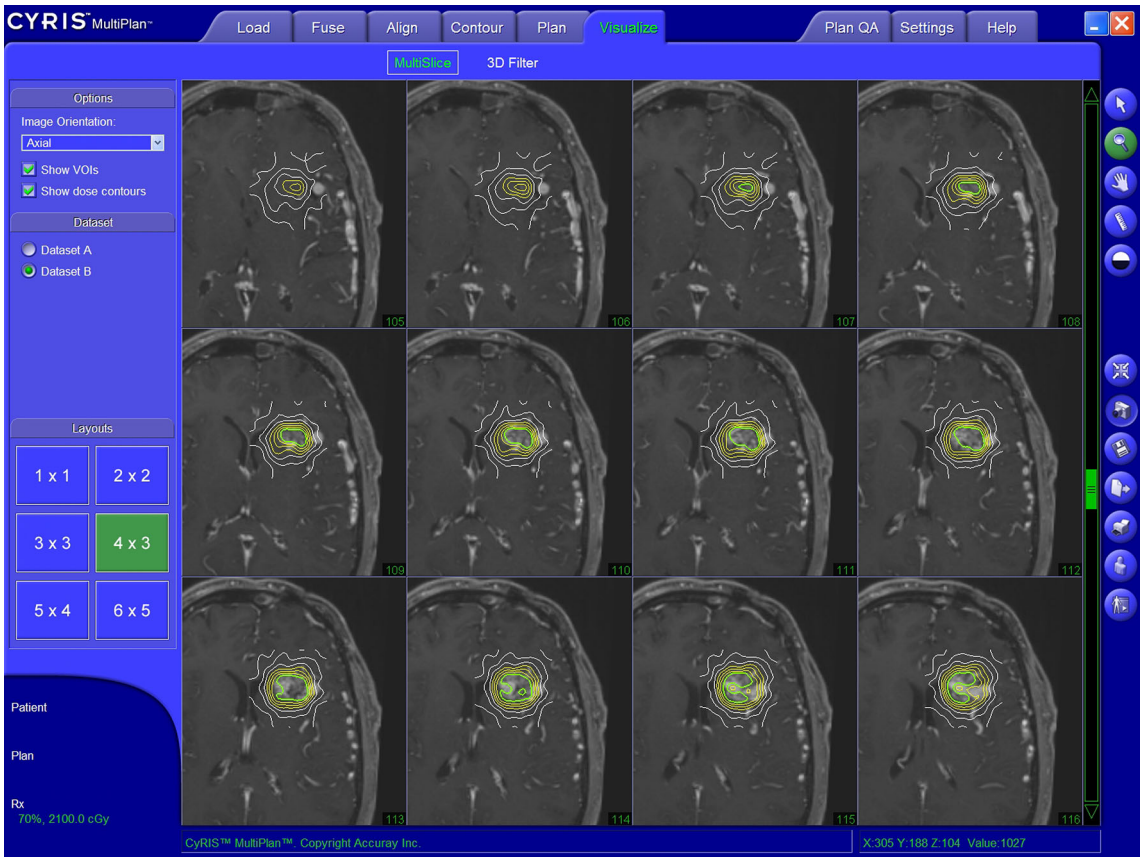

FIGURE 3 | Illustratory target volume planning achieved with the MultiPlan planning software (Accuray Inc., Sunnyvale, CA, USA).

Meier statistics. Factors associated with obliteration within three years were tested in a multivariate Cox regression model. A significance level of $p < 0.05$ was chosen for the tests. SPSS version 25 (IBM) was used for statistical calculations.

RESULTS

Patient Demographics

Of 215 included patients, 49.3% were female, and the median age was 40.4 years (range 18.3–79.8 years). The overall rate of cardiovascular risk factors was low, with arterial hypertension being the main contributor (n = 18). One hundred seventy-four (80.9%) patients had a supratentorial localization of the AVM, while 41 (19.1%) patients presented with infratentorial localization. The majority consisted of Spetzler-Martin grade I to III AVMs (118, 54.9%), while 69 (32.1%) lesions were classified as Spetzler-Martin grade IV or V and 28 (13.0%) were inoperable AVM lesions, classified as Spetzler-Martin grade ≥ IV.

The most frequent presenting symptom was headache (n = 62, 28.8%). AVM associated hemorrhage before treatment was detected in 99 (46.0%) patients. In 15 cases, hemorrhaged AVMs were operated upon to evacuate the hematoma. In 39 cases, the bleeding was eloquently located and did not justify the risk of surgical decompression. In the other 45 cases of the 99 with an associated hemorrhage, the bleeding was small, asymptomatic and did not require hematoma evacuation. Of all patients with an associated hemorrhage, 16 (7.4%) were asymptomatic, 41 (19.1%) had neurological deficits, 13 (6.0%) had headache, 6 (2.8%) presented with epilepsy and 23 (10.7%) had a combination of those symptoms (**Table 1**).

While 114 (53.0%) patients received no previous treatment, 23 (10.7%) were previously subjected to surgery alone or in combination with embolization, 16 (7.4%) were previously subjected to SRS, alone or in combination with embolization, and 62 (28.8%) were previously subjected to embolization alone.

Of the 23 patients who received a previous surgery, 11 were internal referrals and 12 were externally referred to receive CyberKnife SRS at our center. Of the 11 internal referrals, 5 only received surgical hematoma evacuation, because the AVM was non-amenable to resection. Five showed minimal residual AV-shunting on postoperative DSA and one patient had a partial AVM resection.

Treatment Details and Follow-Up Imaging

Of all AVMs treated with CyberKnife SRS, 210 (97.7%) had single targets at the nidus while five (2.3%) had multiple target

TABLE 1 | Patient demographics and characterization of arteriovenous malformations.

Variable		Value
Subjects, N		215
Age, median years ± SD		40.4 ± 13.3
Sex, female		106 (49.3%)
Hypertension		18 (8.4%)
Nicotine abuse		8 (3.7%)
AVM side, left		116 (54.0%)
AVM size	Small (diameter < 3 cm)	121 (56.3%)
	Medium (diameter 3–6 cm)	49 (22.8%)
	Large (diameter > 6 cm)	45 (20.9%)
	Maximum volume	35.7 cm^3
AVM localization	Lobar	148 (68.8%)
	Infratentorial	41 (19.1%)
	Eloquent	72 (33.5%)
AVM venous drainage pattern	Superficial only	136 (63.3%)
	Any deep	79 (36.7%)
Spetzler-Martin grade	I	13 (6.0%)
	II	42 (19.5%)
	III	63 (29.3%)
	IV	48 (22.3%)
	V	21 (9.8%)
	VI	28 (13.0%)
Radiosurgery-based AVM score	Median (IQR)	1.36 [1.11–1.70]
	Range	0.45–4.67
AVM-associated arterial aneurysm		10 (4.7%)
AVM-associated hemorrhage		99 (46.0%)
Previous treatment	None	114 (53%)
	Embolization	62 (28.8%)
	Surgery	10 (4.7%)
	Surgery & embolization	12 (5.6%)
	SRS	6 (2.8%)
	SRS & embolization	10 (4.7%)
	SRS & surgery & embolization	1 (0.5%)
Clinical presentation	Seizure	30 (14.0%)
	Headache	62 (28.8%)
	Focal deficit	63 (29.3%)
	Other deficit	36 (16.7%)
	Asymptomatic	35 (16.3%)

If not otherwise indicated, frequencies are presented as n (%). AVM, arteriovenous malformation; SD, standard deviation; IQR, interquartile range; SRS, stereotactic radiosurgery; Eloquent is any AVM location involving the sensorimotor, language, or visual cortex; the hypothalamus and thalamus; the internal capsule; the brainstem; the cerebellar peduncles; or the deep cerebellar nuclei. Associated arterial aneurysms are flow-related aneurysms located on a feeding artery or within the AVM nidus (so-called intranidal aneurysms). Other deficits include gait ataxia, vertigo, cognitive deficits, and fatigue.

volumes. The median dose was 18 Gy (range, 15–30 Gy). Of all patients treated for AVMs with CyberKnife, all but one patient received a maximum of 25 Gy. There was one patient who received 29.58 Gy. He had a very small high flow AVM/fistula with a volume of 0.4 cc which explains the high focal dose. The median prescription isodose line was 85%. There was a wide range of target volumes (0.1 cm^3 to 35.7 cm^3) with the median being 2.4 cm^3. The Spearman-Rho correlation coefficient between target volume and coverage was 0.157. This value shows that smaller tumors do not manifest an increased coverage or vice versa. The range of follow-up was 5.6 to 165.9 months, with a median value of 40.2 months. All patients were recommended to obtain a DSA after 3 years or if obliteration was suspected in MRI. In all 152 patients who were included in the efficacy analysis (minimum follow-up of three years), 76 (50.0%) were followed-up by DSA while the rest failed to provide a DSA follow-up study, mostly due to its invasive nature and logistic effort (**Table 2**).

Neurological Deficits and Treatment-Related Morbidity

Patients presented with a median Karnofsky performance status of 90% (range, 40%–100%) before SRS. The median Karnofsky performance status did not change at first and last follow-up.

Thirty patients (14.0%) presented with symptomatic epilepsy before SRS treatment. After SRS treatment, 29 patients (13.5%) developed new seizures. Of all 59 patients manifesting symptomatic epilepsy before or after SRS, 36 (16.7%) were adequately controlled with medication.

During the follow-up period, 73 (73.7%) of 99 patients with neurological deficits recovered completely or partially.

There were 11 (5.1%) new neurological deficits after SRS, with ten recovering partially or completely (hemiparesis, cerebellar symptoms, aphasia, cognitive deficits, fatigue) and one visual field deficit not recovering completely. Bivariate analysis revealed that the proportion of patients with new deficits after SRS was higher in those that received previous SRS (17.6% versus 4%, p = 0.015). Similarly, AVMs with a high

TABLE 2 | CyberKnife radiosurgery and follow-up imaging.

Variable		Value
Dose, median Gy (IQR)		18.0 [17.0– 20.0]
Prescription isodose, median % (IQR)		85.0 [70.0–85.0]
Target volume	Median cm^3 (IQR)	2.4 [0.9–5.0]
	Range cm^3	0.1–35.7
Homogeneity index	Median (IQR)	1.18 [1.18–1.43]
Conformity index	Median (IQR)	1.18 [1.12–1.25]
Coverage to GTV	Median (IQR)	96% [92.5–97.7%]
Follow-up period	Median months (IQR)	40.2 [21.6–786]
	Range months	5.6–165.9
Follow-up imaging in all patients	MRI	139 (64.7%)
	MRI and DSA	76 (35.3%)
Follow-up imaging in patients included in efficacy analysis	MRI	76 (50.0%)
	MRI and DSA	76 (50.0%)
Discrepancies between MRI and DSA	MRI inconclusive, DSA shows complete obliteration	10 (5.2%)
	MRI suggests higher grade of obliteration than DSA	0
Post-SRS hemorrhage	Overall	12 (5.6%)
	With pre-SRS hemorrhage (N 93)	6 (6.5%)
	ARUBA-eligible (N 86)	0
Yearly post-SRS hemorrhage risk	Incidence (95% CI)	1.3% [0.7–2.3%]

When not otherwise indicated, frequencies are presented as n (%). SRS, stereotactic radiosurgery; MRI, magnetic resonance imaging; DSA, digital subtraction angiography; IQR, interquartile range; CI, confidence interval; GTV, gross treatment volume.

Spetzler-Martin grading were significantly more at risk for a new deficit after SRS. While patients with a Spetzler-Martin grade I or II lesion developed no new deficit, patients with grade III or IV lesions developed three (2.7%) new deficits and patients with grade V or VI lesions developed eight (16.3%) new deficits ($p < 0.001$). Furthermore, a lower median prescription isodose line was associated with new deficits (70% versus 85%, $p = 0.022$).

Twelve (5.6%) patients developed an AVM related intracerebral hemorrhage after SRS, two of whom died and seven of whom presented with a new neurological deficit. A bivariate risk factor analysis showed that higher single dose (22.5 Gy versus 17.5 Gy, $p = 0.003$) and a lower median prescription isodose line (67.5% versus 85%, $p < 0.001$) were associated to hemorrhage after SRS.

The yearly post-SRS hemorrhage incidence was 1.3% in patients with no or partial obliteration. Four additional deaths were non-related to the AVM or SRS treatment (**Table 3**).

TABLE 3 | Morbidity and mortality.

Variable		Value
Karnofsky performance status before SRS	Median (IQR)	90% [90–100%]
	Range	40–100%
Karnofsky performance status at first follow-up	Median (IQR)	90% [90–100%]
	Range	40–100%
Karnofsky performance status at last follow-up	Median (IQR)	90% [90–100%]
	Range	40–100%
Seizures	None	156 (72.3%)
	Presenting symptom	30 (14.0%)
	Onset after radiosurgery	29 (13.5%)
Headache	None	147 (68.4%)
	Presenting symptom	62 (28.8%)
	Onset after radiosurgery	6 (2.8%)
Neurological deficits before SRS	None	116 (54%)
	Visual field deficits	25 (11.6%)
	Monoparesis	12 (5.6%)
	Hemisyndrome without aphasia	10 (4.7%)
	Vertigo	9 (4.2%)
	Cerebellar symptoms	10 (4.7%)
	Hypesthesia	7 (3.3%)
	Diplopia	7 (3.3%)
	Aphasia	5 (2.3%)
	Fine motor skills	5 (2.3%)
	Facial palsy	3 (1.4%)
	Hemisyndrome with aphasia	3 (1.4%)
	Cognitive deficits	2 (0.9%)
	Fatigue	1 (0.5%)
Course of neurological deficits (N 90) after SRS	No recovery	24 (26.7%)
	Partial recovery	40 (44.4%)
	Full recovery	18 (20.0%)
	Worsened after SRS, no recovery	2 (2.2%)
	Worsened after SRS, partial recovery	10 (11.1%)
New deficits after SRS	Overall	11 (5.1%)
	Facial palsy (full recovery)	1
	Monoparesis (partial recovery)	1
	Coordination (full recovery)	2
	Visual field deficits (no & partial recovery)	3
	Aphasia (partial recovery)	1
	Hemisyndrome (partial recovery)	1
	Cognitive deficits (partial recovery)	1
	Fatigue (full recovery)	1
Death	AVM related	2 (0.9%)
	Non-related to AVM	4 (1.9%)

When not otherwise indicated, frequencies are presented as n (%). AVM, arteriovenous malformation; IQR, interquartile range; SRS, stereotactic radiosurgery.

Treatment Efficacy

Obliteration rates were calculated in 152 patients who were followed-up for at least 3 years. Of those, 72 (47.4%) had a complete AVM obliteration within the first 3 years after SRS and 80 (52.6%) had a persisting AVM lesion (**Table 4**). Of those without complete obliteration after three years, 31 (20.4%) eventually obliterated until last follow-up so that the cumulative complete obliteration rate was 67.7% ($n = 103$).

The median time to complete obliteration was 41.6 months and the median time to partial obliteration was 6.7 months.

There was no significant difference between ARUBA-eligible (**Figure 1**) and ARUBA-non-eligible patients regarding median time to complete (41.6 months versus 42.1 months, $P = 0.605$) or partial obliteration (6.5 months versus 6.7 months, $P = 0.078$, **Figure 4A**).

Kaplan-Meier analysis revealed no significant difference in median time to complete obliteration for patients who received previous SRS versus patients who did not receive previous SRS (41.6 months versus 40.4 months, $P = 0.166$). Similarly, no difference was noted between patients who underwent neuroendovascular embolization before SRS versus patients who were not embolized before SRS (39.3 months versus 41.6 months, $P = 0.604$).

However, patients who received partial surgical resection of the AVM had a shorter median time to complete obliteration (27.8 months versus 43.0 months, $P = 0.028$, **Figure 4B**). In addition, obliteration dynamics significantly varied depending on the Spetzler-Martin grade ($P = 0.007$, **Figure 4C**). While complete obliteration after 3 years was achieved in 67% of patients with Spetzler-Martin grade I and II lesions, the obliteration rate for Spetzler-Martin grades III, IV, V, and VI was 52.3%, 35.7%, 26.3%, and 37.4%, respectively ($P = 0.028$).

A lower radiosurgery-based AVM score ($P = 0.028$), a smaller target volume ($P < 0.001$) and a higher prescription dose ($P = 0.002$) were also significantly associated with complete obliteration within 3 years in bivariate analysis.

When performing a multivariate Cox regression analysis with the above-mentioned significant variables from univariate analysis, only Spetzler-Martin grade ($P = 0.006$) was found as independent predictor of complete obliteration (**Table 4**).

DISCUSSION

We analyzed obliteration dynamics, bleeding events and complications in a large cohort of patients with ruptured and

TABLE 4 | Efficacy of CyberKnife radiosurgery.

Obliteration status 3 years after SRS in patients with ≥ 3 years follow-up (N 152)			**Value**
No obliteration			6 (3.9%)
Partial obliteration			74 (48.7%)
Complete obliteration			72 (47.4%)
Univariate analysis	**Complete obliteration within 3 years (N 72)**	**No complete obliteration within 3 years (N 80)**	**P-Value**
Spetzler-Martin grade			0.028
I	4 (5.6%)	2 (2.5%)	
II	21 (29.2%)	10 (12.5%)	
III	23 (31.9%)	21 (26.3%)	
IV	10 (13.9%)	18 (22.5%)	
V	5 (6.9%)	14 (17.5%)	
VI	9 (12.5%)	15 (18.8%)	
Radiosurgery-based AVM score	1.33 [1.02–1.63]	1.44 [1.19–1.86]	0.028
Dose, Gy	18 [17–21]	17 [16.5–19]	0.002
Target volume, cm³	1.44 [0.52–4.46]	3.69 [1.51–7.89]	< 0.001
Cox-regression multivariate analysis	**Odds ratio and 95% CI**		**P-Value**
Spetzler-Martin grade	2.21 [1.96–2.55]		0.006

When not otherwise indicated, frequencies are presented as n (%). Radiosurgery-based AVM score, dose and target volume are presented as median and interquartile range. AVM, arteriovenous malformation; SRS, stereotactic radiosurgery; MRI, magnetic resonance imaging; DSA, digital subtraction angiography; CI, confidence interval.

unruptured AVMs treated with the frameless CyberKnife SRS system.

After 3 years of follow-up, we found an overall complete obliteration rate of 47.4%. This obliteration rate is consistent with data on Gamma Knife and LINAC-based SRS, where obliteration rates between 30% and 58% were achieved (4, 32–36). The obliteration rate observed in our study must be placed in the context of an unfavorable patient selection with particularly difficult to treat AVMs, including a higher proportion of Spetzler-Martin grade IV to VI AVMs (45.1%) compared to other series (7.5%–22%) (4, 32–36).

Most larger studies on SRS treatment of cerebral AVMs were carried out on Gamma Knife and LINAC systems, while the literature on AVM treatment by CyberKnife is sparse. We found three studies with rather small sample sizes of less than 30 patients that had obliteration rates between 66% and 78% (37–39). One larger study evaluating the three-year outcome of 102 patients treated with CyberKnife SRS (40) found an obliteration rate of 71.5%, which was higher than ours. However, they mainly investigated the treatment efficacy of small AVMs (79% Spetzler-Martin grades I to II, 21% Spetzler-Martin grades III and IV) and did not consider obliteration dynamics, thereby attributing late complete obliteration the same importance as early obliteration. Late complete obliteration could be problematic due to the risk of dangerous rebleeding in the latency period (5).

Regarding safety, the annual hemorrhage incidence after SRS in our treatment cohort was low (1.3%). This is comparable with previously published literature on SRS with hemorrhage rates between 1.3% and 4.9% (4–6, 33, 36, 41). Of note, the yearly hemorrhage incidence was markedly lower compared to the medical arm of the ARUBA trial, where it was 2.2% (25).

During the follow-up period, 73.7% of neurological deficits before SRS either completely or partially resolved after treatment, which was comparable to other studies, which report a partial or full recovery rate around 70% (41).

New neurological deficits occurred in 11 (5.1%) patients, while seven of those were attributed to new hemorrhage. Similarly, two deaths after SRS were secondary to hemorrhage from the treated AVM. The rate of new neurological deficits was comparable to a large meta-analysis on SRS treatment of cerebral AVMs, where it was 8% (42).

Headache was found to be the most prevalent presenting symptom (28.8%) in our study and this proportion was similar to many other AVM studies (33, 36, 40, 42). While 14% of our cohort presented with symptomatic epilepsy before SRS, 13.5% additional patients developed new seizures after SRS. The rate of symptomatic epilepsy at presentation varies in the literature and ranges between 12% and 47% (25, 33, 36, 40–42). New onset of symptomatic epilepsy after SRS ranged between 3% and 10% in other studies (33, 43).

In multivariate analysis, only Spetzler-Martin grade remained an independent predictor of the obliteration status, as has equally been shown in other series (36). The fact that Spetzler-Martin grade is calculated based on AVM size, draining vein status and eloquence sufficiently explains why AVM size alone was not an independent predictor of obliteration.

While efficacy and safety of CyberKnife SRS of our data compared favorably to the literature, our study has several limitations. First, it was a retrospective study and therefore, no statistical power analysis was conducted in advance. Second, CyberKnife does not offer the possibility to coregister stereotactic DSA images with the CT or MRA, making it impossible to compare two patient cohorts with and without stereotactic DSA as a planning basis.

In addition, some patients refused to obtain DSA imaging during follow-up, mostly due to the invasiveness of the procedure, which may introduce a bias in the rate of complete obliteration. This is a common problem in clinical practice that similarly occurred in other large studies on SRS treatment of cerebral AVMs (32, 36, 40). To tackle this frequently observed limitation, one study with 136 patients analyzed the diagnostic

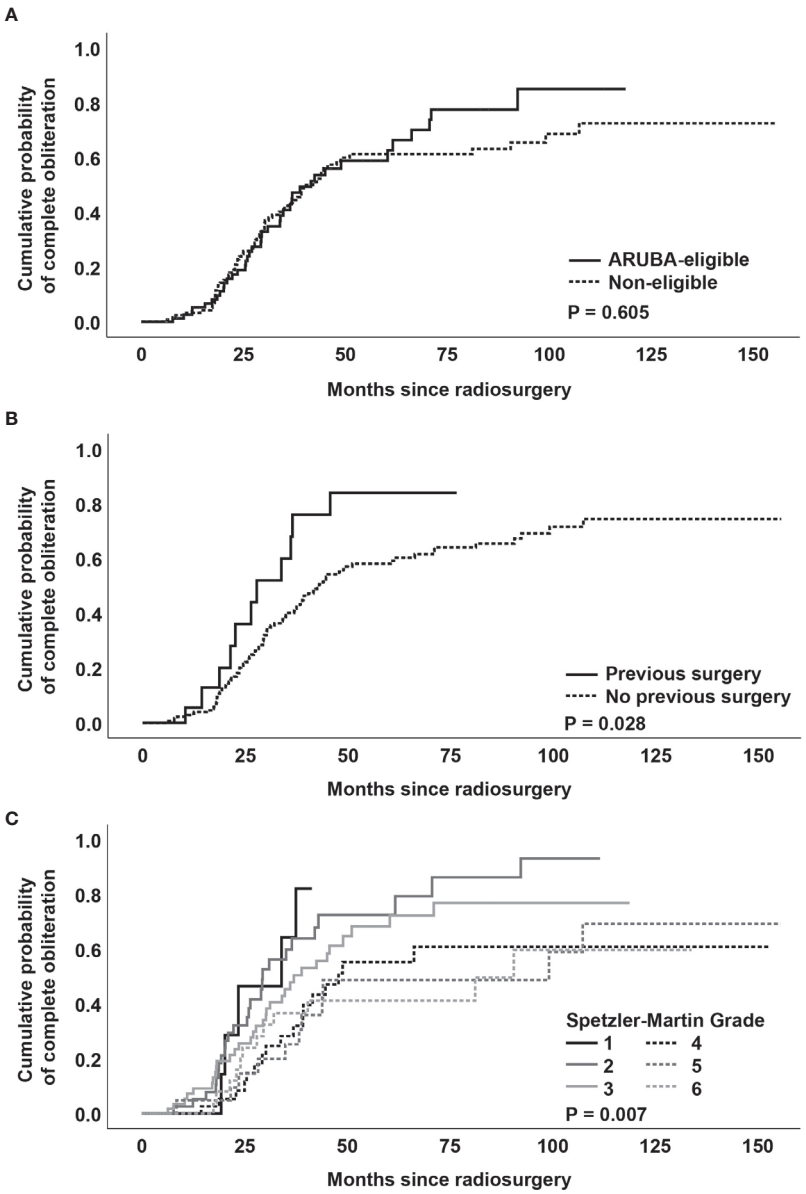

FIGURE 4 | **(A)** Kaplan-Meier analysis of obliteration dynamics stratified by ARUBA-eligibility. **(B)** Kaplan-Meier analysis of obliteration dynamics stratified by previous surgery. **(C)** Kaplan-Meier analysis of obliteration dynamics stratified by Spetzler-Martin grade.

accuracy of MRA regarding AVM obliteration after SRS. They showed a high sensitivity (85%) and specificity (95%) of MRA (31). In addition there is increasing evidence from small studies and case reports that newer time-resolved MRA sequences may be equal or even be better to assess AVM obliteration, when compared to DSA (44–47). While the scope of the present study was not to systematically compare the performance of MRA to DSA follow-up imaging, our obliteration and rebleeding rates were comparable to the literature (as discussed above) which speaks in favor of a correct assessment of obliteration, even in patients who were followed up by MRI only. However, we still advocate larger studies to systematically compare DSA with newer time-resolved MRA sequences in an effort to minimize radiation exposure for patients and potentially overcome the necessity of invasive DSA follow-up imaging in the future.

CONCLUSION

Non-invasive treatment planning, based on MRI and CT angiography, with a frameless SRS robotic system is a safe and effective treatment option in otherwise difficult to treat intracranial AVMs.

Although data on radiotherapy of AVMs is available, this is—to the best of our knowledge—one of the largest series, focusing exclusively on CyberKnife treatment.

Obliteration dynamics and rebleeding rates compare favorably to conventional frame-based radiosurgery devices with stereotactic DSA-guided approaches and thereby might provide higher patient comfort, a less invasive treatment option and lower radiation exposure.

DATA AVAILABILITY STATEMENT

The raw data supporting the conclusions of this article will be made available by the authors upon reasonable request.

ETHICS STATEMENT

The studies involving human participants were reviewed and approved by the ethics committee of the LMU Munich. The patients/participants provided their written informed consent to participate in this study.

AUTHOR CONTRIBUTIONS

AM, CS, and TG: conception and design of the study. FE, TH, TG, and AM acquired the data. TG analyzed the data and drafted the manuscript. FE, TH, JT, FD, CS, and AM critically revised the manuscript. All authors contributed to the article and approved the submitted version.

REFERENCES

1. Al-Shahi R, Bhattacharya JJ, Currie DG, Papanastassiou V, Ritchie V, Roberts RC, et al. Prospective, population-based detection of intracranial vascular malformations in adults: The Scottish Intracranial Vascular Malformation Study (SIVMS). *Stroke* (2003) 34:1163–9. doi: 10.1161/01.STR.0000069018.90456.C9
2. Rutledge WC, Ko NU, Lawton MT, Kim H. Hemorrhage rates and risk factors in the natural history course of brain arteriovenous malformations. *Transl Stroke Res* (2014) 5:538–42. doi: 10.1007/s12975-014-0351-0
3. Steiner L, Lindquist C, Cail W, Karlsson B, Steiner M. Microsurgery and radiosurgery in brain arteriovenous malformations. *J Neurosurg* (1993) 79:647–52. doi: 10.3171/jns.1993.79.5.0647
4. Hirschmann D, Goebl P, Witte FH, Gatterbauer B, Wang WT, Dodier P, et al. Evaluation of the radiosurgical treatment of cerebral arteriovenous malformations: a retrospective single-center analysis of three decades. *J Neurointerv Surg* (2020) 12:401–6. doi: 10.1136/neurintsurg-2019-015332
5. Karlsson B, Lax I, Soderman M. Risk for hemorrhage during the 2-year latency period following gamma knife radiosurgery for arteriovenous malformations. *Int J Radiat Oncol Biol Phys* (2001) 49:1045–51. doi: 10.1016/s0360-3016(00)01432-2
6. Pollock BE, Flickinger JC, Lunsford LD, Bissonette DJ, Kondziolka D. Hemorrhage risk after stereotactic radiosurgery of cerebral arteriovenous malformations. *Neurosurgery* (1996) 38:652–9. doi: 10.1227/00006123-199604000-00004
7. Pollock BE. Gamma Knife Radiosurgery of Arteriovenous Malformations: Long-Term Outcomes and Late Effects. *Prog Neurol Surg* (2019) 34:238–47. doi: 10.1159/000493070
8. Yahya S, Heyes G, Nightingale P, Lamin S, Chavda S, Geh I, et al. Linear accelerator radiosurgery for arteriovenous malformations: Updated literature review. *J Clin Neurosci* (2017) 38:91–5. doi: 10.1016/j.jocn.2016.12.015
9. Lunsford LD, Flickinger JC, Steiner L. The gamma knife. *JAMA* (1988) 259:2544. doi: 10.1001/jama.1988.03720170020017
10. Chen AY, Hsieh Y, McNair S, Li Q, Xu KY, Pappas C. Frame and frameless linear accelerator-based radiosurgery for idiopathic trigeminal neuralgia. *J Radiosurg SBRT* (2015) 3:259–70.
11. van den Berg R, Buis DR, Lagerwaard FJ, Lycklama à Nijeholt GJ, Vandertop WP. Extensive white matter changes after stereotactic radiosurgery for brain arteriovenous malformations: a prognostic sign for obliteration? *Neurosurgery* (2008) 63:1064–9; discussion 9-70. doi: 10.1227/01.neu.0000330413.73983.02
12. Buis DR, Meijer OW, van den Berg R, Lagerwaard FJ, Bot JC, Slotman BJ, et al. Clinical outcome after repeated radiosurgery for brain arteriovenous malformations. *Radiother Oncol* (2010) 95:250–6. doi: 10.1016/j.radonc.2010.03.003
13. Hristov D, Adler JR, Gibbs IC, Dodd R, Marks M, Chang SD, et al. Frameless image guided robotic radiosurgery of arteriovenous malformation localized on spatially correlated digital subtraction and C-arm CT angiography images. *J Neurointerv Surg* (2010) 2:252–4. doi: 10.1136/jnis.2009.001941
14. Lu X-Q, Mahadevan A, Mathiowitz G, Lin P-JP, Thomas A, Kasper EM, et al. Frameless Angiogram-Based Stereotactic Radiosurgery for Treatment of Arteriovenous Malformations. *Int J Radiat Oncol Biol Phys* (2012) 84:274–82. doi: 10.1016/j.ijrobp.2011.10.044
15. Hristov D, Liu L, Adler JR, Gibbs IC, Moore T, Sarmiento M, et al. Technique for targeting arteriovenous malformations using frameless image-guided robotic radiosurgery. *Int J Radiat Oncol Biol Phys* (2011) 79:1232–40. doi: 10.1016/j.ijrobp.2010.05.015
16. Adler JRJr., Chang SD, Murphy MJ, Doty J, Geis P, Hancock SL. The Cyberknife: a frameless robotic system for radiosurgery. *Stereotact Funct Neurosurg* (1997) 69:124–8. doi: 10.1159/000099863
17. Shim YW, Chung TS, Kang WS, Joo JY, Strecker R, Hennig J. Non-invasive follow-up evaluation of post-embolized AVM with time-resolved MRA: a case report. *Korean J Radiol* (2002) 3:271–5. doi: 10.3348/kjr.2002.3.4.271
18. Huston J3rd, Rufenacht DA, Ehman RL, Wiebers DO. Intracranial aneurysms and vascular malformations: comparison of time-of-flight and phase-contrast MR angiography. *Radiology* (1991) 181:721–30. doi: 10.1148/radiology.181.3.1947088
19. Marks MP, Pelc NJ, Ross MR, Enzmann DR. Determination of cerebral blood flow with a phase-contrast cine MR imaging technique: evaluation of normal subjects and patients with arteriovenous malformations. *Radiology* (1992) 182:467–76. doi: 10.1148/radiology.182.2.1732966
20. Oppenheim C, Meder JF, Trystram D, Nataf F, Godon-Hardy S, Blustajn J, et al. Radiosurgery of cerebral arteriovenous malformations: is an early angiogram needed? *AJNR Am J Neuroradiol* (1999) 20:475–81.
21. Hennig J, Scheffler K, Laubenberger J, Strecker R. Time-resolved projection angiography after bolus injection of contrast agent. *Magn Reson Med* (1997) 37:341–5. doi: 10.1002/mrm.1910370306
22. Wang Y, Johnston DL, Breen JF, Huston J3rd, Jack CR, Julsrud PR, et al. Dynamic MR digital subtraction angiography using contrast enhancement, fast data acquisition, and complex subtraction. *Magn Reson Med* (1996) 36:551–6. doi: 10.1002/mrm.1910360408
23. Kauczor HU, Engenhart R, Layer G, Gamroth AH, Wowra B, Schad LR, et al. 3D TOF MR angiography of cerebral arteriovenous malformations after radiosurgery. *J Comput Assist Tomogr* (1993) 17:184–90. doi: 10.1097/00004728-199303000-00005
24. Wowra B, Muacevic A, Tonn JC, Schoenberg SO, Reiser M, Herrmann KA. Obliteration dynamics in cerebral arteriovenous malformations after cyberknife radiosurgery: quantification with sequential nidus volumetry and 3-tesla 3-dimensional time-of-flight magnetic resonance angiography. *Neurosurgery* (2009) 64:A102–9. doi: 10.1227/01.NEU.0000339201.31176.C9
25. Mohr JP, Parides MK, Stapf C, Moquete E, Moy CS, Overbey JR, et al. Medical management with or without interventional therapy for unruptured brain arteriovenous malformations (ARUBA): a multicentre, non-blinded, randomised trial. *Lancet* (2014) 383:614–21. doi: 10.1016/s0140-6736(13)62302-8

26. Spetzler RF, Martin NA. A proposed grading system for arteriovenous malformations. *J Neurosurg* (1986) 65:476–83. doi: 10.3171/jns.1986.65.4.0476
27. Pollock BE, Flickinger JC. A proposed radiosurgery-based grading system for arteriovenous malformations. *J Neurosurg* (2002) 96:79–85. doi: 10.3171/jns.2002.96.1.0079
28. Andrade-Souza YM, Zadeh G, Ramani M, Scora D, Tsao MN, Schwartz ML. Testing the radiosurgery-based arteriovenous malformation score and the modified Spetzler-Martin grading system to predict radiosurgical outcome. *J Neurosurg* (2005) 103:642–8. doi: 10.3171/jns.2005.103.4.0642
29. Pollock BE, Storlie CB, Link MJ, Stafford SL, Garces YI, Foote RL. Comparative analysis of arteriovenous malformation grading scales in predicting outcomes after stereotactic radiosurgery. *J Neurosurg* (2017) 126:852–8. doi: 10.3171/2015.11.JNS151300
30. Sio TT, Jang S, Lee SW, Curran B, Pyakuryal AP, Sternick ES. Comparing gamma knife and cyberknife in patients with brain metastases. *J Appl Clin Med Phys* (2014) 15:4095. doi: 10.1120/jacmp.v15i1.4095
31. Lee CC, Reardon MA, Ball BZ, Chen CJ, Yen CP, Xu Z, et al. The predictive value of magnetic resonance imaging in evaluating intracranial arteriovenous malformation obliteration after stereotactic radiosurgery. *J Neurosurg* (2015) 123:136–44. doi: 10.3171/2014.10.JNS141565
32. Blamek S, Tarnawski R, Miszczyk L. Linac-based stereotactic radiosurgery for brain arteriovenous malformations. *Clin Oncol (R Coll Radiol)* (2011) 23:525–31. doi: 10.1016/j.clon.2011.03.012
33. Kim BS, Yeon JY, Kim JS, Hong SC, Shin HJ, Lee JI. Gamma Knife Radiosurgery for ARUBA-Eligible Patients with Unruptured Brain Arteriovenous Malformations. *J Korean Med Sci* (2019) 34:e232. doi: 10.3346/jkms.2019.34.e232
34. Murray G, Brau RH. A 10-year experience of radiosurgical treatment for cerebral arteriovenous malformations: a perspective from a series with large malformations. *Clin Artic J Neurosurg* (2011) 115:337–46. doi: 10.3171/2011.3.JNS10814
35. Kano H, Lunsford LD, Flickinger JC, Yang HC, Flannery TJ, Awan NR, et al. Stereotactic radiosurgery for arteriovenous malformations, Part 1: management of Spetzler-Martin Grade I and II arteriovenous malformations. *J Neurosurg* (2012) 116:11–20. doi: 10.3171/2011.9.JNS101740
36. Ding D, Yen CP, Xu Z, Starke RM, Sheehan JP. Radiosurgery for patients with unruptured intracranial arteriovenous malformations. *J Neurosurg* (2013) 118:958–66. doi: 10.3171/2013.2.JNS121239
37. Oermann EK, Murthy N, Chen V, Baimeedi A, Sasaki-Adams D, McGrail K, et al. A Multicenter Retrospective Study of Frameless Robotic Radiosurgery for Intracranial Arteriovenous Malformation. *Front Oncol* (2014) 4:298. doi: 10.3389/fonc.2014.00298
38. Gupta R, Moore JM, Amorin A, Appelboom G, Chaudhary N, Iyer A, et al. Long-term follow up data on difficult to treat intracranial arteriovenous malformations treated with the CyberKnife. *J Clin Neurosci* (2019) 61:120–3. doi: 10.1016/j.jocn.2018.10.109
39. Wang X, Wang E, Mei G, Liu X, Zhu H, Pan L, et al. [Cyberknife radiosurgery for cerebral arteriovenous malformations: outlining of the radiosurgical target and obliteration]. *Zhonghua Yi Xue Za Zhi* (2014) 94:2902–6.
40. Colombo F, Cavedon C, Casentini L, Francescon P, Causin F, Pinna V. Early results of CyberKnife radiosurgery for arteriovenous malformations. *J Neurosurg* (2009) 111:807–19. doi: 10.3171/2008.10.JNS08749
41. Steiner L, Lindquist C, Adler JR, Torner JC, Alves W, Steiner M. Clinical outcome of radiosurgery for cerebral arteriovenous malformations. *J Neurosurg* (1992) 77:1–8. doi: 10.3171/jns.1992.77.1.0001
42. Borcek AO, Celtikci E, Aksogan Y, Rousseau MJ. Clinical Outcomes of Stereotactic Radiosurgery for Cerebral Arteriovenous Malformations in Pediatric Patients: Systematic Review and Meta-Analysis. *Neurosurgery* (2019) 85:E629–E40. doi: 10.1093/neuros/nyz146
43. Ding C, Hrycushko B, Whitworth L, Li X, Nedzi L, Weprin B, et al. Multistage stereotactic radiosurgery for large cerebral arteriovenous malformations using the Gamma Knife platform. *Med Phys* (2017) 44:5010–9. doi: 10.1002/mp.12455
44. Yu S, Yan L, Yao Y, Wang S, Yang M, Wang B, et al. Noncontrast dynamic MRA in intracranial arteriovenous malformation (AVM), comparison with time of flight (TOF) and digital subtraction angiography (DSA). *Magn Reson Imaging* (2012) 30:869–77. doi: 10.1016/j.mri.2012.02.027
45. Chang W, Wu Y, Johnson K, Loecher M, Wieben O, Edjlali M, et al. Fast contrast-enhanced 4D MRA and 4D flow MRI using constrained reconstruction (HYPRFlow): potential applications for brain arteriovenous malformations. *AJNR Am J Neuroradiol* (2015) 36:1049–55. doi: 10.3174/ajnr.A4245
46. Li CQ, Hsiao A, Hattangadi-Gluth J, Handwerker J, Farid N. Early Hemodynamic Response Assessment of Stereotactic Radiosurgery for a Cerebral Arteriovenous Malformation Using 4D Flow MRI. *AJNR Am J Neuroradiol* (2018) 39:678–81. doi: 10.3174/ajnr.A5535
47. Kodera T, Arai Y, Arishima H, Higashino Y, Isozaki M, Tsunetoshi K, et al. Evaluation of obliteration of arteriovenous malformations after stereotactic radiosurgery with arterial spin labeling MR imaging. *Br J Neurosurg* (2017) 31:641–7. doi: 10.1080/02688697.2017.1365818

Conflict of Interest: FD is a consultant for Balt, Phenox, and Cerus and received speaker honoraria from Cerenovus and Acandis.

The remaining authors declare that the research was conducted in the absence of any commercial or financial relationships that could be construed as a potential conflict of interest.

frontiers in Oncology

ORIGINAL RESEARCH
published: 22 April 2021
doi: 10.3389/fonc.2021.664455

Lung Stereotactic Body Radiotherapy (SBRT) Using Spot-Scanning Proton Arc (SPArc) Therapy: A Feasibility Study

Gang Liu[1,2], Lewei Zhao[2], An Qin[2], Inga Grills[2], Rohan Deraniyagala[2], Craig Stevens[2], Sheng Zhang[1], Di Yan[2], Xiaoqiang Li[2†] and Xuanfeng Ding[2†]*

[1] Cancer Center, Union Hospital, Tongji Medical College, Huazhong University of Science and Technology, Wuhan, China, [2] Department of Radiation Oncology, Beaumont Health System, Royal Oak, MI, United States

OPEN ACCESS

Edited by:
Rupesh Kotecha,
Baptist Hospital of Miami,
United States

Reviewed by:
Ulrich W. Langner,
Lifespan, United States
Jerry George,
Baptist Health South Florida,
United States

***Correspondence:**
Xuanfeng Ding
xuanfengding@gmail.com

[†]These authors share senior authorship

Specialty section:
This article was submitted to Radiation Oncology, a section of the journal Frontiers in Oncology

Received: 05 February 2021
Accepted: 26 March 2021
Published: 22 April 2021

Citation:
Liu G, Zhao L, Qin A, Grills I, Deraniyagala R, Stevens C, Zhang S, Yan D, Li X and Ding X (2021) Lung Stereotactic Body Radiotherapy (SBRT) Using Spot-Scanning Proton Arc (SPArc) Therapy: A Feasibility Study. Front. Oncol. 11:664455. doi: 10.3389/fonc.2021.664455

Purpose: We developed a 4D interplay effect model to quantitatively evaluate breathing-induced interplay effects and assess the feasibility of utilizing spot-scanning proton arc (SPArc) therapy for hypo-fractionated lung stereotactic body radiotherapy (SBRT). The model was then validated by retrospective application to clinical cases.

Materials and Methods: A digital lung 4DCT phantoms was used to mimic targets in diameter of 3cm with breathing motion amplitudes: 5, 10, 15, and 20 mm, respectively. Two planning groups based on robust optimization were generated: (1) Two-field Intensity Modulated Proton Therapy (IMPT) plans and (2) SPArc plans *via* a partial arc. 5,000 cGy relative biological effectiveness (RBE) was prescribed to the internal target volume (ITV) in five fractions. To quantitatively assess the breathing induced interplay effect, the 4D dynamic dose was calculated by synchronizing the breathing pattern with the simulated proton machine delivery sequence, including IMPT, Volumetric repainting ($IMPT_{volumetric}$), iso-layered repainting ($IMPT_{layer}$) and SPArc. Ten lung patients' 4DCT previously treated with VMAT SBRT, were used to validate the digital lung tumor model. Normal tissue complicated probability (NTCP) of chestwall toxicity was calculated.

Result: Target dose were degraded as the tumor motion amplitude increased. The 4D interplay effect phantom model indicated that motion mitigation effectiveness using SPArc was about five times of $IMPT_{volumetric}$ or $IMPT_{layer}$ using maximum MU/spot as 0.5 MU at 20 mm motion amplitude. The retrospective study showed that SPArc has an advantage in normal tissue sparing. The probability of chestwall's toxicity were significantly improved from 40.2 ± 29.0% (VMAT) ($p = 0.01$) and 16.3 ± 12.0% (IMPT) ($p = 0.01$) to 10.1 ± 5.4% (SPArc). SPArc could play a significant role in the interplay effect mitigation with breathing-induced motion more than 20 mm, where the target D99 of 4D dynamic dose for patient #10 was improved from 4,514 ± 138 cGy [RBE] (IMPT) vs. 4,755 ± 129 cGy [RBE] (SPArc) ($p = 0.01$).

Conclusion: SPArc effectively mitigated the interplay effect for proton lung SBRT compared to IMPT with repainting and was associated with normal tissue sparing.

This technology may make delivery of proton SBRT more technically feasible and less complex with fewer concerns over underdosing the target compared to other proton therapy techniques.

Keywords: lung, stereotactic body radiation therapy, spot-scanning, proton arc therapy, interplay effect

INTRODUCTION

Lung cancer remains a leading cause of cancer mortality in the world (1). Compared to conventional radiotherapy, hypo-fractionated stereotactic body radiotherapy (SBRT) has been proved to improve local tumor control and survival rate for stage I non-small cell lung cancer (NSCLC) patients (2–6). Taking advantage of the unique beam characteristics, Bragg Peak, proton beam therapy could offer a superior dose distribution compared to photon radiotherapy technique in treating locally advanced lung cancer (7). Recently, with the development of pencil beam scanning (PBS) technology, intensity modulated proton therapy (IMPT) offers the potentials to spare the adjacent normal tissues further while maintaining similar or superior target coverage in a more efficient way without using beam specific blocks or compensators compared to passive scatter proton therapy (PSPT) (8–11). However, such scanning technique is susceptible to the interplay effect between proton spot scanning and respiratory induced motion during dose delivery. It eventually leads to an inaccurate dose delivery such as underdose targe or overdoses of the healthy tissue during lung cancer treatment (12, 13). Several motion management strategies were introduced to mitigate the interplay effect, such as repainting, gating, and tracking (14–16), in which volumetric or layer repainting technique has been widely adopted by the proton clinic. With volumetric repainting, the dose delivered during one full volume is equal to 1/N of the prescribed dose, where N was the number of rescans (14). An alternative approach is called iso-layered repainting, in which first delivered several rescans within one energy plane before switching to the next plane with the dose per spot being limited by a maximal MU value (17).

The concept of spot-scanning arc therapy (SPArc) technique was introduced in 2016 to improve the dosimetric plan quality, robustness, and delivery efficiency of proton beam therapy. The technique demonstrated potential clinical benefits in several disease sites or indications (18–23). Whether this novel technique has any potential clinical benefits in the management of stage I non-small cell lung cancer and whether it is robust enough to be implemented in the hypo-fractionated lung SBRT has yet to be explored. Therefore, we proposed a comprehensive study is to 1) to build a lung SBRT model to evaluate the effectiveness of motion interplay mitigation *via* SPArc quantitatively; 2) to validate the model using clinical data sets and exploit the potential benefits.

MATERIALS AND METHODS

In Silico 4D Interplay Phantom Model

Due to the target deformation, motion, and imaging artifact in the four-dimensional computed tomography (4DCT), it is challenging to analyze the interplay effect quantitatively using the patient dataset directly. Previous studies have suggested using a digital lung cancer phantom as a surrogate (24, 25). By introducing a digital phantom employed in a prior study, we built an in silico 4D interplay phantom model to mimic patient's 4DCT datasets while eliminating the artifact and target deformation uncertainties (25). Since most lung tumor motion happens in the superior-inferior (SI) direction (26), a set of digital lung tumor phantoms 4DCT with different breathing induced motion amplitudes (5, 10, 15, and 20 mm in SI direction) were created (25, 27). The target was simulated using a sphere 3 cm in diameter with 1.0 g/cc density (28), close to the average target size measured in the patient group for this study. The gross tumor volume (GTV) was contoured on the lung window through the HU (Hounsfield unit) threshold at each phase image. The internal target volume (ITV) was generated by union GTVs at each phase.

Treatment Planning on the Phantom Model

5,000 cGy relative biological effectiveness [RBE] was prescribed to ITV in five fractions SBRT with RBE = 1.1 for proton plans and RBE = 1.0 for photon plans (29). Two-field IMPT plans were generated using the single field optimization (SFO) technique *via* lateral and posterior beams. SPArc plans were regenerated using a partial arc from 180 to 30° clockwise with a sampling frequency of 2.5°. Both planning strategies used the same robust optimization on average CT with ±5% range and 5 mm setup uncertainties corresponding to 21 scenarios in total with a 3 mm dose grid. The minimum monitor unit (MU) threshold per spot was 0.02 MU based on the IBA proton system (19, 23, 30, 31). Similar objective constraints for organs at risk (OARs) were used in both planning groups. All plans were normalized to guarantee 99% ITV was covered by the prescription dose. The SPArc optimization algorithm starts from a multi-field IMPT with coarse sampling frequency using the worst-case scenario robust optimization and gradually resample the control point to achieve a proton arc plan (18). The algorithm integrated the iterative approaches includes (A) control point re-sampling; (B) control point energy layers re-distribution; (C) energy layers filtration; (D) energy layers re-sampling; and (E) spot number reduction by filtration. Details of the algorithm are described by Ding and Li et al. in 2016 (18).

Interplay Effect Evaluation

The 4D dynamic dose was calculated to assess the interplay effect by synchronizing the breathing pattern with the simulated proton machine delivery sequence (19, 32). To calculate a single fraction 4D dynamic dose, the dose calculated on each phase image was accumulated via the deformable image

registration to the reference phase (expiration end, phase 50%) (19, 32). Ten different starting phases were simulated based on a clinical 360-degree gantry machine parameter with one revolution per minute (RPM) gantry rotation speed, 2 ms spot position switching time, energy layer switching time (ELST) of 1 s, as well as a respiratory motion period of 4 s (19). GTV D99 was assessed along with target motion amplitude variation.

A Quantitative Interplay Effect Mitigation Evaluation

In this study, IMPT treatment delivery simulation using a volumetric repainting technique was denoted as $IMPT_{volumetric}$, and IMPT using an iso-layered repainting technique denoted as $IMPT_{layer}$. To quantitatively evaluate the effectiveness of interplay effect mitigation in lung SBRT, the single fraction 4D dynamic was compared between SPArc without repainting and $IMPT_{volumetric}$, with different numbers of volumetric repainting (rescanning three, five, seven, and nine times respectively) and $IMPT_{layer}$ with a series of maximum MU per spot (from 0.1 to 1.3 MU per spot).

A Retrospective Dosimetric Planning Study

Ten patients with stage I NSCLC previously treated with volumetric modulated Arc therapy (VMAT) based SBRT at our institution were selected. All patients received 4DCT simulation using a helical CT scanner (Philips Brilliance Big Bore, Philips Healthcare System, Cleveland, OH). The GTVs and ITV were generated through the strategies described above as well. The patient characteristics, including tumor location, tumor size in diameter, and tumor motion, are listed in **Table 1**.

Treatment Planning in the Patient Dataset

The VMAT plans were generated using two to four partial arcs (control point frequency as 4°) based on the Elekta HD with 6 MV. The VMAT plan optimization starts from a coarse sampling of gantry position. New sample was added to achieve the desired sampling frequency, in which the Multileaf collimator (MLC) was linearly and gradually interpolated by the adjacent samples (33).

Two-field IMPT and SPArc with partial arc plans were generated, respectively. The prescription dose 5,000 cGy [RBE] was prescribed to 99% of the ITV. For a fair comparison between photon technique and proton technique, robust optimization-based ITV was used considering the same setup uncertainties as 5 mm, but ±5% range uncertainty was considered in proton planning.

Dosimetric Plan Quality Evaluation

The plan quality was evaluated based on the dose–volume histograms (DVHs) of target volume and OARs in the nominal plans. More specifically, all plans were compared for target coverage using conformity index (CI, the target volume covered by RX/the volume covered by RX). Dosimetric index for normal tissue sparing or OARs such as the Dmax or D0.1cc for the spinal cord, ribs and esophagus, Dmean for heart, ipsilateral lung (excluding ITV) as well as chest wall (CW) V30 (the volume received 3,000 cGy [RBE]) were evaluated by comparing SPArc planning group to VMAT and IMPT group.

The integral dose (ID) of radiation delivered to the whole patient body structure or external contour was analyzed (34). The ID definition was as following:

$$\mathrm{ID}(\mathrm{Gy}\cdot\mathrm{L}) = \bar{D}(\mathrm{Gy})\cdot\mathrm{V}(\mathrm{L}) \tag{1}$$

where (Gy) is the mean dose delivered to volume V (L) (where L—liter).

Patient-Specific Interplay Effect Evaluation

Each case's interplay effect was evaluated based on the 4D dynamic dose accumulation method mentioned in *Interplay Effect Evaluation* (19, 32).

Potential Clinical Benefit in Chestwall and Ipsilateral Lung Protection

Late chest wall toxicity after SBRT has been evaluated among three treatment modalities in this study. The probability of chest wall toxicity was calculated based on the odds ratios using the dosimetric parameter chest wall V30 (the volume of chest wall receiving 30 Gy) (35):

$$\begin{aligned} &Probability\ \ of\ \ CW\ \ toxicity\ \ by\ \ V30(cc) \\ &= \frac{e[-3.151 + (0.042 \star V30)]}{1 + e[-3.151 + (0.042 \star V30)]} \end{aligned} \tag{2}$$

TABLE 1 | Patient characteristics.

No.	Tumor Lobe	Tumor Size (mm)	Tumor Motion			
			SI (mm)	RL (mm)	PA (mm)	Offset (mm)
1	RUL	17.0	1.6	1.0	0.2	1.9
2	LUL	33.0	5.0	1.0	3.0	5.9
3	LLL	19.0	5.0	3.0	1.0	5.9
4	LLL	13.0	5.0	2.0	3.0	6.2
5	LUL	22.0	4.0	3.0	4.0	6.4
6	RUL	30.0	5.0	3.0	3.0	6.6
7	RUL	20.0	7.0	4.0	4.0	9.0
8	RUL	32.0	7.0	4.0	5.0	9.5
9	LLL	20.0	10.0	1.0	3.0	10.5
10	LLL	32.0	22.0	4.7	1.9	22.6

SI, superior inferior; RL, right left; PA, posterior anterior; RUL, right upper lobe; LUL, left upper lobe; LLL, left lower lobe; RLL, right lower lobe. Offset = $(SI^2 + RI^2 + PA^2)^{1/2}$.

The incident of radiation pneumonitis for an ipsilateral lung was calculated based on the Lyman–Kutcher–Burman (LKB) model as following (36):

$$\mathrm{NTCP} = \frac{1}{\sqrt{2\pi}} \int_{-\infty}^{t} e^{-\frac{x^2}{2}} dx \tag{3}$$

$$t = \frac{D - TD_{50}}{m \times TD_{50}} \tag{4}$$

where TD_{50} is the tolerance dose for a 50% complication probability for uniform doses to the organ, and m is a dimensionless parameter for determining the slope of the complication probability according to the dose curve. And D is the equivalent dose(EUD), which is the DVH to a single dose value, representing the uniform dose that results in the survival of an equal number of clonogens in a non–homogeneously irradiated tumor. It is defined with the formula as (36):

$$\mathrm{EUD} = \left(\sum_{i=1}^{N} v_i D_i^a\right)^{\frac{1}{a}} \tag{5}$$

where Di is the dose for each bin in a differential DVH, vi is the volume in a specific dose bin i, and N is the unequal fractional sub-volume. The 'a' value is a parameter equal to $1/n$, in which n represents the volume dependence of the complication probability. The parameter set for the lung tissue were taken from Burman et al. (TD50 = 24.5 Gy, m = 0.18, and a = 0.87) (37, 38). According to the LQ model, the dose axis of the DVH was re-scaled to the equivalent dose in 2 Gy per fractions and the method described by Van den Heuvel with assuming α/β ratio of 3 Gy for the ipsilateral normal lung tissue (39, 40).

The dosimetric index from SPArc was utilized as a reference. By comparing with two other treatment technologies (IMPT and VMAT), the differences were assessed with a paired, 2-tailed non-parametric Wilcoxon signed-rank test via SPSS 21.0 software (International Business Machines, Armonk, New York), respectively, and p values less than 0.05 were considered statistically significant.

RESULT

In Silico 4D Interplay Phantom Model

The Interplay Effect Evaluation

The study showed that the dose to target degraded as the tumor motion amplitude increased in the IMPT planning, which was agreed with the previous reports (16, 41, 42). **Figure 1** displayed the target D99 in relationship with various motion amplitudes. SPArc could significantly improve the target coverage compared to IMPT through all the different motion amplitudes, even without any repainting. More specially, the average relative target D99 degradation *via* single fraction 4D dynamic dose accumulation were 2.51 vs 0.00% (p <0.01), 4.01 vs 0.10% (p <0.01), 6.61 vs 1.29% (p <0.01), 8.40 vs 1.70% (p <0.01) for IMPT vs SPArc at different breathing amplitude (5, 10, 15 and 20 mm), respectively.

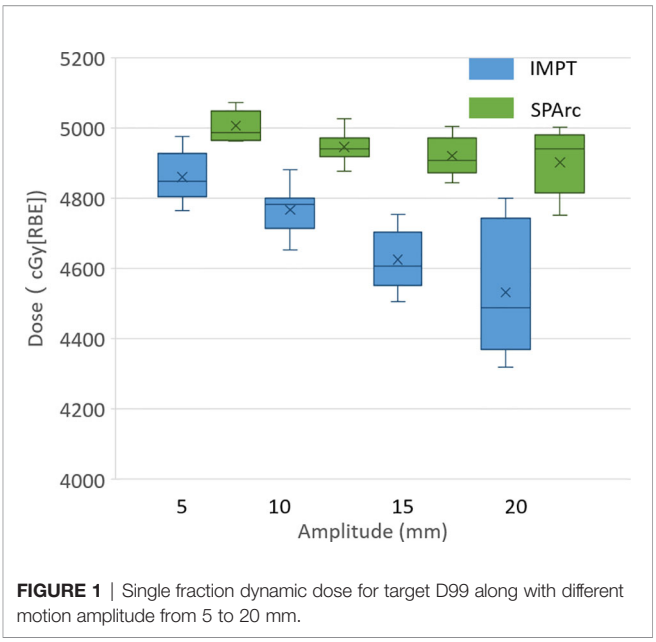

FIGURE 1 | Single fraction dynamic dose for target D99 along with different motion amplitude from 5 to 20 mm.

Comparison of Mitigation Effectiveness in the Interplay Effect With Repainting IMPT

The motion interplay effect can be compensated by increasing the total number of volumetric repainting or constraining the maximum MU per spot using iso-layered repainting. The single fraction 4D dynamic dose accumulation for target D99 with the number of volumetric repainting times and maximum MU per spot for the target motion 10 and 20 mm was displayed in **Figures 2A, B**, respectively. At 10 mm target motion amplitude, GTV D99 was 4,767 ± 63 cGy [RBE] (p <0.01) in IMPT without repainting, which is less than 4,950 ± 41 cGy [RBE] in SPArc. $\mathrm{IMPT_{volumetric}}$ increased GTV D99 to 4,959 ± 76 cGy [RBE] (p = 0.51) and 4,985 ± 66 cGy [RBE] (p = 0.33) with three and five times of volumetric repainting (**Figure 2A**); $\mathrm{IMPT_{layer}}$ increased GTV D99 to 4,931 ± 78 cGy [RBE] (p = 0.39) and 4,981 ± 66cGy [RBE] (p = 0.11) with maximum MU per spot as 0.75 and 0.50 MU respectively (**Figure 2B**), compared to SPArc. It is interesting to find that SPArc is as effective as three to five times of volumetric repainting IMPT or iso-layered repainting with maximum MU per spot as 0.75 to 0.5 MU at 10 mm target motion amplitude.

Moreover, in the target motion with 20 mm amplitude, GTV D99 was 4,532 ± 180 cGy [RBE] (IMPT without repainting) vs 4,902 ± 94 cGy [RBE] (SPArc) (p = 0.01). SPArc was as effective as five to seven times of volumetric repainting or iso-layered repainting with maximum MU per spot as 0.7 to 0.4 MU in IMPT for where GTV D99 received 4,896 ± 75 cGy [RBE] (p = 0.96) and 4,912 ± 26 cGy [RBE] (p = 0.65) for IMPT with volumetric repainting five and seven times, respectively (**Figure 2A**). Meanwhile, GTV D99 reached as 4,841 ± 102 cGy [RBE] (p = 0.09) and 4,929 ± 71 cGy [RBE] (p = 0.65) during $\mathrm{IMPT_{layer}}$ with maximum MU per spot of 0.7 and 0.4 MU (**Figure 2B**), respectively.

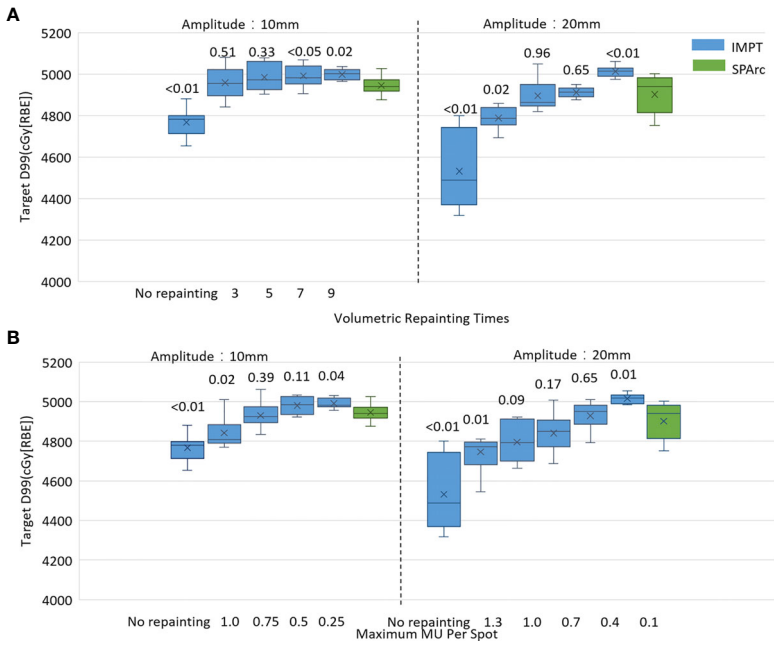

FIGURE 2 | Single fraction 4D dynamic dose comparison between SPArc (green) and **(A)** different number of volumetric repainting times $IMPT_{volumetric,}$ and **(B)** IMPTlayer with different maximum MU per spot.

Retrospective Study Using Patient Dataset

Plan Quality Evaluation

Taking advantage of more degrees of freedom in the optimization through arc(s) trajectory, VMAT and SPArc planning groups demonstrated superior dose conformity to the target. Isodose distributions of patient #10 for treatment plan using VMAT (first column), IMPT (the second column), and SPArc (the third column) was displayed in **Figure 3**.

SPArc improved CI from 0.31 ± 0.08 in IMPT to 0.38 ± 0.10 (p = 0.01). This feature allows SPArc to spare more OARs such as spinal cord and ribs than IMPT. In addition, SPArc plans significantly reduced the Dmean of the ipsilateral lung from 503 ± 1 76 cGy [RBE] to 418 ± 140 cGy [RBE] (p = 0.01) and Dmax of ribs from 4,369 ± 978 cGy [RBE] to 4,151 ± 1,015 cGy [RBE] (p = 0.02) compared to IMPT respectively. V30 of the chest wall was significantly reduced from 30 ± 22 cc to 20 ± 14 cc (p = 0.02) compared to IMPT (**Table 2**).

Compared to VMAT, SPArc significantly reduced the dose to OARs listed in **Table 2**. More specially, SPArc significantly reduced maximum dose to spinal cord: 1,026 ± 494 cGy [RBE] (VMAT) vs 300 ± 530 cGy [RBE] (SPArc) (p = 0.01), esophagus: 1,611 ± 1,361 cGy [RBE] (VMAT) vs 501 ± 1,565 cGy [RBE] (SPArc) (p <0.01), ribs: 4,770 ± 1,059 cGy [RBE] (VMAT) vs 4,151 ± 1,015 cGy [RBE] (SPArc) (p = 0.01). In addition, SPArc significantly reduced the mean dose of the ipsilateral lung from 659 ± 200 cGy [RBE] (VMAT) to 418 ± 140 cGy [RBE] (SPArc) (p = 0.01), and the mean dose of heart from 288 ± 253 cGy [RBE] (VMAT) to 8 ± 11 cGy [RBE] (SPArc) (p = 0.01). The chest wall V30 was also significantly reduced *via* SPArc plan from 60 ± 37 cc to 20 ± 14 cc (p <0.01). The study also found that SPArc (16.13 ± 5.36 Gy·L) significantly reduced ID comparing to both IMPT (18.40 ± 5.79 Gy·L, p = 0.01) and VMAT (38.38 ± 17.10 Gy·L, p = 0.01) planning group.

Interplay Effect Evaluation in the Patient Population

The single fraction 4D dynamic dose accumulation showed that target D99 was degraded due to the interplay effect in IMPT without repainting (**Figure 4**) among the ten patients. Similar to the 4D interplay phantom model, the retrospective study showed a similar trend of target dose coverage degradation with increased breathing-induced motion amplitudes. SPArc significantly mitigated interplay effect compared to IMPT among cases where breathing-induced motion cannot be ignored. Even though the target's motion and shape were complicated as these parameters are patient-specific, the patient cases' trend was consistent with the 4D interplay phantom study (Comparison of Mitigation Effectiveness in the Interplay Effect With Repainting IMPT) when the amplitudes of breathing induced motion is large (**Figure 4**). More specifically, the target D99 of 4D dynamic dose was 4,514 ± 138 cGy [RBE] (IMPT without repainting) vs 4,755 ± 129 cGy [RBE] (SPArc) (p = 0.01) fort the patient #10.

The Probability of Chest Wall Toxicity and Radiation-Induced Pneumonitis

Due to SPArc significantly spared chest wall better than both IMPT and VMAT. The consequence clinic benefit was obvious,

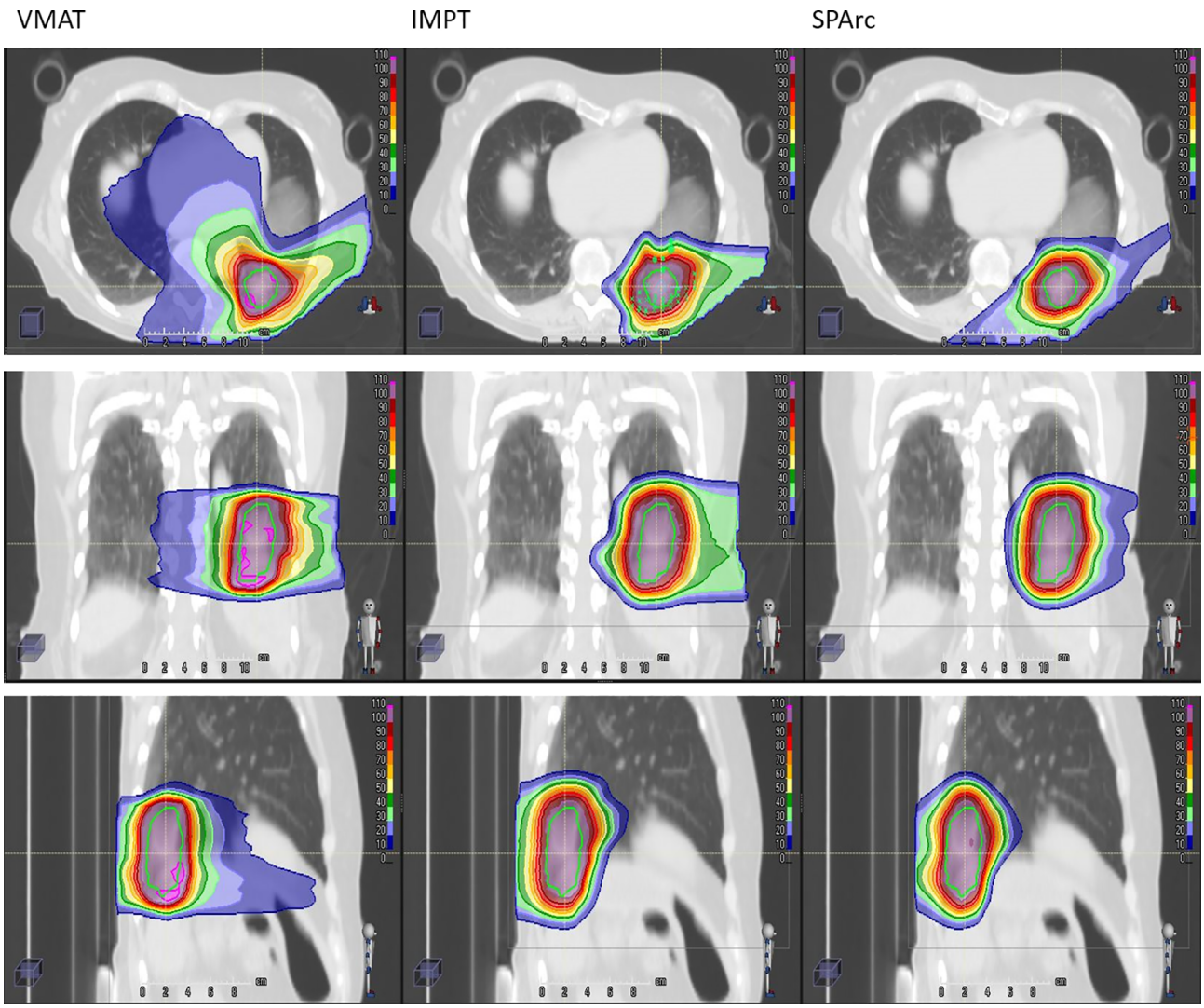

FIGURE 3 | Isodose distributions of patient #10 for treatment plan using VMAT (first column), IMPT (the second column), and SPArc (the third column). The green contour represents ITV. 100% dose is equal to prescription dose.

TABLE 2 | Dosimetry results for the three planning modalities

	VMAT	SPArc	IMPT	p value VMAT vs SPArc	p value IMPT vs SPArc
Spinal Cord Dmax (cGy) [RBE]	1,026 ± 494	300 ± 530	338 ± 604	0.01	0.35
Ipsilateral lung Dmean (cGy) [RBE]	659 ± 200	418 ± 140	503 ± 176	0.01	0.01
Cheat Wall V30 (cc)	60 ± 37	20 ± 14	30 ± 22	<0.01	0.02
Heart Dmean (cGy) [RBE]	288 ± 253	8 ± 11	8 ± 9	0.01	0.83
Esophagus Dmax (cGy) [RBE]	1,611 ± 1,361	501 ± 1,565	541 ± 1,576	<0.01	0.16
Ribs Dmax (cGy) [RBE]	4,770 ± 1,059	4151 ± 1,015	4,369 ± 978	0.01	0.02
ID(Gy·L)	38.38 ± 17.10	16.13 ± 5.36	18.40 ± 5.79	0.01	0.01
CI	0.39 ± 0.12	0.38 ± 0.10	0.31 ± 0.08	0.54	0.01
The probability of CW toxicity(%)	40.2 ± 29.0	10.1 ± 5.4	16.3 ± 12.0	0.01	0.01

ID, integral dose; CW, chest wall.

where the probability of CW toxicity were improved from 40.2 ± 29.0% (VMAT) ($p = 0.01$) and 16.3 ± 12.0 (IMPT) ($p = 0.01$) to 10.1 ± 5.4% (SPArc).

All three treatment modalities were able to spare ipsilateral lung tissue well. The corresponding incidence of radiation pneumonitis was fairly low, all of them were approximate to 0% on average.

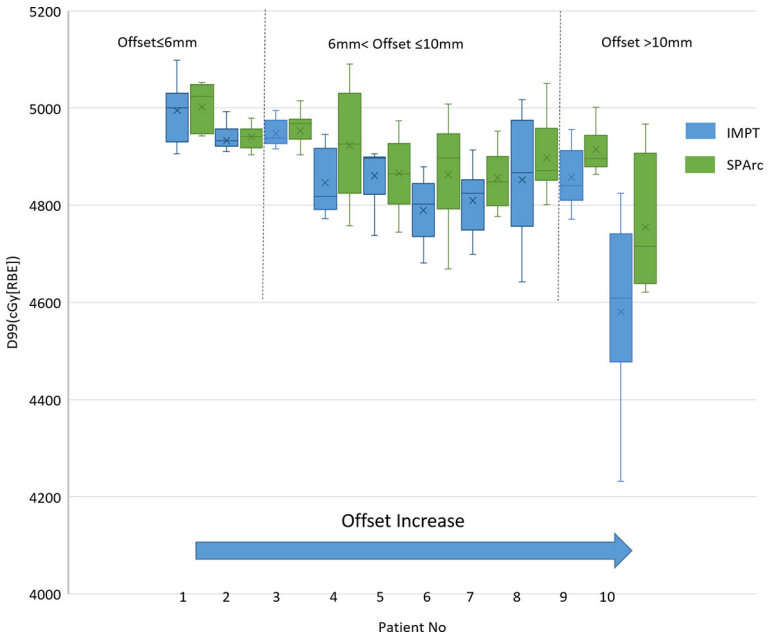

FIGURE 4 | Single fraction dynamic dose for target coverage D99 for ten patients.

DISCUSSION

This is the first study to explore the feasibility of using SPArc in hypo-fractionated treatment in mobile targets and its potential clinical benefits in lung SBRT. We quantify the effectiveness of using SPArc to mitigate the motion interplay effect using digital 4D lung cancer phantom and validate the model through a retrospective dosimetric study. The result confirmed the previous report that the interplay effect led to a deterioration of the dose distribution (16, 41, 42). The larger amplitude in motion, the more deterioration in the target coverage. Such a trend was consistent within the retrospective dosimetric study findings in the ten patient cases (**Figure 4**), even though the tumor shape, size, 3-dimentional tumor motion, and density variation during the breathing cycle were complicated for the patient population. For the patient group with 6 mm <target offset ≤10 mm, the target D99 degradation was 3.36 ± 0.55% on average for IMPT, and 2.05 ± 0.53% SPArc. Thus, it indicated that SPArc or IMPT with repainting was preferred to lung SBRT rather than IMPT alone without repainting. When the target offset >10 mm, the relative target dose D99 degradation was greater than 3% in both phantom and patient cases, indicating that IMPT poses a potential risk in missing part of the target in lung SBRT. In contrast, SPArc could mitigate the target dose degradation caused by interplay effect well in the 4D phantom model. The phantom study indicated that SPArc is as effective as five times of volumetric repainting IMPT in terms of interplay effect mitigation at 10 mm target motion amplitude. Only SI directional and rigid motion being considered in 4D phantom model, it required further investigation since 3D motion and complicated shape changes occurred for the clinical patients. Despite the effectiveness of motion interplay mitigation SPArc offered was compromised in the patient group, it was significantly superior to IMPT without repainting.

The previous study indicated that repainting might not be needed when multiple filed are applied with target amplitude up to 6 mm, because dose blurring effects appear negligible between standard delivery and repainting technique (43). A similar phenomenon was observed in our study as well, where the interplay effect between SPArc and IMPT is very close with target motion less than 6 mm. Additionally, Knopf et al. also demonstrated that IMPT with multiple beams was able to mitigate the interplay effect for targets with large motion amplitude (43), which was confirmed in our study. Our result indicated that SPArc plan could offer superior interplay effect mitigation through applying many beam angles via arc trajectory for the target motion more than10mm, compared to IMPT with two beams.

Lung SBRT for Stage I NSCLC is a highly effective treatment that is being increasingly utilized (4, 44, 45). Lung SBRT is characterized by using a hypo-fractionated treatment course with a biological equivalent dose of at least 100 Gy. Proton lung SBRT offers increased conformality compared to photon lung SBRT; however, there is uncertainty in tumor coverage mainly due to the interplay effect. Thus, proton lung SBRT commonly has been described with passive scattering techniques typically using at least ten fractions (46, 47). Chen et al. reported on using lung SBRT with IMPT with a few patients receiving eight fractions, although the majority had at least ten fractions (48). This study indicated that SPArc's ability to mitigate the interplay effect could improve the normal tissue toxicity while also providing the means to use three to five fraction regimens commonly used with photon SBRT. Even single fractions of photon lung SBRT were

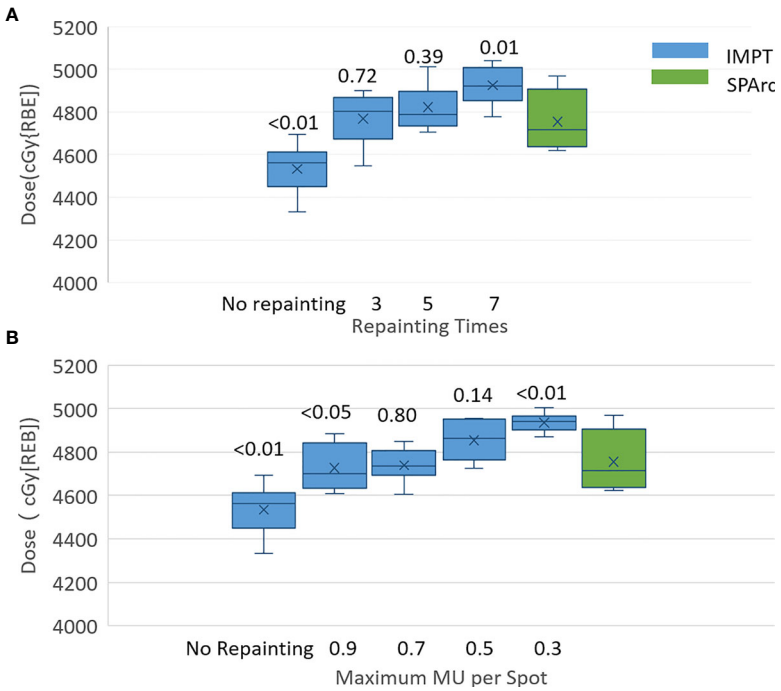

FIGURE 5 | Single fraction 4D dynamic dose of patient #10 for target D99 along with **(A)** volumetric repainting times and **(B)** maximum MU per spot. The top value is the p value for the comparison of target D99 between IMPT with repainting and SPArc without repainting.

shown in RTOG 0915 to have comparable efficacy and toxicity to four fractions (48, 49). The logistical and financial benefits of hypofractionation are attractive in this population of patients with multiple medical comorbidities. SPArc's increased robustness enables the use.

Other motion management strategies such as passive pressure technique, gating, the breath-hold approach could be implemented in the clinical practice, but these procedures prolong treatment time, which causes additional intra-fractionation motion or setup uncertainties (50). This study demonstrated that SPArc could effectively mitigate motion interplay. This new finding of utilizing SPArc to mitigate the interplay effect opens a new direction of motion management strategy by increase the degree of freedom such as arc(s) trajectory to effectively reduce the dosimetric impact from each beam's direction. More specifically, for patient #10, where the breathing-induced motion exceeds 2 cm, the effectiveness of interplay effect mitigation of using SPArc technique reached five times of IMPT with volumetric repainting or IMPT using iso-layered repainting with maximum MU per spot as 0.5 MU at most, in which the corresponding GTV D99 were 4,822 ± 98 cGy [RBE] (p = 0.39) and 4,854 ± 86 cGy [RBE] (p = 0.14) (**Figures 5A, B**).

In general, SBRT is associated with a low incidence of acute and late toxicity. However, late chest well toxicity such as chest pain has been reported, typically mild to moderate. Moreover, chest wall pain commonly occurs with a median time of onset of greater than six months after the treatment. This study shows that SPArc has significantly spared the chest wall V30. Consequently, the probability of CW toxicity was improved considerably from 40.2 ± 29.0% (VMAT) (p = 0.01) and 16.3 ± 12.0% (IMPT) (P = 0.01) to 10.1 ± 5.4% (SPArc), which would improve the probability of chest wall toxicity and patient's life quality.

CONCLUSION

A 4D interplay digital phantom model for mobile lung target was established to evaluate the effectiveness of interplay effect mitigation quantitatively. SPArc, as a novel proton treatment technique, could significantly reduce the dosimetric impact from the interplay effect and potentially reduce the Chestwall pain in lung SBRT.

DATA AVAILABILITY STATEMENT

The raw data supporting the conclusions of this article will be made available by the authors, without undue reservation.

ETHICS STATEMENT

The studies involving human participants were reviewed and approved by Beaumont Health Institutional Review Board. Written informed consent for participation was not required

for this study in accordance with the national legislation and the institutional requirements.

AUTHOR CONTRIBUTIONS

GL contributed to the acquisition, analysis, and interpretation of data and drafted and designed the paper. XL provided technical support. IG and RD contributed to revising the paper and providing clinical inputs. AQ, DY, CS, and SZ provided support in imaging acquisition. LZ contributed to the statistical analysis. XD contributed to the design of the study, revised the draft, and led the research direction. All authors contributed to the article and approved the submitted version.

FUNDING

The study is supported by Ion Beam Application S.A. (IBA, Belgium). The funder was not involved in the study design, collection, analysis, interpretation of data, the writing of this article or the decision to submit it for publication.

REFERENCES

1. Grills IS, Hugo G, Kestin LL, Galerani AP, Chao KK, Wloch J, et al. Image-Guided Radiotherapy via Daily Online Cone-Beam CT Substantially Reduces Margin Requirements for Stereotactic Lung Radiotherapy. *Int J Radiat Oncol Biol Phys* (2008) 70:1045–56. doi: 10.1016/j.ijrobp.2007.07.2352
2. RTOG 0618. Stereotactic body radiation therapy (SBRT) to treat operable early-stage lung cancer patients. Available at: https://ascopubs.org/doi/abs/10.1200/jco.2013.31.15_suppl.7523 (Accessed March 12, 2021).
3. Timmerman RD, Hu C, Michalski JM, Bradley JC, Galvin J, Johnstone DW, et al. Long-term Results of Stereotactic Body Radiation Therapy in Medically Inoperable Stage I Non–Small Cell Lung Cancer. *JAMA Oncol* (2018) 4:1287. doi: 10.1001/jamaoncol.2018.1258
4. Fakiris AJ, McGarry RC, Yiannoutsos CT, Papiez L, Williams M, Henderson MA, et al. Stereotactic body radiation therapy for early-stage non-small-cell lung carcinoma: four-year results of a prospective phase II study. *Int J Radiat Oncol Biol Phys* (2009) 75:677–82. doi: 10.1016/j.ijrobp.2008.11.042
5. Onishi H, Shirato H, Nagata Y, Hiraoka M, Fujino M, Gomi K, et al. Hypofractionated stereotactic radiotherapy (HypoFXSRT) for stage I non-small cell lung cancer: updated results of 257 patients in a Japanese multi-institutional study. *J Thorac Oncol* (2007) 2:S94–100. doi: 10.1097/JTO.0b013e318074de34
6. Uematsu M, Shioda A, Suda A, Fukui T, Ozeki Y, Hama Y, et al. Computed tomography-guided frameless stereotactic radiotherapy for stage I non-small cell lung cancer: a 5-year experience. *Int J Radiat Oncol Biol Phys* (2001) 51:666–70.
7. Newhauser WD, Zhang R. The physics of proton therapy. *Phys Med Biol* (2015) 60:R155–209. doi: 10.1088/0031-9155/60/8/R155
8. Georg D, Hillbrand M, Stock M, Dieckmann K, Pötter R. Can protons improve SBRT for lung lesions? Dosimetric considerations. *Radiother Oncol* (2008) 88:368–75. doi: 10.1016/j.radonc.2008.03.007
9. Zhang X, Li Y, Pan X, Xiaoqiang L, Mohan R, Komaki R, et al. Intensity-Modulated Proton Therapy Reduces the Dose to Normal Tissue Compared With Intensity-Modulated Radiation Therapy or Passive Scattering Proton Therapy and Enables Individualized Radical Radiotherapy for Extensive Stage IIIB Non-Small-Cell Lung Cancer: A Virtual Clinical Study. *Int J Radiat Oncol Biol Phys* (2010) 77:357–66. doi: 10.1016/j.ijrobp.2009.04.028
10. Ding X, Dionisi F, Tang S, Ingram M, Hung C-Y, Prionas E, et al. A comprehensive dosimetric study of pancreatic cancer treatment using three-dimensional conformal radiation therapy (3DCRT), intensity-modulated radiation therapy (IMRT), volumetric-modulated radiation therapy (VMAT), and passive-scattering and modulated-scanning proton therapy (PT). *Med Dosimetry* (2014) 39:139–45. doi: 10.1016/j.meddos.2013.11.005
11. Chang JY, Zhang X, Wang X, Kang Y, Riley B, Bilton S, et al. Significant reduction of normal tissue dose by proton radiotherapy compared with three-dimensional conformal or intensity-modulated radiation therapy in Stage I or Stage III non–small-cell lung cancer. *Int J Radiat Oncol Biol Phys* (2006) 65:1087–96. doi: 10.1016/j.ijrobp.2006.01.052
12. Engwall E, Glimelius L, Hynning E. Effectiveness of different rescanning techniques for scanned proton radiotherapy in lung cancer patients. *Phys Med Biol* (2018) 63:095006. doi: 10.1088/1361-6560/aabb7b
13. Boria AJ, Uh J, Pirlepesov F, Stuckey JC, Axente M, Gargone MA, et al. Interplay Effect of Target Motion and Pencil-Beam Scanning in Proton Therapy for Pediatric Patients. *Int J Particle Ther* (2018) 5:1–10. doi: 10.14338/IJPT-17-00030.1
14. Bernatowicz K, Lomax AJ, Knopf A. Comparative study of layered and volumetric rescanning for different scanning speeds of proton beam in liver patients. *Phys Med Biol* (2013) 58:7905–20. doi: 10.1088/0031-9155/58/22/7905
15. Court LE, Wagar M, Ionascu D, Berbeco R, Chin L. Management of the interplay effect when using dynamic MLC sequences to treat moving targets: Managing the interplay effect. *Med Phys* (2008) 35:1926–31. doi: 10.1118/1.2896083
16. Schätti A, Zakova M, Meer D, Lomax AJ. Experimental verification of motion mitigation of discrete proton spot scanning by re-scanning. *Phys Med Biol* (2013) 58:8555–72. doi: 10.1088/0031-9155/58/23/8555
17. Zenklusen SM, Pedroni E, Meer D. A study on repainting strategies for treating moderately moving targets with proton pencil beam scanning at the new Gantry 2 at PSI. *Phys Med Biol* (2010) 55:5103–21. doi: 10.1088/0031-9155/55/17/014
18. Ding X, Li X, Zhang JM, Kabolizadeh P, Stevens C, Yan D. Spot-Scanning Proton Arc (SPArc) Therapy: The First Robust and Delivery-Efficient Spot-Scanning Proton Arc Therapy. *Int J Radiat Oncol Biol Phys* (2016) 96:1107–16. doi: 10.1016/j.ijrobp.2016.08.049
19. Li X, Kabolizadeh P, Yan D, Qin A, Zhou J, Hong Y, et al. Improve dosimetric outcome in stage III non-small-cell lung cancer treatment using spot-scanning proton arc (SPArc) therapy. *Radiat Oncol* (2018) 13:35. doi: 10.1186/s13014-018-0981-6
20. Chang S, Liu G, Zhao L, Dilworth JT, Zheng W, Jawad S, et al. Feasibility study: spot-scanning proton arc therapy (SPArc) for left-sided whole breast radiotherapy. *Radiat Oncol* (2020) 15:232. doi: 10.1186/s13014-020-01676-3
21. Liu G, Li X, Qin A, Zheng W, Yan D, Zhang S, et al. Improve the dosimetric outcome in bilateral head and neck cancer (HNC) treatment using spot-scanning proton arc (SPArc) therapy: a feasibility study. *Radiat Oncol* (2020) 15:21. doi: 10.1186/s13014-020-1476-9
22. Ding X, Li X, Qin A, Zhou J, Yan D, Stevens C, et al. Have we reached proton beam therapy dosimetric limitations? – A novel robust, delivery-efficient and continuous spot-scanning proton arc (SPArc) therapy is to improve the dosimetric outcome in treating prostate cancer. *Acta Oncol* (2018) 57:435–7. doi: 10.1080/0284186X.2017.1358463
23. Ding X, Zhou J, Li X, Blas K, Liu G, Wang Y, et al. Improving dosimetric outcome for hippocampus and cochlea sparing whole brain radiotherapy using spot-scanning proton arc therapy. *Acta Oncol* (2019) 0:1–8. doi: 10.1080/0284186X.2018.1555374
24. Zhang F, Kelsey CR, Yoo D, Yin F-F, Cai J. Uncertainties of 4-dimensional computed tomography-based tumor motion measurement for lung stereotactic body radiation therapy. *Pract Radiat Oncol* (2014) 4:e59–65. doi: 10.1016/j.prro.2013.02.009
25. Liu G, Hu F, Ding X, Li X, Shao Q, Wang Y, et al. Simulation of dosimetry impact of 4DCT uncertainty in 4D dose calculation for lung SBRT. *Radiat Oncol* (2019) 14:1–25. doi: 10.1186/s13014-018-1191-y
26. Glide-Hurst CK, Hugo GD, Liang J, Yan D. A simplified method of four-dimensional dose accumulation using the mean patient density

representation: 4D dose accumulation using mean patient density representation. *Med Phys* (2008) 35:5269–77. doi: 10.1118/1.3002304
27. Bissonnette J-P, Franks KN, Purdie TG, Moseley DJ, Sonke J-J, Jaffray DA, et al. Quantifying Interfraction and Intrafraction Tumor Motion in Lung Stereotactic Body Radiotherapy Using Respiration-Correlated Cone Beam Computed Tomography. *Int J Radiat Oncol Biol Phys* (2009) 75:688–95. doi: 10.1016/j.ijrobp.2008.11.066
28. Suryanto A, Herlambang K, Rachmatullah P. Comparison of tumor density by CT scan based on histologic type in lung cancer patients. *Acta Med Indones* (2005) 37:195–8.
29. Paganetti H, Niemierko A, Ancukiewicz M, Gerweck LE, Goitein M, Loeffler JS, et al. Relative biological effectiveness (RBE) values for proton beam therapy. *Int J Radiat Oncol Biol Phys* (2002) 53:407–21. doi: 10.1016/S0360-3016(02)02754-2
30. Liu W, Frank SJ, Li X, Li Y, Park PC, Dong L, et al. Effectiveness of robust optimization in intensity-modulated proton therapy planning for head and neck cancers: Robust optimization for IMPT for H&N cancer. *Med Phys* (2013) 40:051711. doi: 10.1118/1.4801899
31. Liu W, Zhang X, Li Y, Mohan R. Robust optimization of intensity modulated proton therapy: Robust optimization of IMPT. *Med Phys* (2012) 39:1079–91. doi: 10.1118/1.3679340
32. Li H, Li Y, Zhang X, Li X, Liu W, Gillin MT, et al. Dynamically accumulated dose and 4D accumulated dose for moving tumors: Dynamic dose and 4D dose. *Med Phys* (2012) 39:7359–67. doi: 10.1118/1.4766434
33. Otto K. Volumetric modulated arc therapy: IMRT in a single gantry arc: Single arc radiation therapy. *Med Phys* (2007) 35:310–7. doi: 10.1118/1.2818738
34. Aoyama H, Westerly DC, Mackie TR, Olivera GH, Bentzen SM, Patel RR, et al. Integral radiation dose to normal structures with conformal external beam radiation. *Int J Radiat Oncol Biol Phys* (2006) 64:962–7. doi: 10.1016/j.ijrobp.2005.11.005
35. Stephans KL, Djemil T, Tendulkar RD, Robinson CG, Reddy CA, Videtic GMM. Prediction of Chest Wall Toxicity From Lung Stereotactic Body Radiotherapy (SBRT). *Int J Radiat Oncol Biol Phys* (2012) 82:974–80. doi: 10.1016/j.ijrobp.2010.12.002
36. Daly ME, Luxton G, Choi CYH, Gibbs IC, Chang SD, Adler JR, et al. Normal Tissue Complication Probability Estimation by the Lyman-Kutcher-Burman Method Does Not Accurately Predict Spinal Cord Tolerance to Stereotactic Radiosurgery. *Int J Radiat Oncol Biol Phys* (2012) 82:2025–32. doi: 10.1016/j.ijrobp.2011.03.004
37. Willner J, Jost A, Baier K, Flentje M. A Little to a Lot or a Lot to a Little?: An Analysis of Pneumonitis Risk from Dose-Volume Histogram Parameters of theLung in Patients with Lung Cancer Treated with 3-D Conformal Radiotherapy. *Strahlenther Onkol* (2003) 179:548–56. doi: 10.1007/s00066-003-1078-0
38. Burman C, Kutcher GJ, Emami B, Goitein M. Fitting of normal tissue tolerance data to an analytic function. *Int J Radiat Oncol Biol Phys* (1991) 21:123–35. doi: 10.1016/0360-3016(91)90172-Z
39. Ricardi U, Filippi AR, Guarneri A, Giglioli FR, Mantovani C, Fiandra C, et al. Dosimetric predictors of radiation-induced lung injury in stereotactic body radiation therapy. *Acta Oncol* (2009) 48:571–7. doi: 10.1080/02841860802520821
40. Zimmermann FB, Geinitz H, Schill S, Thamm R, Nieder C, Schratzenstaller U, et al. Stereotactic hypofractionated radiotherapy in stage I (T1-2 N0 M0) non-small-cell lung cancer (NSCLC). *Acta Oncol* (2006) 45:796–801. doi: 10.1080/02841860600913210
41. Grassberger C, Dowdell S, Lomax A, Sharp G, Shackleford J, Choi N, et al. Motion Interplay as a Function of Patient Parameters and Spot Size in Spot Scanning Proton Therapy for Lung Cancer. *Int J Radiat Oncol Biol Phys* (2013) 86:380–6. doi: 10.1016/j.ijrobp.2013.01.024
42. Seco J, Robertson D, Trofimov A, Paganetti H. Breathing interplay effects during proton beam scanning: simulation and statistical analysis. *Phys Med Biol* (2009) 54:N283–94. doi: 10.1088/0031-9155/54/14/N01
43. Knopf A-C, Hong TS, Lomax A. Scanned proton radiotherapy for mobile targets—the effectiveness of re-scanning in the context of different treatment planning approaches and for different motion characteristics. *Phys Med Biol* (2011) 56:7257–71. doi: 10.1088/0031-9155/56/22/016
44. Zhang Y, Chen Y, Qiu J, Yang J. Dosimetric Comparisons of Lung SBRT with Multiple Metastases by Two Advanced Planning Systems. *Int J Med Phys Clin Eng Radiat Oncol* (2014) 03:252–61. doi: 10.4236/ijmpcero.2014.34032
45. Nagata Y, Takayama K, Matsuo Y, Norihisa Y, Mizowaki T, Sakamoto T, et al. Clinical outcomes of a phase I/II study of 48 Gy of stereotactic body radiotherapy in 4 fractions for primary lung cancer using a stereotactic body frame. *Int J Radiat Oncol Biol Phys* (2005) 63:1427–31. doi: 10.1016/j.ijrobp.2005.05.034
46. Liu Q, Zhu Z, Chen Y, Deng J, Ai D, Liu Q, et al. Phase 2 Study of Stereotactic Body Radiation Therapy for Patients with Oligometastatic Esophageal Squamous Cell Carcinoma. *Int J Radiat Oncol Biol Phys* (2020) 108:707–15. doi: 10.1016/j.ijrobp.2020.05.003
47. Westover KD, Seco J, Adams JA, Lanuti M, Choi NC, Engelsman M, et al. Proton SBRT for medically inoperable stage I NSCLC. *J Thorac Oncol* (2012) 7:1021–5. doi: 10.1097/JTO.0b013e31824de0bf
48. Videtic GM, Paulus R, Singh AK, Chang JY, Parker W, Olivier KR, et al. Long-term Follow-up on NRG Oncology RTOG 0915 (NCCTG N0927): A Randomized Phase 2 Study Comparing 2 Stereotactic Body Radiation Therapy Schedules for Medically Inoperable Patients With Stage I Peripheral Non-Small Cell Lung Cancer. *Int J Radiat Oncol Biol Phys* (2019) 103:1077–84. doi: 10.1016/j.ijrobp.2018.11.051
49. Videtic GM, Paulus R, Singh AK, Chang JY, Parker W, Olivier K, et al. Long-Term Follow-Up on NRG Oncology RTOG 0915 (NCCTG N0927): A Randomized Phase 2 Study Comparing 2 Stereotactic Body Radiation Therapy Schedules for Medically Inoperable Patients with Stage I Peripheral Non–small Cell Lung Cancer. *Int J Radiat Oncol Biol Phys* (2017) 99:S15–6. doi: 10.1016/j.ijrobp.2017.06.052
50. Engwall E, Glimelius L, Hynning E. Effectiveness of different rescanning techniques for scanned proton radiotherapy in lung cancer patients. *Phys Med Biol* (2018) 63:095006. doi: 10.1088/1361-6560/aabb7b

Conflict of Interest: XD, XL, and DY have a patent related to spot-scanning arc therapy.

The remaining authors declare that the research was conducted in the absence of any commercial or financial relationships that could be construed as a potential conflict of interest.

frontiers in Oncology

ORIGINAL RESEARCH
published: 29 April 2021
doi: 10.3389/fonc.2021.654251

Image-Guided Robotic Radiosurgery for the Management of Spinal Ependymomas

Felix Ehret[1,2], Markus Kufeld[2], Christoph Fürweger[2,3], Alfred Haidenberger[2], Paul Windisch[2,4], Carolin Senger[1,5], Melina Kord[1], Malte Träger[1], David Kaul[1,6], Christian Schichor[7], Jörg-Christian Tonn[7] and Alexander Muacevic[2]*

[1] Charité – Universitätsmedizin Berlin, Corporate Member of Freie Universität Berlin and Humboldt-Universität zu Berlin, Department of Radiation Oncology, Berlin, Germany, [2] European Cyberknife Center, Munich, Germany, [3] Department of Stereotaxy and Functional Neurosurgery, University Hospital Cologne, Cologne, Germany, [4] Department of Radiation Oncology, Kantonsspital Winterthur, Winterthur, Switzerland, [5] Charité – Universitätsmedizin Berlin, Corporate Member of Freie Universität Berlin and Humboldt-Universität zu Berlin, Charité CyberKnife Center, Berlin, Germany, [6] German Cancer Consortium (DKTK), Partner Site Berlin, German Cancer Research Center (DKFZ), Heidelberg, Germany, [7] Department of Neurosurgery, Ludwig-Maximilians-University Munich, Munich, Germany

OPEN ACCESS

Edited by:
Alessio Bruni,
University Hospital of Modena, Italy

Reviewed by:
Debra Freeman,
Naples Radiation Oncology,
United States
Young Kwok,
University of Maryland Medical Center,
United States

***Correspondence:**
Felix Ehret
felix.ehret@charite.de
orcid.org/0000-0001-6177-1755

Specialty section:
This article was submitted to Radiation Oncology, a section of the journal Frontiers in Oncology

Received: *15 January 2021*
Accepted: *25 March 2021*
Published: *29 April 2021*

Citation:
Ehret F, Kufeld M, Fürweger C, Haidenberger A, Windisch P, Senger C, Kord M, Träger M, Kaul D, Schichor C, Tonn J-C and Muacevic A (2021) Image-Guided Robotic Radiosurgery for the Management of Spinal Ependymomas. Front. Oncol. 11:654251. doi: 10.3389/fonc.2021.654251

Background: Ependymomas are rare neoplasms of the central nervous system (CNS), usually localized intracranially and most commonly diagnosed in children. Spinal ependymomas are more frequent in young adults. They are either primary lesions or manifest as disseminated seeding of cranial tumors. Data on the management of spinal ependymoma lesions remain scarce, especially concerning stereotactic radiosurgery (SRS) and stereotactic body radiation therapy (SBRT). The purpose of this study is to report the treatment outcomes of two institutions using robotic radiosurgery (RRS) for the treatment of spinal ependymomas.

Materials and Methods: All patients with a histopathologically confirmed diagnosis of an ependymoma WHO grade II or III who were treated with RRS for one or more spinal lesions were included in this analysis.

Results: Twelve patients underwent RRS for the treatment of 32 spinal ependymoma lesions between 2005 and 2020. Two patients were below the age of 18 when treated, whereas nine patients (75%) suffered from a primary spinal ependymoma. The median dose was 15 Gy prescribed to a median isodose of 70%, with 27 lesions (84%) receiving a single-session treatment. The local control (LC) after a median follow-up of 56.7 months was 84%. LC rates at 1, 3, and 5 years were 92, 85, and 77%, respectively. The Kaplan-Meier estimated overall survival after 1, 3, and 5 years were 75, 75, and 64%, respectively. Five patients died, all of them suffering from an anaplastic ependymoma, with widespread CNS tumor progression being the reason for death in four patients. The majority of patients (58%) showed a stable neurological status at the last available follow-up. Overall, the treatment was well tolerated.

Conclusion: RRS appears to be a safe and efficient treatment modality for managing primary and secondary spinal ependymal tumors in patients with multiple lesions and local recurrences.

Keywords: ependymoma, ependymal tumors, radiosurgery, SBRT, spine, CyberKnife

INTRODUCTION

Ependymomas or ependymal tumors are rare neoplasms of the central nervous system (CNS) and of neuroectodermal origin (1, 2). With an estimated annual incidence of 0.43 per 100.000 and year, this tumor entity accounts for 1.7% of all primary CNS tumors (3). Ependymomas are more commonly found in children and young adults, where they represent 4.7% of all CNS tumors (3). These tumors arise from the ependymal lining of the cerebral ventricles, choroid plexus, and central canal of the spinal cord. Locally distinct radial glia cells of the subventricular zone are supposed to be the cells of origin of ependymoma. Spinal ependymomas are more commonly found in young adults, whereas most of the ependymal tumors in children are intracranially located (3–5). Today, nine distinct molecular subgroups based on DNA methylation patterns have been identified, which may guide and advance personalized therapies (1, 6, 7). Today, the mainstay of treatment is the gross total surgical tumor resection as recommended by the European Association of Neuro-Oncology (EANO) (1). Depending on the World Health Organization (WHO) grading, location, and extent of surgical resection, adjuvant radiotherapy and chemotherapy are further components of the multimodal treatment (1, 8). In patients with poor Karnofsky Performance Status (KPS), tumor relapses, widespread disease, and multiple spinal lesions, surgery and conventional radiotherapy may not be repeatable or feasible (1, 2). Stereotactic radiosurgery (SRS) and stereotactic body radiation therapy (SBRT) may be salvage treatment options and help to stop local tumor progression - at least temporarily (9–11). Information on the treatment outcomes after SRS and SBRT for ependymal tumor lesions are scarce, especially concerning spinal ependymomas and robotic radiosurgery (RRS) (10, 12, 13). To the best of our knowledge, only two other reports dedicated to spinal ependymomas are available in the English literature to date (10, 13). Herein, we report the 15-year institutional experience of two treatment centers, including results on local tumor control, treatment characteristics, survival outcomes, and adverse events (AE).

MATERIALS AND METHODS

All patients who were treated at two institutions for a spinal ependymal tumor between 2005 and 2020 were included in this retrospective analysis. Only patients with a histopathological ependymoma diagnosis, including grading according to the WHO CNS tumor classification, were eligible. Indication for RRS was confirmed by an interdisciplinary neurooncological tumor board involving neurosurgeons, neuroradiologists, neuropathologists, and radiation oncologists. Medical history, including pretreatments, treatment plans, neurological deficits, imaging data, and histology, were either stored in a dedicated radiosurgical database or hospital records (14). All patients underwent image-guided RRS using a CyberKnife® robotic radiosurgery system (Accuray Inc., Sunnyvale, CA, USA). Patients only undergoing biopsy for histological confirmation were classified as non-surgical cases. For treatment delivery, contrast-enhanced computed tomography (CT) and magnetic resonance imaging (MRI) scans were acquired for every patient and subsequently overlaid for inverse treatment planning with changing versions of proprietary planning software (MultiPlan, Precision, Accuray Inc., Sunnyvale, CA, USA). Local tumor response, clinical symptoms, and AE were evaluated clinically and by MRI assessment every three months for the first year, then every six months during follow-up or depending on the patients' status and clinical suspicion for tumor progression. The Kaplan-Meier estimate was applied for the respective analyses on the length of local control (LC) and overall survival (OS). LC was defined as an unchanged or decreased tumor volume on follow-up imaging, whereas local failure was defined as an increased tumor volume during follow-up. AE were assessed by the clinical notes of the respective physician and available imaging data. Data were tested for normal distribution by the Shapiro-Wilk test and graphical appearance, including skewness and kurtosis. Normally distributed continuous variables were analyzed with the unpaired student's t-test, non-normally distributed data with the Wilcoxon rank-sum test. All p-values were two-sided and statistical significance was defined as $p<0.05$. Statistical analyses were performed with STATA MP 16.0 (StataCorp, College Station, TX, USA). This study was approved by the institutional review board of the Ludwig-Maximilians-University Munich (20-256 KB).

RESULTS

Patients and Treatment Characteristics

Twelve patients with 32 spinal ependymoma lesions between 2005 and 2020 were included in this analysis. The majority of patients were male (67%). Two patients (17%) were below the age of 18 when treated, with a median age of 34.9 years at the time of RRS. Before treatment, four (33%) patients did not show any symptoms, whereas the remaining eight suffered mostly from motoric weakness or paralysis (58%) and sensory deficits (41%). Most of the treated lesions were located in the thoracic spine (56%), with RRS being the primary treatment modality for the majority of all lesions (59%). Eight treated lesions (25%) were

local recurrences, and five (16%) received adjuvant RRS after incomplete surgical resection. Before RRS, four patients had received multiple cycles of systemic treatments. No patients received chemotherapy during RRS treatment. Nine patients (75%) suffered from a primary spinal ependymoma, whereas the remaining three had a primary ependymal intracranial tumor before developing spinal tumor lesions. The intracranial tumors were initially located in the fourth ventricle, the cerebellum, and the parietal as well as occipital lobes. All patients underwent at least one biopsy or surgical resection of a tumor lesion for histopathological examination. According to the WHO classification of CNS tumors, seven ependymomas (66%) were grade II, with the remaining five being classified as anaplastic ependymomas (grade III). No patient suffered from neurofibromatosis. The median KPS before RRS was 80%, ranging from 30 to 100%. The overall median prescription dose was 15 Gray (Gy), either delivered in a single fraction (range 10 to 16.5 Gy) or three fractions (range 21 to 24 Gy). WHO grade III tumors received doses ranging from 10 to 24 Gy, whereas grade II tumors received doses between 14 and 16.5 Gy. The median prescription isodose was 70%. Twenty-seven of the 32 lesions (84%) were treated with one fraction, the remaining five lesions (16%) of two patients received three fractions. The median irradiated tumor volume was 0.37 cc, ranging from 0.03 cc in a primarily resected lesion to 2.89 cc in an unresected tumor lesion. The patient and treatment characteristics are summarized in **Table 1**.

TABLE 1 | Patient and treatment characteristics.

Number of patients		12	
Number of lesions		32	
Gender (male/female)	8		4
%	67		33
	Median	**Mean**	**Range**
Age (years)	34.9	35.1	13.7 – 71.3
Pretreatment Karnofsky Performance Status (%)	80	80	30 – 100
Follow-up (months)	56.7	55.7	3.2 – 104.2
Tumor volume (cc)	0.37	0.58	0.03 – 2.89
Number of fractions	1	1.3	1 – 3
Dose (Gy)	15	15.6	10 – 24
Prescription isodose (%)	70	71.8	70 – 85
Conformity index	1.32	1.43	1.04 – 2.67
Homogeneity index	1.43	1.39	1.18 – 1.43
Coverage	97.3	93.7	76.0 – 99.9
RRS indication	**Primary treatment**	**Recurrence**	**Adjuvant treatment**
Number of lesions	19	8	5
%	59	25	16
Tumor location	**Cervical**	**Thoracic**	**Lumbar**
Number of lesions	10	18	4
%	31	56	13
Tumor grading (WHO)	**II**		**III**
Number of patients	7		5
%	58		42
Symptoms	**None**	**Dysesthesia/ hypesthesia**	**Weakness/ paralysis**
Number of patients	4	5	7
%	33	41	58

cc, cubic centimeter; Gy, Gray; WHO, World Health Organization.

Local Outcome and Survival Data

The median follow-up time was 56.7 months, ranging from 3.2 to 104.2 months. At the last available follow-up, 27 of the 32 treated lesions were controlled, leading to a local control (LC) rate of 84%. The LC rates after 12, 36, and 60 months were 92%, 85%, and 77%, respectively (**Table 2**, **Figure 1**). The median time to local failure was 28 months. The five local recurrences after RRS occurred in four patients, with three (75%) of them suffering from an anaplastic ependymoma. No significant differences were observed between locally controlled and uncontrolled lesions in regard to dose, prescription isodose, fractions, or tumor volume due to the limited number of events. At the last available follow-up, five (42%) patients had died after a median time of seven months. All were suffering from an anaplastic ependymoma, with widespread CNS tumor progression being the reason for death in four patients. Three of these four tumor-associated deaths occurred in male patients. One patient died from tumor-unrelated causes. The overall survival rates at 12, 36, and 60 months were 75%, 75%, and 64%, respectively (**Table 2**, **Figure 2**). Of the four patients who had not shown symptoms before treatment, two remained stable throughout the follow-up, with the remaining two experiencing onsets of new symptoms (unsteady gait and back pain). The remaining eight patients

TABLE 2 | Local control and overall survival data.

Variable	Time (in months)	%
LC	12	92.8
	24	92.8
	36	85.9
	48	77.3
	60	77.3
OS	12	75.0
	24	75.0
	36	75.0
	48	64.2
	60	64.2

LC, local control; OS, overall survival.

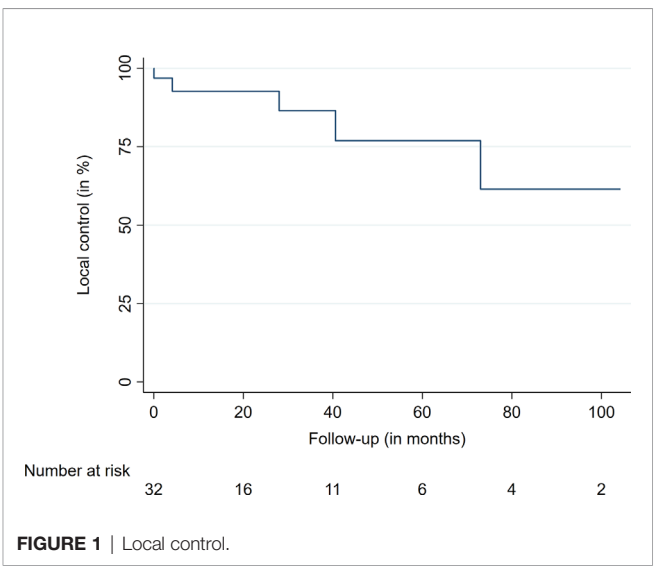

FIGURE 1 | Local control.

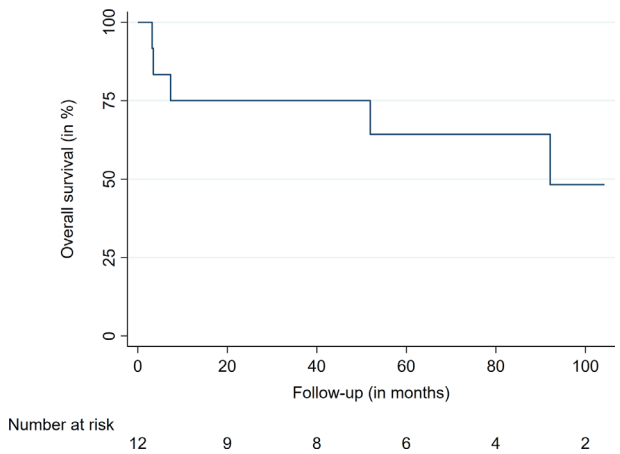

FIGURE 2 | Overall survival.

mostly presented with an unchanged neurological status (5 patients, 62%), with two patients (25%) showing progressing clinical deficits. One patient (12%) who suffered from ataxia fully recovered after treatment and remained symptom-free. The treatment was well tolerated in the majority of patients. One patient who was treated for four lesions in the thoracic spine developed edema at the treatment sites shortly after RRS. He was successfully treated with glucocorticoids. No treatment-related deaths, bleedings, radiation necrosis, or radiation-induced malignancies have been observed.

DISCUSSION

To the best of our knowledge, we report the most extensive series of radiosurgically treated spinal ependymal tumors. With most of the available SRS and SBRT data for ependymomas focusing on intracranial lesions, outcome data for spinal treatments remain sparse (10–12, 15–18). Moreover, the majority of previous studies on SRS utilized GammaKnife (GK)- or conventional linear accelerator (LINAC)-based radiosurgery (11, 12, 15–17, 19–21). Previous studies analyzing SRS and SBRT for intracranial and spinal ependymal tumors observed LC rates typically ranging between 60 and 80% (10, 13, 15, 16, 19–22). It is important to note that previous and the current study populations are heterogeneous, especially concerning age, tumor location, and previous treatments, including the degree of upfront surgical resection. This limits the comparability of the current study and past analyses. Nevertheless, our observed LC of 84% at the last available follow-up is a plausible finding. Shi et al. and Ryu et al. both analyzed cases treated at Stanford University and reported on the radiosurgical treatment of spinal ependymal lesions (10, 13). A total of 13 spinal lesions in 9 patients were treated with RRS in both studies, leading to a LC of 92% (10, 13). Notably, both studies had a shorter median follow-up and sample size than in the current series, which may account for the better results besides varying upfront treatments and the inclusion of intracranial treatments (12 and 54 months vs. 56.7 months) (10, 13). Both studies showed a favorable risk profile (10, 13). Our treatments were also well tolerated, and no severe AE were observed throughout the available follow-up.

Concerning the clinical outcomes, Ryu et al. reported improvement of the two treated patients (13). In contrast, Shi et al. did not report clinical outcomes after treatment (10). Herein, we observed stabilization of pretreatment deficits in most patients. Yet, four patients had either progressive symptoms (two) or developed new neurological deficits (two). Together with our results, RRS appears to be an effective and safe local treatment modality to limit spinal tumor progression and further neurological decline in most cases. Despite the limited sample size and patient heterogeneity, these findings may help to delay or avoid craniospinal irradiation (CSI) or repeated fractionated radiotherapy and associated AE in selected patients (23–26). In regard to the general management of intracranial and spinal ependymoma patients, the EANO have published its recommendations and guidelines in 2017 (1). In case of the spinal ependymoma recommendations, the use of SRS or SBRT is not endorsed and remains unclear, most likely due to the lack of available data and studies (1, 12). On the other hand, fractionated radiotherapy is currently recommended as an adjuvant treatment modality after complete (WHO grade III) and incomplete (WHO II and III) surgical resection in this patient subgroup, with doses ranging from 54 to 59.4 Gy (1). With the increasing availability of SRS and RRS, the number of spinal ependymal treatments may increase and help to clarify its role in the management of this challenging patient group.

Survival of patients with ependymal tumors seems to be mainly dependent on DNA methylation profiles, the extent of surgical resection, and 1q gain (6, 7). Given the recent identification of these genetic parameters and the rarity of the tumor, large prospective validations are lacking (1, 6, 7). Previous studies identified differing predictors of OS and progression-free survival (PFS), including the extent of first surgical resection, WHO grade III, intracranial tumor location as well as age, gender and tumor volume at the time of reirradiation (11, 27, 28). Our study cohort mainly consisted of adult patients (83%), with most of them suffering from a primary spinal ependymoma (75%). This subgroup of patients is known to have a more favorable outcome compared to pediatric patients with intracranial tumors (6, 7, 28). However, all four patients who succumbed to their ependymal tumors in this series were diagnosed with an anaplastic ependymoma (WHO grade III), with two of them suffering from a primary spinal ependymal tumor. Despite the small sample size, one may conclude that anaplastic histopathological features have an impact on OS. This finding is in agreement with previous studies (27, 28). However, DNA methylation data are lacking in our patients, limiting comparability and risk stratification beyond the WHO classification. Further limitations of this study include the retrospective nature, patient heterogeneity, small sample size, and a potential sampling bias. All these factors may limit the drawn conclusions of this study. Nevertheless, this study provides more evidence on the efficacy and safety of RRS for spinal ependymomas.

CONCLUSION

Spinal ependymal tumors may be efficiently treated with RRS, especially in patients with multiple lesions and local recurrences after surgical resection and adjuvant radiotherapy. Most lesions remained controlled, and the treatment was well tolerated. Further neurological decline was prevented in the majority of patients. RRS may be a preferable, time-saving, and non-invasive treatment modality for selected patients.

DATA AVAILABILITY STATEMENT

The data that support the findings of this study are available from the corresponding author, FE, upon reasonable request.

ETHICS STATEMENT

The studies involving human participants were reviewed and approved by the Institutional Review Boards of the Ludwig-Maximilians-University Munich and Charité – Universitätsmedizin Berlin. Written informed consent for participation was not required for this study in accordance with the national legislation and the institutional requirements.

AUTHOR CONTRIBUTIONS

Conception and design of the study: FE. Data acquisition: FE, MKu, CF, AH, CSe, MKo, AM. Data analysis and drafting of the manuscript: FE. Critically revising manuscript: FE, MKu, CF, PW, CSe, MT, DK, CSc, J-CT, AM. All authors contributed to the article and approved the submitted version.

ACKNOWLEDGMENTS

We acknowledge support from the German Research Foundation (DFG) and the Open Access Publication Fund of Charité – Universitätsmedizin Berlin.

REFERENCES

1. Rudà R, Reifenberger G, Frappaz D, Pfister SM, Laprie A, Santarius T, et al. EANO guidelines for the diagnosis and treatment of ependymal tumors. *Neuro Oncol* (2018) 20(4):445–56. doi: 10.1093/neuonc/nox166
2. Dorfer C, Tonn J, Rutka JT. Ependymoma: a heterogeneous tumor of uncertain origin and limited therapeutic options. *Handb Clin Neurol* (2016) 134:417–31. doi: 10.1016/b978-0-12-802997-8.00025-6
3. Ostrom QT, Cioffi G, Gittleman H, Patil N, Waite K, Kruchko C, et al. CBTRUS Statistical Report: Primary Brain and Other Central Nervous System Tumors Diagnosed in the United States in 2012-2016. *Neuro Oncol* (2019) 21 (Suppl 5):v1–v100. doi: 10.1093/neuonc/noz150
4. Khalid SI, Adogwa O, Kelly R, Metha A, Bagley C, Cheng J, et al. Adult Spinal Ependymomas: An Epidemiologic Study. *World Neurosurg* (2018) 111:e53–61. doi: 10.1016/j.wneu.2017.11.165
5. Villano JL, Parker CK, Dolecek TA. Descriptive epidemiology of ependymal tumours in the United States. *Br J Cancer* (2013) 108(11):2367–71. doi: 10.1038/bjc.2013.221
6. Pajtler KW, Witt H, Sill M, Jones DT, Hovestadt V, Kratochwil F, et al. Molecular Classification of Ependymal Tumors across All CNS Compartments, Histopathological Grades, and Age Groups. *Cancer Cell* (2015) 27(5):728–43. doi: 10.1016/j.ccell.2015.04.002
7. Witt H, Gramatzki D, Hentschel B, Pajtler KW, Felsberg J, Schackert G, et al. DNA methylation-based classification of ependymomas in adulthood: implications for diagnosis and treatment. *Neuro Oncol* (2018) 20(12):1616–24. doi: 10.1093/neuonc/noy118
8. Louis DN, Perry A, Reifenberger G, von Deimling A, Figarella-Branger D, Cavenee WK, et al. The 2016 World Health Organization Classification of Tumors of the Central Nervous System: a summary. *Acta Neuropathol* (2016) 131(6):803–20. doi: 10.1007/s00401-016-1545-1
9. Liu EK, Silverman JS, Sulman EP. Stereotactic Radiation for Treating Primary and Metastatic Neoplasms of the Spinal Cord. *Front Oncol* (2020) 10:907. doi: 10.3389/fonc.2020.00907
10. Shi S, Jin MC, Koenig J, Gibbs IC, Soltys SG, Chang SD, et al. Stereotactic Radiosurgery for Pediatric and Adult Intracranial and Spinal Ependymomas. *Stereotact Funct Neurosurg* (2019) 97(3):189–94. doi: 10.1159/000502653
11. Kano H, Su YH, Wu HM, Simonova G, Liscak R, Cohen-Inbar O, et al. Stereotactic Radiosurgery for Intracranial Ependymomas: An International Multicenter Study. *Neurosurgery* (2019) 84(1):227–34. doi: 10.1093/neuros/nyy082
12. Krieger MD, McComb JG. The role of stereotactic radiotherapy in the management of ependymomas. *Childs Nerv Syst* (2009) 25(10):1269–73. doi: 10.1007/s00381-009-0879-6
13. Ryu SI, Kim DH, Chang SD. Stereotactic radiosurgery for hemangiomas and ependymomas of the spinal cord. *Neurosurg Focus* (2003) 15(5):E10. doi: 10.3171/foc.2003.15.5.10
14. Kufeld M, Fürweger C, Drexler CG, Wowra B, Muacevic A. Implementation of a medical database system for a radiosurgery center. *Cureus* (2009) 1:e4.
15. Hoffman LM, Plimpton SR, Foreman NK, Stence NV, Hankinson TC, Handler MH, et al. Fractionated stereotactic radiosurgery for recurrent ependymoma in children. *J Neurooncol* (2014) 116(1):107–11. doi: 10.1007/s11060-013-1259-3
16. Aggarwal R, Yeung D, Kumar P, Muhlbauer M, Kun LE. Efficacy and feasibility of stereotactic radiosurgery in the primary management of unfavorable pediatric ependymoma. *Radiother Oncol* (1997) 43(3):269–73. doi: 10.1016/S0167-8140(97)01926-9
17. Kano H, Yang H-c, Kondziolka D, Niranjan A, Arai Y, Flickinger JC, et al. Stereotactic radiosurgery for pediatric recurrent intracranial ependymomas. *J Neurosurg: Pediatr PED* (2010) 6(5):417. doi: 10.3171/2010.8.Peds10252
18. Hodgson DC, Goumnerova LC, Loeffler JS, Dutton S, Black PM, Alexander E3rd, et al. Radiosurgery in the management of pediatric brain tumors. *Int J Radiat Oncol Biol Phys* (2001) 50(4):929–35. doi: 10.1016/s0360-3016(01)01518-8
19. Lo SS, Abdulrahman R, Desrosiers PM, Fakiris AJ, Witt TC, Worth RM, et al. The role of Gamma Knife Radiosurgery in the management of unresectable gross disease or gross residual disease after surgery in ependymoma. *J Neurooncol* (2006) 79(1):51–6. doi: 10.1007/s11060-005-9112-y
20. Stafford SL, Pollock BE, Foote RL, Gorman DA, Nelson DF, Schomberg PJ. Stereotactic radiosurgery for recurrent ependymoma. *Cancer* (2000) 88 (4):870–5.
21. Mansur DB, Drzymala RE, Rich KM, Klein EE, Simpson JR. The efficacy of stereotactic radiosurgery in the management of intracranial ependymoma. *J Neurooncol* (2004) 66(1-2):187–90. doi: 10.1023/b:neon.0000013472.50749.84
22. Stauder MC, Ni Laack N, Ahmed KA, Link MJ, Schomberg PJ, Pollock BE. Stereotactic radiosurgery for patients with recurrent intracranial ependymomas. *J Neurooncol* (2012) 108(3):507–12. doi: 10.1007/s11060-012-0851-2
23. Merchant TE, Boop FA, Kun LE, Sanford RA. A retrospective study of surgery and reirradiation for recurrent ependymoma. *Int J Radiat Oncol Biol Phys* (2008) 71(1):87–97. doi: 10.1016/j.ijrobp.2007.09.037

24. Bouffet E, Hawkins CE, Ballourah W, Taylor MD, Bartels UK, Schoenhoff N, et al. Survival benefit for pediatric patients with recurrent ependymoma treated with reirradiation. *Int J Radiat Oncol Biol Phys* (2012) 83(5):1541–8. doi: 10.1016/j.ijrobp.2011.10.039
25. Bauman GS, Sneed PK, Wara WM, Stalpers LJ, Chang SM, McDermott MW, et al. Reirradiation of primary CNS tumors. *Int J Radiat Oncol Biol Phys* (1996) 36(2):433–41. doi: 10.1016/s0360-3016(96)00315-x
26. Rao AD, Rashid AS, Chen Q, Villar RC, Kobyzeva D, Nilsson K, et al. Reirradiation for Recurrent Pediatric Central Nervous System Malignancies: A Multi-institutional Review. *Int J Radiat Oncol Biol Phys* (2017) 99(3):634–41. doi: 10.1016/j.ijrobp.2017.07.026
27. Rodríguez D, Cheung MC, Housri N, Quinones-Hinojosa A, Camphausen K, Koniaris LG. Outcomes of malignant CNS ependymomas: an examination of 2408 cases through the Surveillance, Epidemiology, and End Results (SEER) database (1973-2005). *J Surg Res* (2009) 156(2):340–51. doi: 10.1016/j.jss.2009.04.024
28. Pajtler KW, Mack SC, Ramaswamy V, Smith CA, Witt H, Smith A, et al. The current consensus on the clinical management of intracranial ependymoma and its distinct molecular variants. *Acta Neuropathol* (2017) 133(1):5–12. doi: 10.1007/s00401-016-1643-0

Conflict of Interest: FE reports a grant from Ludwig-Maximilians-University Munich and honoraria from Accuray outside the submitted work.

The remaining authors declare that the research was conducted in the absence of any commercial or financial relationships that could be construed as a potential conflict of interest.

frontiers in Oncology

ORIGINAL RESEARCH
published: 27 May 2021
doi: 10.3389/fonc.2021.659987

Clinical Effects of Stereotactic Body Radiation Therapy Targeting the Primary Tumor of Liver-Only Oligometastatic Pancreatic Cancer

Xiaoqin Ji[1†], Yulu Zhao[2†], Chenglong He[3], Siqi Han[3], Xixu Zhu[1], Zetian Shen[1], Cheng Chen[2] and Xiaoyuan Chu[2*]*

[1] Department of Radiation Oncology, Jinling Hospital, Nanjing Clinical School of Nanjing Medical University, Nanjing, China,
[2] Department of Medical Oncology, Jinling Hospital, Nanjing Clinical School of Nanjing Medical University, Nanjing, China,
[3] Department of Medical Oncology, Jinling Hospital, First School of Clinical Medicine, Southern Medical University, Nanjing, China

OPEN ACCESS

Edited by:
Rupesh Kotecha, Baptist Hospital of Miami, United States

Reviewed by:
Stephen Rosenberg, Moffitt Cancer Center, United States
Simon S. Lo, University of Washington, United States
Adeel Kaiser, Baptist Hospital of Miami, United States

***Correspondence:**
Cheng Chen
chencheng1289@126.com
Xiaoyuan Chu
chuxiaoyuan000@163.com

[†]These authors have contributed equally to this work

Specialty section:
This article was submitted to Radiation Oncology, a section of the journal Frontiers in Oncology

Received: *28 January 2021*
Accepted: *03 May 2021*
Published: *27 May 2021*

Citation:
Ji X, Zhao Y, He C, Han S, Zhu X, Shen Z, Chen C and Chu X (2021) Clinical Effects of Stereotactic Body Radiation Therapy Targeting the Primary Tumor of Liver-Only Oligometastatic Pancreatic Cancer. Front. Oncol. 11:659987. doi: 10.3389/fonc.2021.659987

Aim: To investigate the efficacy and safety of stereotactic body radiotherapy (SBRT) targeting the primary tumor for liver-only oligometastatic pancreatic cancer.

Methods: We compared the efficacy and safety of SBRT plus chemotherapy with chemotherapy alone in patients with liver-only oligometastatic pancreatic cancer. The populations were balanced by propensity score-weighted and propensity score-matched analyses based on baseline variables. The primary outcome was overall survival (OS). The secondary outcomes included progression free survival (PFS), local progression, metastatic progression and symptomatic local control.

Results: This is a retrospective study of 89 pancreatic cancer patients with liver-only oligometastasis. Overall, 34 (38.2%) and 55 (61.8%) patients received SBRT plus chemotherapy and chemotherapy alone, respectively. After propensity score matching, 1-year OS rate was 34.0% (95%CI, 17.8-65.1%) in the SBRT plus chemotherapy group and 16.5% (95%CI, 5.9-46.1%) in chemotherapy alone group (P=0.115). The 6-month PFS rate was 29.4% (95%CI, 15.4-56.1) in SBRT plus chemotherapy and 20.6% (95%CI, 8.8-48.6) in chemotherapy alone group (P=0.468), respectively. Further subgroup analysis indicated that the addition of SBRT improved OS in patients with primary tumor located in the head of pancreas (stratified HR, 0.28; 95% CI, 0.09 to 0.90) or good performance status (stratified HR, 0.24; 95% CI, 0.07 to 0.86). In terms of disease control, SBRT delayed local progression of pancreas (P=0.008), but not distant metastatic progression (P=0.56). Besides, SBRT offered significant abdominal/back pain relief (P=0.016) with acceptable toxicities.

Conclusions: The addition of SBRT to chemotherapy in patients with liver-only oligometastatic pancreatic cancer improves the OS of those with primary tumor located in the head of pancreas or good performance status. In addition, it is a safe and effective method for local progression control and local symptomatic palliation in patients with metastatic pancreatic cancer.

Keywords: pancreatic cancer, metastasis, stereotactic body radiotherapy, CyberKnife, pain

INTRODUCTION

Pancreatic cancer has an extremely poor prognosis with a 5-year survival rate of 9% (1). Since the disease presents few, if any, symptoms before it progresses to advanced stage, approximately 80-85% of patients present with Stage III or IV disease at the time of initial diagnosis (2, 3). For metastatic pancreatic patients, the 5-year overall survival (OS) rate is extremely low (about 3%) (1). Systemic chemotherapy combinations, including FOLFIRINOX (5-fluorouracil, folinic acid, irinotecan, and oxaliplatin) and gemcitabine plus nab-paclitaxel (GT), have emerged as standards of care of front-line therapy, increased survival with a median of 11.1 and 8.5 months, respectively (4, 5). In addition, the exploration of immunotherapy and targeted therapy has provided new treatments for these patients (6–9).

The innervation of pancreatic tissue composes the network of sympathetic and parasympathetic systems, yielding an increase in pain sensitivity (10). In most patients with pancreatic cancer, local tumor progression often cause severe symptoms, including abdominal and back pain, biliary obstruction, and pancreatic insufficiency, which severely affect patients' quality of life (2, 6). Some studies indicate that radiation therapy has shown efficacy in improving local control, delaying disease progression and ameliorating local symptoms for pancreatic cancer (11, 12).

Additionally, the locally destructive growth of primary tumor was a significant cause of death for many patients with pancreatic cancer (13). Therefore, local treatment may reduce primary tumor burden and provide better disease control, thereby improving clinical outcomes. You et al. reported that locoregional radiotherapy added to chemotherapy significantly improves OS in chemotherapy-sensitive patients with metastatic nasopharyngeal carcinoma (14). Rusthoven et al. utilized the National Cancer Database (NCDB) and found that compared with androgen deprivation alone, the addition of prostate radiotherapy substantially prolonged the OS of men with metastatic prostate cancer (15). Parker et al. reported that radiotherapy to the primary tumor did not improve OS in patients with newly diagnosed metastatic prostate cancer, but improved failure-free survival (16). Local failure is not a common cause of death in prostate malignancy. However, local progression in pancreatic cancer patients may have significant morbidity and mortality. Thus, in patients with mestastatic pancreatic cancer, radiation therapy targeting the primary tumor may have a different rationale. In the last few years, stereotactic body radiotherapy (SBRT) has emerged as a local treatment for pancreatic cancer with local control rate exceeding 90% at 1 year (17, 18). However, there is few research on the application of SBRT to the primary tumor for metastatic pancreatic cancer.

In this study, we retrospectively investigated the efficacy and safety of SBRT to primary tumor with chemotherapy *vs* chemotherapy alone in patients with liver-only oligometastatic pancreatic cancer at initial diagnosis.

Abbreviations: SBRT, stereotactic body radiotherapy; PFS, progression-free survival; OS, overall survival; CA19–9, carbohydrate antigen 19–9; CT, computed tomography; MRI, magnetic resonance imaging; ^{18}F-FDG-PET/CT, 18-fluorodeoxyglucose positron emission tomography/computed tomography; ECOG, Eastern Cooperative Oncology Group; GTV: gross tumor volume; CTV, clinical tumor volume; PTV, planning tumor volume; BED, biological effective dose; Gy, gray; IPTW, inverse probability of treatment weight; SMD, standardized mean difference. S-1, the prodrug of 5-fluorouracil comprising tegafur, gimeracil, and oteracil; GT, gemcitabine and nab-paclitaxel; GS, gemcitabine and S-1; Gemox, gemcitabine plus oxaliplatin.

METHODS

Patients

This retrospective study was conducted on 89 pancreatic cancer patients with liver-only metastasis at initial diagnosis from January 2010 to December 2019 in Jinling Hospital. They were treated with systemic chemotherapy alone or plus SBRT delivered to the primary tumor. The inclusion criteria of the patients were: (1) Histologically or cytologically confirmed, or clinically diagnosed according to our clinical diagnosis criteria, including typical pancreatic cancer symptoms (abdominal/back pain) and positive carbohydrate antigen 19–9 (CA19-9) value, computed tomography (CT), magnetic resonance imaging (MRI) and 18-fluorodeoxyglucose positron emission tomography/computed tomography (^{18}F-FDG-PET/CT); (2) Oligometastases, with a maximum of 5 metastases in the liver (< 4 cm in size); (3) Comprehensive clinical and imaging examinations prior to treatment proved to be accompanied by liver metastasis at initial diagnosis; (4) Patients who had previously been treated with abdominal radiotherapy, and had a synchronous abdominal cancer or other cancers requiring treatment were excluded. The study was approved by the Ethics Committee of our institution, and written informed consents were obtained from all patients. The main characteristics of all patients are summarized in **Table 1**. Before treatment, data were collected, such as performance status of Eastern Cooperative Oncology Group (ECOG), age, baseline serum carbohydrate antigen 19–9 (CA19-9) concentration, T and N stages.

SBRT

The study used CyberKnife (Accuray Incorporated, Sunnyvale, CA, USA) for localized treatment. Firstly, all patients were implanted with 1-3 gold markers (5.0 × 0.8 mm) under ultrasound or CT guidance. The gold fiducials were placed in the lesion. Then, when the gold fiducial was firmly attached to the surrounding tissue (approximately 7 days), abdominal CT scan (Brilliace Big Bore 16CT Philips Germany) was performed. Before CT positioning, patient was fasted for more than 4 hours. 100-150 ml of oral contrast agent was taken 30, 20 and 10 minutes before the CT scan to clearly show the gastrointestinal tract. Besides, intravenous contrast was also used to better display the lesions. The CT scan range is 15 cm above and below the pancreatic lesion, and the layer thickness is 1 mm.

The gross tumor volume (GTV) was the primary tumor of the pancreas and enlarged lymph nodes (defined as short axis diameter ≥ 1 cm, or PET positive) observed through the imaging. MRI or 18F-FDG-PET/CT were used for target

TABLE 1 | Comparison of baseline variables between SBRT plus chemotherapy and chemotherapy alone groups in the original and matched data sets.

Characteristic	Unmatched cohort			Propensity-score-matched cohort		
	SBRT plus chemotherapy (n = 34)	Chemotherapy alone (n = 55)	P	SBRT plus chemotherapy (n = 23)	Chemotherapy alone (n = 23)	P
Age (years)			0.802			0.768
≤60	17 (50%)	26 (47.3%)		11 (47.8%)	12 (52.2%)	
>60	17 (50%)	29 (52.7%)		12 (52.2%)	11 (47.8%)	
Gender			0.657			0.345
Male	22 (64.7%)	33 (60.0%)		14 (60.9%)	17 (73.9%)	
Female	12 (35.3%)	22 (40.0%)		9 (39.1%)	6 (26.1%)	
Year of diagnosis			0.007			0.760
2010-2014	21 (61.8%)	18 (32.7%)		15 (65.2%)	14 (60.9%)	
2015-2019	13 (38.2%)	37 (67.3%)		8 (34.8%)	9 (39.1%)	
Diagnostic mode			0.514			—
Clinical	5 (14.7%)	7 (12.7%)		0 (0%)	0 (0%)	
Histological/cytological	29 (85.3%)	48 (87.3%)		23 (100%)	23 (100%)	
Performance status			0.030			1.000
0-1	13 (38.2%)	34 (61.8%)		9 (39.1%)	9 (39.1%)	
2	21 (61.8%)	21 (38.2%)		14 (60.9%)	14 (60.9%)	
Primary pancreatic tumor location			0.059			1.000
Head	18 (52.9%)	18 (32.7%)		10 (43.5%)	10 (43.5%)	
Body/tail	16 (47.1%)	37 (67.3%)		13 (56.5%)	13 (56.5%)	
Pre-treatment CA19–9 (U/ml)			0.103			1.000
≤1000	19 (55.9%)	21 (38.2%)		12 (52.2%)	12 (52.2%)	
>1000	15 (44.1%)	34 (61.8%)		11 (47.8%)	11 (47.8%)	
T category※			0.030			0.765
T3	17 (50.0%)	40 (72.7%)		14 (60.9%)	13 (56.5%)	
T4	17 (50.0%)	15 (27.3%)		9 (39.1%)	10 (43.5%)	
N category※			0.676			0.767
N0	17 (50.0%)	25 (45.5%)		11 (47.8%)	10 (43.5%)	
N1	17 (50.0%)	30 (54.5%)		12 (52.2%)	13 (56.5%)	
Chemotherapy regimen			0.198			1.000
GT	2 (5.9%)	1 (1.8%)		2 (8.7%)	1 (4.3%)	
Gemox	11 (32.4%)	13 (23.6%)		6 (26.1%)	6 (26.1%)	
GS	9 (26.5%)	25 (45.5%)		7 (30.4%)	8 (34.8%)	
GP	3 (8.8%)	1 (1.8%)		2 (8.7%)	1 (4.3%)	
G	9 (26.5%)	13 (23.6%)		6 (26.1%)	7 (30.4%)	
Others	0 (0.0%)	2 (3.6%)		0 (0.0%)	0 (0.0%)	
Chemotherapy cycles			0.777			0.873
1	4 (11.8%)	5 (9.1%)		3 (13.0%)	5 (21.7%)	
2	11 (32.4%)	13 (23.6%)		8 (34.8%)	5 (21.7%)	
3	5 (14.7%)	7 (12.7%)		3 (13.0%)	3 (13.0%)	
4	8 (23.5 %)	15 (27.3%)		6 (26.1%)	6 (26.1%)	
>4	6 (17.6%)	15 (27.3%)		3 (13.1%)	4 (17.4%)	

CA19-9, carbohydrate antigen 19–9; SBRT, stereotactic body radiotherapy; GT, gemcitabine and nab-paclitaxel; Gemox, gemcitabine plus oxaliplatin; GS, gemcitabine and S-1; GP, gemcitabine and nedaplatin; G, gemcitabine. ※According to the American Joint Committee on Cancer and the Union for International Cancer Control stage system (7th edition).

delineation. Radiation oncologists delineated GTV on axial slices of the contrast-enhanced CT. Since our center performs tracking (Synchrony), internal target volume (ITV) is not requried. The clinical tumor volume (CTV) was equivalent to GTV. The planning tumor volume (PTV) margin was 0-5 mm from the GTV, depending on the disease location and size. We used oral meglumine diatrizoate to clearly display the gastrointestinal tract and MRI images to determine the junction between tumor and gastrointestinal structures, thereby helping to modify PTV to avoid overlapping of gastrointestinal organs. Average total prescribed dose was 41.1 gray (Gy) (range of 25-50 Gy), which was given in 5-7 fractions. Because the median number of fractions was 5, organs at risk (OAR) dose constraints applied for five fraction SBRT was used in this study. The dose-volume constraints for OARs are summarized in **Appendix Table 1**. Respiration synchronous tracking (Synchrony) was used to track the movement of the fiducials for simultaneous irradiation. The delivery of SBRT was performed between cycles of chemotherapy, usually once a day. SBRT usually takes about 1 h, and it is difficult for patients with severe pain to maintain the same posture over a long time. Thus, 10 mg of morphine were taken half an hour before SBRT to relieve the patient's pain and help complete the treatment.

Chemotherapy

Chemotherapy regimens were mostly gemcitabine-based chemotherapy (up to 97.8%), including gemcitabine plus nab-paclitaxel, gemcitabine plus oxaliplatin, gemcitabine plus S-1, gemcitabine monotherapy and so on (**Table 1**). Concurrent

administration of systemic therapy and SBRT was avoided if possible. Most patients continue chemotherapy after radiotherapy.

Symptom Assessment

Before treatment, patients were asked at baseline to identify a "target symptom" (pain), which is their main complaint that they hope to relieve. At each follow-up visit, they were asked to describe the severity of target symptom compared to baseline. The pain was scored using the visual analogue scale, and was classified into the none (score 0), mild (score 1–3), moderate (score 4–6) and severe pain (score 7–10). The symptom score is always collected as part of the clinical visits.

Outcomes and Follow Up

After completion of treatment, patients were followed-up every 3-5 weeks in the first 6 months and every 3 months afterwards until the death. Treatment results and side effects were evaluated on the basis of clinical examinations, laboratory examination, CT, MRI, bone scan, and ^{18}F-FDG-PET/CT. Toxicity was evaluated according to the National Cancer Institute Common Terminology Criteria for Adverse Events version 5.0. The primary efficacy outcome was OS, defined as the time from the start of treatment to the death due to any cause. Secondary outcomes included progression-free survival (PFS) (defined as the time from the start of treatment to progression at any site or death), local progression (defined as the progression of tumors in the pancreas from the start of treatment) and metastatic progression (defined as new metastases or progression of existing metastases from the start of treatment). Death without the event of interest was a competing event, and patients lost to follow-up without the event were censored.

Statistical Analysis

We compared baseline and matched characteristics using Pearson χ^2 or Fisher's exact test for categorical data. To address the imbalance of potential confounders between the SBRT plus chemotherapy and chemotherapy alone groups, propensity scores-matched analysis was performed for treatment groups (19). The propensity score model included T stage, N stage, gender, age, performance status, primary pancreatic tumor location, CA19–9, and year of diagnosis. Then, matched pairs were formed between patients treated by SBRT plus chemotherapy and those treated by chemotherapy alone using a one-to-one nearest neighbor calliper with width of 0.3 (the maximum allowable difference in propensity scores). On the basis of the propensity score matching, a stabilized inverse probability of treatment weighting (IPTW) was calculated (20, 21). Weights were truncated at the 5th and 95th percentile to reduce potential data sparsity. To assess balance before and after matching and weighting, the standardized mean difference (SMD) was calculated. SMD value of 0.1 or less indicated optimal balance. Kaplan-Meier estimators were calculated for each group and were compared using the log-rank test. Cox proportional hazards regression model was used to compare the relative treatment efficacy between treatment groups. Within the matched patient group, the heterogeneity of treatment efficacy was assessed with tests of interaction and subgroup analyses, which explored the effect of gender, age, performance status, primary pancreatic tumor location, CA19–9, year of diagnosis, T stage and N stage. An HR less than 1.00 favored SBRT plus chemotherapy. Competitive risk analysis (Gray's test) (22) was used to estimate the cumulative incidence of local progression for pancreatic lesions and the cumulative incidence of metastatic progression. Statistical analysis was done using SPSS version 24.0 and R version 3.6.3. All tests were displayed on both sides, with 95% CIs and relevant p values.

RESULTS

Patient Characteristics and Treatment Features

Between January 01, 2010, and December 31, 2019, 89 patients with metastatic pancreatic cancer were included in this study, of whom 34 received SBRT plus chemotherapy and 55 received chemotherapy alone. The median time interval from diagnosis to the start of treatment was 8 days (0-28 days). The baseline characteristics of all patients were presented in **Table 1**. Patients who received SBRT plus chemotherapy had a higher ratio of poor performance status (ECOG=2, 61.8% *vs* 38.2%, P=0.030) and advanced T stage (T4, 50.0% *vs* 27.3%, P=0.030). Patients were more likely to receive SBRT from 2010 to 2014 (Year of diagnosis, 61.8% *vs* 32.7%, P=0.007). To eliminate the influence of these differences on subsequent analysis, we matched the two groups for all covariates by propensity score matching (**Appendix Table 2** and **Appendix Figure 1**). The baseline characteristics were well balanced between two groups after matching (**Table 1**).

Before SBRT, 12 patients received no chemotherapy, 13 patients received 1-cycle of chemotherapy, 5 patients received 2-cycles chemotherapy, and 4 patients received ≥ 3-cycles chemotherapy. The median number of chemotherapy cycles was 1 (range of 0-6) before SBRT. Almost all patients received systemic chemotherapy after radiotherapy. The median time interval from initial treatment to SBRT was 13 days (0-114 days). The median PTV was 77.5 cm3 (range of 17.8-355.7 cm3). The treatment duration was 5-9 days. Median total prescribed dose was 42.5 gray (Gy) (range of 25-50 Gy), which was given in 5-7 fractions. The median prescription isodose was 73%. The SBRT planning and delivery variables are shown in **Appendix Table 3**.

Survival Analysis

Median follow-up time for all patients was 20.9 months (95% CI,17.7-24.1 months). In unmatched analysis, the median OS was 8.9 months (95% CI, 5.7-18.8 months) for SBRT plus chemotherapy group and 7.5 months (95% CI, 6.0-9.6 months) for chemotherapy alone group. The 1-year OS rate was 39.4% (95% CI, 24.1–64.3%) for SBRT plus chemotherapy group and 21.3% (95% CI, 11.9–38.0) for chemotherapy alone group. Compared with the control group, the SBRT group has no survival advantage (log-rank P=0.059; **Figure 1A**; **Table 2**). This is consistent with the result of the propensity-score-matched analysis. The rates of OS at 1-year survival for SBRT plus chemotherapy and chemotherapy alone groups were 34.0%

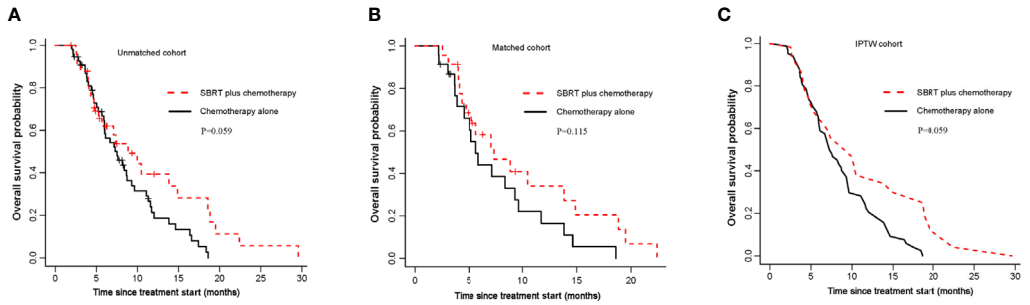

FIGURE 1 | Kaplan-Meier curves for OS. **(A)** OS of the unmatched cohort; **(B)** shows OS of the propensity score matched group; **(C)** shows OS of the inverse probability of treatment weight-adjusted group. SBRT, stereotactic body radiotherapy.

(95%CI, 17.8-65.1%) and 16.5% (95%CI, 5.9-46.1%), respectively (log-rank P= 0.115; **Figure 1B**; **Table 2**). In the IPTW analysis, SBRT still was not associated with a significant OS benefit. The 1-year OS rate was 38.0% in SBRT plus chemotherapy group versus 22.2% in the chemotherapy alone group (log-rank P=0.059; **Figure 1C**; **Table 2**).

To explore whether SBRT would benefit selected patients, we performed subgroup analyses of the matched cohort. The P values for interaction were not significant in most of the prespecified subgroups, indicating that there was no significant difference on OS between subgroups (**Figure 2A**). Notably, the addition of SBRT was beneficial for OS in patients with primary tumor located in the head of pancreas (stratified HR, 0.28; 95% CI, 0.09 to 0.90; P=0.193 for interaction; **Figures 2A**, **B**) or those with good performance status (stratified HR, 0.24; 95% CI, 0.07 to 0.86; P=0.115 for interaction; **Figures 2A**, **C**).

Compared with chemotherapy alone group, the SBRT plus chemotherapy group also did not have the survival advantage on PFS (**Appendix Figure 2**; **Table 2**). Subgroup analyses in the matched cohort showed that there was no beneficial effect of SBRT on PFS across all subgroups (**Appendix Figure 3**).

Local Progression and Metastatic Progression

By competing risk analysis in the unmatched groups, the cumulative incidence of local progression within the pancreas was 22.1% (95%CI, 8.2-40.2) for SBRT plus chemotherapy group and 53.2% (95%CI, 37.5-66.6) for chemotherapy alone group at 12 months. The addition of SBRT significantly delayed disease progression in the pancreas (SHR, 0.40; 95% CI, 0.19-0.84; P=0.016; **Figure 3A** and **Table 2**). This is consistent with the result of the propensity-score-matched analysis. The cumulative incidence of local progression in the pancreas was 14.2% (95%CI, 3.2-33.2) for SBRT plus chemotherapy group and 53.3% (95%CI, 27.8-73.4) for chemotherapy alone group at 12 months (SHR, 0.23; 95% CI, 0.08-0.69; P=0.008; **Figure 3B** and **Table 2**).

As for metastatic progression, the cumulative incidence was 61.6% (95%CI, 41.9-76.4) for SBRT plus chemotherapy group

TABLE 2 | Summary of estimated treatment effect for main outcome measures in unmatched, propensity Matched and IPTW groups.

	Unmatched			Propensity Matched			IPTW		
	SBRT plus chemotherapy	**Chemotherapy alone**	**P**	**SBRT plus chemotherapy**	**Chemotherapy alone**	**P**	**SBRT plus chemotherapy**	**Chemotherapy alone**	**P**
OS rate			0.059			0.115			0.059
6-months	62.0%	60.5%		58.3%	44.0%		66.0%	61.9%	
12-months	39.4%	21.3%		34.0%	16.5%		38.0%	22.2%	
PFS rate			0.113			0.468			0.093
6-months	29.3%	19.2%		29.4%	20.6%		28.4%	19.3%	
12-months	8.4%	2.4%		0%	5.2%		6.8%	2.1%	
Local progression rate			0.016			0.008	–	–	–
6-months	12.6%	34.6%		8.7%	36.7%		–	–	–
12-months	22.1%	53.2%		14.2%	53.3%		–	–	–
Metastatic progression rate			0.086			0.56	–	–	–
6-months	61.6%	78.2%		66.2%	71.8%		–	–	–
12-months	88.1%	95.3%		100%	94.4%		–	–	–
Local symptomatic palliation rate			0.015			0.016	–	–	–
3-months	78.8%	52.8%		87.0%	54.5%		–	–	–

IPTW, inverse probability of treatment weight; SBRT, stereotactic body radiotherapy.

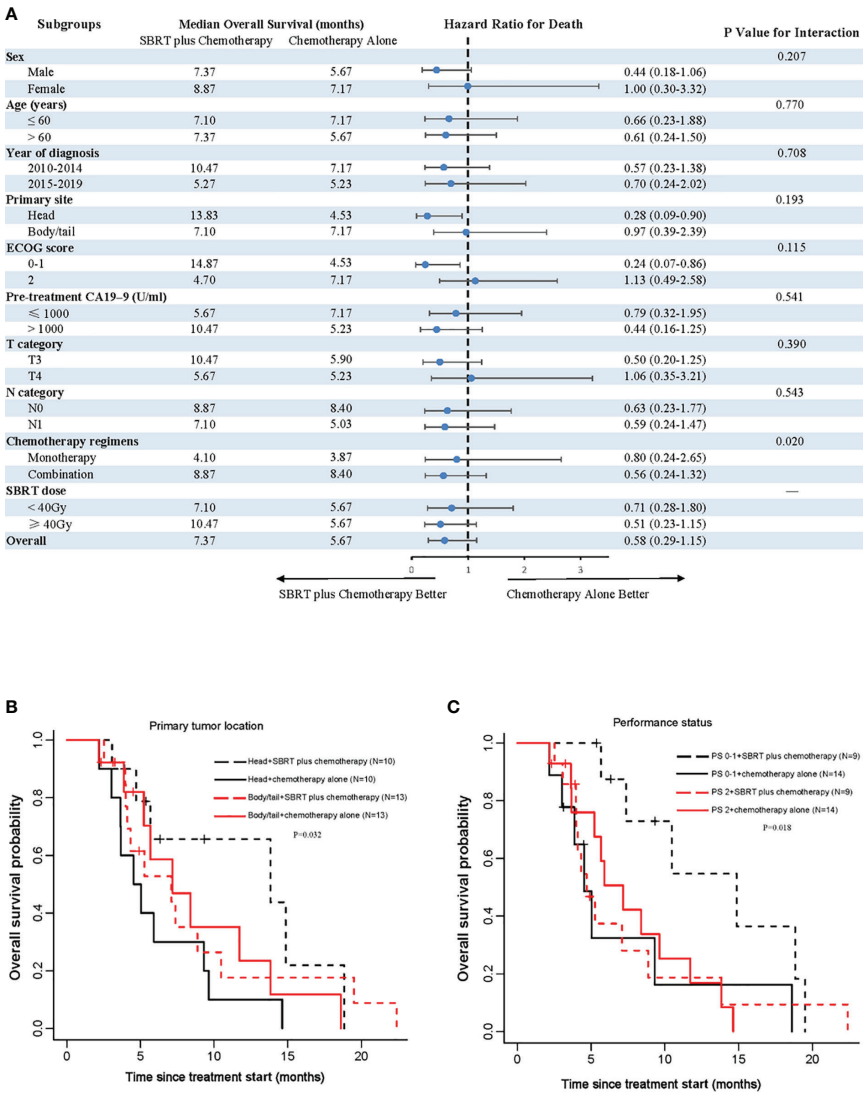

FIGURE 2 | Analyses of OS in matched population. **(A)** Forest plot of subgroup analyses of OS; **(B)** shows OS of the primary tumor location; **(C)** shows OS of performance status. SBRT, stereotactic body radiotherapy; PS, performance status.

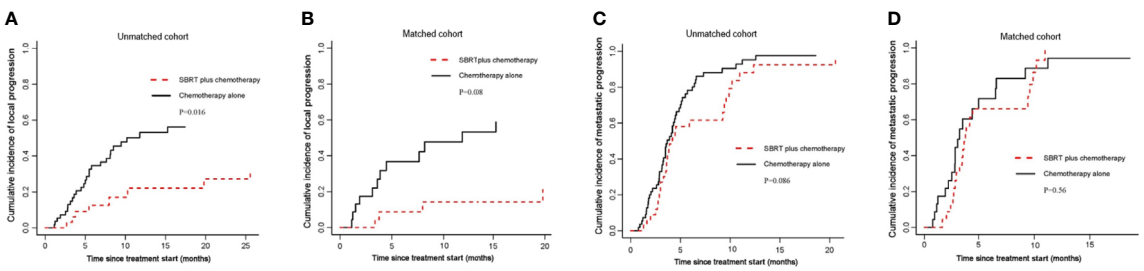

FIGURE 3 | Cumulative incidence curves for the probability of each competing event. **(A)** cumulative incidence of local progression in the unmatched group; **(B)** cumulative incidence of local progression in the matched group; **(C)** cumulative incidence of metastatic progression in the unmatched group; **(D)** cumulative incidence of metastatic progression in the matched group.

and 78.2% (95%CI, 63.8-87.5) for chemotherapy alone group at 6 months in the unmatched groups. The addition of SBRT did not delay metastatic progression (P=0.086; **Figure 3C** and **Table 2**). This is consistent with the result of the propensity-score-matched analysis. The cumulative incidence of metastatic progression was 66.2% (95%CI, 41.6-82.4) for SBRT plus chemotherapy group and 71.8% (95%CI, 44.2-87.4) for chemotherapy alone group at 6 months (SHR, 0.83; 95% CI, 0.44-1.55; P=0.56; **Figure 3D** and **Table 2**).

Symptom Palliation

The definition of symptom palliation is that moderate or severe symptoms at baseline should be improved, mild symptoms should be controlled, and the occurrence of other symptoms should be prevented (23). With these criteria, we compared changes of the pain symptom from baseline to 3 months (improved: moderate or severe at baseline, mild or nil at 3 months; controlled: mild at baseline, mild or nil at 3 months; prevented: nil at baseline, nil at 3 months). Patients who had died by 3 months were considered as without symptom palliation. Symptomatic palliation was assessed using a scoring system, such as visual analogue scoring for pain. After propensity matching, in SBRT plus chemotherapy group, the symptom of 13 patients was improved, that of 7 patients was controlled and that of 0 patient was prevented. In chemotherapy alone group, the symptom of 5 patients was improved, that of 7 patients was controlled, that of 0 patient was prevented, and 1 patient was lost to follow-up. The pain palliation rate was 87.0% for the SBRT plus chemotherapy group and 54.5% for the chemotherapy alone group at 3 months (**Table 2**). Palliation were observed with the addition of SBRT for abdominal/back pain (P=0.016). As shown in **Figure 4**, the proportion of patients with moderate or severe symptoms significantly decreased in SBRT plus chemotherapy group over time.

Toxicity

Mild toxic effects were recorded for patients, including grade 1 and grade 2 of transient fatigue, anorexia, nausea, and vomiting. Overall, there were no significant differences in hepatotoxic, nephrotoxic, and hematologic toxic effects between two groups. Due to the adverse effects of radiotherapy, one patient presented with duodenal ulcer bleeding (grade 3), and the symptom was improved after endoscopic intervention. Since this patient had a positive history of duodenal ulcer, we suppose that SBRT may cause its recurrence. Thus, for patients with a history of gastric or duodenal ulcers, dose constraints may have to be individualized. The details on the comparison of toxicity between the SBRT plus chemotherapy group and the chemotherapy alone group were summarized in **Appendix Table 4**.

DISCUSSION

Although chemotherapy remains the primary treatment method for metastatic pancreatic cancer, the use of SBRT has been increasing. However, the clinical efficacy of SBRT to primary tumor for patients with metastatic pancreatic cancer was unclear. To solve this problem, we performed propensity-matched analyses of 89 patients who were newly diagnosed with metastatic pancreatic cancer. These patients were divided into two groups: SBRT plus chemotherapy group and chemotherapy alone group. Our study showed that the addition of SBRT did not improve OS. However, subgroup analysis showed that SBRT improved OS in patients with primary tumor located in the head of pancreas or good performance status. This is probably due to that patients with good fitness can withstand intensive combination therapy. Therefore, consideration of the tumor location and performance status may be a reasonable step towards individualized therapy.

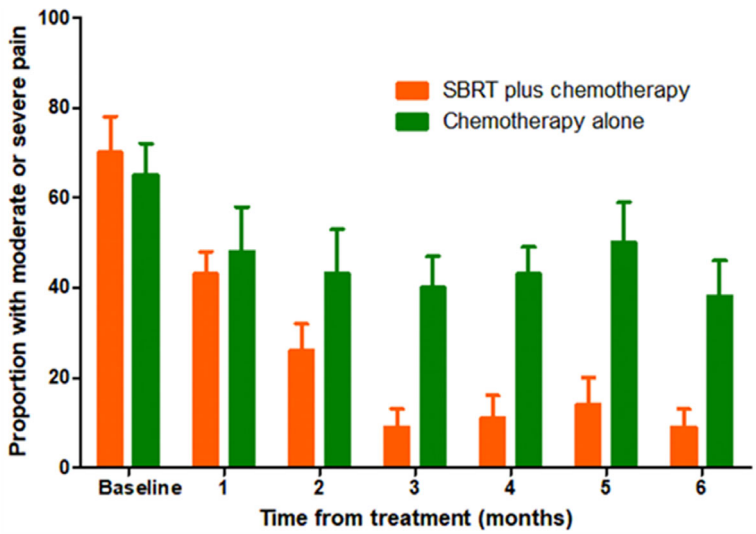

FIGURE 4 | Proportion of patients with moderate or severe abdominal/back pain over time in the matched group.

There have been few studies investigating the role of SBRT in the local control of primary tumors of metastatic pancreatic cancer. Lischalk et al. (24) analyzed 20 patients with pathologically diagnosed metastatic adenocarcinoma of the pancreas. SBRT was conducted on the primary pancreatic tumor in five fractions to a total dose of 25-30 Gy. The 1-year local control rate and OS rate were 43% and 53%, respectively. Koong et al. (25) retrospectively analyzed patients with metastatic pancreatic cancer who received stereotactic ablative radiotherapy to the primary tumor. They found the median OS was 7 months, with a cumulative incidence of local failure at 1 year of 25%. However, these studies only had SBRT treatment group and lacked a control group. In our study, patients were divided into SBRT plus chemotherapy group and chemotherapy alone group. The result revealed that the addition of SBRT improved local disease control. However, the improvement in disease control did not transform into a benefit in OS, which may be partly due to the high proportion of patients who developed distant metastatic progression (66.2% *vs* 71.8%, P=0.56).

SBRT to the primary tumor in the case of metastatic pancreatic tumor has a different rationale than the oligometastatic pathway being explored in other disease sites. Many patients with pancreatic malignancy may experience significant morbidity/mortality from local progression of their disease. SBRT in this setting may provide significant benefit. This is different rationale to potentially pursue SBRT than the oligometastatic disease paradigm (SABR-COMET et) that local ablation to all sites may improve outcomes (26, 27). As has been observed recently, radiating a single site in oligometastatic disease is unlikely to provide benefit in patients (28). However, in the context of that single site being a significant cause of morbidity and mortality with local progression, SBRT may provide a significant benefit in this population—but should be tested in a prospective trial.

In addition to the limited life expectancy, the primary pancreatic tumor may cause severe local symptoms, leading to poor life quality (29). Amelioration of symptoms, especially abdominal or back pain, should be given priority in the treatment for metastatic pancreatic cancer. A recent systematic review (10) of the effects of SBRT on pain relief in patients with locally advanced pancreatic carcinoma reported a global overall response rate of 84.9%. Similarly, Su et al. (30) showed that SBRT effectively relieved the abdominal pain of 65% of patients with acceptable toxicities. In our study, in addition to providing good local disease control, SBRT offered improvement in pain control for patients with metastatic pancreatic cancer. Patients with metastatic pancreatic cancer may be treated with SBRT for symptom relief or delaying symptom progression.

This study was mainly limited due to its retrospective nature at a single institution, relatively small sample size, and limited metastatic disease burden with a focus on liver-only oligmetastatic patients. Additionally, there were a variety of types of chemotherapy and number of chemotherapy cycles in this study. However, there was no significant difference in chemotherapy regimens and the number of chemotherapy cycles between two groups. The result in this paper should be further verified with a larger sample size and extended to other metastatic sites of pancreatic cancer.

In conclusion, our study showed a benefit of the combination of SBRT with chemotherapy for pancreatic-specific disease control and palliation of cancer-related symptoms with acceptable toxicities in pancreatic cancer patients with liver-only oligometastasis. Although the addition of SBRT did not improve OS in all patients, it prolonged OS in patients with primary tumor located in the head of pancreas or good performance status. Therefore, the further research is needed to study the role of SBRT in carefully selected patients and as a consolidation therapy after chemotherapy.

DATA AVAILABILITY STATEMENT

The raw data supporting the conclusions of this article will be made available by the authors, without undue reservation.

ETHICS STATEMENT

The study was approved by the Ethics Committee of Jinling Hospital, and written informed consents were obtained from all patients. The patients/participants provided their written informed consent to participate in this study.

AUTHOR CONTRIBUTIONS

XC and CC designed the study. XJ, CH and ZS collected the data. XJ, SH and YZ wrote the manuscript. XC and XZ analyzed and interpreted the data. All authors contributed to the article and approved the submitted version.

FUNDING

This work was supported by grants from Natural Science Foundation of Jiangsu Province (BK20181238 to XC).

SUPPLEMENTARY MATERIAL

The Supplementary Material for this article can be found online at: https://www.frontiersin.org/articles/10.3389/fonc.2021.659987/full#supplementary-material

Supplementary Figure 1 | Plot of the balance evaluated before and after matching/weighting.

Supplementary Figure 2 | Kaplan-Meier curves for PFS. **(A)** PFS of the unmatched cohort; **(B)** PFS of the propensity score matched group; **(C)** PFS of the inverse probability of treatment weight-adjusted group. PFS, progression-free survival; SBRT, stereotactic body radiotherapy.

Supplementary Figure 3 | Forest plot of PFS subgroup analyses in matched study population. PFS, progression-free survival; SBRT, stereotactic body radiotherapy.

REFERENCES

1. Siegel RL, Miller KD, Jemal A. Cancer Statistics, 2020. *CA: A Cancer J Clin* (2020) 70(1):7–30. doi: 10.3322/caac.21590
2. Mizrahi JD, Surana R, Valle JW, Shroff RT. Pancreatic Cancer. *Lancet* (2020) 395(10242):2008–20. doi: 10.1016/S0140-6736(20)30974-0
3. Alistar A, Morris BB, Desnoyer R, Klepin HD, Hosseinzadeh K, Clark C, et al. Safety and Tolerability of the First-in-Class Agent CPI-613 in Combination With Modified FOLFIRINOX in Patients With Metastatic Pancreatic Cancer: A Single-Centre, Open-Label, Dose-Escalation, Phase 1 Trial. *Lancet Oncol* (2017) 18(6):770–8. doi: 10.1016/S1470-2045(17)30314-5
4. Conroy T, Desseigne F, Ychou M, Bouché O, Guimbaud R, Bécouarn Y, et al. FOLFIRINOX Versus Gemcitabine for Metastatic Pancreatic Cancer. *New Engl J Med* (2011) 364(19):1817–25. doi: 10.1056/NEJMoa1011923
5. Von Hoff DD, Ervin T, Arena FP, Chiorean EG, Infante J, Moore M, et al. Increased Survival in Pancreatic Cancer With Nab-Paclitaxel Plus Gemcitabine. *New Engl J Med* (2013) 369(18):1691–703. doi: 10.1056/NEJMoa1304369
6. Grossberg AJ, Chu LC, Deig CR, Fishman EK, Hwang WL, Maitra A, et al. Multidisciplinary Standards of Care and Recent Progress in Pancreatic Ductal Adenocarcinoma. *CA: A Cancer J Clin* (2020) 70(5):375–403. doi: 10.3322/caac.21626
7. Foley K, Kim V, Jaffee E, Zheng L. Current Progress in Immunotherapy for Pancreatic Cancer. *Cancer Lett* (2016) 381(1):244–51. doi: 10.1016/j.canlet.2015.12.020
8. Moore MJ, Goldstein D, Hamm J, Figer A, Hecht JR, Gallinger S, et al. Erlotinib Plus Gemcitabine Compared With Gemcitabine Alone in Patients With Advanced Pancreatic Cancer: A Phase III Trial of the National Cancer Institute of Canada Clinical Trials Group. *J Clin Oncol* (2007) 25(15):1960–6. doi: 10.1200/JCO.2006.07.9525
9. Philip PA, Benedetti J, Corless CL, Wong R, O'Reilly EM, Flynn PJ, et al. Phase III Study Comparing Gemcitabine Plus Cetuximab Versus Gemcitabine in Patients With Advanced Pancreatic Adenocarcinoma: Southwest Oncology Group–directed Intergroup Trial S0205. *J Clin Oncol* (2010) 28(22):3605. doi: 10.1200/JCO.2009.25.7550
10. Buwenge M, Macchia G, Arcelli A, Frakulli R, Fuccio L, Guerri S, et al. Stereotactic Radiotherapy of Pancreatic Cancer: A Systematic Review on Pain Relief. *J Pain Res* (2018) 11:2169. doi: 10.2147/JPR.S167994
11. Rosati LM, Kumar R, Herman JM. Integration of Stereotactic Body Radiation Therapy Into the Multidisciplinary Management of Pancreatic Cancer. *Semin Radiat Oncol* (2017) 27(3):256–67. doi: 10.1016/j.semradonc.2017.02.005
12. Hammel P, Huguet F, van Laethem J-L, Goldstein D, Glimelius B, Artru P, et al. Effect of Chemoradiotherapy vs Chemotherapy on Survival in Patients With Locally Advanced Pancreatic Cancer Controlled After 4 Months of Gemcitabine With or Without Erlotinib: The LAP07 Randomized Clinical Trial. *Jama* (2016) 315(17):1844–53. doi: 10.1001/jama.2016.4324
13. Iacobuzio-Donahue CA, Fu B, Yachida S, Luo M, Abe H, Henderson CM, et al. DPC4 Gene Status of the Primary Carcinoma Correlates With Patterns of Failure in Patients With Pancreatic Cancer. *J Clin Oncol* (2009) 27(11):1806. doi: 10.1200/JCO.2008.17.7188
14. You R, Liu Y-P, Huang P-Y, Zou X, Sun R, He Y-X, et al. Efficacy and Safety of Locoregional Radiotherapy With Chemotherapy vs Chemotherapy Alone in De Novo Metastatic Nasopharyngeal Carcinoma: A Multicenter Phase 3 Randomized Clinical Trial. *JAMA Oncol* (2020) 6(9):1345–52. doi: 10.1001/jamaoncol.2020.1808
15. Rusthoven CG, Jones BL, Flaig TW, Crawford ED, Koshy M, Sher DJ, et al. Improved Survival With Prostate Radiation in Addition to Androgen Deprivation Therapy for Men With Newly Diagnosed Metastatic Prostate Cancer. *J Clin Oncol* (2016) 34(24):2835–42. doi: 10.1200/JCO.2016.67.4788
16. Parker CC, James ND, Brawley CD, Clarke NW, Hoyle AP, Ali A, et al. Radiotherapy to the Primary Tumour for Newly Diagnosed, Metastatic Prostate Cancer (STAMPEDE): A Randomised Controlled Phase 3 Trial. *Lancet* (2018) 392(10162):2353–66. doi: 10.1016/S0140-6736(18)32486-3
17. Trakul N, Koong AC, Chang DT. Stereotactic Body Radiotherapy in the Treatment of Pancreatic Cancer. *Semin Radiat Oncol* (2014) 24(2):140–7. doi: 10.1016/j.semradonc.2013.11.008
18. Comito T, Cozzi L, Zerbi A, Franzese C, Clerici E, Tozzi A, et al. Clinical Results of Stereotactic Body Radiotherapy (SBRT) in the Treatment of Isolated Local Recurrence of Pancreatic Cancer After R0 Surgery: A Retrospective Study. *Eur J Surg Oncol (EJSO)* (2017) 43(4):735–42. doi: 10.1016/j.ejso.2016.12.012
19. Renehan AG, Malcomson L, Emsley R, Gollins S, Maw A, Myint AS, et al. Watch-and-Wait Approach Versus Surgical Resection After Chemoradiotherapy for Patients With Rectal Cancer (the OnCoRe Project): A Propensity-Score Matched Cohort Analysis. *Lancet Oncol* (2016) 17(2):174–83. doi: 10.1016/S1470-2045(15)00467-2
20. Cole SR, Hernán MA. Constructing Inverse Probability Weights for Marginal Structural Models. *Am J Epidemiol* (2008) 168(6):656–64. doi: 10.1093/aje/kwn164
21. Rajyaguru DJ, Borgert AJ, Smith AL, Thomes RM, Conway PD, Halfdanarson TR, et al. Radiofrequency Ablation Versus Stereotactic Body Radiotherapy for Localized Hepatocellular Carcinoma in Nonsurgically Managed Patients: Analysis of the National Cancer Database. *J Clin Oncol* (2018) 36(6):600–8. doi: 10.1200/JCO.2017.75.3228
22. Fine JP, Gray RJ. A Proportional Hazards Model for the Subdistribution of a Competing Risk. *J Am Stat Assoc* (1999) 94(446):496–509. doi: 10.1080/01621459.1999.10474144
23. Muers MF, Stephens RJ, Fisher P, Darlison L, Higgs CM, Lowry E, et al. Active Symptom Control With or Without Chemotherapy in the Treatment of Patients With Malignant Pleural Mesothelioma (MS01): A Multicentre Randomised Trial. *Lancet* (2008) 371(9625):1685–94. doi: 10.1016/S0140-6736(08)60727-8
24. Lischalk JW, Burke A, Chew J, Elledge C, Gurka M, Marshall J, et al. Five-Fraction Stereotactic Body Radiation Therapy (SBRT) and Chemotherapy for the Local Management of Metastatic Pancreatic Cancer. *J gastrointestinal Cancer* (2018) 49(2):116–23. doi: 10.1007/s12029-016-9909-2
25. Koong AJ, Toesca DA, Baclay JRM, Pollom EL, von Eyben R, Koong AC, et al. The Utility of Stereotactic Ablative Radiation Therapy for Palliation of Metastatic Pancreatic Adenocarcinoma. *Pract Radiat Oncol* (2020) 10(4):274–81. doi: 10.1016/j.prro.2020.02.010
26. Palma DA, Olson R, Harrow S, Gaede S, Louie AV, Haasbeek C, et al. Stereotactic Ablative Radiotherapy Versus Standard of Care Palliative Treatment in Patients With Oligometastatic Cancers (SABR-COMET): A Randomised, Phase 2, Open-Label Trial. *Lancet* (2019) 393(10185):2051–8. doi: 10.1016/S0140-6736(18)32487-5
27. Palma DA, Olson R, Harrow S, Gaede S, Louie AV, Haasbeek C, et al. Stereotactic Ablative Radiotherapy for the Comprehensive Treatment of Oligometastatic Cancers: Long-Term Results of the SABR-COMET Randomized Trial. *Int J Radiat Oncol Biol Phys* (2020) 108(3):S88–9. doi: 10.1016/j.ijrobp.2020.07.2251
28. McBride S, Sherman E, Tsai CJ, Baxi S, Aghalar J, Eng J, et al. Randomized Phase II Trial of Nivolumab With Stereotactic Body Radiotherapy Versus Nivolumab Alone in Metastatic Head and Neck Squamous Cell Carcinoma. *J Clin Oncol* (2021) 39(1):30–7. doi: 10.1200/JCO.20.00290
29. Freelove R, Walling A. Pancreatic Cancer: Diagnosis and Management. *Am Family physician* (2006) 73(3):485–92.
30. Su T-S, Liang P, Lu H-Z, Liang J-N, Liu J-M, Zhou Y, et al. Stereotactic Body Radiotherapy Using CyberKnife for Locally Advanced Unresectable and Metastatic Pancreatic Cancer. *World J Gastroenterol: WJG* (2015) 21(26):8156. doi: 10.3748/wjg.v21.i26.8156

Conflict of Interest:: The authors declare that the research was conducted in the absence of any commercial or financial relationships that could be construed as a potential conflict of interest.

frontiers in Oncology

ORIGINAL RESEARCH
published: 28 May 2021
doi: 10.3389/fonc.2021.642314

Image-Guided Robotic Radiosurgery for the Treatment of Same Site Spinal Metastasis Recurrences

Felix Ehret[1,2*], *Lucas Mose*[2], *Markus Kufeld*[2], *Christoph Fürweger*[2,3], *Paul Windisch*[2,4], *Alfred Haidenberger*[2], *Christian Schichor*[5], *Jörg-Christian Tonn*[5] *and Alexander Muacevic*[2]

[1] Charité—Universitätsmedizin Berlin, Corporate Member of Freie Universität Berlin and Humboldt-Universität zu Berlin, Department of Radiation Oncology, Berlin, Germany, [2] European Cyberknife Center, Munich, Germany, [3] Department of Stereotaxy and Functional Neurosurgery, University Hospital Cologne, Cologne, Germany, [4] Department of Radiation Oncology, Kantonsspital Winterthur, Winterthur, Switzerland, [5] Department of Neurosurgery, Ludwig-Maximilians-University Munich, Munich, Germany

OPEN ACCESS

Edited by:
John Varlotto,
Marshall University, United States

Reviewed by:
Peter Carlos Gerszten,
University of Pittsburgh Medical Center, United States
Samuel Chao,
Case Western Reserve University, United States
Dwight E. Heron,
Bon Secours Health System, United States

***Correspondence:**
Felix Ehret
felix.ehret@charite.de
orcid.org/0000-0001-6177-1755

Specialty section:
This article was submitted to Radiation Oncology, a section of the journal Frontiers in Oncology

Received: 15 December 2020
Accepted: 18 March 2021
Published: 28 May 2021

Citation:
Ehret F, Mose L, Kufeld M, Fürweger C, Windisch P, Haidenberger A, Schichor C, Tonn J-C and Muacevic A (2021) Image-Guided Robotic Radiosurgery for the Treatment of Same Site Spinal Metastasis Recurrences. Front. Oncol. 11:642314. doi: 10.3389/fonc.2021.642314

Background: Due to recent medical advancements, patients suffering from metastatic spinal disease have a prolonged life expectancy than several decades ago, and some will eventually experience relapses. Data for the retreatment of spinal metastasis recurrences occurring at the very same macroscopic spot as the initially treated lesion are limited. Previous studies mainly included recurrences in the boundary areas as well as other macroscopic parts of the initially affected vertebrae. This study exclusively analyzes the efficacy and safety of spinal reirradiation for recurrences on the same site utilizing single-session robotic radiosurgery.

Materials and Methods: Patients between 2005 and 2020 who received radiotherapy for a spinal metastasis suffering from a local recurrence were eligible for analysis. Only patients undergoing a single-session reirradiation were included. All recurrences must have been occurred in the same location as the initial lesion. This was defined as a macroscopic recurrence on computed tomography occurring at the same site as the initial spinal metastasis. All other lesions, including those in the boundary areas or other parts of the initially affected vertebrae, were excluded.

Results: Fifty-three patients with fifty-three lesions were retreated for spinal metastases. The median dose and number of fractions for the initial radiotherapy were 36 Gy and 15, respectively. Eleven patients were initially treated with stereotactic body radiotherapy. Retreatment was performed with a median dose of 18 Gy prescribed to a median isodose of 70%. The local control was 77% after a median follow-up of 22.2 months. Patients experiencing a second recurrence received a lower dose ($p = 0.04$), mostly below 18 Gy, and had a worse coverage ($p = 0.01$) than those showing local tumor control. 51% of patients experienced an improvement in pain control after treatment delivery. Besides, four vertebral compression fractures (7% of patients) but no other adverse events higher than grade 2 were observed.

Conclusion: Single-session robotic radiosurgery appears to be a safe, time-saving, and effective treatment modality for spinal metastasis recurrences occurring in the same initial location if a considerable dose and coverage can be applied. Treatment results are comparable to reirradiated metastases in the boundary areas.

Keywords: SBRT, radiosurgery, spinal metastasis, spine, recurrence, CyberKnife, reirradiation (ReRT)

INTRODUCTION

Due to recent medical advancements, patients suffering from metastatic disease have a prolonged life expectancy than several decades ago (1). In addition to projected demographic changes, this shift is expected to lead to an increasing number of patients needing therapy for spinal metastases within the upcoming years. Today, about 180.000 patients in the United States are suffering from spinal metastases, and approximately 10% of them will experience spinal cord compression as a potentially life-threatening complication (2–5). With the development, implementation, and general availability of conventional fractionated external-beam radiotherapy (EBRT) and stereotactic body radiation therapy (SBRT), many patients with spinal metastases can be treated effectively and non-invasively. Primary treatment results regarding local control (LC), pain, and quality of life (Qol) are sound (6, 7). However, with the increased life expectancy after irradiation, chances of local recurrence or even further development of spinal metastases increase. So far, single-session and multisession SBRT up to 5 fractions showed 1-year-LC rates around 80% for spinal metastases, even for radioresistant tumor entities (6, 8–11). Still, this implies that a substantial number of patients will experience the need for a follow-up treatment thanks to current and future improvements in systemic therapies, which increase the overall life expectancy for patients with metastatic disease. Thus, dedicated treatment options for recurrent spinal metastases are needed. These should respect the previous irradiation and associated risks for myelopathies and vertebral compression fractures (VCFs) (12). Reirradiation for spinal metastases seems feasible and effective, but the number of reports is still limited (12–15). Finally, data on the efficacy and safety of reirradiation with single-session robotic radiosurgery (RRS) are particularly limited (12, 14). Besides, previous reports often included spinal recurrences in the boundary area or previously irradiated field and other parts of the initially affected vertebrae, and not just same site relapses (16, 17). This may potentially compromise patient and data homogeneity, which could limit the overall generalizability of the reported results. Thus, the objective of this study is to analyze the treatment results of RRS for preirradiated spinal metastasis recurrences occurring at the very same spot as the initial macroscopic lesion. To date, data for this specific patient cohort are sparse. Besides, all tumors were exclusively and primarily treated in one session, and we compare our results with the existing SBRT literature.

MATERIALS AND METHODS

Fifty-three patients treated for a spinal metastasis recurrence between 2005 and 2020 were included in this retrospective single-center study. Only patients undergoing primary single-session RRS for a retreatment for relapse on the same site as the initial tumor were eligible for analysis. This type of lesion was defined as a macroscopic osteolytic, osteoblastic, or mixed recurrence on computed tomography (CT) occurring at the same site as the initial macroscopic spinal metastasis. Patients undergoing initial surgical treatment for their relapse before RRS and local recurrences in the boundary area of the previous irradiation as well as other parts of the affected vertebrae were excluded. All patient data, including medical history, previous treatments, and follow-up data, were prospectively stored in a dedicated database for radiosurgery and retrospectively analyzed. Diagnosis of spinal metastasis recurrence was made by an interdisciplinary team consisting of radiation oncologists, neurosurgeons, and neuroradiologists.

Treatment Procedure and Outcome

As formerly described, every patient underwent thin-sliced, contrast-enhanced CT and magnetic resonance imaging (MRI) scans for treatment planning and delivery. Obtained images were overlaid for inverse treatment planning, which was done with a dedicated planning software (MultiPlan, Precision, Accuray Inc., Sunnyvale, CA, USA). All treatments were delivered in a single session utilizing a CyberKnife® robotic radiosurgery system (Accuray Inc., Sunnyvale, CA, USA). For tracking, the X-sight spine tracking algorithm (Accuray Inc., Sunnyvale, CA, USA) has been used for all treatment sessions without any application of fiducials (18, 19). The gross tumor volume (GTV) comprised all visible tumor tissue identified on MRI and CT scans. For vertebral body metastases, a 2 mm margin was added. Besides, no further margins have been added to the planning target volume (PTV), given the accuracy of RRS (19). Radioresistant tumors included renal cell carcinoma, gastrointestinal tumors, non-small cell lung cancer, sarcomas, head and neck tumors, thyroid cancer as well as melanomas. Radiosensitive tumors included breast, cervical, uterine, and prostate cancer. The metastases of cancers of unknown primary were deemed intermediate. This classification was in accordance with the work of Yamada et al. (20). Dose constraints for organs at risk were respected for patients following the data of the AAPM TG101 if medically appropriate and feasible as well as subject to changes for individual cases (21). Dose constraints were as follows: ≤0.35/≤1.2 cc of the spinal cord could receive 10.0/7.0 Gy, with a maximum point dose of 14.0 Gy in ≤0.35 cc. Adverse events (AE) and toxicity were reported according to the Common Terminology Criteria for Adverse Events (CTCAE) up to version 5, depending on the date of the AE occurrence. Local control (LC) was defined as an unchanged or decreased tumor

volume on follow-up imaging. Local failure (LF) was defined as an increased tumor volume during follow-up.

Statistical Analyses

Time of LC, local progression-free survival (including LFs and death of any cause) (l-PFS), and overall survival (OS) were calculated according to the Kaplan-Meier estimate. Differences in survival or other time-to-event differences were analyzed with a log-rank test. Continuous variables were tested for normality utilizing the Shapiro Wilk test and the graphic appearance, including skewness and kurtosis. Subsequent analyses were done with unpaired t-tests or Wilcoxon rank-sum tests according to the results of the normality testing, For categorical testing, the Fisher's exact test was utilized if the number of events was less than five in each group; for scenarios with more than five events for each group, the Chi-square test was applied. Descriptive statistics utilized mean, median, frequencies, proportions, and ranges depending on the analyzed variable. Data were analyzed using STATA 16.0 MP (StataCorp, College Station, TX, USA). P-values equal to or less than 0.05 were considered significant.

RESULTS

Patients and Treatment Characteristics

Patient, pretreatment, and treatment characteristics are summarized in **Tables 1** and **2**. A total of 53 patients with a median follow-up of 22.2 months were included in this analysis. The initial treatment was mainly fractionated (41/53 patients, 77.3%), with a median dose of 36 Gy. The median time to recurrence was 17.2 months. A total of five patients (9%) experienced a recurrence within six months of upfront treatment, three of them after three months. Four of them received EBRT; one underwent SBRT. For the recurrences, a median dose of 18 Gy prescribed to a median isodose of 70% was applied. The median and mean max doses to the spinal cord were 13.4 and 13.7 Gy, respectively. Most of the lesions were osteolytic, located in the lumbar spine, and caused pain. The majority of treated entities were deemed radioresistant. The renal cell carcinoma was the most frequently treated tumor in this cohort. Forty patients had further metastatic disease; thirteen were only suffering from the spinal metastasis recurrence. Only four patients (7%) had brain metastases at the time of treatment delivery. Most patients were suffering from further bone metastases (58%), abdominal metastases (34%), and lung metastases (11%). Four patients (7%) suffered from VCFs after reirradiation. Besides, the reirradiation was well tolerated; no patients experienced other AE grade 2 or higher. No myelopathy or bleeding events were observed after retreatment.

TABLE 1 | Patient characteristics.

Total number of patients included		53	
Gender (male/female, %)	34 (64)	19 (36)	
	Median	**Mean**	**Range**
Age (years)	61.9	62.5	36.3 – 89.4
Pretreatment Karnofsky Performance Status (%)	90	91.8	70 – 100
Follow-up (months)	22.2	34.7	1.4 – 154.3
Tumor location	**Cervical**	**Thoracic**	**Lumbar**
Number of patients	11	19	23
%	21	36	43
Lesion type	**Osteolytic**	**Osteoblastic**	**Mixed**
Number of patients	32	20	1
%	60	38	2
Symptoms	**Pain**	**Radiculopathy**	**Weakness**
Number of patients	21	7	2
%	40	13	4
Only spinal metastasis, no other distant metastasis	**Yes**	**No**	
Number of patients	13	40	
%	23	77	
Tumor entities		**Number of patients**	
Renal		14	
Breast		10	
Prostate		8	
Lung		7	
Head and neck		2	
Colorectal		2	
Other		10	
Radiosensitivity	**Sensitive**	**Intermediate**	**Resistant**
Number of patients	18	2	33

Local Outcome and Survival Data

The comparison between locally-controlled and uncontrolled patients is summarized in **Table 3**. The outcome and survival data are outlined in **Table 4**. Overall, 12 of 53 patients experienced a second recurrence of their spinal metastasis after a median and mean time of 14.7 and 22.7 months, respectively. This equals a crude LC of 77.3%. Overall, the prescription dose and coverage were lower in patients suffering from TF ($p = 0.04$ and $p = 0.01$, respectively). The minimal dose within the tumor showed a trend but did not reach significance ($p = 0.07$). Most of the recurrences occurred in patients with prescription doses of 18 or less Gy ($p = 0.04$, 9/12 patients, 75%) (**Figure 1**). Besides, most LFs were present in patients with a coverage less than 94% ($p = 0.01$, 9/12 patients, 75%).

The median survival was 28.7 months (**Figure 2**). The LC after 12, 24, and 36 months was 85.1%, 72.9%, and 72.9%, respectively (**Table 4** and **Figure 3**). The respective l-PFS and OS were 72.2%, 47.0%, 36.6% and 82.0%, 58.9%, and 43.1% (**Table 4**, **Figures 2** and **4**). The OS did not significantly differ for patients receiving more than 35 Gy or less for their first treatment ($p = 0.15$). LC rates did not differ for patients receiving their reirradiation within or after 12 months of initial treatment delivery ($p = 0.90$). Radiosensitivity did not have a significant impact on LFs. For 29 patients, clinical status was obtainable at last follow-up, with 51% of patients experiencing a subjective improvement in pain control. Moreover, 20% had a stable pain level and 29% showed worsening of their subjective pain at their last follow-up. Notably, most patients in this study experienced a significant decrease in their overall performance

TABLE 2 | Pretreatment and treatment characteristics.

Pretreatment	Median	Mean	Range
Dose (Gy)	36	33	14 – 50.4
Number of fractions	15	13.9	1 – 28
Time to recurrence (months)	17.2	27.9	2.5 – 236
Patients with a time to recurrence of less than six months (%)		5 (9)	
Patients treated with one fraction (%)		12 (23)	
Patients treated with two to five fractions (%)		3 (6)	
Patients additionally treated with surgery (%)		5 (9)	
Treatment	**Median**	**Mean**	**Range**
Tumor volume (cc)	25.7	35.5	1.5 – 115.5
Prescription dose (Gy)	18	18.7	15 – 22
Prescription isodose (%)	70	68.3	60 – 75
Max tumor dose (Gy)	27.1	27.4	20.7 – 34.5
Min tumor dose (Gy)	11.7	12.5	8.3 – 20.3
Max dose spinal cord (Gy)	13.4	13.7	1.8 – 21.8
Conformity index	1.28	1.31	1.13 – 1.74
Homogeneity index	1.43	1.47	1.33 – 1.67
Coverage	93.7	92.5	76.6 – 99.9

cc, cubic centimeter; Gy, Gray.

TABLE 3 | Comparison between locally-controlled and uncontrolled patients.

Variable	Local control	Treatment failure	p-value
	Mean (±SD)		
Age	61.3 (2.3)	62.7 (2.8)	0.76
Time to first recurrence (months)	28.9 (6.1)	24.5 (5.6)	0.94
Pretreatment fractions (number)	13.0 (1.4)	16.8 (2.4)	0.20
Pretreatment dose (Gy)	32.2 (1.5)	35.7 (3.0)	0.30
Tumor volume (cc)	36.3 (5.0)	38.6 (7.7)	0.82
Dose (Gy)	18.9 (0.2)	17.9 (0.5)	0.04
Max dose (Gy)	27.7 (0.4)	26.6 (0.9)	0.13
Min dose (Gy)	12.9 (0.5)	11.2 (0.4)	0.07
Coverage (%)	93.6 (0.6)	89.5 (1.9)	0.01

SD, standard deviation; Gy, Gray; cc, cubic centimeter.

TABLE 4 | Outcome and survival data.

Variable	Time (in months)	Value (%)	95% Confidence interval (%)
LC	12	85.1	71.4 – 92.6
	24	72.9	55.9 – 84.2
	36	72.9	55.9 – 84.2
I-PFS	12	72.2	57.7 – 82.5
	24	47.0	32.1 – 60.5
	36	36.6	22.5 – 50.7
OS	12	82.0	68.2 – 90.2
	24	58.9	43.2 – 71.6
	36	43.1	28.0 – 57.4

LC, local control; I-PFS, local progression-free survival; OS, overall survival.

status and progressed due to metastatic disease, partially limiting dedicated clinical pain evaluations regarding the preirradiated spinal metastasis. At last follow-up, thirty-six patients (68%) had disease progression or succumbed to their illness.

DISCUSSION

This is one of the largest reports exclusively analyzing patients treated with single-session RRS for their spinal metastasis recurrence (12–14). Only recurrences which occurred at the very same spot as the initial macroscopic metastatic lesion were included. So far, only sparse data are available for this patient cohort. The objective was to investigate whether this dedicated subgroup of recurrences behaves differently when irradiated with SBRT. Besides, the reported follow-up herein is more extensive compared to most of the previous studies (12, 13). In general, spinal metastases are a common and considerable oncologic challenge. With the recent advancements in systemic and local treatments, more patients will experience spinal metastasis recurrences in the foreseeable future. However, only a few studies have reported dedicated results for SBRT for the treatment of spinal metastasis recurrences until today (12, 13). Thus, further evaluation of treatment options that may achieve long-term LC and pain relief are needed.

Local Control and Survival

According to recent reviews, SBRT for the reirradiation of spinal metastasis has shown 1-year LC rates between 66% and 90% (12, 14). Overall, the current data quality on spinal reirradiation with SBRT for spinal metastasis are not only limited but mostly based on retrospective single-center trials like the current study. One large retrospective multicenter analysis showed favorable results for single-session treatments (13). Notably, most reports included recurrences that generally occurred in previously irradiated fields, while this study exclusively included recurrences literally at the same spot as the initial lesion, trying to improve data homogeneity. Our findings, however, are mostly comparable to the previous reports (12–14, 23). Moreover, this report only included patients receiving one fraction. Many preirradiated patients in the literature underwent more than one fraction. The most common fractionation schemes included 3 x 9 Gy, 3 x 8 Gy, 3 x 7 Gy, 5 x 6 Gy, 5 x 5 Gy, and 5 x 4 Gy, with comparable LC rates (12–14). Notably, a single-session treatment reduces the time patients need to spend for their treatment and care. This is especially important for patients receiving palliative care. As previously described, 1-year LC rates are around 80% with the formerly mentioned doses and fractions. In this study, 85% of patients had their metastasis controlled after 12 months. This is also in agreement with the patients treated with one fraction, as reported by Hashmi et al. (13). Notably, they reported better LC rates for single-session treatments compared to multisession irradiations (13). As most published series only report 1-year LC rates due to poor overall survival of the study cohorts, respective median follow-up times are mostly around 12 months (12, 13). Thus, not much data are available on the LC beyond this period after undergoing SBRT. Herein, many patients were alive after two years, showing a LC of 73% at that time. After three years, 16 patients were still alive, with a LC rate of 73%. Despite limited data and the small sample sizes, SBRT may achieve satisfactory 2-year and 3-year LC rates (13). However, it remains unclear what factors may influence LC rates in this patient group. In contrast to Garg and colleagues as

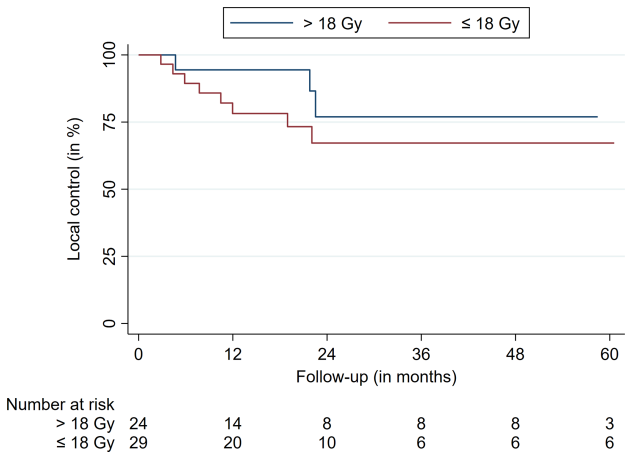

FIGURE 1 | Local control stratified for a prescription dose cutoff at 18 Gy.

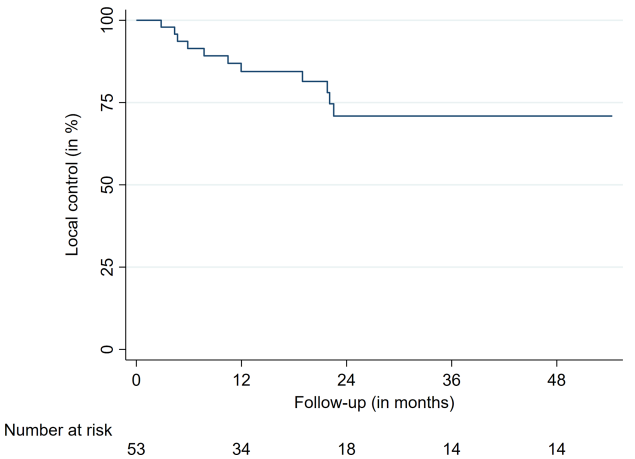

FIGURE 3 | Overall local control.

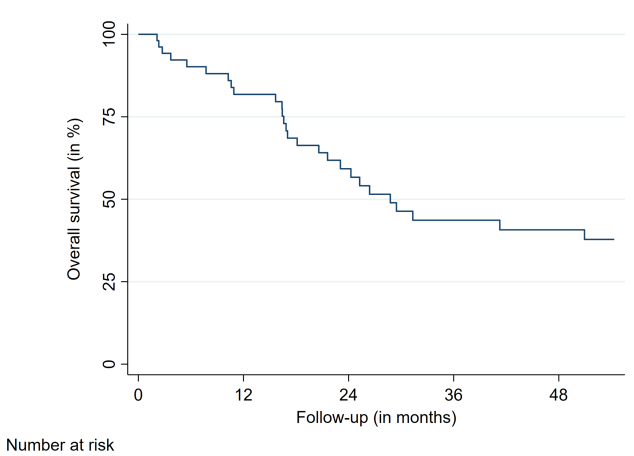

FIGURE 2 | Overall survival.

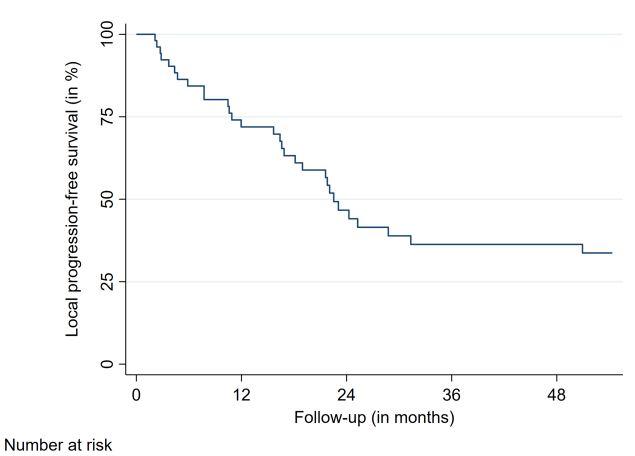

FIGURE 4 | Local progression-free survival.

well as Choi and colleagues, we did not find significant associations between pretreatment doses of less than 35 Gy or the time to reirradiation less than 12 months with OS and LF (16, 24). Overall, it remains unclear to which extent the primary treatment influences the outcome of the reirradiation. Nevertheless, we did see the trend that patients receiving lower prescription doses (<18 Gy) experienced most of the documented LFs. Considering that doses around 24 Gy delivered in one fraction show reasonable LC rates for the initial treatment of spinal metastasis, it may decrease the chance of LF if doses of at least 19 Gy in one fraction may be applied (25). Besides, patients with a minimal dose of 13 Gy or less experienced significantly more local recurrences. Moreover, patients with a coverage of more than 94% did show fewer recurrences. Whereas previous studies and reports discussed the role of radiosensitivity as a potential factor influencing the LC rate, we did not find any significant associations herein (20, 26). However, this may be due to the small sample size, low number of LFs, and proportions of included tumor entities.

Despite the fear of associated toxicity and adverse events with a limited life expectancy, treating physicians should anticipate increased survival in this patient subgroup in the future and, thus, should try to apply a considerable dose with respective coverage to prevent LFs before systemic disease progression. Overall, treatment planning should be carefully evaluated for this specific patient subgroup. This is especially important for patients only suffering from spinal metastasis while having a controlled primary tumor side and a low systemic tumor burden. Finally, the applied single-session RRS treatment achieved LC in most of the cases, but the majority of patients suffered from additional metastases at the time of treatment, which ultimately led to an overall disease progression. Finally, most other reports

did not report on the further disease status of patients, i.e., presence and number, as well as the location of other metastases, limiting accurate comparisons.

Toxicity

Spinal reirradiation with SBRT at the same macroscopic location is still not a very commonly reported situation. In this study, we observed tolerable toxicity, mostly following the dose constraints of the AAPM TG 101 (21). No adverse events higher than grade 2 were observed after treatment delivery. The four occurring VCFs except one did not need any additional medical or surgical treatment. Previously published studies reported similar toxicities, with the majority of AE related to fatigue. An overall VCF rate of 12% was reported among the four studies reporting VCFs as a dedicated adverse event in a recent review (12). With a VCF rate of 7%, single-session RRS seems to have a slightly lower fracture risk as compared to the hypofractionated schemes that were applied in the other studies. However, in contrast to the VCF rate of 4.5% in the study of Hashmi et al., the risk seems to be slightly higher (13). Yet, data are limited, and no definite conclusions can be drawn considering that the majority of studies did not report on the occurrence of VCF (12, 14). Besides VCF, myelopathy is an associated complication after spinal irradiation. In this study, no myelopathies were observed in our group of 53 patients. This is in agreement with the existing literature as myelopathies still rarely occur after reirradiation (crude risk 1.2%) (12, 13). Overall, and given the limited data available for modern SBRT for spinal metastasis reirradiation, it remains unclear what other factors may contribute to adverse events higher than grade 2.

Pain

Pain control has always been a substantial treatment goal for the treatment of spinal metastases. This goal is similar for the retreatment of spinal lesions. While repeated EBRT with various fractionation schemes showed a notable effect in around 60% of patients in multiple studies, some data are available on SBRT for the control of pain after reirradiation (12, 22, 27). Moreover, given the heterogeneity of reporting outcomes for spinal treatments – something which is especially true for reirradiation procedures –, limited conclusions can be drawn from the available data (12–14, 28). Current studies show pain control rates between 65% and 81% (12, 13). As for the dynamic of pain control and improvement, Garg and colleagues reported better pain levels on the Brief Pain Inventory (BPI) after three months of treatment delivery (24). This improvement was also present after six months (24). Herein, we report an improvement rate of 51% at last follow-up, which may be caused by the limited clinical information and subjective assessment method. Considering the limited data we can provide on pain control, more studies are needed to assess the actual treatment efficiency. Notably, most cases in this report had widespread metastatic disease, especially bone metastases, with respective symptoms that limited the possibility to exactly determine the symptoms just caused by the spinal recurrence alone.

Future Challenges

As depicted by the SPINO consortium, the reporting of studies for spinal metastasis is particularly heterogeneous (28). Considering the 15-year span it took to treat about 50 patients with a spinal recurrence occurring in the exact location as previously, the frequency of spinal reirradiation for this small subgroup of patients poses a considerable challenge to report standardized outcomes. This is mainly due to various changes in the field and improved radiation techniques in the past 15 years. With respect to the increasing life expectancy of patients with spinal metastasis, patients experiencing recurrences should be assessed in a comparable way to create reliable evidence on reirradiation treatment options. According to the SPINO consortium, various clinician-based (SINS, Bilsky grade, MRC, KPS,…) and patient-reported outcomes (SF36, BPI, SOSGOQ,…) should be implemented (28). Besides these recommendations and in consideration of the available literature, single-session RRS may be an appropriate tool for spinal reirradiation, especially in palliative settings. Ultimately, prospective trials are necessary to determine the ideal management on spinal reirradiation.

Limitations

This study has several inherent limitations given its retrospective nature and design. First, the sample size is limited due to the single-center study design. Second, no standardized outcome measures for the pain assessment were available. The analysis of the pain data was limited to chart reviews. Third, we included all patients who met the criteria for their recurrence, potentially causing a sampling bias due to this convenient sampling approach. This may be reflected by an imbalance of patients receiving EBRT and SBRT as their initial treatment.

CONCLUSION

Single-session RRS appears to be a safe and effective treatment modality for spinal metastases reoccurring at the same macroscopic location after initial irradiation. Treatment results are comparable to reirradiated metastases in the boundary areas. Toxicity can be effectively limited if appropriate dose constraints are considered. Given the practicability, single-session RRS may be a well-suited treatment option given the less time-consuming treatment delivery if reasonable doses with an adequate coverage can be applied.

DATA AVAILABILITY STATEMENT

The data that support the findings of this study are available from the corresponding author, FE, upon reasonable request.

ETHICS STATEMENT

The studies involving human participants were reviewed and approved by the Ludwig-Maximilians-University Munich.

Written informed consent for participation was not required for this study in accordance with the national legislation and the institutional requirements.

AUTHOR CONTRIBUTIONS

Conception and design of the study: FE. Data acquisition: FE, LM, MK, CF, AH, and AM. Data analysis and drafting of the manuscript: FE. Critically revising manuscript: FE, CF, PW, CS, J-CT, and AM. All authors contributed to the article and approved the submitted version.

ACKNOWLEDGMENTS

We acknowledge support from the German Research Foundation (DFG) and the Open Access Publication Fund of Charité – Universitätsmedizin Berlin.

REFERENCES

1. Spratt DE, Beeler WH, de Moraes FY, Rhines LD, Gemmete JJ, Chaudhary N, et al. An Integrated Multidisciplinary Algorithm for the Management of Spinal Metastases: An International Spine Oncology Consortium Report. *Lancet Oncol* (2017) 18(12):e720–30. doi: 10.1016/s1470-2045(17)30612-5
2. Hernandez RK, Adhia A, Wade SW, O'Connor E, Arellano J, Francis K, et al. Prevalence of Bone Metastases and Bone-Targeting Agent Use Among Solid Tumor Patients in the United States. *Clin Epidemiol* (2015) 7:335–45. doi: 10.2147/CLEP.S85496
3. Patchell RA, Tibbs PA, Regine WF, Payne R, Saris S, Kryscio RJ, et al. Direct Decompressive Surgical Resection in the Treatment of Spinal Cord Compression Caused by Metastatic Cancer: A Randomised Trial. *Lancet* (2005) 366(9486):643–8. doi: 10.1016/s0140-6736(05)66954-1
4. Li S, Peng Y, Weinhandl ED, Blaes AH, Cetin K, Chia VM, et al. Estimated Number of Prevalent Cases of Metastatic Bone Disease in the US Adult Population. *Clin Epidemiol* (2012) 4:87–93. doi: 10.2147/clep.S28339
5. Wong DA, Fornasier VL, MacNab I. Spinal Metastases: The Obvious, the Occult, and the Impostors. *Spine (Phila Pa 1976)* (1990) 15(1):1–4. doi: 10.1097/00007632-199001000-00001
6. Ahmed KA, Stauder MC, Miller RC, Bauer HJ, Rose PS, Olivier KR, et al. Stereotactic Body Radiation Therapy in Spinal Metastases. *Int J Radiat Oncol Biol Phys* (2012) 82(5):e803–9. doi: 10.1016/j.ijrobp.2011.11.036
7. Jawad MS, Fahim DK, Gerszten PC, Flickinger JC, Sahgal A, Grills IS, et al. Vertebral Compression Fractures After Stereotactic Body Radiation Therapy: A Large, Multi-Institutional, Multinational Evaluation. *J Neurosurg Spine* (2016) 24(6):928–36. doi: 10.3171/2015.10.Spine141261
8. Chang EL, Shiu AS, Mendel E, Mathews LA, Mahajan A, Allen PK, et al. Phase I/II Study of Stereotactic Body Radiotherapy for Spinal Metastasis and Its Pattern of Failure. *J Neurosurg Spine* (2007) 7(2):151–60. doi: 10.3171/spi-07/08/151
9. Gerszten PC, Burton SA, Ozhasoglu C, Welch WC. Radiosurgery for Spinal Metastases: Clinical Experience in 500 Cases From a Single Institution. *Spine (Phila Pa 1976)* (2007) 32(2):193–9. doi: 10.1097/01.brs.0000251863.76595.a2
10. Chang U-K, Youn SM, Park SQ, Rhee CH. Clinical Results of Cyberknife(r) Radiosurgery for Spinal Metastases. *J Korean Neurosurg Soc* (2009) 46(6):538–44. doi: 10.3340/jkns.2009.46.6.538
11. Heron DE, Rajagopalan MS, Stone B, Burton S, Gerszten PC, Dong X, et al. Single-Session and Multisession CyberKnife Radiosurgery for Spine Metastases-University of Pittsburgh and Georgetown University Experience. *J Neurosurg Spine* (2012) 17(1):11–8. doi: 10.3171/2012.4.Spine11902
12. Myrehaug S, Sahgal A, Hayashi M, Levivier M, Ma L, Martinez R, et al. Reirradiation Spine Stereotactic Body Radiation Therapy for Spinal Metastases: Systematic Review. *J Neurosurg Spine* (2017) 27(4):428–35. doi: 10.3171/2017.2.Spine16976
13. Hashmi A, Guckenberger M, Kersh R, Gerszten PC, Mantel F, Grills IS, et al. Re-Irradiation Stereotactic Body Radiotherapy for Spinal Metastases: A Multi-Institutional Outcome Analysis. *J Neurosurg Spine* (2016) 25(5):646–53. doi: 10.3171/2016.4.Spine151523
14. Myrehaug S, Soliman H, Tseng C, Heyn C, Sahgal A. Re-Irradiation of Vertebral Body Metastases: Treatment in the Radiosurgery Era. *Clin Oncol (R Coll Radiol)* (2018) 30(2):85–92. doi: 10.1016/j.clon.2017.11.005
15. Boyce-Fappiano D, Elibe E, Zhao B, Siddiqui MS, Lee I, Rock J, et al. Reirradiation of the Spine With Stereotactic Radiosurgery: Efficacy and Toxicity. *Pract Radiat Oncol* (2017) 7(6):e409–17. doi: 10.1016/j.prro.2017.05.007
16. Choi CY, Adler JR, Gibbs IC, Chang SD, Jackson PS, Minn AY, et al. Stereotactic Radiosurgery for Treatment of Spinal Metastases Recurring in Close Proximity to Previously Irradiated Spinal Cord. *Int J Radiat Oncol Biol Phys* (2010) 78(2):499–506. doi: 10.1016/j.ijrobp.2009.07.1727
17. Damast S, Wright J, Bilsky M, Hsu M, Zhang Z, Lovelock M, et al. Impact of Dose on Local Failure Rates After Image-Guided Reirradiation of Recurrent Paraspinal Metastases. *Int J Radiat Oncol Biol Phys* (2011) 81(3):819–26. doi: 10.1016/j.ijrobp.2010.06.013
18. Muacevic A, Staehler M, Drexler C, Wowra B, Reiser M, Tonn JC. Technical Description, Phantom Accuracy, and Clinical Feasibility for Fiducial-Free Frameless Real-Time Image-Guided Spinal Radiosurgery. *J Neurosurg Spine* (2006) 5(4):303–12. doi: 10.3171/spi.2006.5.4.303
19. Fürweger C, Drexler C, Kufeld M, Muacevic A, Wowra B, Schlaefer A. Patient Motion and Targeting Accuracy in Robotic Spinal Radiosurgery: 260 Single-Fraction Fiducial-Free Cases. *Int J Radiat Oncol Biol Phys* (2010) 78(3):937–45. doi: 10.1016/j.ijrobp.2009.11.030
20. Yamada Y, Katsoulakis E, Laufer I, Lovelock M, Barzilai O, McLaughlin LA, et al. The Impact of Histology and Delivered Dose on Local Control of Spinal Metastases Treated With Stereotactic Radiosurgery. *Neurosurg Focus* (2017) 42(1):E6. doi: 10.3171/2016.9.Focus16369
21. Benedict SH, Yenice KM, Followill D, Galvin JM, Hinson W, Kavanagh B, et al. Stereotactic Body Radiation Therapy: The Report of AAPM Task Group 101. *Med Phys* (2010) 37(8):4078–101. doi: 10.1118/1.3438081
22. Chow E, van der Linden YM, Roos D, Hartsell WF, Hoskin P, Wu JS, et al. Single Versus Multiple Fractions of Repeat Radiation for Painful Bone Metastases: A Randomised, Controlled, Non-Inferiority Trial. *Lancet Oncol* (2014) 15(2):164–71. doi: 10.1016/s1470-2045(13)70556-4
23. Thibault I, Campbell M, Tseng CL, Atenafu EG, Letourneau D, Yu E, et al. Salvage Stereotactic Body Radiotherapy (SBRT) Following In-Field Failure of Initial SBRT for Spinal Metastases. *Int J Radiat Oncol Biol Phys* (2015) 93(2):353–60. doi: 10.1016/j.ijrobp.2015.03.029
24. Garg AK, Wang XS, Shiu AS, Allen P, Yang J, McAleer MF, et al. Prospective Evaluation of Spinal Reirradiation by Using Stereotactic Body Radiation Therapy: The University of Texas MD Anderson Cancer Center Experience. *Cancer* (2011) 117(15):3509–16. doi: 10.1002/cncr.25918
25. Gong Y, Xu L, Zhuang H, Jiang L, Wei F, Liu Z, et al. Efficacy and Safety of Different Fractions in Stereotactic Body Radiotherapy for Spinal Metastases: A Systematic Review. *Cancer Med* (2019) 8(14):6176–84. doi: 10.1002/cam4.2546
26. Bernard V, Bishop AJ, Allen PK, Amini B, Wang XA, Li J, et al. Heterogeneity in Treatment Response of Spine Metastases to Spine Stereotactic Radiosurgery Within "Radiosensitive" Subtypes. *Int J Radiat Oncol Biol Phys* (2017) 99(5):1207–15. doi: 10.1016/j.ijrobp.2017.08.028
27. Huisman M, van den Bosch MA, Wijlemans JW, van Vulpen M, van der Linden YM, Verkooijen HM. Effectiveness of Reirradiation for Painful Bone Metastases: A Systematic Review and Meta-Analysis. *Int J Radiat Oncol Biol Phys* (2012) 84(1):8–14. doi: 10.1016/j.ijrobp.2011.10.080
28. Laufer I, Lo SS, Chang EL, Sheehan J, Guckenberger M, Sohn MJ, et al. Population Description and Clinical Response Assessment for Spinal Metastases: Part 2 of the SPIne Response Assessment in Neuro-Oncology

(SPINO) Group Report. *Neuro Oncol* (2018) 20(9):1215–24. doi: 10.1093/neuonc/noy047

Conflict of Interest: FE reports a grant from Ludwig-Maximilians-University Munich and honoraria from Accuray outside the submitted work.

The remaining authors declare that the research was conducted in the absence of any commercial or financial relationships that could be construed as a potential conflict of interest.

frontiers in Oncology

ORIGINAL RESEARCH
published: 15 June 2021
doi: 10.3389/fonc.2021.667993

Cost-Effectiveness Analysis of Local Treatment in Oligometastatic Disease

*Dirk Mehrens[1], Marcus Unterrainer[1], Stefanie Corradini[2], Maximilian Niyazi[2], Farkhad Manapov[2], C. Benedikt Westphalen[3], Matthias F. Froelich[4], Moritz Wildgruber[1], Max Seidensticker[1], Jens Ricke[1], Johannes Rübenthaler[1] and Wolfgang G. Kunz[1]**

[1] Department of Radiology, University Hospital, LMU Munich, Munich, Germany, [2] Department of Radiation Oncology, University Hospital, LMU Munich, Munich, Germany, [3] Department of Medicine III, University Hospital, LMU Munich, Munich, Germany, [4] Department of Radiology and Nuclear Medicine, University Medical Centre Mannheim, Medical Faculty Mannheim-University of Heidelberg, Mannheim, Germany

OPEN ACCESS

Edited by:
Rupesh Kotecha,
Baptist Hospital of Miami,
United States

Reviewed by:
Vivek Verma,
Allegheny General Hospital,
United States
Moshe Schaffer,
Ben-Gurion University of the Negev,
Israel
Erqi Pollom,
Stanford University, United States

***Correspondence:**
Wolfgang G. Kunz
wolfgang.kunz@med.lmu.de

Specialty section:
This article was submitted to Radiation Oncology, a section of the journal Frontiers in Oncology

Received: 15 February 2021
Accepted: 31 May 2021
Published: 15 June 2021

Citation:
Mehrens D, Unterrainer M, Corradini S, Niyazi M, Manapov F, Westphalen CB, Froelich MF, Wildgruber M, Seidensticker M, Ricke J, Rübenthaler J and Kunz WG (2021) Cost-Effectiveness Analysis of Local Treatment in Oligometastatic Disease. Front. Oncol. 11:667993. doi: 10.3389/fonc.2021.667993

Background: In certain malignancies, patients with oligometastatic disease benefit from radical ablative or surgical treatment. The SABR-COMET trial demonstrated a survival benefit for oligometastatic patients randomized to local stereotactic ablative radiation (SABR) compared to patients receiving standard care (SC) alone. Our aim was to determine the cost-effectiveness of SABR.

Materials and Methods: A decision model based on partitioned survival simulations estimated costs and quality-adjusted life years (QALY) associated with both strategies in a United States setting from a health care perspective. Analyses were performed over the trial duration of six years as well as a long-term horizon of 16 years. Model input parameters were based on the SABR-COMET trial data as well as best available and most recent data provided in the published literature. An annual discount of 3% for costs was implemented in the analysis. All costs were adjusted to 2019 US Dollars according to the United States Consumer Price Index. SABR costs were reported with an average of $11,700 per treatment. Deterministic and probabilistic sensitivity analyses were performed. Incremental costs, effectiveness, and cost-effectiveness ratios (ICER) were calculated. The willingness-to-pay (WTP) threshold was set to $100,000/QALY.

Results: Based on increased overall and progression-free survival, the SABR group showed 0.78 incremental QALYs over the trial duration and 1.34 incremental QALYs over the long-term analysis. Treatment with SABR led to a marginal increase in costs compared to SC alone (SABR: $304,656; SC: $303,523 for 6 years; ICER $1,446/QALY and SABR: $402,888; SC: $350,708 for long-term analysis; ICER $38,874/QALY). Therapy with SABR remained cost-effective until treatment costs of $88,969 over the trial duration (i.e. 7.6 times the average cost). Sensitivity analysis identified a strong model impact for ongoing annual costs of oligo- and polymetastatic disease states.

Conclusion: Our analysis suggests that local treatment with SABR adds QALYs for patients with certain oligometastatic cancers and represents an intermediate- and long-term cost-effective treatment strategy.

Keywords: OMD, cost-effectiveness (economics), radiation therapy (radiotherapy), cancer, SABR

INTRODUCTION

Metastatic cancers are considered incurable in a variety of tumor entities. The treatment of choice is systemic therapy. The state of oligometastatic disease (OMD) was introduced in the mid 90s as a subcategory of metastatic cancer. With only a limited number of metastases confined to a few organs, this state may represent a less aggressive tumor biology and open the possibility of treatment in a curative intent (1). However, the oligometastatic state is not fully defined and established (2), and studies regarding treatment are still unfolding (3).

Treatment options include ablative surgery, stereotactic ablative radiotherapy (SABR) and other local ablative procedures like thermal ablation and radioablation, which show different efficacy depending on anatomic location (4). Considering treatment of several metastases in different locations with particularities of their anatomy and composition, SABR has proven to be a targeted treatment option with only few side effects (5, 6) and sufficient local tumor control (7).

The SABR-COMET trial is one of the first phase II trials to compare treatment of patients with one to five metastases of varying tumor entities with standard care (SC) to additional SABR (SABR) (8). The trial demonstrated that combined treatment extended progression-free survival (PFS) and overall survival (OS), all while maintaining quality of life (QoL).

Given this new local treatment option, our aim was to determine the cost-effectiveness of SABR compared to SC, taking into account PFS, OS and QoL.

METHODS

Model Structure

Our analysis followed recommendations of the Second Panel on Cost-Effectiveness in Health and Medicine (9). We developed a partitioned survival model using decision-analytic software (Treeage Healthcare Pro 2020, Version 20.1.2-v20200326; Treeage, Williamstown, MA) to assess the cost-effectiveness of SABR versus SC over the trial duration of 6 years, using a cycle length of 1 month. Furthermore, long-term survival data was obtained from the Surveillance, Epidemiology, and End Results (SEER) Program (10). The partitioned survival analysis model allows to simulate a patient cohort over time as patients advance along mutually exclusive health states. During each cycle, patients could therefore remain in the oligometastatic state, progress to the polymetastatic disease (PMD) state or die. The only absorbing state was death.

Model Input Parameters

Progression and Survival Probabilities

All individuals started in the oligometastatic state. Monthly overall and progression-free survival rates were derived from the Kaplan-Meier analysis of the SABR-COMET trial (**Supplementary Figure 1**). Therefore, no adjustment for the age-related death rate was necessary. For modeling long-term survival, we referred to the Surveillance, Epidemiology, and End Results Program (SEER) using the SEER*Explorer. OS data were pooled from the database for the metastatic stage of the most frequent cancer entities in the SABR-COMET trial (breast, colorectal, lung, prostate) and fitted with respect to the proportion in the study population. The OS course in the SEER data was used to extrapolate the trial OS curve beyond the trial period. In detail, the curve was expanded beginning from the latest reported OS percentage from the trial and continued with the SEER survival curve at that same percentage. Because of missing data in terms of PFS, we also applied this data to extrapolate the long-term course of PFS; for this we additionally assumed the same proportionality of OS to PFS as in the SABR COMET trial (**Supplementary Table 1**). An overview of the model structure is shown in **Figure 1**.

Costs

The analysis was performed in a United States setting from a health care perspective. The ongoing treatment costs for standard care of OMD and PMD states were derived from Reyes et al. (11) and accumulated. These accumulated cost data were used to reflect average annual health expenditures for the patient population that was investigated in the SABR-COMET trial. It further allowed to model the differences in

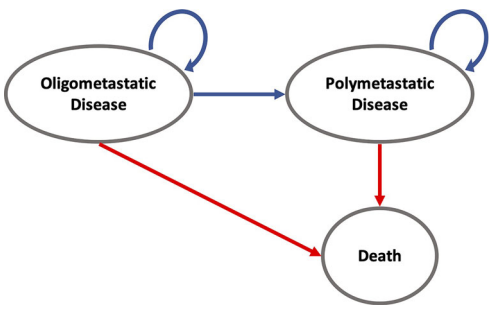

FIGURE 1 | State-transition diagram for modeling cost and effectiveness for the SABR and SC strategies over time intervals. For example, patients in the oligometastatic disease state can either remain in the oligometastatic state, transition to the polymetastatic disease state, or die. Death is an absorbing state and will discontinue the individual simulation.

therapy costs during the time intervals spent in the OMD or PMD state. 55% of patients in the SABR group as well as 63.6% of patients in the SC group received systemic therapy. Because of missing information in terms of drug administration, costs were distributed proportionally in the OMD and PMD group. Costs for single treatment of SABR were pooled from assorted papers comprising different fraction numbers and localization of treatment (12–16). Costs for palliative radiotherapy were derived from Medicare coverage data (17).

23 patients in the SC group and 16 patients in the SABR group obtained salvage radiotherapy. 9 patients of the SABR group received additional salvage SABR. Total costs for additional radiotherapy were accumulated per group and factored in as cost items at the beginning of the simulation as data concerning the time of administration was not available; this approximation will slightly alter the costs as these would not be discounted before the actual time of administration. An additional cumulative single time cost was added for the last 180 days of treatment before death (18).

Therapy-related adverse events higher than or equal to grade 2 occurred in 19 patients in the SABR group and 3 patients in the SC group. Costs for treatment (19–21) and disutility (22–26) were pooled from the literature and added as one-time cost and disutility at the beginning of the analysis. An overview of the input parameters is given in **Table 1**. An annual discount of 3% for costs was implemented in the analysis according to current recommendations (9). All costs were adjusted to 2019 US Dollars according to the United States Consumer Price Index.

Utilities

Therapy effectiveness was measured in quality-adjusted life years (QALYs), calculated by multiplying years spent in OMD and PMD states by assigned utility weights. Utility weights for OMD were obtained from the FACT-G-Score used in the SABR-COMET trial and converted to EQ-5D according to Teckle et al. (27). Utility weights for PMD were derived from the literature (24, 26, 28–34). A discount of 3% for utilities was implemented in the analysis (9).

Cost-Effectiveness Analysis

Treatment strategies were compared in terms of net monetary benefits, incremental costs, incremental effectiveness, and incremental cost-effectiveness ratios (ICERs). The willingness-to-pay was set to $100,000 per QALY as in recent studies (35). Net monetary benefits combine costs and effectiveness in one measure: net monetary benefit = (effectiveness × willingness-to-pay) minus costs.

Sensitivity Analysis

We used comprehensive deterministic and probabilistic sensitivity analysis (PSA) to test the robustness of the model. Deterministic one-way sensitivity analysis was performed to identify variables that significantly influence the model outcomes. The ranges for deterministic sensitivity analysis were determined by the 95% confidence interval of the initial probabilities and by ±20% for costs. Moreover, PSA allows simultaneous alteration of multiple model input parameters using distributions according to probability density functions for second order Monte Carlo simulation runs (n=10,000) (36). The model input parameters were assigned appropriate distributions as indicated in **Table 1**. Utilities were varied with a beta distribution. Treatment costs were modeled by gamma distribution. Beta distributions were used for disutilities as well as PFS and OS data.

RESULTS

Base Case Analysis

In the base case analysis of the total study population over the trial duration of 6 years, SABR led to an increased effectiveness of 0.78 QALY at increased costs of $1,133. The ICER was $1,446 per QALY. When additional long-term SEER data were applied, SABR led to an increased effectiveness of 1.34 QALY at additional costs of $52,180. The corresponding ICER was $38,874 per QALY. Adverse events only had a minor effect on our results with a loss of 0.002 QALYs for SABR and 0.0008 QALYs for SC. Incremental costs for treatment of adverse events amounted to $1,443 for the SABR group and $997 for the SC arm.

Deterministic Sensitivity Analysis

The results of the deterministic one-way sensitivity analysis are presented in **Figure 2**. Costs of systemic therapy of PMD and OMD possessed the strongest impact on ICER regarding the trial duration as well as costs of OMD state on long-term survival. Higher costs of OMD state and lower costs of PMD led to unfavorable ICER values whereas lower costs for therapy of OMD state and higher costs of PMD state led to favorable ICER values. These effects were reversed for the SC strategy. SABR remained cost-effective even when the costs for SABR and salvage SABR were increased 7.6 times during the trial duration and stayed cost-effective when raised up to 8 times for long-term survival (see **Figure 3**).

Probabilistic Sensitivity Analysis

Overall, SABR was cost-effective in 100% of Monte Carlo simulation runs with an ICER of $1,105 per QALY during the trial duration and $38,740 per QALY for long-term survival in 99.95% of Monte Carlo simulation runs, indicating robustness of the model. In 47% of simulations, SABR was the dominant strategy when analyzed with SABR-COMET data, meaning that it provided better outcomes at lower costs.

The mean incremental effectiveness was positive, meaning that SABR on average led to increased QALYs. Moreover, the mean values for the ICERs were below the willingness-to-pay threshold. The detailed results of the PSA are shown in **Table 2**.

DISCUSSION

This study evaluated the economic impact of SABR in the treatment of oligometastatic cancer patients. The analysis

TABLE 1 | Detailed Model Input Parameters.

Model Input	Base Case Value	Range for Sensitivity Analysis*	Distribution	Reference
Initial Probabilities				
oligometastatic state	1			Palma et al. (8)
polymetastatic state	0			
death	0			
Survival Probabilities				
OS for SC				Palma et al. (8)
1st year	0.88			
2nd year	0.58			
3rd year	0.38	± 15%	ß	
4th year	0.18			
5th year	0.18			
6th year	0.18			
OS for SABR				
1st year	0.88			
2nd year	0.69			
3rd year	0.62			
4th year	0.52			
5th year	0.42			
6th year	0.42			
PFS for SC				
1st year	0.19			
2nd year	0.13			
3rd year	0.07			
4th year	0.04			
6th year	0			
5th year	0			
PFS for SABR				
1st year	0.5			
2nd year	0.38			
3rd year	0.3			
4th year	0.21			
5th year	0.18			
6th year	0.18			
Health Care Costs				
Annual costs for metastatic disease				
cumulative	$ 97,440	$ 77,952 - 116,928	y	adapted from Reyes et al. (11)
Annual costs for progressive metastatic disease				
cumulative	$ 189,840	$ 151,872 - 227,808	y	adapted from Reyes et al. (11)
End of life costs				
Last 180 Days	$ 19,174	$ 15,339 - 23,009	y	Bekelman et al. (16)
Palliative RT costs				
unit costs	$ 11,070	$ 8,856 - 13,284	y	Agarwal et al. (17)
SABR costs				
cumulative	$ 11,700	$ 8,190 - 14,040	y	Hess et al. (12); Kim et al., 2015; Lanni et al. (14); Shah et al. (15); Kim et al., 2016
Utilities				
OMD	0.82	0.70 - 0.90	ß	Palma et al. (8) calculated from Teckle et al. (27)
PMD	0.59	0.50 - 0.70	ß	Lloyd et al. (28); Lee at al. (29); Farkilla et al. (30); Petrou and Campbell (31); Llyod et al. (29), Hudgens et al. (32); Paracha et al. (33); Paracha et al. (26); Nafees et al. (24)
Adverse Events				
Disutility	SABR: -0.002 SC: -0.0008	± 10%	ß	Palma et al. (8) Hagiwara et al. (22); Chouaid et al. (23); Wehler et al., 2018; Paracha et al. (26)
Treatment costs	SABR: $ 1,443 SC: $ 997	SABR: $ 1,154 - 1,732 SC: $ 798 - 1,196	y	Palma et al. (8) Wong et al. (19) Copley-Merriman et al. (20); Ting et al. (21)

*Detailed model input parameters. Survival probabilities and utility for OMD were derived from the SABR-COMET trial. All costs, transitions probabilities for long term survival as well as utility for PMD and disutility from adverse events were derived from the literature. Ranges for deterministic sensitivity analysis were determined by the 95% confidence interval of the initial probabilities and by ±20% for costs. For PSA y-distribution for costs and ß-distribution for utilities was applied. All costs were converted to 2019 USD. *The minimum and maximum values for ranges were derived from reported 95% confidence intervals or from calculated 95% confidence intervals with the use of variance estimates as available.*

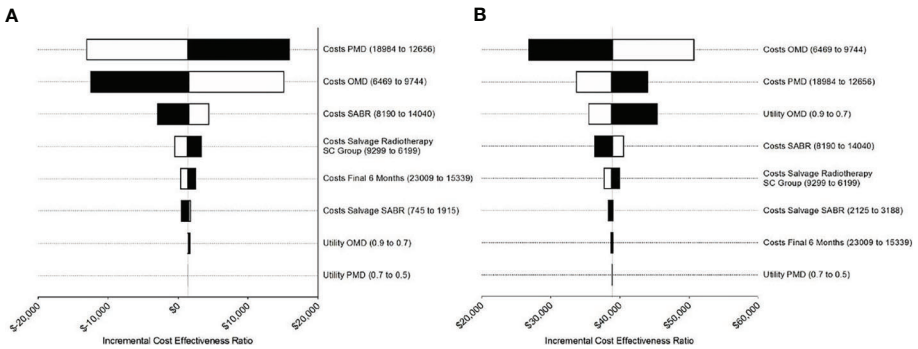

FIGURE 2 | Tornado diagrams for the sensitivity analysis during **(A)** the trial duration and **(B)** long-term simulation extrapolated based on SEER survival data. **(A)** Costs for PMD and OMD demonstrated the strongest impact on ICER during trial duration. **(B)** For long-term analysis costs for PMD influenced ICER the most followed by costs for PMD and utility for OMD.

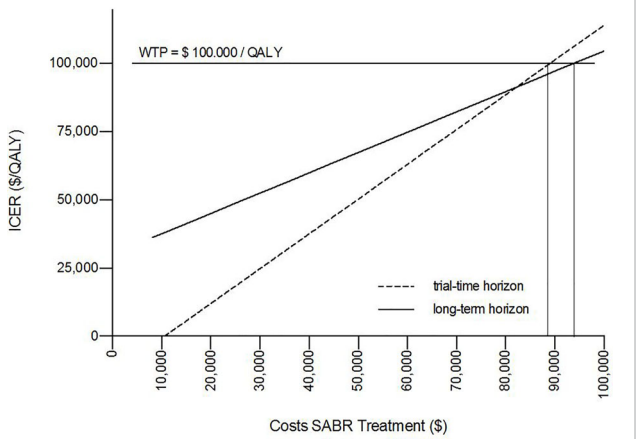

FIGURE 3 | One-way sensitivity analysis proved cost-effectiveness for SABR up to unit costs of $88,696 over the trial duration and $93,750 for long-term survival for a willingness-to-pay (WTP) threshold of $100,000/QALY.

indicates that SABR is a cost-effective treatment option compared to SC alone. Additional costs of SABR were partly amortized due to longer progression-free survival in the OMD state, which was accompanied with lower treatment costs of systemic treatment. As expected, DSA demonstrated a relevant impact of treatment costs on the ICER. Yet even with an increase in SABR treatment costs up to about sevenfold, the SABR treatment strategy remained cost-effective.

The SABR-COMET trial is the first basket study to prove survival benefits of SABR treatment in patients with OMD across different cancer entities. Previous cost-effectiveness analysis indicated cost-effectiveness for SABR in oligometastatic prostate cancer and NSCLC (37, 38). Recently, two economic analyse have also analyzed the cost-effectiveness of the SABR-COMET trial (39, 40). Kumar et al. (39) assessed that treatment with SABR is cost-effective in 99.8% of cases at a WTP threshold of $100,000 per QALY, with an ICER of $28,906 per QALY in a US health care setting after a 10-year horizon. Qu et al. (40) showed that SABR is cost-effective over a lifetime horizon in 97% of cases at a WTP threshold of $100,000 per QALY with an ICER of $54,564 per QALY. Kumar et al. used SEER data for long-term analysis over 10 years in total with an increased ICER of $79,406 per QALY if costs for treatment were continued. A detailed comparison of methods and results of these studies is provided in **Table 3**. These data provide external validation and demonstrate robustness of the cost-effectiveness of SABR. Similar to our analysis, Kumar et al. showed cost-effectiveness for SABR up to a 10-fold increase in treatment costs.

In contrast to our study, Kumar et al. assumed treatment with SC for all patients and did not include costs for salvage or palliative radiotherapy. Qu et al. used data directly from the SABR-COMET trial, which is not publicly available in its entirety. Moreover, the discount rate was adapted according to Canadian guidelines for the Economic Evaluation of Health Technologies with 1.5% and not 3% as in Kumar et al. and our study. Qu et al. report a non-linear relationship between the number of lesions and the PFS hazard ratio (HR) with the need of decreasing the HR by 0.047 for each additional metastasis to maintain cost-effectiveness for SABR.

Further studies including phase III trials are required to validate the results. Several studies are ongoing at the moment. These include the phase III of the SABR-COMET trial, namely SABR-COMET-3 (41) and SABR-COMET-10 (42), investigating the impact of SABR on patients with 1-3 metastases or 4-10 metastases respectively. By analyzing these two subpopulations, Palma et al. will help to clarify the uncertainty up to which number of metastases patients benefit from SABR. Further phase III trials include the SARON study comparing SC versus SABR and SC for oligometastatic NSCLC with 1-5 metastases in up to a maximum of 3 organs (43), NRG-BR002 investigating systemic therapy versus SABR or surgery combined with systemic therapy in breast cancer with less than 4 metastases (44), and the HALT trial examining the effect of SABR under tyrosine kinase inhibitor (TKI) therapy versus TKI treatment alone in metastatic disease with equal to or less than 3 sites of metastases (45).

TABLE 2 | Cost-effectiveness analysis results.

Trial duration **Patient group**	**Cost ($)**	**IC ($)**	**Effect (QALY)**	**IE (QALY)**	**NMB ($)**	**ICER ($/QALY)**	**Acceptability at WTP (%)**
SABR	304,459	1,105	2.58	0.78	-46,000	1,412	100
SC	303,354		1.80		-123,149		
Long-term analysis							
Patient group	**Cost ($)**	**IC ($)**	**Effect (QALY)**	**IE (QALY)**	**NMB ($)**	**ICER ($/QALY)**	**Acceptability at WTP (%)**
SABR	403,149	52,072	3.37	1.34	-66,632	38,740	99.95
SC	351,077		2.02		-148,975		

Results of cost-effectiveness analysis. SABR proved to be cost effective over the trial duration as well as long-term analysis with an ICER of $1,405 and $38,740 respectively. The willingness-to-pay was set to $100,000 per QALY. SABR, stereotactic ablative radiotherapy; SC, standard care; NMB, net monetary benefit; ICER, incremental cost-effectiveness ratio; IC, incremental cost; IE, incremental effectiveness; WTP, willingness-to-pay threshold.

TABLE 3 | Comparison of SABR-COMET cost-effectiveness analysis.

	Mehrens et al.	**Kumar et al.**	**Qu et al.**
Region	US	US	Canada/US
Year	2019	2019	2018
Perspective	healthcare	healthcare/societal	healthcare
Model	PSA	Markov	Markov
Duration	16 years	10 years	20 years
Cycle length	monthly	monthly	3 months
WTP	100,000 USD	100,000 USD	100,000 CAD
Discount	3%	3%	1.50%
Analysis	BCS/DSA/PSA	BCS/DSA/PSA	BCS/DSA/PSA
Input			
Survival data	SEER	SEER	Weibull
Cost SABR	11,700 USD/treatment	12,242 USD/treatment	8,378 CAD/ metastasis (1-5)
Cost SC (annually)	97,440 USD 189,840 USD (cancer progression)	96,468 USD 185,436 USD (cancer progression)	chemotherapy 20,813 CAD base cost 14,510 CAD base cost terminal 94,760 CAD
Results (healthcare)			
Total cost			
SABR	403,149 USD	460,161 USD	169,693 CAD
SC	351,007 USD	405,901 USD	135,452 CAD
Effectiveness			
SABR	3.37	4.84	2.77
SC	2.02	2.96	1.85
ICER	38,740 USD	28,906 USD	37,157 CAD 54,564 USD
Acceptability SABR	99.95%	99.8%	97%
Miscellaneous	SABR cost-effective until 93,750 USD	SABR cost-effective until 145,688 USD cost-effective for a hazard ratio from 0.3 until 0.76	to remain cost-effective, the HR must decrease by approx. 0.047 for each additional metastasis

Comparison of different cost-effectiveness analysis of the SABR-COMET trial. Results stated are from a healthcare perspective and only long-term survival data were compared. Currency as well as year of the respective analysis were not adapted. Our study demonstrated similar results as the analysis of Kumar et al. Input parameters as well as results from Qu et al. differed from our study as well as from Kumar et al. In probability sensitivity analysis SABR was cost-effective in nearly all of the iterations. PSA, Partitioned survival analysis; BCS, Base case scenario; DSA, Deterministic sensitivity analysis; USD, US-Dollar; CAD, Canadian Dollar.

The study results should be interpreted with knowledge of the following limitations. First, the current state of evidence on SABR in OMD is still limited by the sample size of the underlying trial; current phase III trials are ongoing. Second, the FACT-G score was stated only for whole populations of study groups. No distinction was made between progression-free and progressive patients. Data on progression-related decrease in QoL were not publicly available from the SABR-COMET study. Third, no information was provided concerning which patients received systemic therapy. Therefore, in our analysis we used the same percentage for treatment with systemic therapy in the progression-free as well as the progressive patient group to avoid introducing any bias. Fourth, because of rapidly changing treatment regimens, specifying a cost for systemic treatment may remain a source of inaccuracy.

Fifth, missing information on which treatment was administered and the inclusion of diverse tumor entities represents a challenge for precise estimation of costs for systemic cancer treatment. This may influence cost-effectiveness as one-dimensional sensitivity analysis

demonstrated a great impact of costs for systemic treatment on the ICER. We therefore chose a restrictive approach for our cost-effectiveness analysis, which still indicated cost-effectiveness for the SABR group. Sixth, long-term survival data was obtained from SEER-Program with only OS being available. We deployed these data to also model PFS. Moreover, changes in systemic therapy with more efficient treatments (46, 47) as well as technical advances in planning and performing SABR with accompanying reduction of costs (7) have to be taken into account to obtain an authentic cost estimate in the future.

In conclusion, local treatment with SABR adds QALYs for patients with oligometastatic disease across selected cancer entities in SABR-COMET and represents an intermediate- and long-term cost-effective treatment strategy.

AUTHOR CONTRIBUTIONS

DM: Investigation, Data Curation, Formal analysis, Writing - Original Draft, Software. MU: Validation, Writing - Review and Editing. SC: Validation, Writing - Review and Editing. K-MN Validation, Writing - Review and Editing. FM: Validation, Writing - Review and Editing. CW: Validation, Writing - Review and Editing. MF: Validation, Writing - Review and Editing. MW: Validation, Writing - Review and Editing. MS: Validation, Writing - Review and Editing. JeR: Validation, Writing - Review and Editing. JoR: Validation, Writing - Review and Editing. WK: Conceptualization, Methodology, Validation, Supervision, Project administration. All authors contributed to the article and approved the submitted version.

DATA AVAILABILITY STATEMENT

Publicly available datasets were analyzed in this study. This data can be found here: https://pubmed.ncbi.nlm.nih.gov/32484754/ DOI: 10.1200/JCO.20.00818.

SUPPLEMENTARY MATERIAL

The Supplementary Material for this article can be found online at: https://www.frontiersin.org/articles/10.3389/fonc.2021.667993/full#supplementary-material

REFERENCES

1. Pitroda SP, Khodarev NN, Huang L, Uppal A, Wightman SC, Ganai S, et al. Integrated Molecular Subtyping Defines a Curable Oligometastatic State in Colorectal Liver Metastasis. *Nat Commun* (2018) 9(1):1793. doi: 10.1038/s41467-018-04278-6
2. Lievens Y, Guckenberger M, Gomez D, Hoyer M, Iyengar P, Kindts I, et al. Defining Oligometastatic Disease From a Radiation Oncology Perspective: An ESTRO-ASTRO Consensus Document. *Radiother Oncol* (2020) 148:157–66. doi: 10.1016/j.radonc.2020.04.003
3. Palma DA, Salama JK, Lo SS, Senan S, Treasure T, Govindan R, et al. The Oligometastatic State—Separating Truth From Wishful Thinking. *Nat Rev Clin Oncol* (2014) 11(9):549–57. doi: 10.1038/nrclinonc.2014.96
4. Palma DA, Bauman GS, Rodrigues GB. Beyond Oligometastases. *Int J Radiat Oncol Biol Phys* (2020) 107(2):253–6. doi: 10.1016/j.ijrobp.2019.12.023
5. Arnett ALH, Mou B, Owen D, Park SS, Nelson K, Hallemeier CL, et al. Long-Term Clinical Outcomes and Safety Profile of SBRT for Centrally Located Nsclc. *Adv Radiat Oncol* (2019) 4(2):422–8. doi: 10.1016/j.adro.2019.01.002
6. Baumann BC, Wei J, Plastaras JP, Lukens JN, Damjanov N, Hoteit M, et al. Stereotactic Body Radiation Therapy (SBRT) for Hepatocellular Carcinoma: High Rates of Local Control With Low Toxicity. *Am J Clin Oncol* (2018) 41(11):1118–24. doi: 10.1097/COC.0000000000000435
7. Tsang MWK. Stereotactic Body Radiotherapy: Current Strategies and Future Development. *J Thoracic Dis* (2016) 8(Suppl 6):S517–27. doi: 10.21037/jtd.2016.03.14
8. Palma DA, Olson R, Harrow S, Gaede S, Louie AV, Haasbeek C, et al. Stereotactic Ablative Radiotherapy for the Comprehensive Treatment of Oligometastatic Cancers: Long-Term Results of the SABR-COMET Phase II Randomized Trial. *J Clin Oncol* (2020) JCO2000818. doi: 10.1101/2020.03.26.20044305
9. Sanders GD, Neumann PJ, Basu A, Brock DW, Feeny D, Krahn M, et al. Recommendations for Conduct, Methodological Practices, and Reporting of Cost-effectiveness Analyses: Second Panel on Cost-Effectiveness in Health and Medicine. *JAMA* (2016) 316(10):1093–103. doi: 10.1001/jama.2016.12195
10. *Seer*Explorer: An Interactive Website for SEER Cancer Statistics*. Surveillance Research Program, National Cancer Institute. Available at: https://seer.cancer.gov/explorer/.
11. Reyes C, Engel-Nitz NM, DaCosta Byfield S, Ravelo A, Ogale S, Bancroft T, et al. Cost of Disease Progression in Patients With Metastatic Breast, Lung, and Colorectal Cancer. (1549-490X (Electronic)). doi: 10.1634/theoncologist.2018-0018
12. Hess G, Barlev A, Chung K, Hill JW, Fonseca E. Cost of Palliative Radiation to the Bone for Patients With Bone Metastases Secondary to Breast or Prostate Cancer. *Radiat Oncol* (2012) 7(1):168. doi: 10.1186/1748-717X-7-168
13. Kim H, Rajagopalan MS, Beriwal S, Huq MS, Smith KJ. Cost-Effectiveness Analysis of Single Fraction of Stereotactic Body Radiation Therapy Compared With Single Fraction of External Beam Radiation Therapy for Palliation of Vertebral Bone Metastases. *Int J Radiat Oncol Biol Phys* (2015) 91(3):556–63. doi: 10.1016/j.ijrobp.2014.10.055
14. Lanni TB Jr., Grills IS, Kestin LL, Robertson JM. Stereotactic Radiotherapy Reduces Treatment Cost While Improving Overall Survival and Local Control Over Standard Fractionated Radiation Therapy for Medically Inoperable Non-Small-Cell Lung Cancer. *Am J Clin Oncol* (2011) 34(5):494–8. doi: 10.1097/COC.0b013e3181ec63ae
15. Shah A, Hahn SM, Stetson RL, Friedberg JS, Pechet TTV, Sher DJ. Cost-Effectiveness of Stereotactic Body Radiation Therapy Versus Surgical Resection for Stage I Non–Small Cell Lung Cancer. *Cancer* (2013) 119(17):3123–32. doi: 10.1002/cncr.28131
16. Kim H, Gill B, Beriwal S, Huq MS, Roberts MS, Smith KJ. Cost-Effectiveness Analysis of Stereotactic Body Radiation Therapy Compared With Radiofrequency Ablation for Inoperable Colorectal Liver Metastases. *Int J Radiat Oncol Biol Phys* (2016) 95(4):1175–83. doi: 10.1016/j.ijrobp.2016.02.045
17. Agarwal A, Dayal A, Kircher SM, Chen RC, Royce TJ. Analysis of Price Transparency Via National Cancer Institute–Designated Cancer Centers' Chargemasters for Prostate Cancer Radiation Therapy. *JAMA Oncol* (2020) 6(3):409–12. doi: 10.1001/jamaoncol.2019.5690
18. Bekelman JE, Halpern SD, Blankart CR, Bynum JP, Cohen J, Fowler R, et al. Comparison of Site of Death, Health Care Utilization, and Hospital Expenditures for Patients Dying With Cancer in 7 Developed Countries. *Jama* (2016) 315(3):272–83. doi: 10.1001/jama.2015.18603
19. Wong W, Yim YM, Kim A, Cloutier M, Gauthier-Loiselle M, Gagnon-Sanschagrin P, et al. Assessment of Costs Associated With Adverse Events in Patients With Cancer. *PloS One* (2018) 13(4):e0196007. doi: 10.1371/journal.pone.0196007
20. Copley-Merriman C, Stevinson K, Liu FX, Wang J, Mauskopf J, Zimovetz EA, et al. Direct Costs Associated With Adverse Events of Systemic Therapies for Advanced Melanoma: Systematic Literature Review. *Med (Baltimore)* (2018) 97(31):e11736. doi: 10.1097/MD.0000000000011736

21. Ting J, Tien Ho P, Xiang P, Sugay A, Abdel-Sattar M, Wilson L. Cost-Effectiveness and Value of Information of Erlotinib, Afatinib, and Cisplatin-Pemetrexed for First-Line Treatment of Advanced Egfr Mutation-Positive non-Small-Cell Lung Cancer in the United States. *Value Health* (2015) 18 (6):774–82. doi: 10.1016/j.jval.2015.04.008
22. Hagiwara Y, Shiroiwa T, Shimozuma K, Kawahara T, Uemura Y, Watanabe T, et al. Impact of Adverse Events on Health Utility and Health-Related Quality of Life in Patients Receiving First-Line Chemotherapy for Metastatic Breast Cancer: Results From the SELECT BC Study. *Pharmacoeconomics* (2018) 36 (2):215–23. doi: 10.1007/s40273-017-0580-7
23. Chouaid C, Agulnik J, Goker E, Herder GJ, Lester JF, Vansteenkiste J, et al. Health-Related Quality of Life and Utility in Patients With Advanced non-Small-Cell Lung Cancer: A Prospective Cross-Sectional Patient Survey in a Real-World Setting. *J Thorac Oncol* (2013) 8(8):997–1003. doi: 10.1097/JTO.0b013e318299243b
24. Nafees B, Stafford M, Gavriel S, Bhalla S, Watkins J. Health State Utilities for non Small Cell Lung Cancer. *Health Qual Life Outcomes* (2008) 6:84. doi: 10.1186/1477-7525-6-84
25. Lachaine J, Mathurin K, Barakat S, Couban S. Economic Evaluation of Arsenic Trioxide Compared to All-Trans Retinoic Acid + Conventional Chemotherapy for Treatment of Relapsed Acute Promyelocytic Leukemia in Canada. *Eur J Haematol* (2015) 95(3):218–29. doi: 10.1111/ejh.12475
26. Paracha N, Abdulla A, MacGilchrist KS. Systematic Review of Health State Utility Values in Metastatic Non-Small Cell Lung Cancer With a Focus on Previously Treated Patients. *Health Qual Life Outcomes* (2018) 16(1):179. doi: 10.1186/s12955-018-0994-8
27. Teckle P, McTaggart-Cowan H, Van der Hoek K, Chia S, Melosky B, Gelmon K, et al. Mapping the FACT-G Cancer-Specific Quality of Life Instrument to the EQ-5D and SF-6D. (1477-7525 (Electronic)). doi: 10.12968/ijpn.1997.3.5.275
28. Lloyd AJ, Kerr C, Penton J, Knerer G. Health-Related Quality of Life and Health Utilities in Metastatic Castrate-Resistant Prostate Cancer: A Survey Capturing Experiences From a Diverse Sample of UK Patients. *Value Health* (2015) 18(8):1152–7. doi: 10.1016/j.jval.2015.08.012
29. Lee JY, Ock M, Jo MW, Son WS, Lee HJ, Kim SH, et al. Estimating Utility Weights and Quality-Adjusted Life Year Loss for Colorectal Cancer-Related Health States in Korea. *Sci Rep* (2017) 7(1):5571. doi: 10.1038/s41598-017-06004-6
30. Farkkila N, Sintonen H, Saarto T, Jarvinen H, Hanninen J, Taari K, et al. Health-Related Quality of Life in Colorectal Cancer. *Colorectal Dis* (2013) 15 (5):e215–22. doi: 10.1111/codi.12143
31. Petrou S, Campbell N. Stabilisation in Colorectal Cancer. *Int J Palliat Nurs* (1997) 3(5):275–80. doi: 10.12968/ijpn.1997.3.5.275
32. Hudgens S T-SG, De Courcy J, Kontoudis I, Tremblay G, Forsythe A, Lloyd A. Real-World Evidence on Health States Utilities in in Metastatic Breast Cancer Patients: Data From a Retrospective Patient Record Form Study and A Cross-Sectional Patient Survey. *Value Health* (2016) 19(3):A157. doi: 10.1016/j.jval.2016.03.1466
33. Paracha N, Thuresson PO, Moreno SG, MacGilchrist KS. Health State Utility Values in Locally Advanced and Metastatic Breast Cancer by Treatment Line: A Systematic Review. *Expert Rev Pharmacoecon Outcomes Res* (2016) 16 (5):549–59. doi: 10.1080/14737167.2016.1222907
34. Lloyd A, Nafees B, Narewska J, Dewilde S, Watkins J. Health State Utilities for Metastatic Breast Cancer. *Br J Cancer* (2006) 95(6):683–90. doi: 10.1038/sj.bjc.6603326
35. Cameron D, Ubels J, Norström F. On What Basis are Medical Cost-Effectiveness Thresholds Set? Clashing Opinions and an Absence of Data: A Systematic Review. *Global Health Action* (2018) 11(1):1447828–1447828. doi: 10.1080/16549716.2018.1447828
36. Sheppard CW. Computer Simulation of Stochastic Processes Through Model-Sampling (Monte Carlo) Techniques. *FEBS Lett* (1969) 2 Suppl 1:S14–s21. doi: 10.1016/0014-5793(69)80071-2
37. Lester-Coll NH, Decker RH, Yu JB. Cost-Effectiveness Analysis of Stereotactic Body Radiation Therapy for Pulmonary Oligometastases. *Int J Radiat Oncol Biology Phys* (2014) 90(1):S585–6. doi: 10.1016/j.ijrobp.2014.05.1761
38. Parikh NR, Nickols NG, Rettig M, King CR, Raldow AC, Steinberg ML, et al. Cost-Effectiveness of Metastasis-Directed Therapy in the Setting of Oligometastatic Hormone-Sensitive Prostate Cancer. *J Clin Oncol* (2019) 37 (7_suppl):147–7. doi: 10.1200/JCO.2019.37.7_suppl.147
39. Kumar A, Straka C, Courtney PT, Vitzthum L, Riviere P, Murphy JD. Cost-Effectiveness Analysis of Stereotactic Ablative Radiation Therapy in Patients With Oligometastatic Cancer. *Int J Radiat Oncol Biol Phys* (2020). doi: 10.1016/j.ijrobp.2020.09.045
40. Qu XM, Chen Y, Zaric GS, Senan S, Olson RA, Harrow S, et al. Is SABR Cost-Effective in Oligometastatic Cancer? An Economic Analysis of the SABR-COMET Randomized Trial. *Int J Radiat Oncol Biol Phys* (2020). doi: 10.1016/j.ijrobp.2020.12.001
41. Olson R, Mathews L, Liu M, Schellenberg D, Mou B, Berrang T, et al. Stereotactic Ablative Radiotherapy for the Comprehensive Treatment of 1-3 Oligometastatic Tumors (SABR-COMET-3): Study Protocol for a Randomized Phase III Trial. *BMC Cancer* (2020) 20(1):380. doi: 10.1186/s12885-020-06876-4
42. Palma DA, Olson R, Harrow S, Correa RJM, Schneiders F, Haasbeek CJA, et al. Stereotactic Ablative Radiotherapy for the Comprehensive Treatment of 4-10 Oligometastatic Tumors (SABR-COMET-10): Study Protocol for a Randomized Phase III Trial. *BMC Cancer* (2019) 19(1):816. doi: 10.1186/s12885-019-5977-6
43. Conibear J, Chia B, Ngai Y, Bates AT, Counsell N, Patel R, et al. Study Protocol for the SARON Trial: A Multicentre, Randomised Controlled Phase III Trial Comparing the Addition of Stereotactic Ablative Radiotherapy and Radical Radiotherapy With Standard Chemotherapy Alone for Oligometastatic Non-Small Cell Lung Cancer. *BMJ Open* (2018) 8(4):e020690. doi: 10.1136/bmjopen-2017-020690
44. Chmura SJ WK, Al-Hallaq HA, Borges VF, Jaskowiak NT, Matuszak M, Milano MT, et al. NRG-BR002: A Phase IIR/III Trial of Standard of Care Therapy With or Without Stereotactic Body Radiotherapy (SBRT) and/or Surgical Ablation for Newly Oligometastatic Breast Cancer (NCT02364557). *J Clin Oncol* (2019) 35(TPS1117-TPS1117). doi: 10.1200/JCO.2019.37.15_suppl.TPS1117
45. McDonald F GM, Popat S, Andratschke N, Kilburn L, Toms C, Bliss J. HALT: Targeted Therapy Beyond Progression With or Without Dose-Intensified Radiotherapy in Oligoprogressive Disease in Oncogene Addicted Lung Tumours. . *Lung Cancer* (2017) 103:57. doi: 10.1016/S0169-5002(17)30175-7
46. Wartman LD. The Future of Cancer Treatment Using Precision Oncogenomics. *Cold Spring Harbor Mol Case Stud* (2018) 4(2):a002824. doi: 10.1101/mcs.a002824
47. Falzone L, Salomone S, Libra M. Evolution of Cancer Pharmacological Treatments at the Turn of the Third Millennium. *Front Pharmacol* (2018) 9:1300. doi: 10.3389/fphar.2018.01300

Conflict of Interest: The authors declare that the research was conducted in the absence of any commercial or financial relationships that could be construed as a potential conflict of interest.

frontiers in Oncology

ORIGINAL RESEARCH
published: 16 July 2021
doi: 10.3389/fonc.2021.640461

Efficacy and Prognostic Factors of Trans-Arterial Chemoembolization Combined With Stereotactic Body Radiation Therapy for BCLC Stage B Hepatocellular Carcinoma

Changchen Jiang, Shenghua Jing, Han Zhou, Aomei Li, Xiangnan Qiu, Xixu Zhu and Zetian Shen *

Department of Radiation Oncology, Jinling Hospital, Medical School of Nanjing University, Nanjing, China

OPEN ACCESS

Edited by:
Alexander Muacevic, Ludwig Maximilian University of Munich, Germany

Reviewed by:
Khaled Elsayad, University of Münster, Germany
Raquel Bar-Deroma, Rambam Health Care Campus, Israel

***Correspondence:**
Zetian Shen
zetian_shen66@163.com

Specialty section:
This article was submitted to Radiation Oncology, a section of the journal Frontiers in Oncology

Received: *11 December 2020*
Accepted: *01 July 2021*
Published: *16 July 2021*

Citation:
Jiang C, Jing S, Zhou H, Li A, Qiu X, Zhu X and Shen Z (2021) Efficacy and Prognostic Factors of Trans-Arterial Chemoembolization Combined With Stereotactic Body Radiation Therapy for BCLC Stage B Hepatocellular Carcinoma. Front. Oncol. 11:640461. doi: 10.3389/fonc.2021.640461

Purpose: This study aimed to evaluate the efficacy and safety of trans-arterial chemoembolization (TACE) followed by stereotactic body radiation therapy (SBRT) in treating Barcelona Clinic Liver Cancer (BCLC) stage B hepatocellular carcinoma (HCC) not amenable to resection and radiofrequency ablation (RFA).

Methods: From February 2012 to January 2017, a total of 57 BCLC stage B HCC patients who were unsuitable candidates for resection and RFA treated with TACE combined with CyberKnife SBRT were included in this retrospective study. Patients underwent TACE for a median of two times (1–5 times) before SBRT. SBRT prescription doses ranged from 30 Gy to 50 Gy in 3–5 fractions.

Results: The median follow-up time was 42 months. The objective response rate (CR + PR) was 85.9%, and the disease control rate (CR + PR + SD) was 96.5%. The local control (LC) rates were 91.1% and 84.3% at 1 and 2 years, respectively. The 1-, 2-, 3-year overall survival (OS) and the median survival time were 73.2%, 51.4%, 32.4% and 26.6 months, respectively. The 1-, 2-, and 3-year progression-free survival (PFS) were 34.2%, 21.6%, and 9%, respectively, with a median PFS time of 9.7 months. A subgroup analysis was conducted in 32 patients with AFP ≥ 200 ng/ml before TACE. OS was significantly prolonged in those with AFP that decreased by more than 75% than those with AFP that decreased by less than 75% (P = 0.018) after SBRT. The treatment was well tolerated with only one patient (1.8%) developed grade 3 gastrointestinal toxicity, and another patient developed non-classical RILD. In multivariate analysis, tumor length ≥ 10 cm and AFP ≥ 200 ng/ml were independent poor prognostic factors for OS.

Conclusion: The combination of TACE and Cyberknife SBRT showed optimal efficacy with acceptable toxicity for BCLC stage B HCC.

Keywords: hepatocellular carcinoma, trans-arterial chemoembolization, CyberKnife, stereotactic body radiation therapy, BCLC B

INTRODUCTION

Primary liver cancer is the sixth most commonly diagnosed cancer, and its mortality rate ranks fourth around the world. According to the estimates of GLOBOCAN 2018 statistics produced by the International Agency for Research on Cancer of the World Health Organization, there are about 841,000 new cases and 782,000 deaths due to liver cancer annually. The ratio of death to new cases is as high as 0.9 (1). China is the worst-hit area of primary liver cancer with a 5-year survival rate of around 10% (2). Liver resection and transplantation are the main radical treatments and associated with superior clinical outcome, but liver cancer is difficult to diagnose early and progresses rapidly. Only 15% of patients could receive surgical treatment when diagnosed. For patients with Barcelona Clinic Liver Cancer (BCLC) stage B hepatocellular carcinoma (HCC), trans-arterial chemoembolization (TACE) is the recommended therapy. However, the tumor response rate after TACE and local control (LC) rate for those with tumors larger than 5 cm, multiple intrahepatic lesions, cirrhosis, or portal vein tumor thrombus (PVTT) are still not satisfactory (3, 4). All these data highlight the unmet need of optimizing the loco-regional therapy effect in the management of HCC.

The National Comprehensive Cancer Network (NCCN) guidelines recommended that TACE combined with radiotherapy could improve the LC rate and prolong the survival time of patients with unresectable HCC, which was more effective than TACE and sorafenib (5, 6). However, the role of conventional radiotherapy in HCC has long been overlooked because of the low tolerance of the whole liver to radiation. Delivering high tumoricidal dose without causing radiation-induced liver disease (RILD) and affecting adjacent stomach, duodenum, and other endangered organs is difficult (7). In recent years, with the improvements of radiotherapy technology, SBRT, a highly conformal radiation therapy with high geometric precision and accuracy, can deliver a potent dose to target lesions while reducing the dose to adjacent normal tissues, providing a new therapeutic option for inoperable HCC patients. TACE combined with SBRT might have synergistic effects in the treatment of patients with inoperable HCC (8–11). Theoretically, TACE is well controlled in the tumor center but poorly controlled in the oxygen-rich area around the tumor, whereas SBRT is poorly controlled in the hypoxic area in the large tumor center but has a good curative effect in the oxygen-rich area around the tumor. The combination of the two treatment strategies can compensate for each other's deficiencies and give full play to their advantages. Thus, in this study, we retrospectively analyzed the clinical outcome of combined CyberKnife SBRT and TACE in the treatment of BCLC stage B HCC. The results are reported as follows.

MATERIALS AND METHODS

Clinical Data

From February 2012 to January 2017, a total of 57 patients with BCLC stage B primary liver cancer who received TACE combined with CyberKnife SBRT treatment in Nanjing Jinling Hospital were included in this retrospective study. Inclusion criteria: 1. Patients were diagnosed as HCC by biopsy, and the imaging manifestations were nodular or lumpy; 2. BCLC stage B, Child–Pugh score A–B7 and ECOG 0–1; 3. Unsuitable for resection, liver transplantation, or local ablation therapies according to the comprehensive assessment of hepatobiliary surgery experts, oncologists, interventional experts, and radiologists; 4. Remaining healthy liver > 700 ml. Exclusion criteria: 1. Portal vein thrombus, lymph node involvement, and extrahepatic metastasis; 2. ECOG ≥ 2; 3. Poor liver function with Child–Pugh score of C; 4. Diffuse liver cancer or nonmeasurable lesion, tumor number ≥ 4; 5. Other life-threatening conditions, such as cardiac ischemia or cerebrovascular accident within the last 6 months.

From February 2012 to January 2017, a total of 57 patients received the combined TACE and CyberKnife SBRT treatment as presented above. In our study, 44 (77.2%) patients were hepatitis B carriers. All patients had BCLC stage B disease. The median tumor size was 8.4 cm (range, 4.5–16.3 cm). None of the patients had previously received any other treatment, and no patient dropped out after TACE. The median number of TACE is 2 (range, 1–5). The CyberKnife SBRT prescription doses ranged from 30 Gy to 50 Gy in 3–5 fractions. The median BED10 was 100 Gy (range, 48–124 Gy). The median interval between TACE and SBRT was 37 days (23–69 days). Baseline patient and tumor characteristics are displayed in **Table 1**.

Treatment

TACE: Percutaneous puncture of the femoral artery with Seldinger technique was performed. The catheter was inserted into the hepatic artery or celiac axis under the guidance of DSA. Contrast agent was injected into the catheter to determine the location, size, number, and supply artery of the tumor. After the target lesion is determined, a catheter will be inserted to the feeding artery branch. A mixture of 5–20 ml of lipiodol and chemotherapy agents such as 30–40 mg/m^2 cisplatinum, 20–40 mg THP, or 500–1500 mg fluorouracil glycosides was slowly injected through the catheter to the tumor site. The amount of the mixture emulsion should depend on the tumor size and arterial blood flow. Thereafter, gelatin sponge particle gelfoam embolization was conducted. Liver enhanced MRI and CT scans were performed 3 to 4 weeks after TACE to evaluate the lesion and short-term efficacy. TACE was repeated 1 to 5 times at intervals of 4 to 6 weeks. The median interval between the last cycle of TACE and CyberKnife SBRT was 37 days (23–69 days).

CyberKnife SBRT: All patients were implanted with 3–6 gold fiducials (size of 6.0 mm × 0.8 mm) within or around the tumor using a CT-guided 19 G needle. A CT plain and enhanced scan was performed about 7 days after the implantation. At this time, edema and local hemorrhage subsided, and the gold fiducials were relatively stable and immobile.

Patients were placed in a supine position and used a vacuum pad to fix the body. CT scanning was conducted, and the slice thickness was 1 mm. Hepatic scans ranged 15 cm above and below the lesions. The gross target volume (GTV) was defined as visible liver tumors at the arterial phase or at the delayed portal

TABLE 1 | Baseline patient and tumor characteristics of the 57 patients.

Item	Cases	Percentage(%) or median
Age		
<65	29	50.9
≥65	28	49.1
Gender		
Male	46	80.7
Female	11	19.3
HBVs Ag		
positive	44	77.2
negative	13	22.8
Pre-TACE AFP (ng/ml)		
<200	25	43.9
≥200	32	56.1
AST(U/L)		
≤40	19	33.3
>40	38	66.7
Total bilirubin (mg/dl)		
≥2	9	84.2
<2	48	15.8
Size of largest lesion		
≥10cm	17	8.4 (4.5-16.3)cm
<10cm	40	
Number of lesions		
1	37	64.9
2-3	20	35.1
Child-Pugh score		
A	47	82.5
B	10	17.5
BED10, Gy		
≥100	30	100 (48-124)
<100	27	
Dose/Fraction		
45-48Gy/3F	14	24.6
40-48Gy/4F	7	12.3
30-50Gy/5F	36	63.2
Number of TACE		
1-2	36	2 (1-5)
>2	21	

phase on the CT or MRI scan. The planning target volume (PTV) was defined as GTV plus a margin of 3 to 5 mm. After expansion, the area of the PTV should be adjusted according to the adjacent critical organs at risk. According to the tumor size, location, and critical organ constrains, patients were treated with prescription dose ranging from 30 Gy to 50 Gy for 3–5 times. Respiratory synchronization and gold standard tracking technology were adopted during the treatment. The prescribed isodose line should encompass >95% of PTV. Dose constraints for critical structures are shown in **Table 2**.

Follow-Up and Evaluation

Enhanced upper abdominal CT and MRI were conducted 1 month after the completion of CyberKnife treatment, every 3 months in the first 2 years, and then every 6 months thereafter. According to the Modified Response Evaluation Criteria in Solid Tumors (12), the assessment results were divided into complete response (CR), partial response (PR), progressive disease (PD), and stable disease (SD). LC was defined as no progression within the PTV (patients undergoing liver transplantation or resection after the combined treatment were censored). Progression-free survival (PFS) was defined as the period from the beginning of TACE to the radiological progression of any lesion, appearance of new lesions, or the time at which the patient passed away, whichever occurred first. Overall survival (OS) was defined from the date of starting TACE until death or the final follow-up. Toxicity assessment was based on the National Cancer Institute Common Terminology Criteria for Adverse Events version 4.0. Liver-specific toxicity consists of classic and non-classic RILD. Classic RILD was defined as an increase in alkaline phosphatase exceeding two times the upper limit of normal, and non-classic RILD was defined as an increase in transaminase over five times the upper limit of normal, under the circumstances of lack of disease progression or malignant ascites (13).

Statistical Analysis

SPSS 22.0 statistical software was used for data analysis. LC, PFS, and OS were calculated using the Kaplan–Meier method. Univariate analyses were used to investigate the relationship between all independent variables and OS. Any factors that were significant in univariate analyses were incorporated into multivariate analyses using the Cox proportional hazards model. $P < 0.05$ was considered statistically significant.

RESULTS

LC

After CyberKnife SBRT, liver MRI and/or abdominal CT was evaluated in all patients. CR occurred in 11 patients (19.3%), 38 (66.6%) patients achieved PR, 6 (10.5%) patients showed SD, and 2 (3.5%) cases developed PD. The objective response rate (ORR = CR + PR) was 85.9%. The disease control rate (DCR = CR + PR + SD) was 96.5%. The 1- and 2-year LC rates were 91.1% and 84.3%, respectively (**Figure 1**).

TABLE 2 | Dose constraints for critical organs.

Critical organs	Dose constraints (treatment in 3–5 fractions)					
	45-48Gy/3F		40-48Gy/4F		30-50Gy/5F	
	Volume	Dose	Volume	Dose	Volume	Dose
Remaining healthy liver	≥700cc	≤5.7Gy/fx	≥700cc	≤4.8Gy/fx	≥700cc	≤4.2Gy/fx
Stomach	Any point	7.4Gy/fx	Any point	6.8Gy/fx	Any point	6.4Gy/fx
Duodenum	Any point	7.4Gy/fx	Any point	6.8Gy/fx	Any point	6.4Gy/fx
Renal cortex	≥200cc	≤4.8Gy/fx	≥200cc	≤4Gy/fx	≥200cc	≤3.5Gy/fx
Spinal cord	Any point	7.3Gy/fx	Any point	6.5Gy/fx	Any point	6Gy/fx

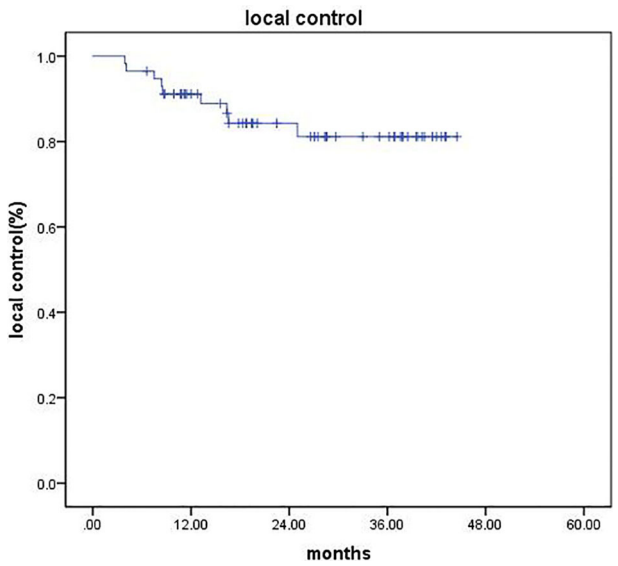

FIGURE 1 | Kaplan–Meier analysis of LC.

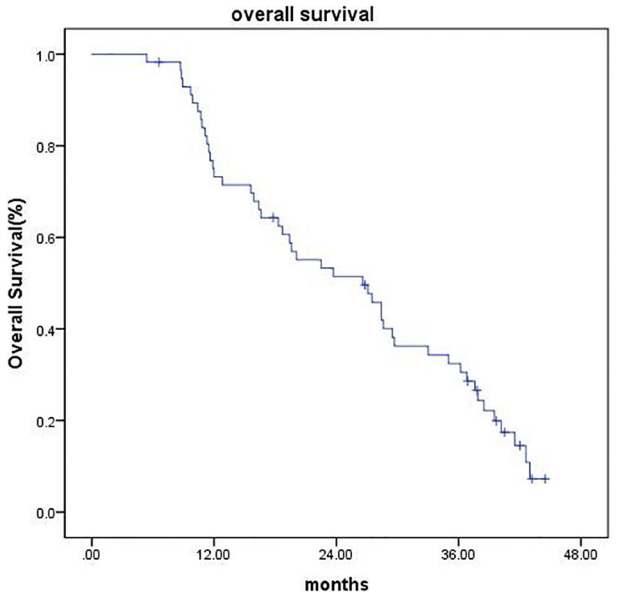

FIGURE 2 | Kaplan–Meier estimates of OS.

PFS and OS

As of the last follow-up date (February 25, 2020), the median follow-up time was 42 months (range, 6.6–44.5 months). Four patients (7.0%) were lost to follow-up at the time of analysis, 1 patient (1.7%) underwent surgical resection, and 1 patient (1.7%) underwent liver transplantation, all of which were recorded as censored. The median OS was 26.6 months (95% CI 18.27–34.92), and the 1-, 2-, and 3-year OS were 73.2%, 51.4%, and 32.4%, respectively (**Figure 2**). The median PFS was 9.7 months (95% CI 7.42–11.97), and the PFS was 34.2%, 21.6%, and 9% at 1, 2, and 3 years, respectively (**Figure 3**).

Prognostic Factors for OS

The univariate analysis of OS identified five poor prognostic factors, including tumor diameter ≥ 10 cm, multiple nodules, AFP ≥ 200 ng/ml, BED10 < 100 Gy, and TACE times > 2. The significant factors of univariate analysis were enrolled in the multivariate analysis using the Cox proportional hazards regression model. The results showed that tumor diameter ≥ 10 cm and pretreatment AFP ≥ 200 ng/ml were associated with poorer OS (**Table 3**).

Subgroup Analysis of AFP Determined OS

A subgroup analysis was performed on 32 patients with pretreatment AFP ≥ 200 ng/ml. Within 3 months after CyberKnife SBRT, the AFP of 18 patients (56.3%) decreased by more than 75%, and their OS was significantly longer than those whose AFP decreased by less than 75% (P = 0.018) (**Figure 4**).

Side Effects

Patients mainly experienced grade 1 or 2 fatigue; nausea; vomiting; and hematological toxicity such as anemia, leukopenia, thrombocytopenia, hyperbilirubinemia, and AST elevation. Grade

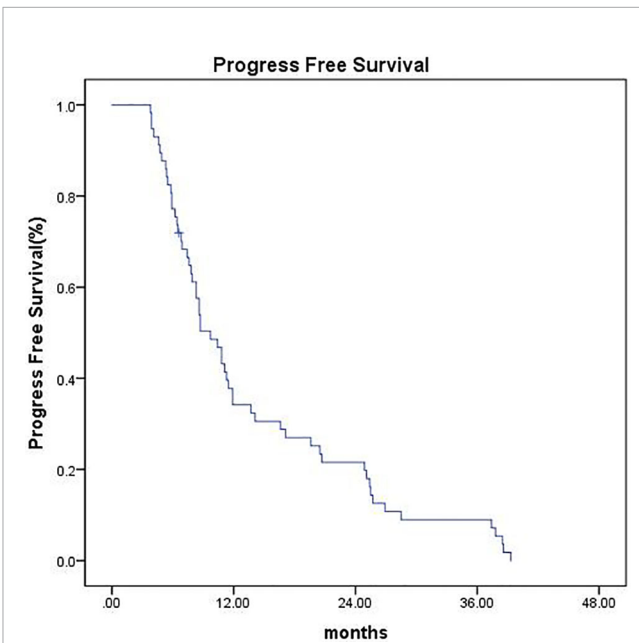

FIGURE 3 | Kaplan–Meier estimates of PFS.

3 or above adverse events included anemia (3.5%), leukopenia (5.3%), thrombocytopenia (7.1%), AST elevation (5.3%), and hyperbilirubinemia (7%). Three months after the treatment, no patient developed classic RILD, but one patient presented non-classic RILD. One patient developed gastric ulcer 5 months after treatment (**Table 4**). The adverse effects gradually improved after symptomatic treatment. No patients had gastrointestinal perforation, and no treatment-related deaths were found. Before

TABLE 3 | Univariate and multivariate analyses of prognostic factors for OS.

	Univariate HR (95%CI)	P value	Multivariate HR (95%CI)	P value
Gender (male *vs.* female)	0.930 (0.65-1.32)	0.687	—	—
Age (≥65 *vs.* <65)	1.204 (0.67-2.14)	0.529	—	—
HB *vs.* Ag (positive *vs.* negative)	0.883 (0.44-1.74)	0.720	—	—
AFP (≥200 *vs.* <20ng/ml)	0.351 (0.18-0.65)	0.001	0.294 (0.15-0.55)	0.000
AST(>40 *vs.* ≤40U/L)	0.913 (0.66-1.25)	0.573	—	—
Total Bilirubin (≥2 *vs.* <2mg/dl)	1.016 (0.67-1.52)	0.938	—	—
Tumor size (≥10 *vs.* <10cm)	0.477 (0.34-0.66)	0.000	0.430 (0.30-0.61)	0.000
Tumor number(single *vs.* Multiple)	0.670 (0.49-0.90)	0.009	—	—
Child-Pugh score (A *vs.* B)	0.736 (0.50-1.06)	0.104	—	—
TACE(1-2 *vs.* >2)	0.697 (0.51-0.93)	0.016	—	—
BED10 (≥100 *vs.* <100Gy)	1.619 (1.19-2.20)	0.002	—	—

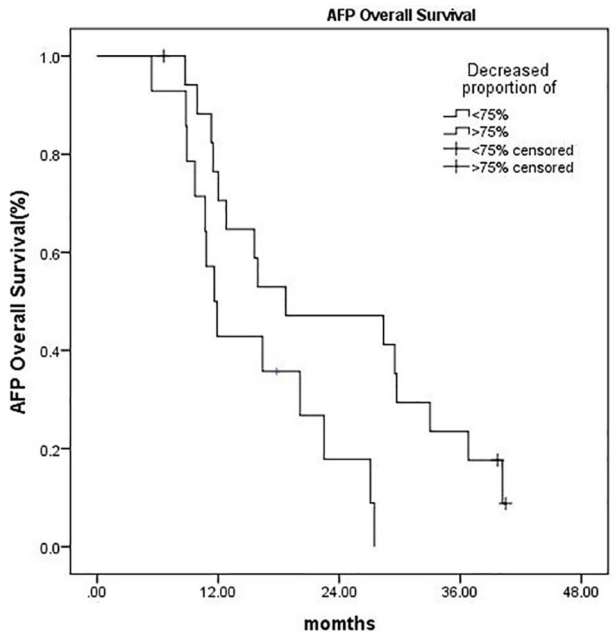

FIGURE 4 | Kaplan–Meier OS curves:AFP decreased more than 75% *vs.* AFP decreased by less than 75% (P = 0.018).

TACE treatment, 82.5% of patients had a Child–Pugh score of A, and 17.5% of patients had a Child–Pugh score of B. However, after 1 month of CyberKnife treatment, 47.4% of patients had a Child–Pugh score of A, and 45.6% of patients had a Child–Pugh score of B.

DISCUSSION

The current guidelines formulated by the NCCN and American Association for the Study of Liver Diseases recommend TACE as the preferred treatment for inoperable HCC. According to the treatment algorithm of the BCLC, TACE is considered as the first-line treatment for intermediate-stage HCC patients who are not suitable for surgical resection or tumor ablation. However, TACE alone demonstrated a dismal CR rate of only 0%–4.8%, and patients cannot achieve satisfactory long-term survival, the 5-year cumulative survival rate of which is only 1%–8% (14). When the tumor size is 5–7 and ≥8 cm, the 2-year OS is only 42% and 0%, respectively (15). Hence, TACE alone might not be sufficient for managing large tumors. Y. Kawamura (16) found that TACE alone can only eradicate 22%–50% of tumor tissues as determined by pathological examination and can minimally eradicate the tumor completely. Thus, TACE was considered as a palliative treatment. To improve the tumor response rate and prolong survival, a large number of studies currently considered the concept of combining TACE with another local therapy, including RFA (17), percutaneous ethanol injection (PEI) (18), and radiotherapy. However, some lesions are unsuitable for RFA and PEI. For example, when the tumor is adjacent to the liver capsule, ablation treatment may lead to rupture of the liver capsule and thus may cause tumor dissemination. Moreover, patients whose tumors are located close to important large blood vessels, bile duct, or gallbladder or deep inside the liver including PVTT are not candidates for percutaneous puncture ablation.

A meta-analysis (5) of 25 studies involving a total of 2,577 patients with unresectable HCC showed the benefits of TACE combined with radiotherapy (mainly three-dimensional conformational radiotherapy) with CR, PR, and 1–5 year OS rates being significantly higher in the combined treatment group than in the chemoembolization alone group (P < 0.001). However, the pooled analysis indicated that the adverse events including gastrointestinal ulcers (OR, 12.80; 95% CI 1.57–104.33), ALT elevation (OR, 2.46; 95% CI 1.30–4.65), and total bilirubin (OR, 2.16; 95% CI 1.05–4.45) were also increased in the combined treatment group. CyberKnife SBRT, which features high-precision radiotherapy, makes up for the deficiency of conventional radiotherapy (19). Several reports indicated that SBRT has a high LC rate and safety in the treatment of liver tumors (8, 19–22). However, the LC rate of SBRT alone in treating increased tumor volume is not satisfactory (10, 23).

In recent years, an increasing number of studies have demonstrated that combination therapy benefits LC compared with monotherapy in the treatment of unresectable HCC (9, 24). In a retrospective study of adjuvant SBRT following TACE in patients who were unsuitable for surgical resection with tumors ≥ 3 cm, Jacob et al. (9) reported that the local recurrence rate was significantly lower in the TACE plus SBRT group compared with the TACE alone group (P = 0.04). Baek Gyu Jun (24) conducted a propensity score matching analysis on HCC patients with tumor

TABLE 4 | Side effects after SBRT.

	Grade1-2, n (%)	Grade 3, n (%)	Grade 4, n (%)	Grade 5, n (%)
Fatigue	19 (33.3)	0 (0)	0 (0)	0 (0)
Nausea	13 (22.8)	0 (0)	0 (0)	0 (0)
Vomiting	8 (14.0)	0 (0)	0 (0)	0 (0)
Gastric ulcer	0 (0)	1 (1.8)	0 (0)	0 (0)
Anemia	10 (17.5)	2 (3.5)	0 (0)	0 (0)
Leukopenia	18 (31.6)	2 (3.5)	1 (1.8)	0 (0)
Thrombocytopenia	26 (45.6)	3 (5.3)	1 (1.8)	0 (0)
Elevation of AST	17 (29.8)	3 (5.3)	0 (0)	0 (0)
Hyperbilirubinemia	11 (19.3)	4 (7)	0 (0)	0 (0)
Non-classic RILD	0 (0)	1 (1.8)	0 (0)	0 (0)

size ≤ 5 cm and found that the TACE+SBRT group showed significantly higher 1- and 3-year LC rates (91.1% and 89.9%, respectively) than the TACE alone group (69.9% and 44.8%, respectively; $P < 0.001$). A phase 2 trial of SBRT as a local salvage treatment after incomplete TACE in patients with HCC < 10 cm was conducted. The results demonstrated that TACE+SBRT treatment achieved promising tumor response rate and LC rate (8). A total of 57 patients with BCLC stage B HCC were enrolled in our study with a median tumor size of 8.4 (range, 4.5–16.3) cm. After the treatment, CR occurred in 11 patients (19.3%). ORR occurred in 49 patients (85.9%), which was superior to 17%–62% in previous studies of TACE alone (25). LC rates at 1 and 2 years were 91.1% and 84.3%, which were comparable to those achieved in previous studies (26, 27).

Clinical data have shown that TACE combined with SBRT in the treatment of unresectable HCC has better long-term survival than TACE or SBRT alone (10, 28). Tiffany CL (28) conducted a propensity score matching analysis including 49 cases of TACE and SBRT combined therapy and 98 cases of TACE alone. The results showed that the median PFS and OS of the combined treatment group were 7.6 and 23.9 months, respectively. The PFS at 1 and 3 years was significantly improved in the combined treatment group ($P = 0.012$). Meanwhile, the 1- and 3-year OS was also significantly prolonged in the TACE plus SBRT group ($P = 0.003$). Ting-Shi Su (10) found that in unresectable HCC with tumor size ≥ 5 cm, patients who received TACE followed by SBRT achieved longer OS than those who only received SBRT monotherapy. In our study, the median OS was 26.6 months (95% CI 18.277–34.923). The 1-, 2-, and 3-year OS rates were 73.2%, 51.4%, and 32.4%, respectively. The median PFS was 9.7 months (95% CI 7.427–11.973). The PFS at 1, 2, and 3 years was 34.2%, 21.6%, and 9%, respectively. Previous studies reported that SBRT treatment for unresectable HCC has a 2-year OS of 34%–68.7% and PFS up to 33.8%–48% (8–11), which are slightly better than the results in our study. This is probably because the median tumor size in most of these studies was around 5 cm, whereas the tumor volume in our study was relatively large, with a median tumor diameter of 8.4 cm. C.L Chiang (27) retrospectively evaluated the efficacy of TACE combined with SBRT as initial therapy in BCLC stage B-C HCC. The median prescription dose in an equivalent dose of 2 Gy per fraction (EQD2, $\alpha/\beta = 10$) was 37.3 Gy, and BED10 was 44.76 Gy. The median OS was 19.8 months. Subgroup analysis found that the median OS of BCLC stage B patients was 25.7 months, and the median PFS was 9.1 months (95% CI, 7.2–19.8). The OS in our study seems more favorable than that in the above study, which may be due to the higher prescription dose in our study (100 Gy for mBED10). Higher effective biological dose might result in better LC and long-term survival rate.

Although 30%–40% of primary liver cancer is negative for AFP (29), it is still a sensitive tumor marker for the detection of HCC and a useful predictive factor due to its specificity for patient survival after locoregional or systemic treatment in HCC (30, 31). A South Korean study reported that AFP normalization within 3 months after SBRT was a prognostic surrogate for OS and PFS in patients with small HCC (32). The prognostic value of AFP normalization after SBRT is still unknown due to the lack of randomized controlled studies and several other factors. First, there is no uniform standard of the optimal decrement of the AFP level. Second, the cut-off value of pretreatment AFP that would be adequate in order to apply AFP normalization as a surrogate is still unknown. In this study, we found that pretreatment AFP level ≥ 200 ng/ml was an independent adverse prognostic factor for OS. In addition, we conducted a subgroup analysis, which indicated that within 3 months after CyberKnife SBRT, the OS was significantly increased in patients whose AFP decreased by more than 75% compared with those whose AFP decreased by less than 75%. Moreover, the difference was statistically significant ($P = 0.018$). This result was consistent with previous reports of Erhua Yao (33).

With regard to the side effects, TACE combined with CyberKnife SBRT was well tolerated, with the majority of adverse effects being grade 1 and 2. No patient exhibited classic RILD, but one patient had liver transaminase elevation without disease progression, which is defined as non-classic RILD. One patient developed gastric ulcer, whose target lesion was adjacent to the stomach. The maximum point dose reached 7 Gy*5fx, which might exceed the tolerance of the stomach. The toxic reaction could be gradually repaired after symptomatic treatment. The treatment-related adverse effects for most patients were tolerable, which may be due to the fact that 82.5% of the patients in this study had a Child–Pugh score of A. In addition, the interval between the last TACE and CyberKnife was more than 3 weeks, exceeding the time window of liver function repair, which was conducive to the recovery of liver function. Consistent with the opinion of most previous studies, TACE combined with SBRT was well tolerated

in the treatment of HCC patients with Child–Pugh score of A/B7 (8). However, Lasley (34) found that the hepatotoxicity of patients with Child–Pugh score of B was increased compared with that of patients with Child–Pugh score of A after SBRT, suggesting that the use of this treatment should be cautioned in patients with Child–Pugh score of B. The latest technology, MRI-based radiotherapy can provide real-time visualization of both the tumor and nearby organs, potentially reduce toxicity to critical structures. Superior to CT-guided radiotherapy, this technology has the potential to define tolerances to gastrointestinal and hepatobiliary structures, which might increase the number of patients eligible for high-dose ablative liver radiotherapy (35).

This study has several limitations. First, this is a retrospective cohort study from a single SBRT center, and the results might not be generalizable. Second, the number of enrolled patients is relatively small. Further randomized controlled studies are needed to address the limitations and determine the intended population, the most appropriate time for SBRT, the optimal number of TACE before SBRT, and the formulation of prescription dose and fractions in combination therapy. Recently, a randomized phase 3 trial (IMbrave150) showed that atezolizumab plus bevacizumab can prolong OS and PFS than sorafenib in patients with advanced unresectable BCLC B-C HCC (36). Immunotherapy has become the new standard of care for advanced HCC. Further studies are warranted to investigate the optimal algorithm of these therapeutic options in advanced unresectable HCC.

CONCLUSION

In conclusion, treatment with TACE plus CyberKnife SBRT was associated with optimal efficacy and acceptable toxicity in patients with unresectable BCLC B HCC.

DATA AVAILABILITY STATEMENT

The original contributions presented in the study are included in the article/supplementary material. Further inquiries can be directed to the corresponding author.

ETHICS STATEMENT

The studies involving human participants were reviewed and approved by Jinling Hospital review board. The patients/participants provided their written informed consent to participate in this study.

AUTHOR CONTRIBUTIONS

CJ: project design, data collection, assembly, analysis, manuscript writing. SJ: data collection and assembly. HZ: data collection and assembly. AL: Investigation. XQ: data collection and assembly. XZ: project design. ZS: project conception and design, data interpretation. All authors contributed to the article and approved the submitted version.

FUNDING

This work was supported by grants from: 1. The Nanjing Municipal Science and Technology Committee of Jiangsu Province, China (grant number: 201803050). 2. The Jiangsu Post-doctoral Research Funding Program, China (grant number: 2020Z305).

REFERENCES

1. Bray F, Ferlay J, Soerjomataram I, Siegel RL, Torre LA, Jemal A. Global Cancer Statistics 2018: GLOBOCAN Estimates of Incidence and Mortality Worldwide for 36 Cancers in 185 Countries. *CA: A Cancer J Clin* (2018) 68 (6):394–424. doi: 10.3322/caac.21492
2. Chen W, Zheng R, Baade PD, Zhang S, Zeng H, Bray F, et al. Cancer Statistics in China, 2015. *CA Cancer J Clin* (2016) 66(2):115–32. doi: 10.3322/caac.21338
3. Lo CM, Ngan H, Tso WK, Liu CL, Lam CM, Poon RT, et al. Randomized Controlled Trial of Transarterial Lipiodol Chemoembolization for Unresectable Hepatocellular Carcinoma. *Hepatology* (2002) 35(5):1164–71. doi: 10.1053/jhep.2002.33156
4. Llovet JM, Real MI, Montaña X, Planas R, Coll S, Aponte J, et al. Arterial Embolisation or Chemoembolisation Versus Symptomatic Treatment in Patients With Unresectable Hepatocellular Carcinoma: A Randomised Controlled Trial. *Lancet* (2002) 359(9319):1734–9. doi: 10.1016/S0140-6736(02)08649-X
5. Huo YR, Eslick GD. Transcatheter Arterial Chemoembolization Plus Radiotherapy Compared With Chemoembolization Alone for Hepatocellular Carcinoma: A Systematic Review and Meta-Analysis. *JAMA Oncol* (2015) 1(6):756–65. doi: 10.1001/jamaoncol.2015.2189
6. Yoon SM, Ryoo BY, Lee SJ, Kim JH, Shin JH, An JH, et al. Efficacy and Safety of Transarterial Chemoembolization Plus External Beam Radiotherapy *vs.* Sorafenib in Hepatocellular Carcinoma With Macroscopic Vascular Invasion: A Randomized Clinical Trial. *JAMA Oncol* (2018) 4(5):661–9. doi: 10.1001/jamaoncol.2017.5847
7. Lawrence TS RJ, Anscher MS, Jirtle RL, Ensminger WD, Fajardo LF. Hepatic Toxicity Resulting From Cancer Treatment. *Int J Radiat Oncol Biol Phys* (1995) 31(5):1237–48. doi: 10.1016/0360-3016(94)00418-K
8. Kang JK, Kim MS, Cho CK, Yang KM, Yoo HJ, Kim JH, et al. Stereotactic Body Radiation Therapy for Inoperable Hepatocellular Carcinoma as a Local Salvage Treatment After Incomplete Transarterial Chemoembolization. *Cancer* (2012) 118(21):5424–31. doi: 10.1002/cncr.27533
9. Jacob R, Turley F, Redden DT, Saddekni S, Aal AK, Keene K, et al. Adjuvant Stereotactic Body Radiotherapy Following Transarterial Chemoembolization in Patients With Non-Resectable Hepatocellular Carcinoma Tumours of ≥3 Cm. *Hpb* (2015) 17(2):140–9. doi: 10.1111/hpb.12331
10. Su T-S, Lu HZ, Cheng T, Zhou Y, Huang Y, Gao YC, et al. Long-Term Survival Analysis in Combined Transarterial Embolization and Stereotactic Body Radiation Therapy Versus Stereotactic Body Radiation Monotherapy for Unresectable Hepatocellular Carcinoma >5 Cm. *BMC Cancer* (2016) 16 (1):834. doi: 10.1186/s12885-016-2894-9
11. Takeda A, Sanuki N, Tsurugai Y, Iwabuchi S, Matsunaga K, Ebinuma H, et al. Phase 2 Study of Stereotactic Body Radiotherapy and Optional Transarterial Chemoembolization for Solitary Hepatocellular Carcinoma Not Amenable to Resection and Radiofrequency Ablation. *Cancer* (2016) 122(13):2041–9. doi: 10.1002/cncr.30008
12. Lencioni R, Llovet JM. Modified RECIST (mRECIST) Assessment for Hepatocellular Carcinoma. *Semin Liver Dis* (2010) 30(1):52–60. doi: 10.1055/s-0030-1247132

13. Pan CC, Kavanagh BD, Dawson LA, Li XA, Das SK, Miften M, et al. Radiation-Associated Liver Injury. *Int J Radiat Oncol Biol Phys* (2010) 76(3 Suppl):S94–100. doi: 10.1016/j.ijrobp.2009.06.092
14. Jansen MC, van Hillegersberg R, Chamuleau RA, van Delden OM, Gouma DJ, van Gulik TM. Outcome of Regional and Local Ablative Therapies for Hepatocellular Carcinoma: A Collective Review. *Eur J Surg Oncol* (2005) 31 (4):331–47. doi: 10.1016/j.ejso.2004.10.011
15. Shim SJ, Seong J, Han KH, Chon CY, Suh CO, Lee JT. Local Radiotherapy as a Complement to Incomplete Transcatheter Arterial Chemoembolization in Locally Advanced Hepatocellular Carcinoma. *Liver Int* (2005) 25(6):1189–96. doi: 10.1111/j.1478-3231.2005.01170.x
16. Kawamura Y, Ikeda K, Seko Y, Hosaka T, Kobayashi M, Saitoh M, et al. Heterogeneous Type 4 Enhancement of Hepatocellular Carcinoma on Dynamic CT Is Associated With Tumor Recurrence After Radiofrequency Ablation. *AJR Am J Roentgenol* (2011) 197(4):W665–73. doi: 10.2214/AJR.11.6843
17. Zhen-Wei Peng M, Yao-Jun Zhang M, Hui-Hong Liang M, Xiao-Jun Lin M, Rong-Ping Guo M, Chen, PhD MM-S. Recurrent Hepatocellular Carcinoma Treated With Sequential Transcatheter Arterial Chemoembolization and RF Ablation Versus RF Ablation Alone: A Prospective Randomized Trial. *Radiology* (2012) 262:689–700. doi: 10.1148/radiol.11110637
18. Wang W, Shi J, Xie WF. Transarterial Chemoembolization in Combination With Percutaneous Ablation Therapy in Unresectable Hepatocellular Carcinoma: A Meta-Analysis. *Liver Int* (2010) 30(5):741–9. doi: 10.1111/j.1478-3231.2010.02221.x
19. Bujold A, Massey CA, Kim JJ, Brierley J, Cho C, Wong RK, et al. Sequential Phase I and II Trials of Stereotactic Body Radiotherapy for Locally Advanced Hepatocellular Carcinoma. *J Clin Oncol* (2013) 31(13):1631–9. doi: 10.1200/JCO.2012.44.1659
20. Kwon JH, Bae SH, Kim JY, Choi BO, Jang HS, Jang JW, et al. Long-Term Effect of Stereotactic Body Radiation Therapy for Primary Hepatocellular Carcinoma Ineligible for Local Ablation Therapy or Surgical Resection. Stereotactic Radiotherapy for Liver Cancer. *BMC Cancer* (2010) 10:475. doi: 10.1186/1471-2407-10-475
21. Andolino DL, Johnson CS, Maluccio M, Kwo P, Tector AJ, Zook J, et al. Stereotactic Body Radiotherapy for Primary Hepatocellular Carcinoma. *Int J Radiat Oncol Biol Phys* (2011) 81(4):e447–53. doi: 10.1016/j.ijrobp.2011.04.011
22. Huang W-Y, Jen YM, Lee MS, Chang LP, Chen CM, Ko KH, et al. Stereotactic Body Radiation Therapy in Recurrent Hepatocellular Carcinoma. *Int J Radiat Oncol Biol Physics* (2012) 84(2):355–61. doi: 10.1016/j.ijrobp.2011.11.058
23. Que JY, Lin L-C, Lin K-L, Lin C-H, Lin Y-W, Yang C-C. The Efficacy of Stereotactic Body Radiation Therapy on Huge Hepatocellular Carcinoma Unsuitable for Other Local Modalities. *Radiat Oncol* (2014) 9(1):120. doi: 10.1186/1748-717X-9-120
24. Jun BG, Kim SG, Kim YD, Cheon GJ, Han KH, Yoo JJ, et al. Combined Therapy of Transarterial Chemoembolization and Stereotactic Body Radiation Therapy Versus Transarterial Chemoembolization for </=5cm Hepatocellular Carcinoma: Propensity Score Matching Analysis. *PLoS One* (2018) 13(10):e0206381. doi: 10.1371/journal.pone.0206381
25. Schwarz RE, Abou-Alfa GK, Geschwind JF, Krishnan S, Salem R, Venook AP, et al. Nonoperative Therapies for Combined Modality Treatment of Hepatocellular Cancer: Expert Consensus Statement. *HPB (Oxford)* (2010) 12(5):313–20. doi: 10.1111/j.1477-2574.2010.00183.x
26. Buckstein M, Kim E, Fischman A, Blacksburg S, Facciuto M, Schwartz M, et al. Stereotactic Body Radiation Therapy Following Transarterial Chemoembolization for Unresectable Hepatocellular Carcinoma. *J Gastrointestinal Oncol* (2018) 9 (4):734–40. doi: 10.21037/jgo.2018.05.01
27. Chiang CL, Chan MKH, Yeung CSY, Ho CHM, Lee FAS, Lee VWY, et al. Combined Stereotactic Body Radiotherapy and Trans-Arterial Chemoembolization as Initial Treatment in BCLC Stage B–C Hepatocellular Carcinoma. *Strahlenther Und Onkol* (2018) 195(3):254–64. doi: 10.1007/s00066-018-1391-2
28. Wong TC, Chiang CL, Lee AS, Lee VH, Yeung CS, Ho CH, et al. Better Survival After Stereotactic Body Radiation Therapy Following Transarterial Chemoembolization in Nonresectable Hepatocellular Carcinoma: A Propensity Score Matched Analysis. *Surg Oncol* (2019) 28:228–35. doi: 10.1016/j.suronc.2019.01.006
29. Zhao L, Mou DC, Peng JR, Huang L, Wu ZA, Leng XS. Diagnostic Value of Cancer-Testis Antigen mRNA in Peripheral Blood From Hepatocellular Carcinoma Patients. *World J Gastroenterol* (2010) 16(32):4072–8. doi: 10.3748/wjg.v16.i32.4072
30. Chan SL, Mo FK, Johnson PJ, Hui EP, Ma BB, Ho WM, et al. New Utility of an Old Marker: Serial Alpha-Fetoprotein Measurement in Predicting Radiologic Response and Survival of Patients With Hepatocellular Carcinoma Undergoing Systemic Chemotherapy. *J Clin Oncol* (2009) 27(3):446–52. doi: 10.1200/JCO.2008.18.8151
31. Tsai MC, Wang JH, Hung CH, Kee KM, Yen YH, Lee CM, et al. Favorable Alpha-Fetoprotein Decrease as a Prognostic Surrogate in Patients With Hepatocellular Carcinoma After Radiofrequency Ablation. *J Gastroenterol Hepatol* (2010) 25(3):605–12. doi: 10.1111/j.1440-1746.2009.06115.x
32. Jung J, Yoon SM, Han S, Shim JH, Kim KM, Lim YS, et al. Alpha-Fetoprotein Normalization as a Prognostic Surrogate in Small Hepatocellular Carcinoma After Stereotactic Body Radiotherapy: A Propensity Score Matching Analysis. *BMC Cancer* (2015) 15:987. doi: 10.1186/s12885-015-2017-z
33. Yao E, Chen J, Zhao X, Zheng Y, Wu X, Han F, et al. Efficacy of Stereotactic Body Radiotherapy for Recurrent or Residual Hepatocellular Carcinoma After Transcatheter Arterial Chemoembolization. *BioMed Res Int* (2018) 2018:5481909. doi: 10.1155/2018/5481909
34. Lasley FD, Mannina EM, Johnson CS, Perkins SM, Althouse S, Maluccio M, et al. Treatment Variables Related to Liver Toxicity in Patients With Hepatocellular Carcinoma, Child-Pugh Class A and B Enrolled in a Phase 1-2 Trial of Stereotactic Body Radiation Therapy. *Pract Radiat Oncol* (2015) 5 (5):e443–9. doi: 10.1016/j.prro.2015.02.007
35. Witt JS, Rosenberg SA, Bassetti MF. MRI-Guided Adaptive Radiotherapy for Liver Tumours: Visualising the Future. *Lancet Oncol* (2020) 21:e74–82. doi: 10.1016/S1470-2045(20)30034-6
36. Finn RS, Qin S, Ikeda M, Galle PR, Ducreux M, Kim TY, et al. Atezolizumab Plus Bevacizumab in Unresectable Hepatocellular Carcinoma. *N Engl J Med* (2020) 382:1894–905. doi: 10.1056/NEJMoa1915745

Conflict of Interest: The authors declare that the research was conducted in the absence of any commercial or financial relationships that could be construed as a potential conflict of interest.

Advantages of publishing in Frontiers

OPEN ACCESS
Articles are free to read for greatest visibility and readership

FAST PUBLICATION
Around 90 days from submission to decision

HIGH QUALITY PEER-REVIEW
Rigorous, collaborative, and constructive peer-review

TRANSPARENT PEER-REVIEW
Editors and reviewers acknowledged by name on published articles

Frontiers
Avenue du Tribunal-Fédéral 34
1005 Lausanne | Switzerland

Visit us: www.frontiersin.org
Contact us: frontiersin.org/about/contact

REPRODUCIBILITY OF RESEARCH
Support open data and methods to enhance research reproducibility

DIGITAL PUBLISHING
Articles designed for optimal readership across devices

FOLLOW US
@frontiersin

IMPACT METRICS
Advanced article metrics track visibility across digital media

EXTENSIVE PROMOTION
Marketing and promotion of impactful research

LOOP RESEARCH NETWORK
Our network increases your article's readership